Author:
Earl, Simeon J

Title:
Estimation of subsurface electrical resistivity values in 3D.

Estimation of Subsurface Electrical Resistivity Values in 3D

Simeon J. Earl

Department of Engineering Mathematics
University of Bristol

A Thesis submitted to The University of Bristol
for the degree of Doctor of Philosophy
in the Faculty of Engineering

July 1998

Abstract

The viability of electrical resistivity surveys (ERS) depends on schemes for inverting measurements into accurate subsurface resistivity values. These inversion schemes typically involve a forward modelling capability and a method for calculating the rate of change of each measurement with respect to each resistivity value (i.e. the Jacobian matrix). Directly calculating the Jacobian matrix (the perturbation method) is unpopular because it is time consuming.

A suite of numerical methods for solving Poisson's equation over a 3D finite-difference grid, including a non-iterative 3D method, was developed and tested for various resistivity distributions. Method-dependent preferred orientations were discovered for the homogeneous case. However, for non-homogeneous cases the time taken was dominated by the heterogeneities. To minimise the time taken, a set of guidelines was developed on the basis of numerical experiments.

It is common for measurements to be inverted using a pre-computed Jacobian for the homogeneous case, sometimes with the addition of a fast updating method which assumes that the Jacobian does not vary widely from the homogeneous case. Another method uses the adjoint to the forward problem where the elements of the Jacobian are calculated utilising solutions from additional forward problems. This method is fast but includes a second order approximation.

This adjoint method has been tested against the perturbation method using a numerical simulation having a complex distribution of highly variable resistivities. Inversions of synthetic measurements using these two approaches, to calculate the Jacobian, produced large differences in the estimated of resistivity values; the perturbation method was more accurate. Correction schemes were applied to the adjoint method but yielded little or no improvement.

Comparing Jacobian matrices calculated by the above approaches for the same resistivities showed differences of many orders of magnitude and changes in sign. Similarly, these matrices were seen to change vastly during the course of inversions. By considering individual measurements in the matrices calculated from the solution and the best result which was given by the perturbation method, it was seen that regions of low resistivity were associated with the dominant elements and that the depth of the investigation increased when the electrodes overlaid these low resistivity regions.

To stabilise inversions using the adjoint method, it was necessary to

stiffen the smoothness constraint, as is also the case for noisy measurements (Sasaki [1992]). Smooth results are seen in the literature when either the adjoint or approximate methods are used with noise free data (e.g. Sasaki [1992], Loke & Barker [1995]). Consequently, it is concluded that errors in Jacobian matrices, as well as errors in the measurements, degrade the accuracy of the estimation of resistivity values. There is a need to improve the 'fast' methods currently used to calculate the Jacobians, particularly when close to a solution.

It is common for the resistivity of a geological formation to be anisotropic. The methods developed here are capable of modelling and interpreting structures with anisotropic resistivity.

In memory of my father

Acknowledgements

Firstly, I would like to thank both my supervisors: Gordon Reece, at the University of Bristol, for his many pearls of wisdom in how to develop methods for doing research and programming, and Peter Jackson, at the British Geological Surveys (BGS), for the many practical suggestions and enlightening conversations on Electrical Resistivity Tomography and related subjects. Also, they instigated and arranged an E.P.S.R.C. Case award in conjunction with BGS.

As a member of the Applied Nonlinear Maths group I had access to a wealth of knowledge which was practical, interesting or fun, and I would like to thank all the group past and present. In particular, I would like to thank Stuart Doole for the many helpful suggestions, not least in the tips on hacking Postscript and Gabriel Lord for the knowledge and references to Numerical Analysis he gave me, and for organising the department cricket team. I would also like to thank Mario, Martin, Jonathan R. and Nigel for their help with Latex and Nigel for the five-a-side football. Many thanks to the 'Ploy Masters' for organising many ploys for the PGs and RAs.

I would like to thank various members of the Department of Engineering Maths. The foremost among them are the secretaries, in particular, Sue and Gina who between them organised my travel for my many visits to BGS.

I would like to thank the Engineering Geology and Geophysics Group At BGS, because during my visits was made to feel part of the group and their help and unique insight into geology. I would particularly to thank Rob Flint for all his help with computers and I would like to wish him all the best with his PhD. Also I would like to thank Janet.

Finally, I wish to thank all my friends and family for all their support and advice. In particular I would like to thank my mother, Eifion, Mike and Mike for their time in pointing out parts which bore little relation to the English language.

Declaration

This thesis entitled "Estimation of Subsurface Electrical Resistivity Values in 3D" is submitted for the degree of Doctor of Philosophy at the University of Bristol and has not been submitted, in part or total, for another degree or diploma at any other institution or examining body.

The work reported in this thesis was carried out by the author in the Department of Engineering Mathematics at University of Bristol and in the Coastal and Engineering Geology Group at the British Geological Survey's site in Keyworth (near Nottingham) from October 1994 to June 1998 under the supervision of Dr. G. Reece of the University of Bristol and Dr. P Jackson of the British Geological Survey. The help received has been acknowledged and the views expressed are solely those of the author.

Simeon J. Earl

July 1998

Contents

Chapter 1

Introduction

1.1 Background

Various non-destructive and non-invasive methods can be used to obtain knowledge of the structure and properties of a given solid object, without damaging the object. An example is the use of X-rays to find the location of a tumour or fracture. The use of invasive investigative techniques will sometimes have the unfortunate effect of changing the nature and characteristics of the object under investigation. For example, a borehole will draw water to it, thus changing the groundwater level in the soil around it.

The technique which has been investigated in detail is electrical resistivity tomography (ERT) and, in particular, its application to the field of geophysics. Even with the resistivity information that will be provided by our technique it will not always be possible to ascertain the actual type of mineral/rock/deposit that form the region of subsurface under investigation. However, it is possible to estimate its location and size.

In studying the resistivity of the subsurface, there are other properties that are of interest apart from the structure; these include pore space, grain size, density, permeability and pore contents. Such properties are useful, in particular to the oil industry, in order to give an accurate estimation of the amount of oil in any particular field, together with a measure of its ease of extraction. Needless to say, some investigative techniques are better at identifying certain properties than others. It is possible to build up a fuller picture of the subsurface by using more than one of these.

There are various types of surveying techniques. The best known is seismic surveying, which uses the reflections of sound waves to produce a good

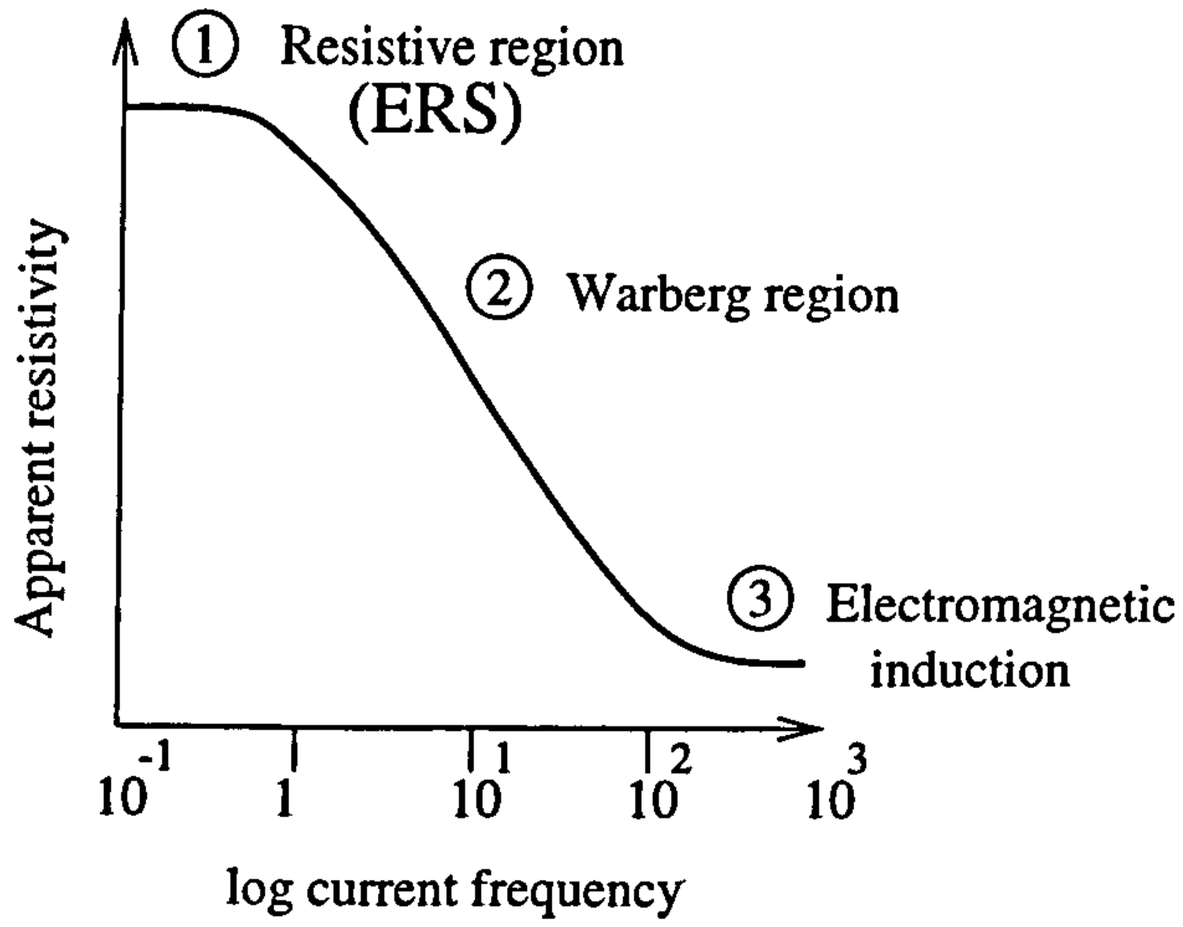

Figure 1.1: The relationship between apparent resistivity and measuring current frequency (from Kearey & Brooks [1991]) which illustrates the regions in which the electrical methods work.

representation of the structure. This is the most widely used technique as it is reasonably easy to interpret because the sound waves travel in relatively straight lines. Another method is ground penetrating radar. Other methods use anomalies in the gravitational, magnetic and potential fields. Electrical methods can be divided into three, see figure 1.1, according to the frequency of the electrical current used, namely high (3), medium (2) and low (1). It is the low frequency technique which will be investigated. The reason for using AC (0 to 5Hz) rather than DC is to alleviate the problem of capacitance occurring in the subsurface. An example of how capacitance occurs is given in figure 1.2. This (low frequency) AC can be modelled as DC because the unwanted capacitance is not modelled and at such low frequency any inductance is effectively resistive. This low frequency method AC is called electrical resistivity surveying (ERS).

ERS is used to produce images of the resistivity distribution of the subsurface. The resistivity of the subsurface does not necessarily deliver useful information, even though it gives details of the structure of the subsurface, identifying both faults and beds. The method is useful for finding conductive minerals, which mainly take the form of salts. However, as most rock is of high resistivity, the current will tend to flow though any water present, particularly if it contains salts, as the ions produce a much lower resistance than the rock. Therefore ERS is useful for investigating both the level of groundwater and monitoring the pollutants, specifically ionised pollutants, that are flowing within it. Therefore, the resistivity distribution

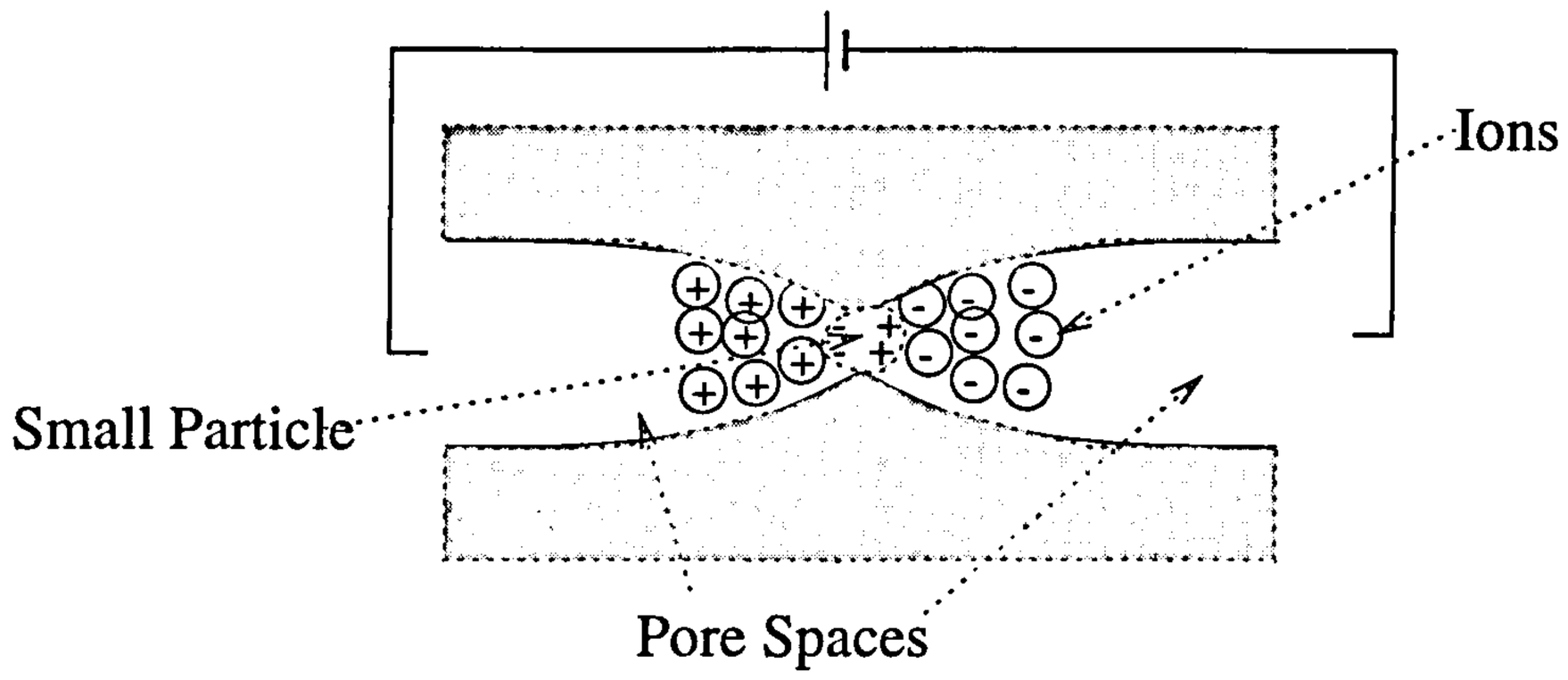

Figure 1.2: Capacitance in blocked pore spaces (from Kearey & Brooks [1991]).

contains information on the pore space, including both size and contents of the pores. If this method is used in conjunction with others, such implicit information can be investigated further and clarified.

For us be able to deduce these properties, ERT must produce not only a schematic representation of the resistivities but also fairly accurate values of the resistivities themselves. Some of the methods of interpretation used (reviewed in chapter 4) may be fast but yield inaccurate resistivity values. The aim of this work will be to produce a method of interpreting ERS which is more accurate and reasonably quick. The algorithms and techniques developed in later chapters are designed to solve fully 3D problems, even if the test problem (in chapter 6) is a 2D grid of 3D zones. The reason for this, is that the ground is a 3D space and it is not best modelled by trying to force 1D or 2D methods upon it.

1.2 Electrical resistivity tomography

This section introduces ERT and shows how electrodes are arranged in geophysical surveys. It also introduces some of the terminology used in later chapters.

Most applications of ERT resemble figure 1.3, where the subject of the investigation, which has a resistivity distribution (ρ), is surrounded by electrodes. When any given set of electrodes is used they either supply electrical current (current electrodes) or are used to measure potential difference (potential electrodes). A series of measurements is taken from a combination of current electrodes and potential electrodes. These measurements are then interpreted to produce an image of the resistivity distribution.

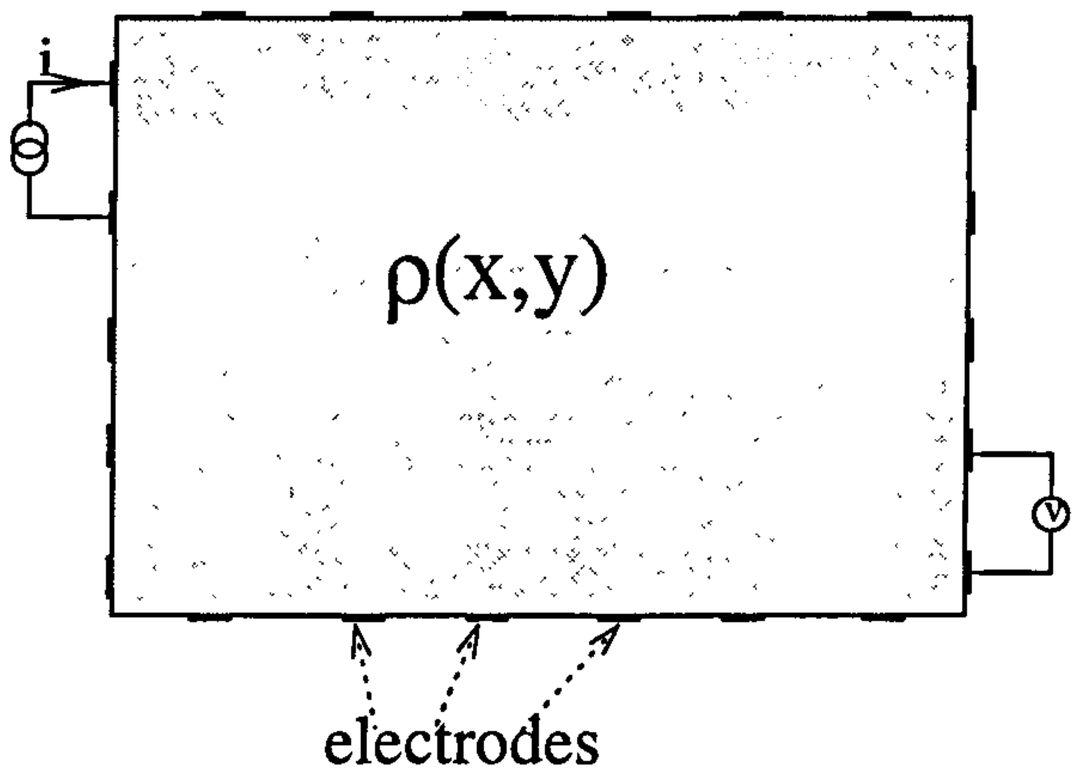

Figure 1.3: A 2D schematic of electrical resistivity tomography as usually applied.

Most of the published methods use a model of the material which consists of zones (or blocks)[1] which tend to be box shaped. The subject of the investigation as seen in figure 1.3 is made up of these zones. The methods use the model to calculate synthetic measurements of potentials to compare with the actual measurements as a part of the interpretation algorithms. The difference between actual and modelled measurements can also be used as a convergence criterion.

Applications, which resemble figure 1.3, can be used in medical imaging (Barber & Brown [1984], Powell, Barber & Freeston [1987]), fault detection in materials (Santosa [1995]) and in the imaging of core samples (Lovell & Jackson [1991]). The technique used in figure 1.3 has advantages over the surveys used in the field. The greatest of these is to have definite boundaries and the ability to apply electrodes to all of them. This means that current can be passed through the centre of the subject easily. It also means that any external influences can be removed so that the measurements will not suffer from any pre-existing electrical fields. Another advantage is that given that the boundaries are defined all the current will stay within these boundaries thus making the problem mathematically simpler because it is possible that the resistivity can be uniquely determined Kohn & Vogelius [1984].

Surveys used in the field can be divided into two types, firstly where electrodes are placed both in boreholes and on the surface and secondly, those where the electrodes are only placed on the surface. The techniques developed in later chapters will work for both cases since they work independently of the location of electrodes. However, the surveys with electrodes on the surface will be the main

[1]The terminology varies from author to author. We shall refer to "zones" in what follows.

examples used. The results displayed in chapter 6 relate to electrodes only placed on the surface of the ground.

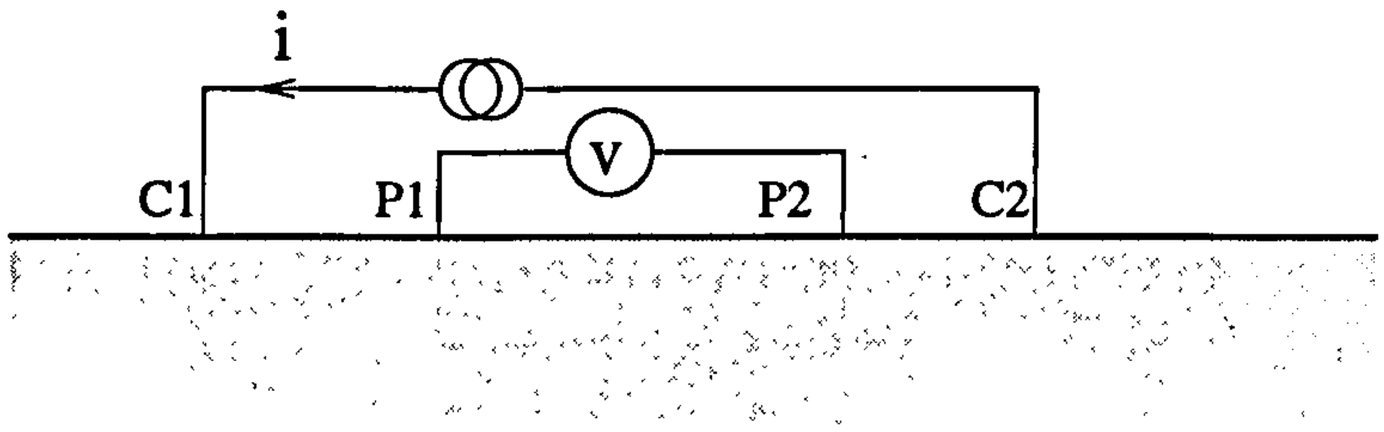

Figure 1.4: A schematic of electrical resistivity survey with surface electrodes. This is known as the dipole–dipole survey.

Figure 1.4 shows the basic structure of a survey. There are two current electrodes, $C1$ being the current source electrode and $C2$ being the current sink electrode. $P1$ and $P2$ are the two electrodes between which the potential difference is measured. The most important difference between figure 1.4 and 1.3, is that only one boundary is defined, i.e. the surface of the ground. The surface is taken to be flat plane to ease the mathematics but there are various techniques which can be used for uneven ground (Sasaki [1994]). The other boundaries are assumed to be theoretically infinitely far from the electrodes. (However, the numerical model considers these boundaries to be at a large finite distance.)

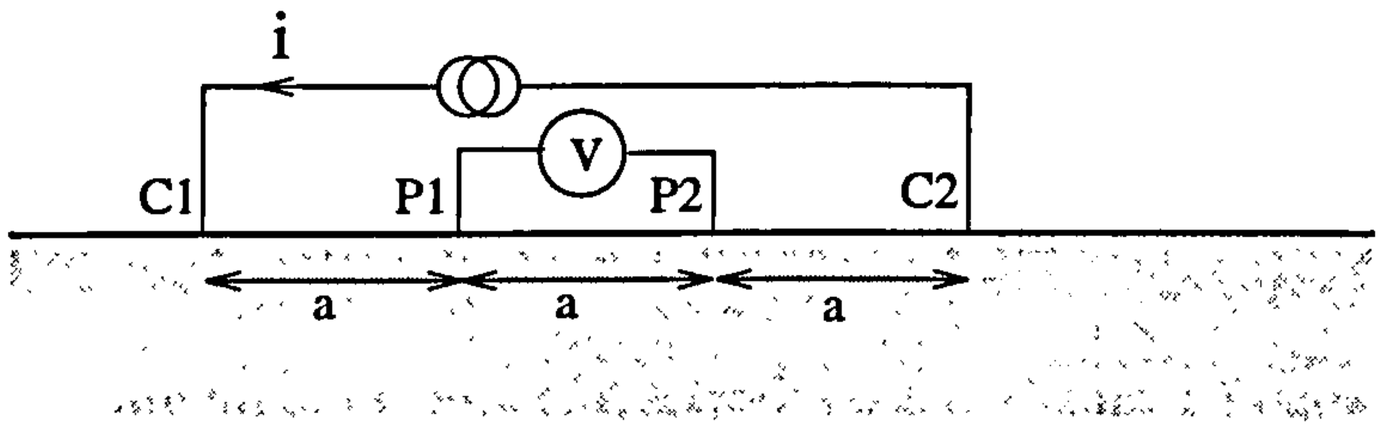

Figure 1.5: A Wenner electrode configuration.

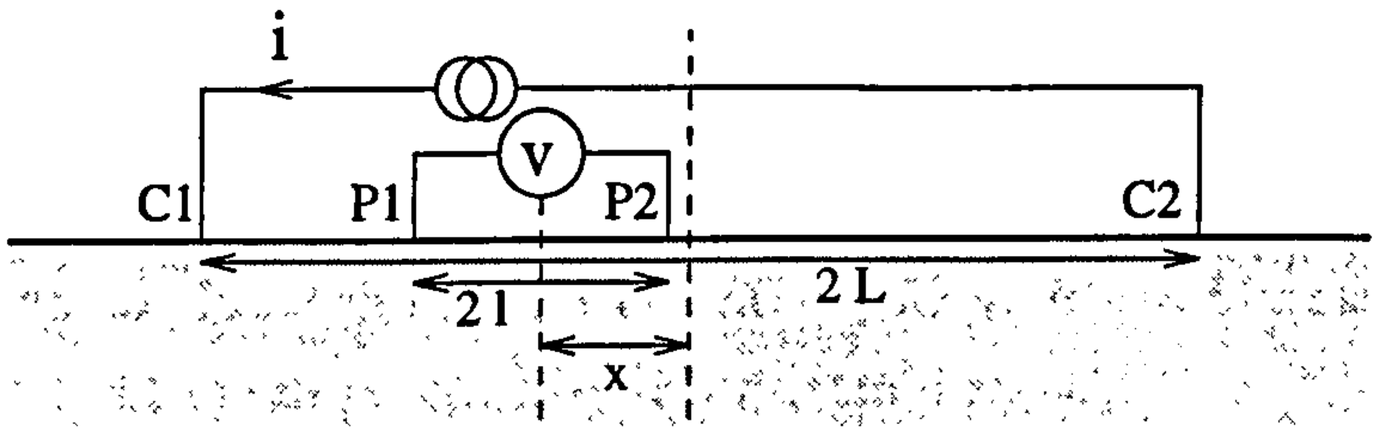

Figure 1.6: A Schlumberger electrode configuration.

Figures 1.5 and 1.6 are two types of dipole–dipole which are widely used in practice. Both have the potential electrodes placed on a straight line between the

current electrodes. It is not necessarily the case with all dipole–dipole surveys that the potential electrodes need to be between the current electrodes.

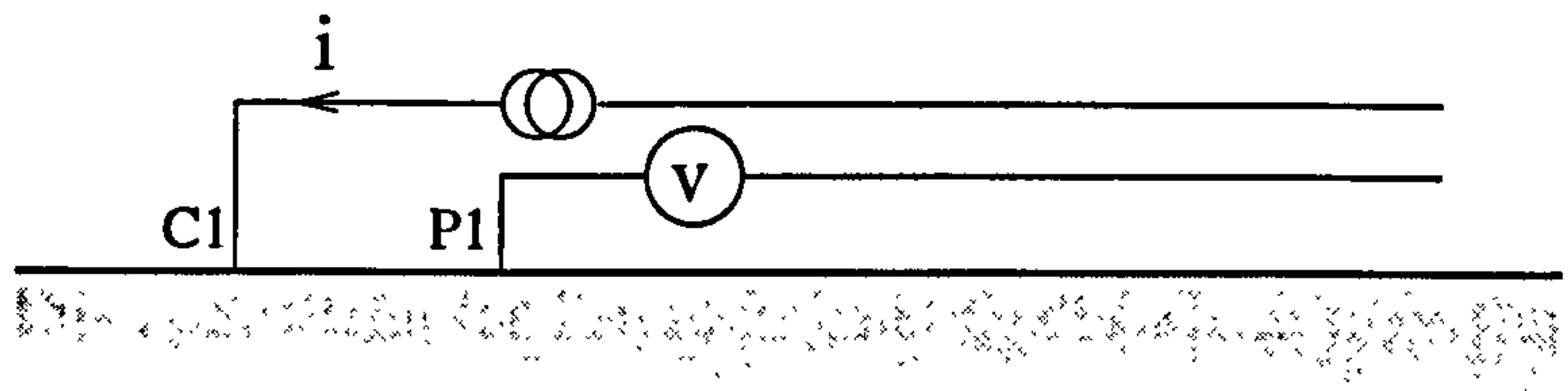

Figure 1.7: A schematic of pole–pole .

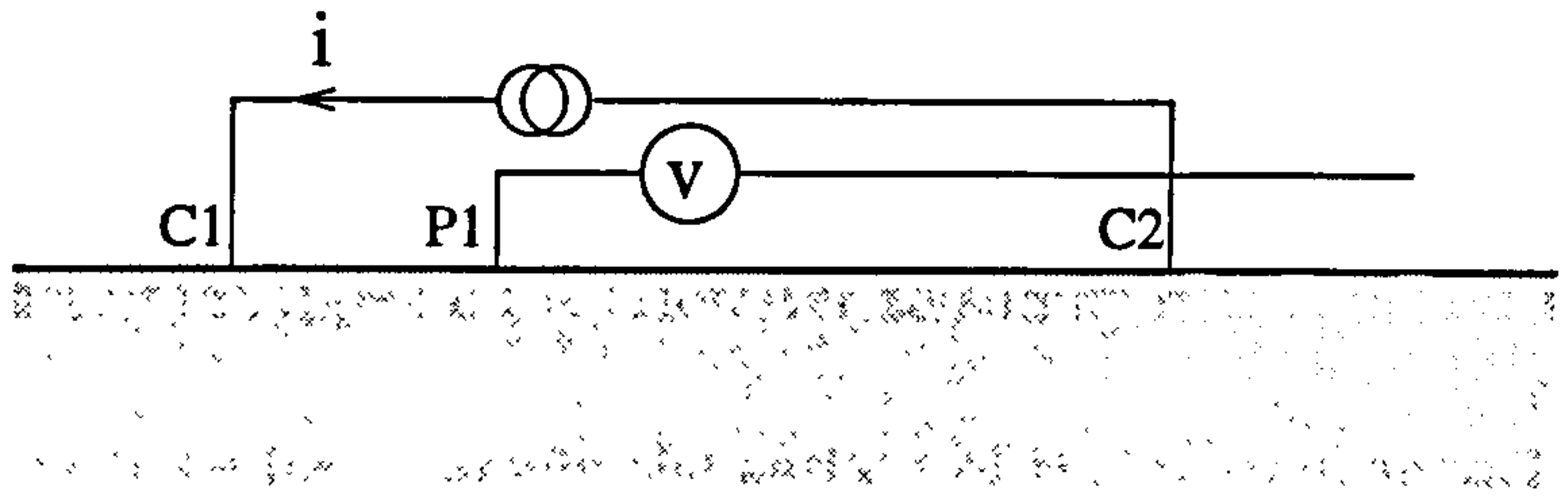

Figure 1.8: A schematic of dipole–pole .

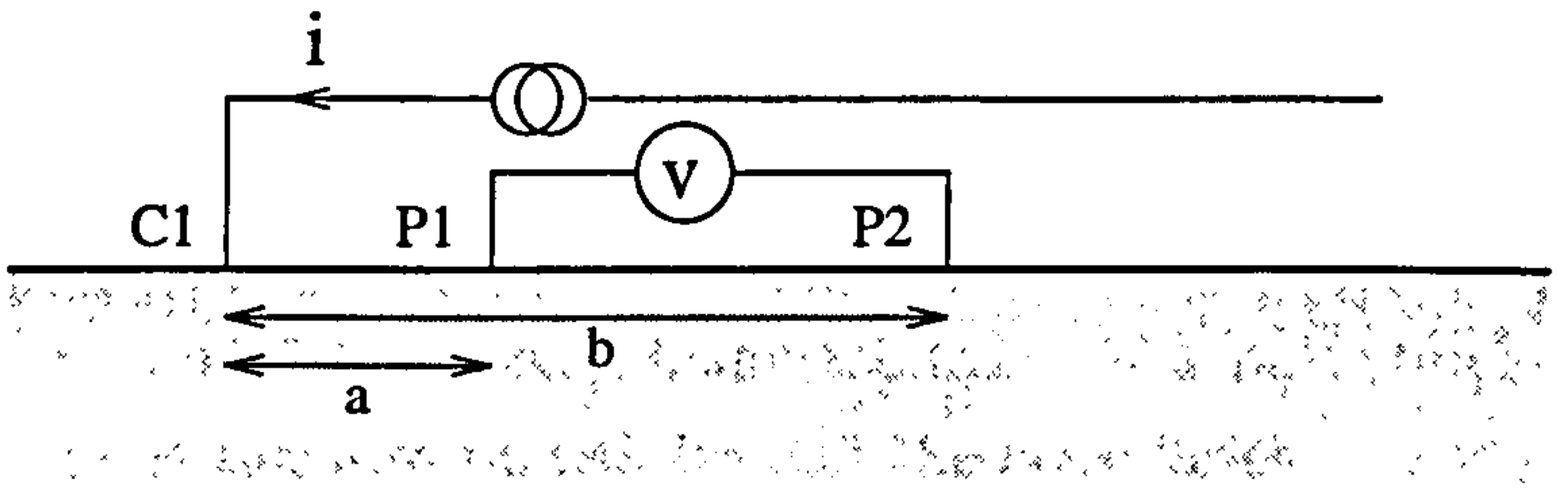

Figure 1.9: A schematic of pole–dipole .

There are other layouts of electrodes used. Figure 1.7 shows a schematic of a pole–pole survey. This is often used because it makes the mathematics of the interpretation much simpler and as such tends to be used for testing new methods. Figure 1.8 is a dipole–pole electrode formation which appears not to be widely used, (given the lack of mention in any of the papers reviewed). Both pole–pole and dipole–pole surveys tend to suffer much more from background electrical fields as they measure an absolute value for the potential whereas methods which use a dipole are measuring a change in potential over a certain distance.

Figure 1.9 shows a schematic of a pole–dipole. This is the type which is used by the British Geological Survey (BGS) and as such is the type which will be used in later chapters. It is also be called a "half Schlumberger" array although it will from now on be referred to as a pole–dipole survey. It does not suffer from the

errors which can occur when measuring with a single pole. However, measuring a potential difference does tend to make the measurements smaller. Figure 1.9 also defines a and b values where a is the distance between $C1$ and $P1$ and b is the distance between $C1$ and $P2$. The length of $\frac{a}{3}$ can be used as a rough estimate of the depth to which most of the current being used is likely to flow. As will be seen in chapter 7 this is not true for heterogeneous media which may vary widely from the homogeneous case.

The implementation of all the methods which involve a pole rather than a dipole place the other electrode far enough away from the region being surveyed so as not to effect the other electrodes. However, when these various pole methods are modelled these electrodes are assumed to be outside the boundaries of the survey.

The model used for representing the current behaviour of subsurface is described in detail in Appendix A. However to summarise, it includes:-

- One finite boundary, namely the surface of the ground, modelled by a Neumann boundary condition, i.e. no current flows through the boundary.

- Five infinite boundaries. These are in practice taken to be far enough away from the zones to have negligible effect. These are modelled by Dirichet boundary conditions, i.e. the potential is set at a fixed value.

- A current source, the survey being modelled is a pole–dipole survey. The current sink is taken to be well beyond the boundaries.

- Measurements are taken from potential electrodes.

- The ground is assumed to be continuous and connected. This means that there is no point which can take an arbitrary value of potential.

- It is assumed that the ground can be modelled by a finite difference grid. This is analogous to using a 3D grid of nodes connected by resistors (as in figure 1.10).

If Kirchoff Laws are solved for every node on the grid then there exists a solution for all the potentials, given the values of all the resistors, the size and location of the current source and the boundaries. This produces a set of simultaneous equations for the value of the potential which can be written in the form

$$\underline{\mathbf{A}}\mathbf{x} = \mathbf{b} \tag{1.1}$$

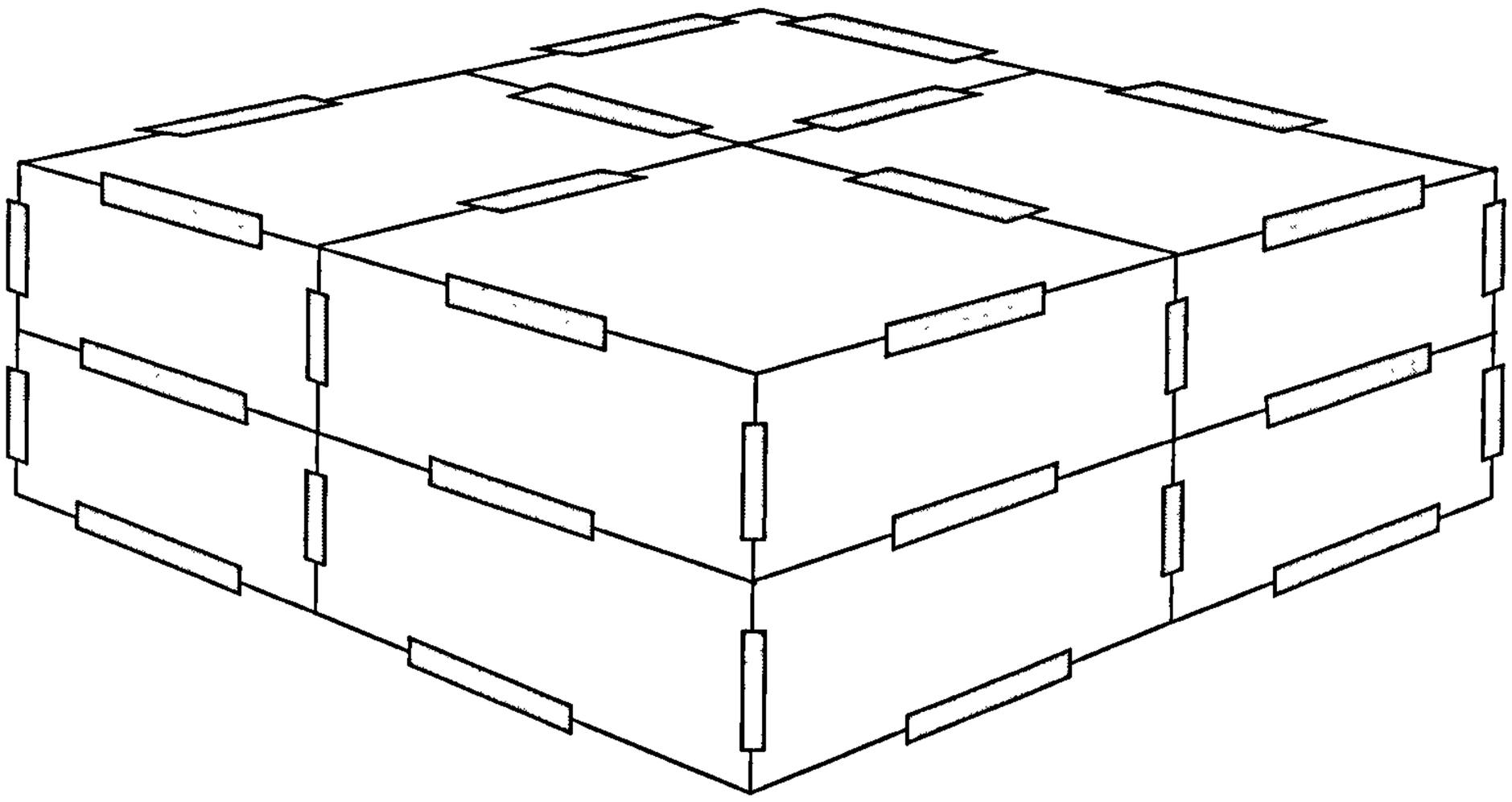

Figure 1.10: 3D resistor grid.

where $\underline{\mathbf{A}}$ is a matrix containing the conductances, $\mathbf{b}$ contains the sources and boundary conditions, and $\mathbf{x}$ is a vector of the unknowns. If the grid cells tends to be infinitely small, then Poisson's equation (1.2) can be derived in the same form as steady state heat conduction.

$$\nabla.(k\nabla\phi) = \sigma \tag{1.2}$$

where k is the conductivity (is the inverse of resistivity), σ is the source term and ϕ (or T) is the value of potential, whether it is electrical potential (or temperature).

This method could be adapted to solve equivalent problems which contain anisotropic resistivities. Although no anisotropic medium has been actually modelled, this is a direction in which further research should be pursued. In appendix A, one method of modelling anisotropy is given (the same as in Carslaw & Jaeger [1959]). This involves k being a matrix. If the matrix is a diagonal matrix for the whole volume of the ground being modelled, then the present network of resistor model would work. This does not imply that the whole space has to be homogeneous as well as being anisotropic.

There are a number of limitations on ERSs, as set out below, which are quoted from Kearey & Brooks [1991]:-

1. Interpretations are ambiguous. Consequently, independent geophysical and geological controls are necessary to discriminate between valid alternative interpretations of resistivity data.

2. Interpretation is limited to simple structural configurations. Any deviations from these simple situations may be impossible to interpret.

3. Topography and the effects of near-surface resistivity variations can mask the effects of deeper variations.

4. The depth of penetration of the method is limited by the maximum electrical power that can be introduced into the ground and by the practical difficulties of laying out long lengths of cable. The practical depth limit for most surveys is about 1km.

1, 3 and 4 appear to be correct and 2 can be overcome by using an appropriate control in the method for interpretation. An example of this can be seen in the test problem used in the inversions in chapter 6.

1.3 Forward problem

This section introduces the "forward problem": given ρ and σ (e.g. from a survey) find the value of ϕ at various locations using equation (1.2).

The forward problem is solved over a finite difference grid using knowledge of the location of the current electrodes, the size of the current applied and the resistivity distribution, to calculate the value of the potential for every node on the grid. Therefore, to model a whole survey, the number of forward problems which need to be calculated is proportional to the number of different locations of the which there is a $C1$ electrode[2]. If only one calculation is used per $C1$ location, then there will be only one forward problem per $C1$ location, therefore number of forward problems to be solved would be equal to the number of locations $C1$. However, this is not the case if more than one grid is used. In the program used during the interpretation in chapter 6 two grids were used. The reason for this is discussed below and it is the reason for the problem discussed in section 5.4.2.

The modelling of the surveys described in section 1.2 requires a means of accurately modelling the boundaries. The simplest boundary to model is the surface of the ground, which is a Neumann boundary, i.e. no current flows through the boundary. All the other boundaries are an infinite distance from the electrodes. Thus, as it is not possible to solve the heterogeneous case analytically, these infinite boundaries have to be modelled by finite boundaries. Such theoretical boundaries

[2]This is true for pole–dipole surveys. In general, it is proportional to the number of different sets of source electrodes.

are modelled by Dirichet boundary conditions where either the potentials are set to zero or the homogeneous values taken from the analytic solution of the homogeneous case. Instead of using one large grid, two grids are used, where a large but sparse grid is used to calculate the boundaries and the starting point for a smaller grid with a finer mesh which includes all the electrodes. This is tending towards a multigrid approach.

The forward problem amounts to solving Poisson's equation, (see equation (1.2)) with a point source. This is discretised over a finite difference grid as used in Reece [1986] and Williams [1996]. It is possible to solve Poisson's equation analytically for a point source with a homogeneous resistivity distribution. For heterogeneous resistivity distributions numerical methods have to be used. The numerical methods used are discussed in chapter 2 and these include a direct method, the conjugate gradient method and other iterative methods. The accuracy of these methods is dependent on the discretisation and grid size and not on the methods themselves as they are all unconditionally convergent to the solution apart from the conjugate gradient method. There are various properties of these methods which affect the time taken to obtain the solution.

1.4 Inverse problem

The interpretation of either real or test data, will be referred to as the "inverse problem", i.e. given σ and a sparse, incomplete set of ϕ, trying to reconstructed ρ. It is however, only one example of a group of problems which come under the name of inverse problems. Inverse problems have a number of associated traits which are regularly (though not invariably) encountered. The traits are: the data is inconsistent and sparse, and the solution space has an infinite number of minima (an infinite number of solutions may exist). This means that finding the correct solution can be hard, or even impossible. One of the means of getting around this last trait is to introduce constraints (or a set of constraints) to the problem. This can have the effect of reducing the number of minima in the solution space (i.e. reduce the number of possible solutions). In doing so, it is likely that it is only possible to get into the neighbourhood of the solution, or maybe only close to the neighbourhood of the solution.

There are various methods which are used to solve[3] the inverse problem.

[3] "Solve" in most of these cases means producing *a* solution, not necessarily a solution even close to reality.

A number of these techniques are described in chapter 4 and where the algorithms were given in any particular papers these have been included. The method previewed in section 4.2 and used in chapter 6 is a smoothness-constraint least-squares inversion scheme.

The part of this scheme which is investigated in detail is the calculation of the Jacobian matrix. It is a fundamental part of most of the inversion schemes used in solving the inverse problem. Chapter 7 compares the Jacobian matrices calculated at various points in the calculation of the inverse problem.

1.5 Objectives

There are a number of important geophysical properties that geologists would like to be able to determine in any subsurface. These include properties like porosity and the content of the pore space, e.g. oil or water. There are other linked properties such as the concentration of ionised pollutants in the ground water and the monitoring of such pollutants. This implicitly includes the structure of the rock/ground in any particular region. Such properties cannot be found by using one type of surveying technique in isolation but require the comparison of values obtained from a number of differing surveying techniques. In order to predict these, the methods for interpreting surveys must be accurate if a reliable answer is to be obtained. One of the surveying techniques geologists wish to use is ERS. They need a reliable method of inversion which is accurate, does not take too long to run and will distinguish gradual changes as well as sharp changes in the value of resistivity.

What is needed is a method of inversion which produces accurate values of the resistivity. There are also other restraints, such as the accuracy of the resistivity values and speed. On a practical note if it is possible to process overnight the data collected in one day out in the field, then the speed of the interpretation process is fast enough. Furthermore, if an interesting feature, whether is it the edge of a pollutant or a complex fault, then a greater concentration of measurements can be taken in that particular area so as to give a more accurate picture.

In general the objectives are to increase the speed whilst retaining the accuracy of the interpretation of the data. In the forward problem the objective is to find a technique for picking the fastest method for a particular problem. There are only two types of problem which are of particular interest. The first of these is the fast solution of complicated resistivity distributions starting reasonably far from the solution. In the case where the forward problem is used to calculate

synthetic measurements. The second is for the same type of distributions as the first problem but starting close to the solution. This is analogous to the way in which the perturbation method[4] for calculating the Jacobian matrix uses the forward problem.

The most time consuming part of an inversion scheme is the calculation of the Jacobian matrix. The objectives are not only to increase the speed of the calculation but also reduce the number of terms that determine the time taken for the calculation of this matrix. It will also be demonstrated that the accurate calculation of the Jacobian increases the overall accuracy of the inversion scheme.

[4]This is one of the methods for calculating the Jacobian. See section 6.3.1 for more details on this method.

Chapter 2

Methods for Solving the Forward Problem

2.1 Introduction

This chapter introduces various techniques for solving the forward problem. The objectives (discussed in section 1.5) give some criteria by which these methods may be judged. The ideal method should be fast, robust and accurate. It would help if the methods were able to use other information, for example, an initial condition that is reasonably close to the solution.

The schemes described in this chapter can be split into three types:-

1. Non-iterative methods.

2. Stationary Iterative methods.

3. Non-stationary Iterative methods.

The difference between the first and the other two types is obvious. The difference between the second two is more subtle, and in order to explain the difference, the term "stationary" should be defined (per the definition used in Barrett, Berry, Chan, Demmel, Donato, Dongarra, Eijkhout, Pozo, Romine & Van der Vorst [1994]). Most iterative methods can be expressed in the form

$$x^{(k)} = Bx^{(k-1)} + c \tag{2.1}$$

For the method to be "stationary", B and c do not depend on the iteration count k. An example of a stationary method is point iteration. Most of the non-stationary methods are based on the conjugate gradients method.

The non-iterative method, described in section 2.2, uses the structure of the $\underline{A}$ matrix. In particular, the fact that the $\underline{A}$ matrix can be written as a block tridiagonal matrix. Physically, the blocks actually represent planes of nodes. There are other methods that could be used but most rely on being able to store the whole of the $\underline{A}$ matrix. This is neither practical nor possible, in most cases, for even relatively small 3D forward problems, since the number of elements in $\underline{A}$ is the square of the number of nodes[1].

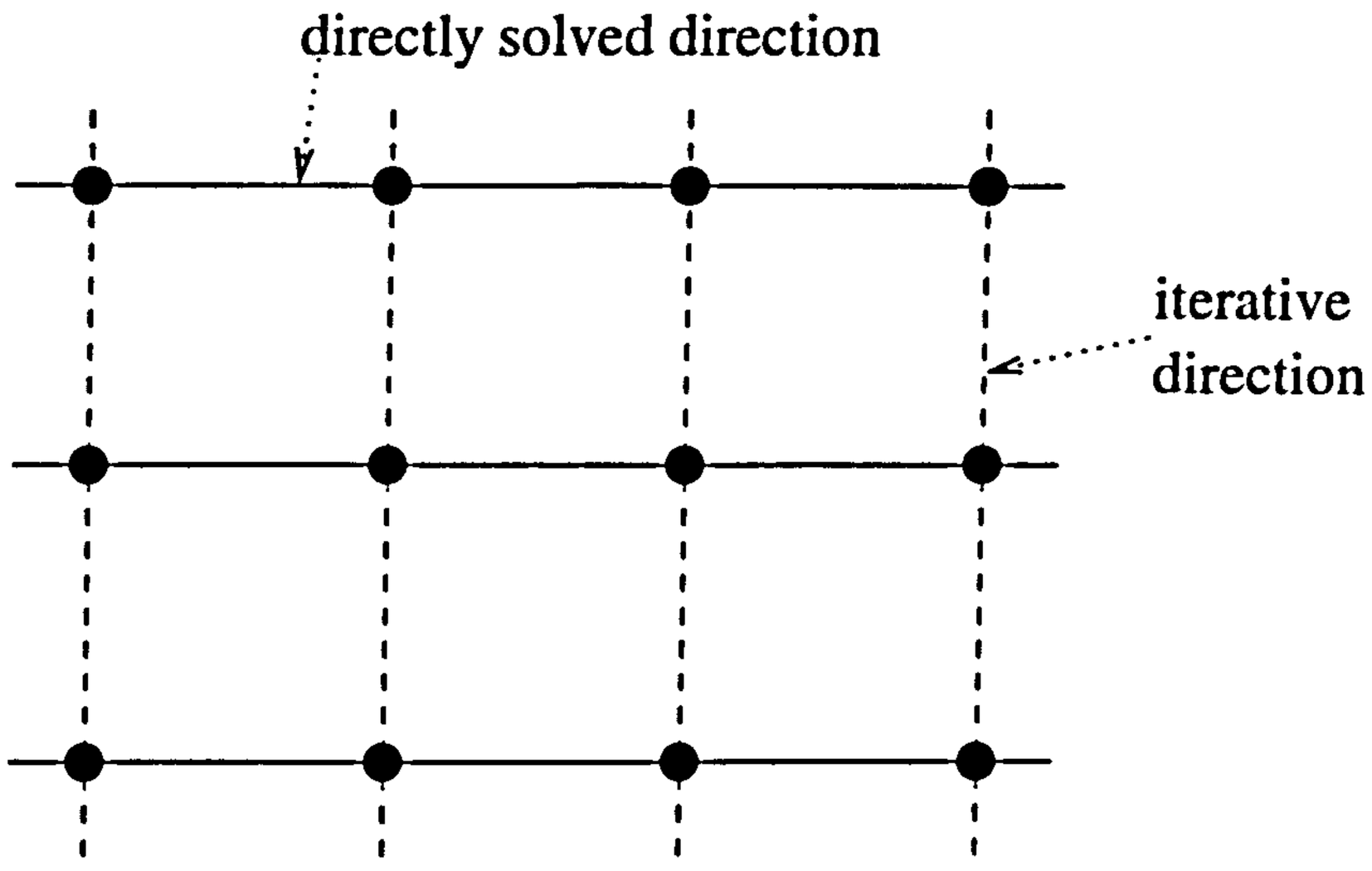

Figure 2.1: Detail of compound methods.

The stationary iterative methods described in section 2.3 are similar to the Gauss-Seidel method. The first, point iteration, is the same as Gauss-Seidel but the floating point divisions are done before the first iterations, therefore changing the problem to a normalised version. The line iteration and panel iteration methods use the non-iterative solver to directly in lines or panels nodes and iterate in other directions (see figure 2.1, where the third direction, not drawn, is solved either iteratively or directly depending which method is being used). The reasoning behind these latter two composite methods is to have fewer iterations but make them more efficient, although each iteration takes longer.

Two non-stationary methods were investigated (for the purposes of this chapter). These were the basic conjugate gradient method[2] and a variant in the form of GMRES (generalised minimal residual) Method. This connects with work done by Zhang, Mackie & Madden [1995] and Spitzer & Wurmstich [1995].

[1] This includes the boundary nodes.

[2] Recommended in private communication with Gene Golub and Andy Wathen.

2.2 Complete inversion

This is a non-iterative method, and as its name suggests solves equation (1.1) "exactly"[3] without any iterative steps. The method does however take full advantage of the structure of $\underline{\mathbf{A}}$. $\underline{\mathbf{A}}$ is a heptadiagonal matrix which is very large for most problems[4] and this means that $\underline{\mathbf{A}}^{-1}$ is not only large but it is a "full" matrix and therefore, if calculable, is almost certainly not easily storable. This also implies that means that finding $\underline{\mathbf{A}}^{-1}$ by Gaussian elimination or LU decomposition, etc, is not practicable (or usually possible for actual surveys). The complete inversion method used here, is an extension of an algorithm developed by Buzbee in (Buzbee, Golub & Nielson [1970] and Buzbee, Dorr, George & Golub [1971]). The reason that this algorithm can be used is because $\underline{\mathbf{A}}$ can be written as a block tridiagonal matrix.

Choose a direction (in this case k which is n nodes long)

for $k = 1, 2, ..., n$

$\underline{\mathbf{M}}_1 = \underline{\mathbf{D}}_k - \underline{\mathbf{C}}_k.\underline{\mathbf{E}}_{k-1}$

$\mathbf{v_1} = \mathbf{b_k} - \underline{\mathbf{C}}_\mathbf{k}.\mathbf{b_{k-1}}$

Solve $\underline{\mathbf{M}}_1.\underline{\mathbf{M}}_2 = \underline{\mathbf{E}}_k$ for $\underline{\mathbf{M}}_2$

Solve $\underline{\mathbf{M}}_1.\mathbf{b_k} = \mathbf{v_1}$ for $\mathbf{b_k}$

$\underline{\mathbf{E}}_k = \underline{\mathbf{M}}_2$

end

$\mathbf{x_n} = \mathbf{b_n}$

for $k = n - 1, ..., 2, 1$

$\mathbf{x_k} = \mathbf{b_{k+1}} - \underline{\mathbf{E}}_\mathbf{k}.\mathbf{x_{k+1}}$

end

Figure 2.2: Method for Complete Inversion

In figure 2.2 $\underline{\mathbf{M}}_1$ and $\underline{\mathbf{M}}_2$ are two matrices and $\mathbf{v_1}$ is a vector used during the algorithm. $\mathbf{x_k}$ is a set of vectors which together make up $\mathbf{x}$ in the same way $\mathbf{b_k}$ makes up $\mathbf{b}$. The matrices $\underline{\mathbf{C}}_k$, $\underline{\mathbf{D}}_k$ and $\underline{\mathbf{E}}_k$ are the blocks from arranging $\underline{\mathbf{A}}$ in such

[3]Exactly, means that it produces the exact answer to the set of simultaneous equations but not necessarily the exact answer to the continuous problem.

[4]The number of nodes for the test problem in chapter 6 is $25 \times 15 \times 15$ which means that $\underline{\mathbf{A}}$ is a square matrix with 5625 rows.

a way that it is block tridiagonal matrix.

$$\underline{\mathbf{A}} = \begin{pmatrix} \underline{\mathbf{D}}_1 & & & & & \\ \underline{\mathbf{C}}_2 & \underline{\mathbf{D}}_2 & \underline{\mathbf{E}}_2 & & & \\ & \underline{\mathbf{C}}_3 & \underline{\mathbf{D}}_3 & \underline{\mathbf{E}}_3 & \cdot & \\ & & \ddots & \ddots & \ddots & \\ & & & \underline{\mathbf{C}}_{n-1} & \underline{\mathbf{D}}_{n-1} & \underline{\mathbf{E}}_{n_1} \\ & & & & & \underline{\mathbf{D}}_n \end{pmatrix}$$

$\underline{\mathbf{C}}_k$ and $\underline{\mathbf{E}}_k$ are diagonal matrices, however only $\underline{\mathbf{C}}_k$ can be stored in such away to take advantages of this, as $\underline{\mathbf{E}}_k$ is altered during the algorithm in such away that, off diagonal terms are added. $\underline{\mathbf{D}}_k$ is actually a pentadiagonal matrix, which is in essence a 2D problem. In practice the two "Solve" statements in figure 2.2 are done together by Gaussian elimination and back substitution as $\underline{\mathbf{M}}_1$ has no special structure.

Even with this algorithm, which saves memory, more memory is required than any of the other methods discussed in this chapter. But it will solve mildly realistic problems even if it does take a long time. The major advantages of this method being:-

1. No matter how complex the problem it will take the same time to produce the solution.
2. No initial conditions are needed.

If the only purpose of the method were to model potentials produced from current sources with a complex resistivity distribution then this might be a technique to consider. The second advantage is a drawback in our problems considering the *a priori* knowledge, which takes the form of a good initial condition (starting point).

2.3 Iterative methods

This section investigates and develops three stationary iterative methods. These methods can be explained using equation 1.1 but are intuitively explained using a stencil, see figure 2.3. The 'iterative' part of the methods is based around a Gauss-Seidel method, which we call point iteration, and is the first of the methods which will be discussed. The other two techniques, line iteration and panel iteration, are forms of composite methods.

The idea behind using a composite method is to reduce the number of iterations. The drawback is that each iteration is computationally more expensive.

Both methods are a cross between point iteration and complete inversion. The iterative part is not a value but a vector (a line or plane of points in the grid).

2.3.1 Point iteration

Point iteration is a variant on the Gauss-Seidel method. Both methods work by using the potential value at the nodes and calculate a weighted mean, where the weights are the conductances (which are calculated from the resistivity values and the mesh size). This updates the potential value in $\mathbf{x}$, so that when the neighbouring nodes are calculated it use the new value from the previous node.

Like all iterative methods of this type there exists a stencil. This is shown in figure 2.3. These stencils can show update in both space and time but as this is a steady state problem the time element can be ignored. The central node in updated using the values of the surrounding nodes and the associated conductance values.

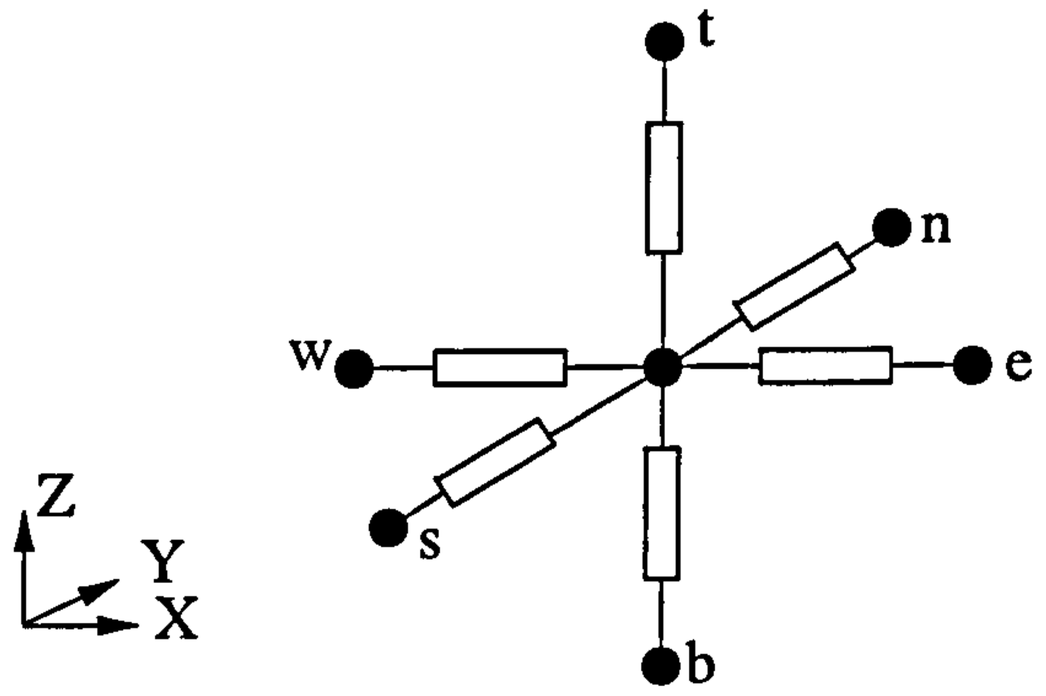

Figure 2.3: Point iteration stencil.

The equation for Gauss-Seidel is

$$x_i^{(k+1)} = \frac{b_i - \sum_{j<i} a_{i,j} x_j^{(k+1)} - \sum_{j>i} a_{i,j} x_j^{(k)}}{a_{i,i}} \tag{2.2}$$

The disadvantage of the Gauss-Seidel method is the need for a floating point division for every node in the grid. This is a very time consuming operation compared with floating pointing addition and multiplication. The equation for point iteration is

$$x_i^{(k+1)} = \left(\frac{b_i}{a_{i,i}}\right) - \sum_{j<i} \left(\frac{a_{i,j}}{a_{i,i}}\right) x_j^{(k+1)} - \sum_{j>i} \left(\frac{a_{i,j}}{a_{i,i}}\right) x_j^{(k)} \tag{2.3}$$

As can be seen, the two methods are equivalent except that in point iteration the values of $\left(\frac{a_{i,j}}{a_{i,i}}\right)$ and $\left(\frac{b_i}{a_{i,i}}\right)$ are calculated prior to the start of the iterations. The effect of this is that the same number of variables are being stored without any

floating point division in the iterations. This makes a very considerable difference to the speed of each iterative step, which is not only because we perform one fewer operation, but also because floating point division is much slower than multiplication. If $\frac{1}{a_{i,i}}$ is multiplied instead the method is then roughly 5% slower and takes up more space in the memory.

The following is relevant for all similar iterative methods, which have a direction of the iteration. Point iteration updates $\mathbf{x}$ as it goes through an iteration, which means it solves faster in some directions, namely the direction of the iteration. This can be used as an advantage by setting up the method so that it iterates from one corner, then iterates from another corner and so on until all corners have been iterated. Therefore, a single "iteration" commences from each of the corners in turn of the 3D grid, thus iterating through the grid eight times. This method was implemented and seems to work very well. There is a second improvement, which is to use more knowledge about the problem being solved. In this case, we know that there is a point current source, therefore if all calculations are started from the current source and radiate outwards, the result of the previous calculation can be utilised in next calculation, thereby increasing efficiency. This has not been implemented due to the complexity of ensuring that the calculations are carried out in the correct sequence within the rectangular grid, putting it outside the scope of this work.

2.3.2 Line iteration

This algorithm was described by Reece [1986]. The method works by solving each line of nodes as a one dimensional problem. The solutions of the lines have a 2D point iteration applied to them. This process is shown in figure 2.4.

Figure 2.4 gives the pseudo-code of the line iteration implemented. There is a moderation to the original version in that the method starts by directly solving all the lines. This allows the first iterative part of the method to be more efficient as it iterates away from a line of nodes (in the case of a point source) rather than starting with a point. The code for this can be found on the CD ROM (with the main components of the algorithm being found in procedure 'solve' and its subprocedures).

This method, like point iteration has a direction of iteration. Unlike point iteration there are 4 different directions for the iteration of any particular line being solved. The four directions come from starting at each of the four corners of a rectangle where each point represents a directly solved line of nodes. The direction of the line being solved can be rotated to two other directions. However, in practice

```
Choose a direction, in this case k which is p nodes long,
with the other two directions being i with m nodes and
j with n nodes

        for i = 1, 2, ..., m
                for j = 1, 2, ..., n
                        Solve for all lines in i
                end
        end
        While error > max. error then
                for k = 1, 2, ..., p
                        for i = 1, 2, ..., m
                                for j = 1, 2, ..., n
                                        Point Iterate in j k plane
                                end
                        end
                        for j = 1, 2, ..., n
                                Solve for all lines in i
                        end
                end
                Calculate error
        end
```

Figure 2.4: Method for line iteration

the implementation which has been used for calculating the results in chapter 3 uses half of these, excluding the reverse directions. An improvement to this would be to use the same suggestion put forward at the end of section 2.3.1, i.e. starting from the current source[5]. This could work by taking the two directions of the point iteration and solving the lines in the same direction. A second improvement would be to solve the lines through the source and radiate from these lines.

[5]This is consistent with the recommendations in Reece [1986] to work from high values to low ones, thereby achieving much more rapid convergence.

2.3.3 Panel iteration

This algorithm was developed to take advantage of the complete inversion method. It is very similar to line iteration except that instead of solving lines of nodes this method solves panels (planes) of nodes, which by their very nature are 2D, with point iteration applied to the third direction. This is a very similar to line iteration in that it involves a 2-step process. This can be seen by comparing figure 2.5 with figure 2.4.

Choose a direction, in this case k which is p nodes long, with the other two direction being i with m nodes and j with n nodes

```
for i = 1, 2, ..., m
        Solve for all j − k planes
end
While error > max. error then
    for k = 1, 2, ..., p
        for i = 1, 2, ..., m
            for j = 1, 2, ..., n
                Point Iterate in i lines
            end
        end
        Solve for all j − k planes
    end
    Calculate error
end
```

Figure 2.5: Method for panel iteration

This method, like point iteration (and line iteration) has a direction of iteration, except there are only 2 different directions to be iterated in for each particular orientation of the panels. The method can be improved by using the source optimisation method described briefly at the end of section 2.3.1.

No rotation of the direction of iteration has been attempted, although this may be possible. The main reason was the practicalities of implementation, namely the requirement of either twice or three times as much memory and/or a lot of book keeping.

2.4 Conjugate gradient methods

This section investigates two non-stationary iterative methods, conjugate gradients and one of its variants GMRES. Conjugate gradients, and its variants, are widely discussed in the numerical analysis literature, Golub & Van Loan [1988], Barrett et al. [1994]. These methods are widely used in various computationally intensive linear algebra problems which solve equation 1.1, for example, in the field of computational fluid dynamics. However, these methods are not so widely used in ERT, although they are discussed in Spitzer & Wurmstich [1995] and Zhang et al. [1995].

The conjugate gradient method will only converge if the $\underline{\mathbf{A}}$ matrix is symmetric[6] positive[7] definite[8]. Unfortunately, in general, $\underline{\mathbf{A}}$ is not a symmetric matrix, although it is always positive definite due to the physical constraints of the problem. Both Spitzer & Wurmstich [1995] and Barrett et al. [1994], contain comparisons of the conjugate gradient methods, and its variants, from which a variant was sought. It should be noted that Spitzer & Wurmstich [1995] also found that it was not possible to use the basic conjugate gradient method for solving only homogeneous forward problems[9].

The variant chosen was GMRES[10] since it has no requirement for $\underline{\mathbf{A}}$ to be a symmetric matrix.

The GMRES method has a few drawbacks. These are mainly concentrated on the amount of memory needed. Not only does $\underline{\mathbf{A}}$ have to be stored but so do the results of at least the last five iterations. This method is not totally guaranteed to converge[11], and was never coded up and tested.

So far in this section we have looked at finding a method to solve unsymmetric $\underline{\mathbf{A}}$. However, since the basic conjugate gradient method is very efficient it would therefore be preferable to use a matrix which is symmetric. Hence, a method to convert $\underline{\mathbf{A}}$ into a symmetric matrix is required. Let us consider the 1D case.

---

[6] Symmetric is when the matrix is its own mirror image in the leading diagonal, i.e. $a_{i,j} = a_{j,i}$.

[7] Positive is when all the eigenvalues are positive.

[8] Definite is when all the eigenvalues are non zero.

[9] It was found that it also had to be on a uniform grid.

[10] Choice of GMRES confirmed in a private communication with Andy Wathen

[11] Convergence is only guaranteed to if the results of n iterations can be stored, where n is the number of rows in $\underline{\mathbf{A}}$.

If $\mathbf{A} \epsilon \Re^{\mathbf{n \times n}}$ is a positive definite and $\mathbf{b} \epsilon \Re^{\mathbf{n}}$ and solve $\mathbf{Ax} = \mathbf{b}$ for $\mathbf{x} \epsilon \Re^{\mathbf{n}}$

$\mathbf{x^{(0)}}$ is an initial guess

For $j = 1, 2, ...$

Solve $\mathbf{r}$ from $\underline{\mathbf{M}}\mathbf{r} = \mathbf{b} - \underline{\mathbf{A}}\mathbf{x^{(0)}}$

$\mathbf{v^{(1)}} = \frac{\mathbf{r}}{\|\mathbf{r}\|_2}$

$\mathbf{s} := \|\mathbf{r}\|_2 \mathbf{e_1}$

for $i = 1, 2, ..., m$

Solve w from $\underline{\mathbf{M}}\mathbf{r} = \mathbf{b} - \underline{\mathbf{A}}\mathbf{v^{(i)}}$

for $j = 1, 2, ..., i$

$h_{k,i} = \left(w, \mathbf{v^{(i)}}\right)$

$\mathbf{w} = \mathbf{w} - \mathbf{h_{k,i}} \mathbf{v^{(i)}}$

end

$h_{i+1,i} = \|\mathbf{w}\|_2$

$\mathbf{v^{(i+1)}} = \frac{\mathbf{w}}{\mathbf{h_{i+1,i}}}$

apply $J_1, ..., J_{i-1}$ on $(h_{1,i}, ..., h_{i+1,i})$

construct J_i, acting on ith and $(i+1)$st component of $h_{.,i}$ such that $(i+1)$st of $J_i h_{.,i}$ is 0

$s := J_i s$

if $s(i+1)$ is small enough then

(UPDATE(x,i) and quit)

end

UPDATE(x,i)

check convergence; continue if necessary

end

Figure 2.6: Method for generalised minimal residual

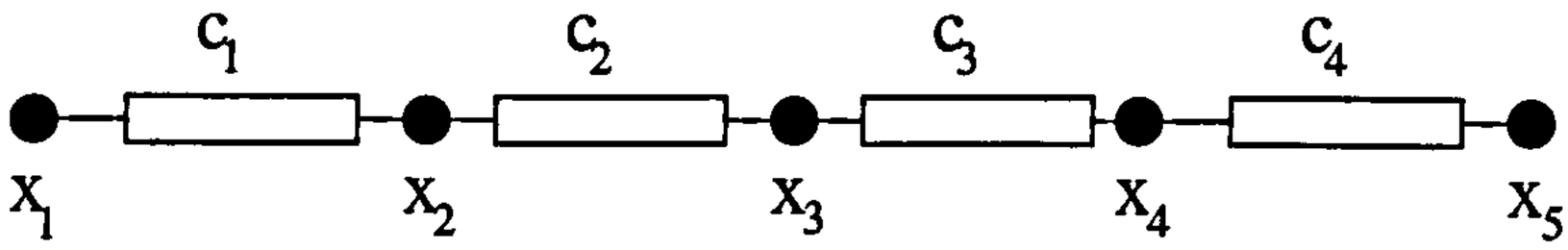

Figure 2.7: 1D forward problem with five nodes.

In this case $\underline{\mathbf{A}}$ would look like

$$\underline{\mathbf{A}} = \begin{pmatrix} 1 & 0 & 0 & 0 & 0 \\ \frac{c_1}{c_1+c_2} & 1 & \frac{c_2}{c_1+c_2} & 0 & 0 \\ 0 & \frac{c_2}{c_2+c_3} & 1 & \frac{c_3}{c_2+c_3} & 0 \\ 0 & 0 & \frac{c_3}{c_3+c_4} & 1 & \frac{c_4}{c_3+c_4} \\ 0 & 0 & 0 & 0 & 1 \end{pmatrix} \tag{2.4}$$

The reason for choosing such a large problem is to display an internal node. A diagonal matrix $\underline{\mathbf{S}}$ is chosen such that

$$\underline{\mathbf{S}}\,\underline{\mathbf{A}} = \begin{pmatrix} 1 & 0 & 0 & 0 & 0 \\ c_1 & (c_1+c_2) & c_2 & 0 & 0 \\ 0 & c_2 & (c_2+c_3) & c_3 & 0 \\ 0 & 0 & c_3 & (c_3+c_4) & c_4 \\ 0 & 0 & 0 & 0 & 1 \end{pmatrix} \tag{2.5}$$

$\underline{\mathbf{S}}$ is the leading diagonal of the matrix shown above. It can be seen that $\underline{\mathbf{S}}\,\underline{\mathbf{A}}$ is very nearly a symmetric matrix and the conjugate gradient method may solve the above problem but it is not guaranteed.

It is possible to perform column operations on $\underline{\mathbf{SA}}$, which are contained in a matrix $\underline{\mathbf{S}}$, so that

$$\underline{\mathbf{P}}\,\underline{\mathbf{S}}\,\underline{\mathbf{A}} = \begin{pmatrix} 1 & c_1 & 0 & 0 & 0 \\ c_1 & (c_1^2+c_1+c_2) & c_2 & 0 & 0 \\ 0 & c_2 & (c_2+c_3) & c_3 & 0 \\ 0 & 0 & c_3 & (c_3+c_4+c_4^2) & c_4 \\ 0 & 0 & 0 & c_4 & 1 \end{pmatrix} \tag{2.6}$$

Now this is a symmetric matrix. But we wish to solve $\underline{\mathbf{A}}\mathbf{x} = \mathbf{b}$, which is the same as solving

$$\underline{\mathbf{P}}\,\underline{\mathbf{S}}\,\underline{\mathbf{A}}\mathbf{x} = \underline{\mathbf{P}}\,\underline{\mathbf{S}}\mathbf{b} \tag{2.7}$$

The matrices $\underline{\mathbf{P}}$ and $\underline{\mathbf{S}}$ cannot be singular. This is because as $\underline{\mathbf{S}}$ is a diagonal matrix and $\underline{\mathbf{P}}$ is an identity matrix plus two off - diagonal elements. In general, there is

the same number of off diagonal terms as there are boundary nodes in the original forward problem. In practice these extra matrix multiplications should have little effect on the time taken to carry out the calculations. This method will only work for specific problems. There are various limitations on the above technique, e.g. the resistivity from east to west must be the same as from west to east, i.e. not like a diode.

If $\mathbf{A} \epsilon \Re^{\mathbf{n} \times \mathbf{n}}$ is a symmetric positive definite and $\mathbf{b} \epsilon \Re^{\mathbf{n}}$ and solve $\underline{\mathbf{A}}\mathbf{x} = \mathbf{b}$ for $\mathbf{x} \epsilon \Re^{\mathbf{n}}$

needs correcting

$k = 0$

$\mathbf{x_0} = \mathbf{0}$ or an initial start position

$\mathbf{r_0} = \mathbf{b}$

While $\mathbf{r_k} \neq \mathbf{0}$

$k = k + 1$

if $k = 1$

$\mathbf{p_1} = \mathbf{r_0}$

else

$\beta_k = \frac{\mathbf{r_{k-1}^T r_{k-1}}}{\mathbf{r_{k-2}^T r_{k-2}}}$

$\mathbf{p_k} = \mathbf{r_{k-1}} + \beta \mathbf{p_{k-1}}$

end

$\alpha = \frac{\mathbf{r_{k-1}^T r_{k-1}}}{\mathbf{p_k^T A r_k}}$

$\mathbf{x_k} = \mathbf{x_{k-1}} + \alpha \mathbf{p_k}$

$\mathbf{p_k} = \mathbf{r_{k-1}} - \alpha \mathbf{A p_k}$

end

$\mathbf{x} = \mathbf{x_k}$

Figure 2.8: Method for conjugate gradients

The algorithm for the conjugate gradient technique without the matrix manipulation is given at figure 2.8. This is not a practical algorithm as it stands, as $\mathbf{r_k}$ will never reach zero in a numerical calculation. Therefore another criterion must be chosen, e.g. $\mathbf{r}.\mathbf{r}$ becoming less than a certain value, as was used in this case. In figure 2.8, $\mathbf{r_*}$ and $\mathbf{p_*}$ are vectors which are updated during each iteration. Both α and β are constants calculated during each iteration.

Chapter 3

Results of Methods for Solving the Forward Problem

3.1 Introduction

This chapter displays and discusses the results of the numerical techniques given in chapter 2. There has been a lot of work done on the conjugate gradient method including a little in applying the technique to ERS (Spitzer & Wurmstich [1995], Zhang et al. [1995]). Point iteration ought to exhibit similar properties to Gauss - Seidel. Line iteration has been used before in this field e.g. Williams [1996], Jackson, Busby, Meldrum & Reece [1988] & Jackson, Earl & Reece [1997], but there is little work on its behaviour. During this chapter two attributes of the methods will be discussed.

The first is the speed (efficiency) of the methods and in particular the impact of the size and shape[1] of the grid. This follows a 'well trodden' path for measuring the speed of a method and the memory space required. In general, ERS do not use uniform grids of homogeneous resistivity distributions. The grid uniformity and the resistivity distribution are connected in that both are needed to produce the conductances (in the conjugate gradient method) or relative conductances (the other methods) contained in the $\underline{A}$ matrix. Speed is important to the solution of the inverse problem because all the measurements are calculated during each iteration. This involves solving many heterogeneous forward problems.

The second depends on the starting point $\mathbf{x_0}$, particularly when it is

[1]Shape refers to the ratio of number of nodes in each direction rather than the actual physical dimensions.

close to the solution. This is of interest to the perturbation method[2] for calculating the Jacobian, where forward problems are solved numerous times, starting from a position very close to the solution.

The issue of convergence, which is important when considering all numerical methods, is less of a problem in solving this forward problem since the methods are unconditionally convergent. However, the speed of conversion can be slow for some methods as will be seen in section 3.2.

All the timings in this chapter where produced using a 90Mhz Pentium PC. The code used can be found on the CD ROM and is written in C. Each timing refers to the time taken for just the calculation using the algorithm. All of the methods use the same basic setup files but the complete inversion and the conjugate gradient methods store the $\underline{\mathbf{A}}$ matrix in different ways to the other methods.

3.2 Results on speed of the methods

This section presents the results of a number of numerical experiments run on the methods discussed in chapter 2. These experiments come in two forms, the first deals with the issue of size and shape of the grid, and the second with the effect of resistivity distribution. The results of both forms of experiments are intended to be the basis for choosing which particular method should be used for particular problems.

However, before discussing the results of the size and shape experiments, the task set for each method, for the purposes of comparison, needs to be explained. The task set had to be symmetric in all directions so as to eliminate the effect of rotation i.e. if the number of nodes in each direction differed then if the task was rotated in any way this may effect the time taken to complete the task, which would not be attributable to the method used. Thus making a level playing field. This meant that the type of boundaries used had to be the same and the source term symmetric. Therefore, within such constraints there were two possiblies, namely, to have a point source in the centre of a 3D cube or to have an uniform source term over the whole cube. The latter was chosen, since the former needed a node centred on the centre of the cube which only occurs when there is an odd number of nodes in each direction[3]. This constraint would reduce the number of data points which

[2]See section 6.3.1 for details of the perturbation method

[3]This need to have a node at a the location of a point source is a major constraint on the grids used to model the surveys.

could be collected. In the task set the grid cells were uniform i.e. identical to all the other cells in the task. The conductivity was set a at $1W/mK$ and the uniform source was set at 100 Joules per m^3. The size of the cube was set at $1m^3$. The boundaries were Dirichet and set at zero, whilst initially all nodes were zero[4].

The size of any grid should give a clear indication of how long a forward problem should take to solve. Although a number of other factor which are explored in this section and section 3.3 also have an effect. However for the complete inversion method the time to produce the solution is only dependent on the number of nodes in each direction. For the other techniques there is also the question of the convergence criteria. As it happens the conjugate gradient method has a built in convergence criterion, but the other methods require a convergence criterion to be defined. The one chosen resembles the one in conjugate gradients. The criterion being the sum of the modulus of the change in each potential value, divided by the number of nodes, being less than 10^{-6}.

Given the above, the speed of all methods will be dependent on the size of the task set. As such it should be possible to predict the time taken to solve a particular problem on a particular computer. Leaving aside the factor relating to the using a different machine, the time taken will be proportional to the number of nodes in each direction. Therefore

$$t = k.x^a.y^b.z^c \tag{3.1}$$

and for the case where there are equal number of nodes in all directions then

$$t = k.x^a.y^b.z^c = k.n^d \tag{3.2}$$

where $x = y = z = n$ and $d = a + b + c$. x, y and z are the number of nodes in each direction and n is the number of nodes in one direction. All results ignore the time to setup the arrays containing all the conductances, sources and initial conditions.

The first of the methods tested is the complete inversion method. This method is completely dependent on the size and shape of the grid. Therefore the results here apply to any combination of sources and all realistic resistivity distributions.

The logarithmic version of figure 3.1 is in appendix B.1 in figure B.1 which shows that as the number nodes increases the time taken tends to

[4]The problem being modelled is a heat conduction problem and the units of "zero" is in Kelvin but the value is better considered as the value in Kelvin minus the initial value.

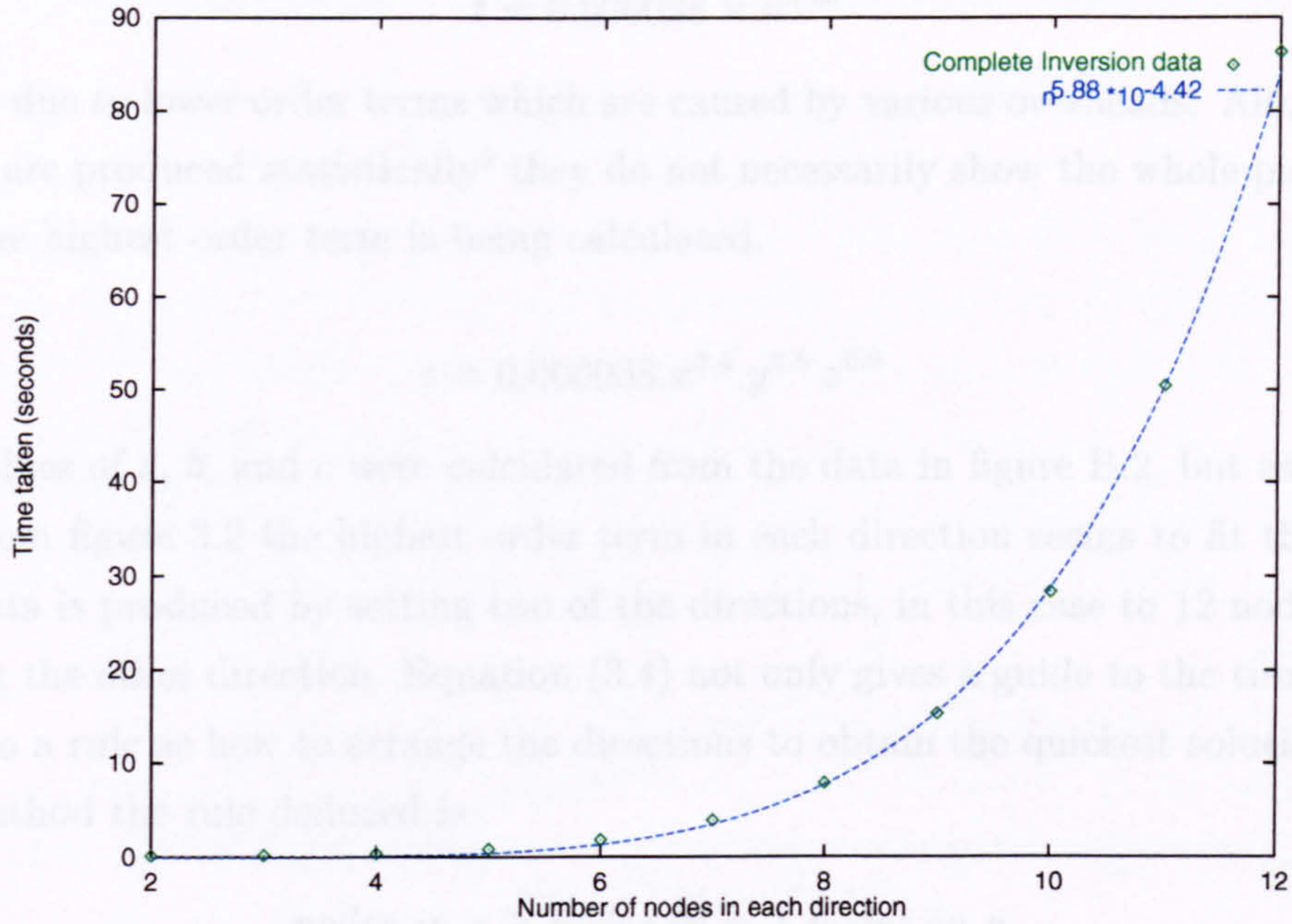

Figure 3.1: Time taken against number of nodes in each direction of a cube, for complete inversion.

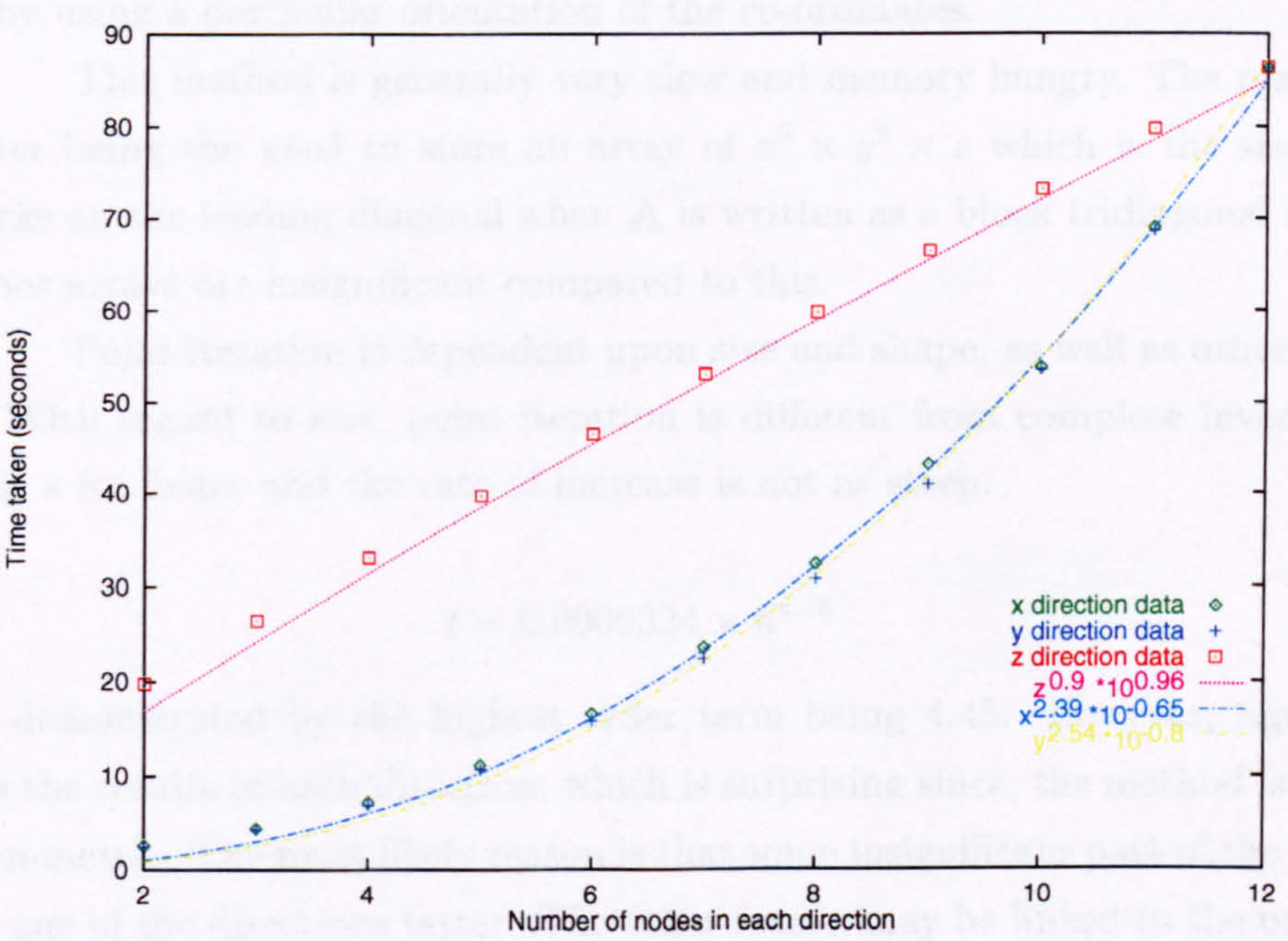

Figure 3.2: Time taken against number of nodes in one of the direction with 12 nodes in both of the others, for complete inversion.

$$t = 0.000038 \times n^{5.88} \tag{3.3}$$

This is due to lower order terms which are caused by various overheads. Also, as the values are produced statistically[5] they do not necessarily show the whole picture as only the highest order term is being calculated.

$$t = 0.000038.x^{2.4}.y^{2.5}.z^{0.9} \tag{3.4}$$

The values of a, b, and c were calculated from the data in figure B.2, but as can be seen from figure 3.2 the highest order term in each direction seems to fit the data. The data is produced by setting two of the directions, in this case to 12 nodes, and varying the other direction. Equation (3.4) not only gives a guide to the time taken but also a rule as how to arrange the directions to obtain the quickest solution. For this method the rule deduced is

$$nodes\ in\ z \geq nodes\ in\ x \geq nodes\ in\ y$$

It should be noted that this due to the way in which this method was set up i.e. the direction in which Buzbee's method has been used, but the method will solve better by using a particular orientation of the co-ordinates.

This method is generally very slow and memory hungry. The reason for the latter being the need to store an array of $x^2 \times y^2 \times z$ which is the size of all the blocks on the leading diagonal when $\underline{\underline{A}}$ is written as a block tridiagonal matrix. The other arrays are insignificant compared to this.

Point iteration is dependent upon size and shape, as well as others properties. With regard to size, point iteration is different from complete inversion in that it is a lot faster and the rate of increase is not as steep.

$$t = 0.0000324 \times n^{4.48} \tag{3.5}$$

This is demonstrated by the highest order term being 4.48. However, figure 3.4 displays the results at each direction, which is surprising since, the method is meant to be symmetric. The most likely reason is that some insignificant part of the coding making one of the directions faster. The other reason may be linked to the ordering of the changes in direction. In figure 3.4 the lines do not intersect the points and actually full below them. They do intersect if a constant is added. The reason for this is that the method seems to have some large lower order terms which can be

[5]Regression lines are plotted on log - log plots (the ones shown in appendix B.1).

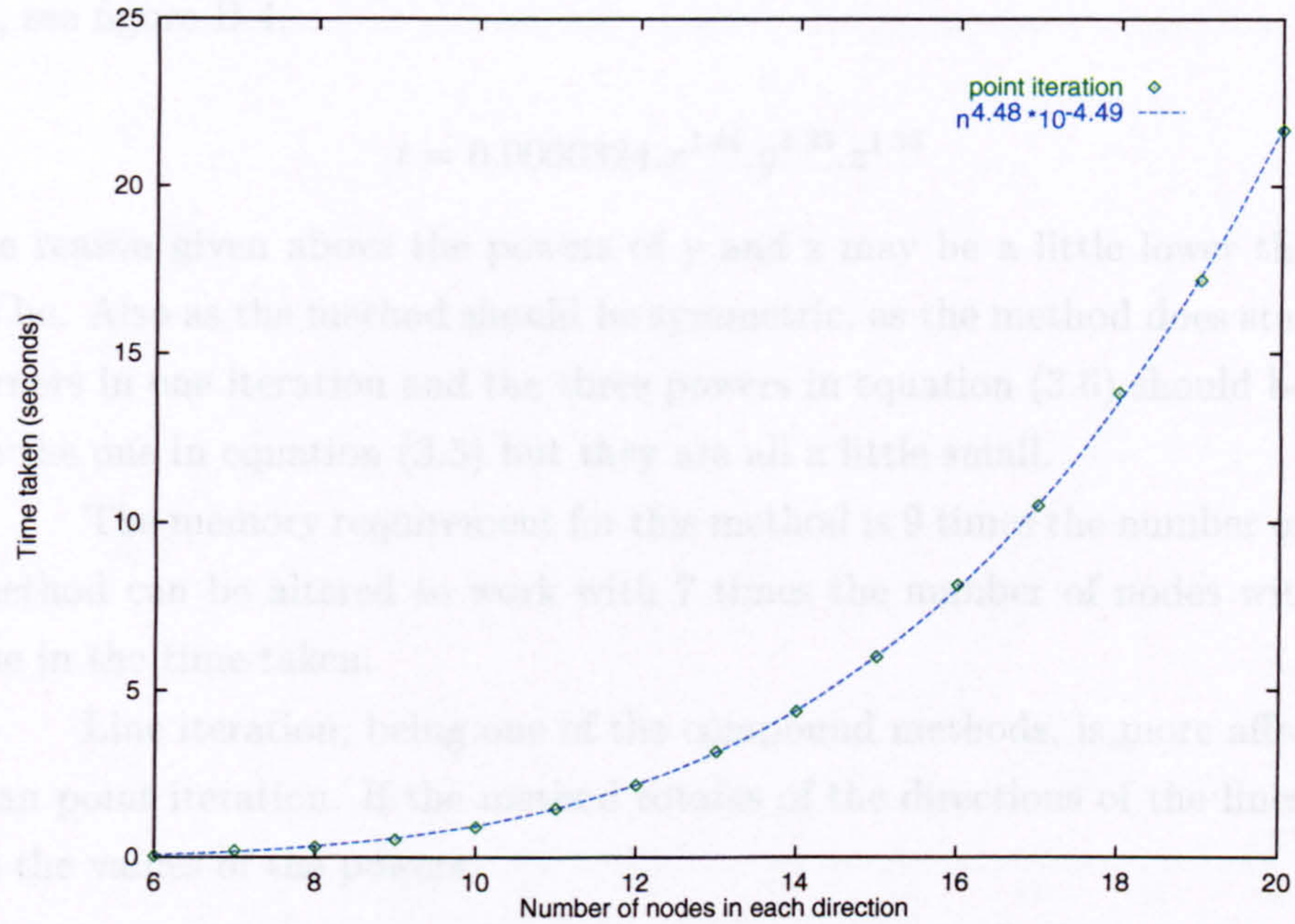

Figure 3.3: Time taken against number of nodes in each direction of a cube, for point iteration.

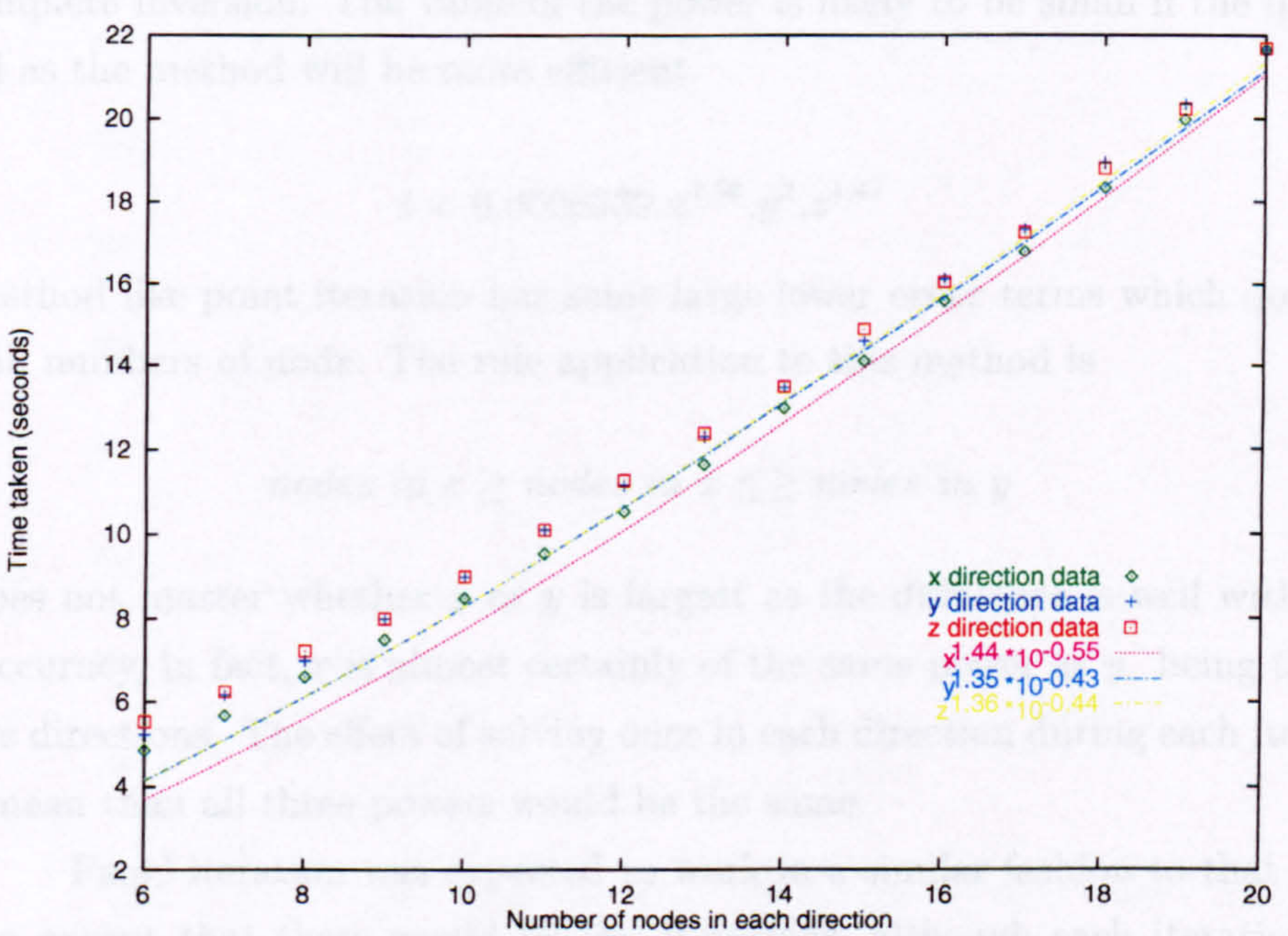

Figure 3.4: Time taken against number of nodes in one of the direction with 12 nodes in both of the others, for point iteration.

seen to have an effect on size of the region in which the regression lines could be drawn, see figure B.4.

$$t = 0.0000324.x^{1.44}.y^{1.35}.z^{1.36} \tag{3.6}$$

For the reason given above the powers of y and z may be a little lower than they should be. Also as the method should be symmetric, as the method does start at all the corners in one iteration and the three powers in equation (3.6) should be added to give the one in equation (3.5) but they are all a little small.

The memory requirement for this method is 9 times the number of nodes. The method can be altered to work with 7 times the number of nodes with a 5% increase in the time taken.

Line iteration, being one of the compound methods, is more affected by size than point iteration. If the method rotates of the directions of the lines would change the values of the powers.

$$t = 0.0000339 \times n^{5.5} \tag{3.7}$$

Equation (3.7) shows that this order of the method is between that of point iteration and complete inversion. The value of the power is likely to be small if the lines are rotated as the method will be more efficient.

$$t = 0.0000339.x^{1.98}.y^{2}.z^{1.47} \tag{3.8}$$

This method like point iteration has some large lower order terms which dominate for small numbers of node. The rule application to this method is

$$nodes\ in\ z \geq nodes\ in\ x \leq\geq nodes\ in\ y$$

as it does not matter whether x or y is largest as the difference is well within the order accuracy, in fact, x is almost certainly of the same power as y. being the two iterative directions. The effect of solving once in each direction during each iteration would mean than all three powers would be the same.

Panel iteration was expected to work in a similar fashion to that of line iteration except that there would be less iterations, although each iteration may take a little longer. The actual values of the time taken are less than those of line iteration.

$$t = 0.00001 \times n^{5.9} \tag{3.9}$$

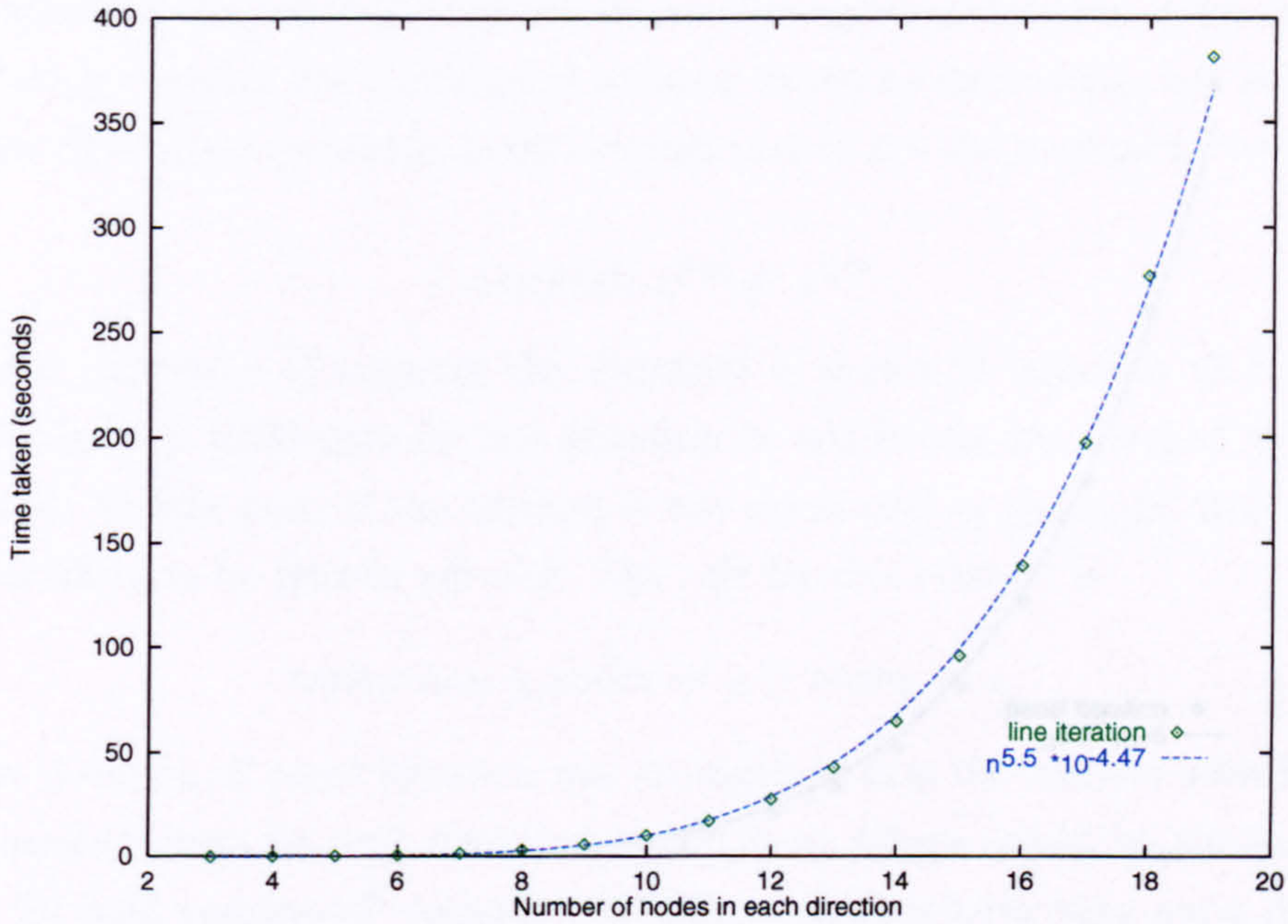

Figure 3.5: Time taken against number of nodes in each direction of a cube, for line iteration.

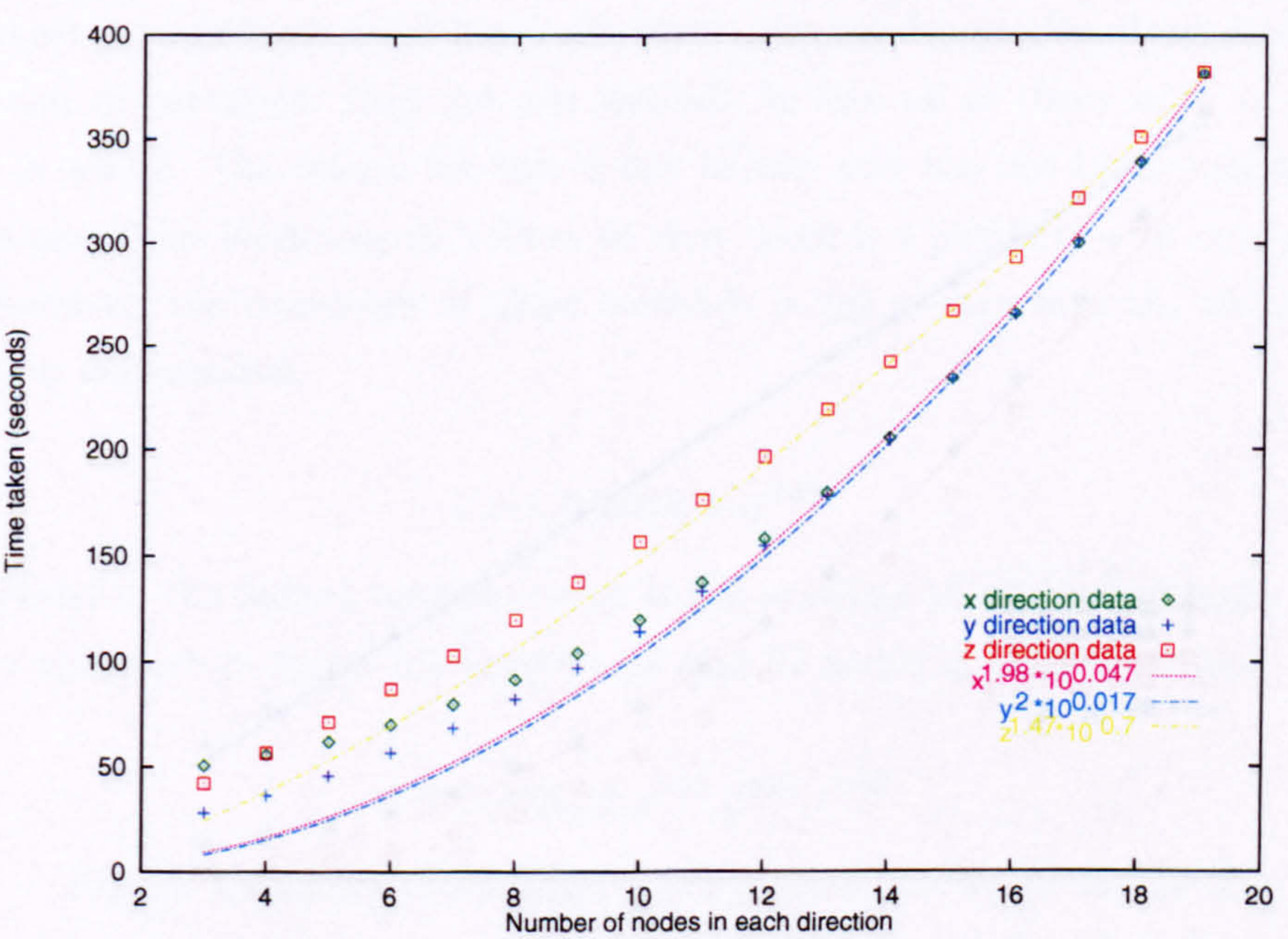

Figure 3.6: Time taken against number of nodes in one of the directions with 12 nodes in both of the others, for line iteration.

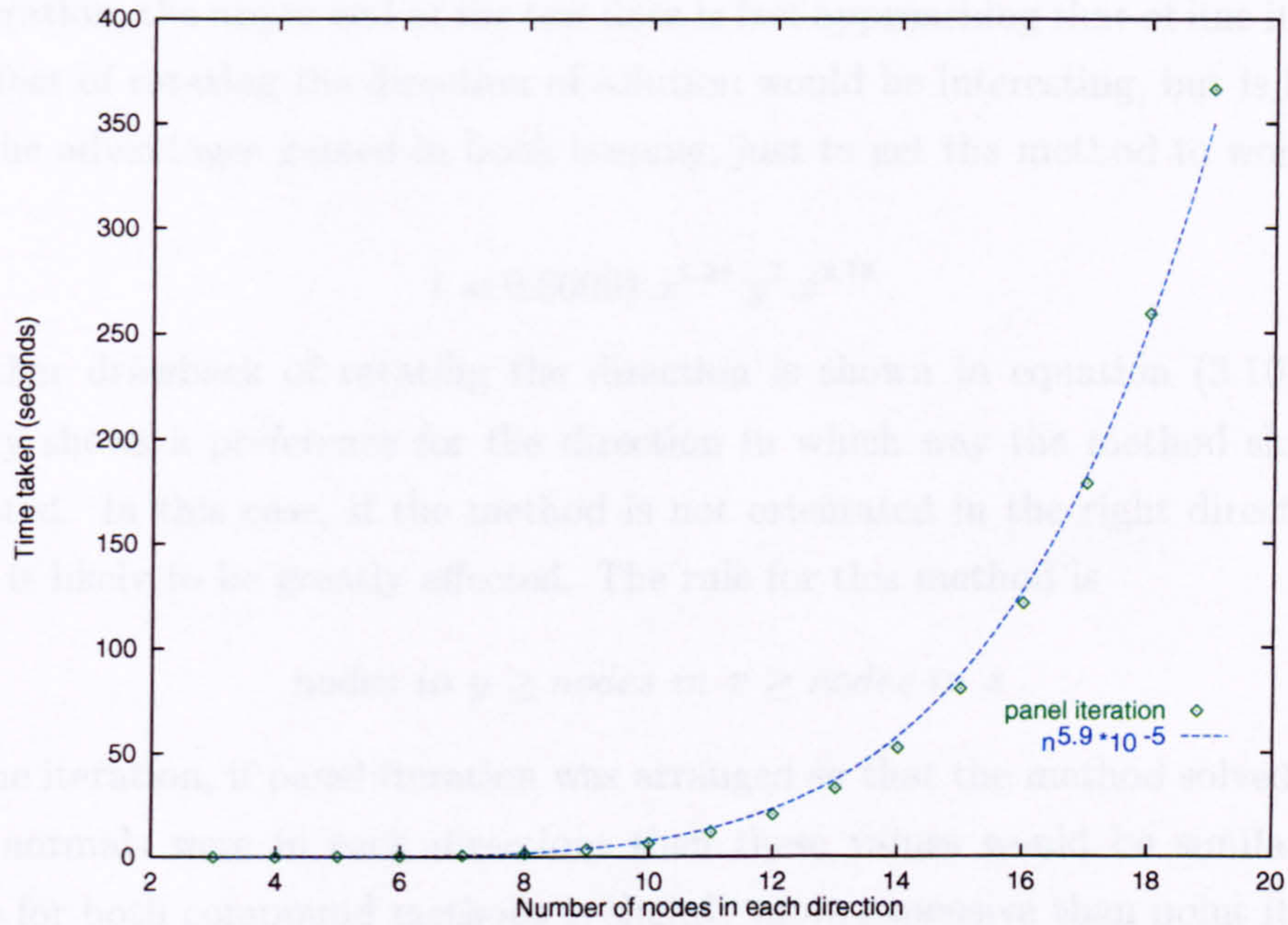

Figure 3.7: Time taken against number of nodes in each direction of a cube, for panel iteration.

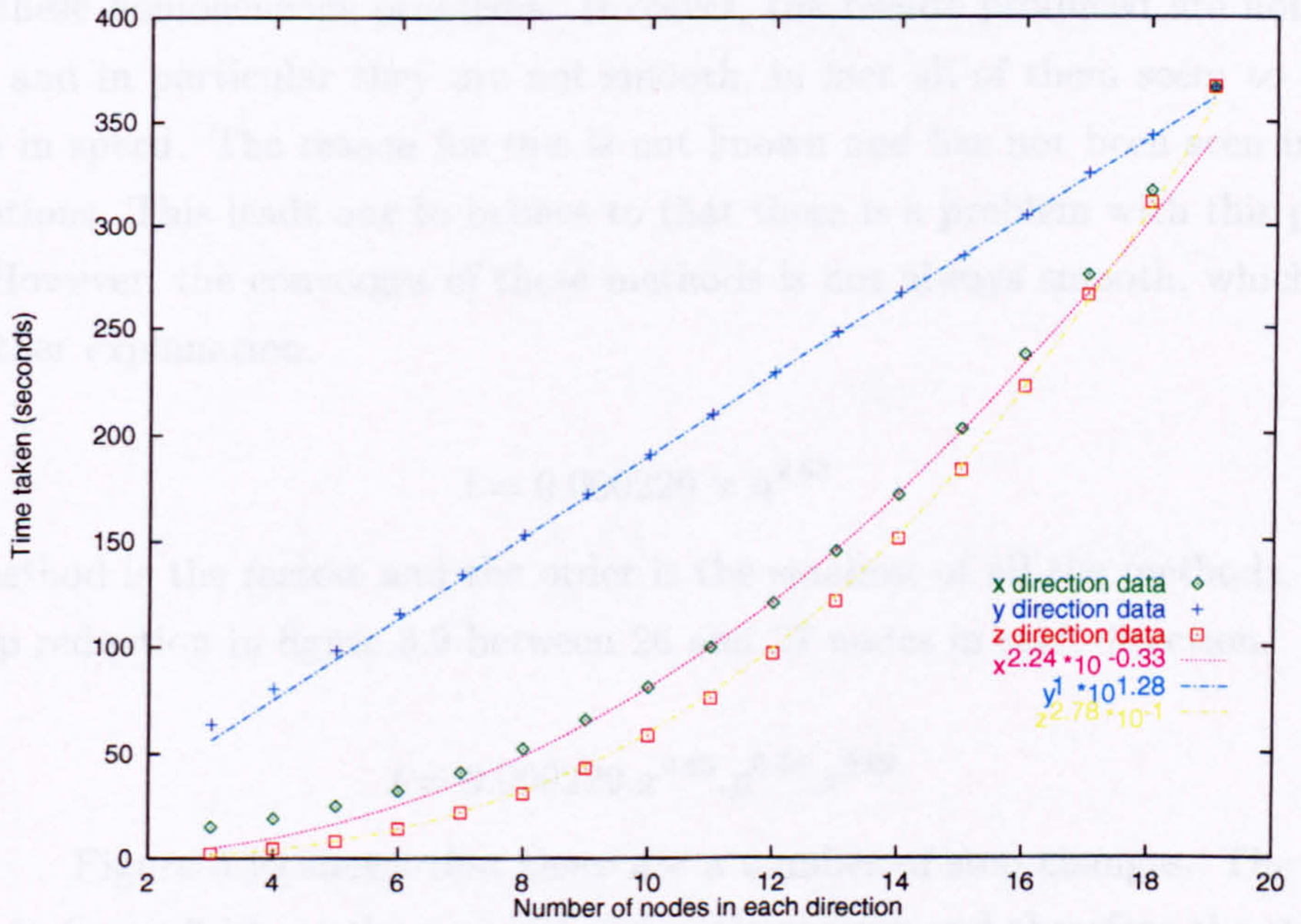

Figure 3.8: Time taken against number of nodes in one of the directions with 12 nodes in both of the others, for panel iteration.

However, this is the highest power of any of the methods and although quicker than line iteration, the upper end of the test data is fast approaching that of line iteration. The effect of rotating the direction of solution would be interesting, but is likely to loose the advantages gained in book keeping, just to get the method to work.

$$t = 0.00001.x^{2.24}.y^{1}.z^{2.78} \tag{3.10}$$

The other drawback of rotating the direction is shown in equation (3.10) which strongly shows a preference for the direction in which way the method should be orientated. In this case, if the method is not orientated in the right direction the timing is likely to be greatly affected. The rule for this method is

$$nodes\ in\ y \geq nodes\ in\ x \geq nodes\ in\ z$$

Like line iteration, if panel iteration was arranged so that the method solved planes whose normals were in each directions then these values would be similar. The storage for both compound methods is slightly more expensive than point iteration due to the arrays needed during calculation.

The conjugate gradient method is a widely used method in other fields and the results of Spitzer & Wurmstich [1995] are an useful guide to how this method solves these homogeneous problems. However, the results produced are not as expected and in particular they are not smooth, in fact all of them seem to exhibit a jump in speed. The reason for this is not known and has not been seen in other publications. This leads one to believe to that there is a problem with this piece of code. However, the converges of these methods is not always smooth, which could be another explanation.

$$t = 0.000229 \times n^{2.63} \tag{3.11}$$

This method is the fastest and the order is the smallest of all the methods. There is a step reduction in figure 3.9 between 26 and 27 nodes in each direction.

$$t = 0.000229.x^{0.65}.y^{0.64}.z^{0.69} \tag{3.12}$$

Figure 3.10 shows that there are a number of step changes. The values plotted in figure 3.10 are the mean of eight calculations and therefore the step is a repeatable result. Equation (3.12) uses the values across the step changes but the lines of data points between the step changes are nearly at the power of 1.

Having looked at the effect of size and shape on the time taken, we now turn to look at the effect (if any) of resistivity. In order to measure the effect, a

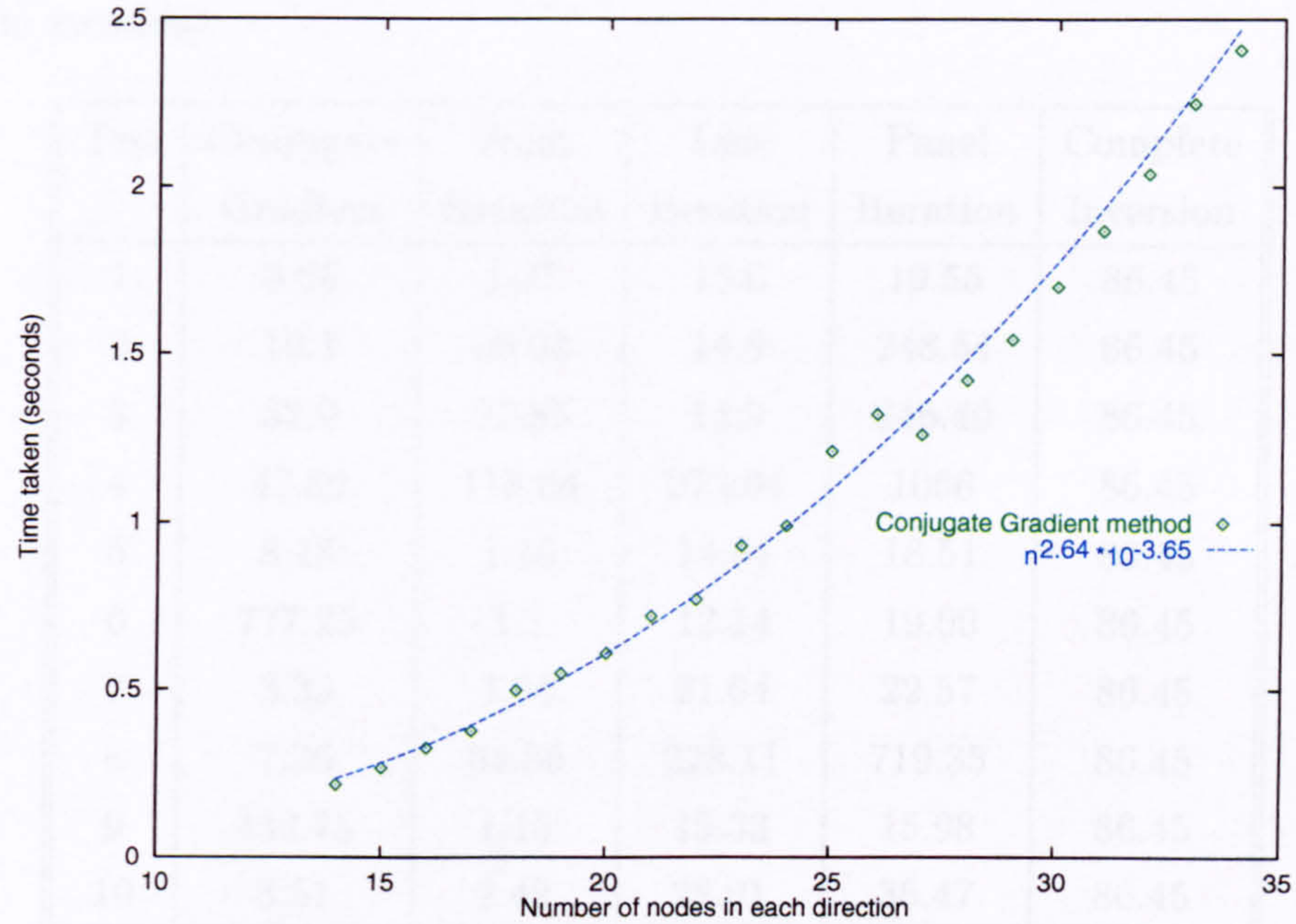

Figure 3.9: Time taken against number of nodes in each direction of a cube, for the conjugate gradient Method.

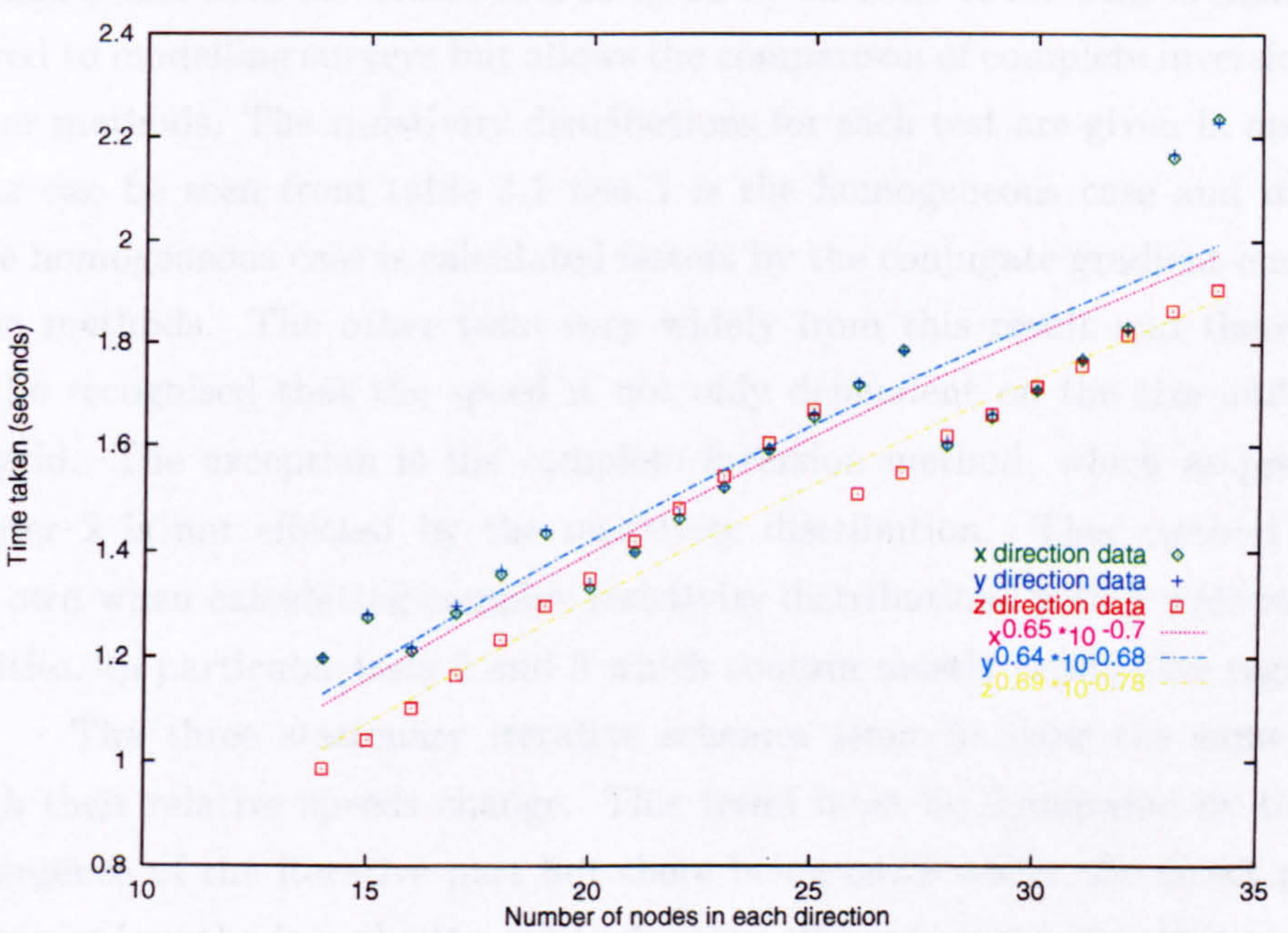

Figure 3.10: Time taken against number of nodes in one of the direction with 12 nodes in both of the others, for the conjugate gradient method.

Table 3.1: Results of various tests of the effect of different resistivity distribution (time in seconds).

Test	Conjugate Gradient	Point Iteration	Line Iteration	Panel Iteration	Complete Inversion
1	0.66	1.27	15.6	19.55	86.45
2	10.1	28.02	14.9	248.54	86.45
3	32.9	27.85	14.9	246.40	86.45
4	42.89	118.04	273.04	1066	86.45
5	8.18	1.16	14.61	18.51	86.45
6	777.25	1.1	12.14	19.00	86.45
7	3.35	1.54	21.04	22.57	86.45
8	7.36	64.86	228.11	719.35	86.45
9	432.75	1.15	15.33	15.98	86.45
10	3.51	2.42	28.01	36.47	86.45

different test task was set, namely a much closer model to that of the ERS, with a source and a sink near the centre of a 12 by 12 by 12 node cube. This is small when compared to modelling surveys but allows the comparison of complete inversion with the other methods. The resistivity distributions for each test are given in appendix B.2. As can be seen from table 3.1 test 1 is the homogeneous case and it shows that the homogeneous case is calculated fastest by the conjugate gradient and point iteration methods. The other tests vary widely from this result and therefore it should be recognised that the speed is not only dependent on the size and shape of the grid. The exception is the complete inversion method, which as predicted in chapter 2 is not effected by the resistivity distribution. This method comes into its own when calculating complex resistivity distributions with a wide range of resistivities. In particular tests 4 and 8 which contain mostly conductive regions.

The three stationary iterative schemes seem to show the same trend although their relative speeds change. This trend must be dominated by the rate of convergence of the iterative part but there being cases where the direct part of the compound methods make the methods more efficient. panel iteration seems to suffer most when there is a slow rate of convergence in the iterative scheme which is almost certainly due to the direct part of each iteration being comparatively time consuming. However, both the compound methods seem to be relatively stable in

the time taken compared with the other two iterative methods. The results for the conjugate gradient method are interesting. There is a huge variation in the time taken. The reasons for this are not obvious except to say it can react very badly to certain distributions.

The heterogeneous resistivity distributions, in most cases, take longer to calculate than the homogeneous case. The most obvious factor that could cause this slow down is the boundary between two regions of resistivity. Let us consider boundaries between two regions, see figure 3.11. If the current is flowing from left to

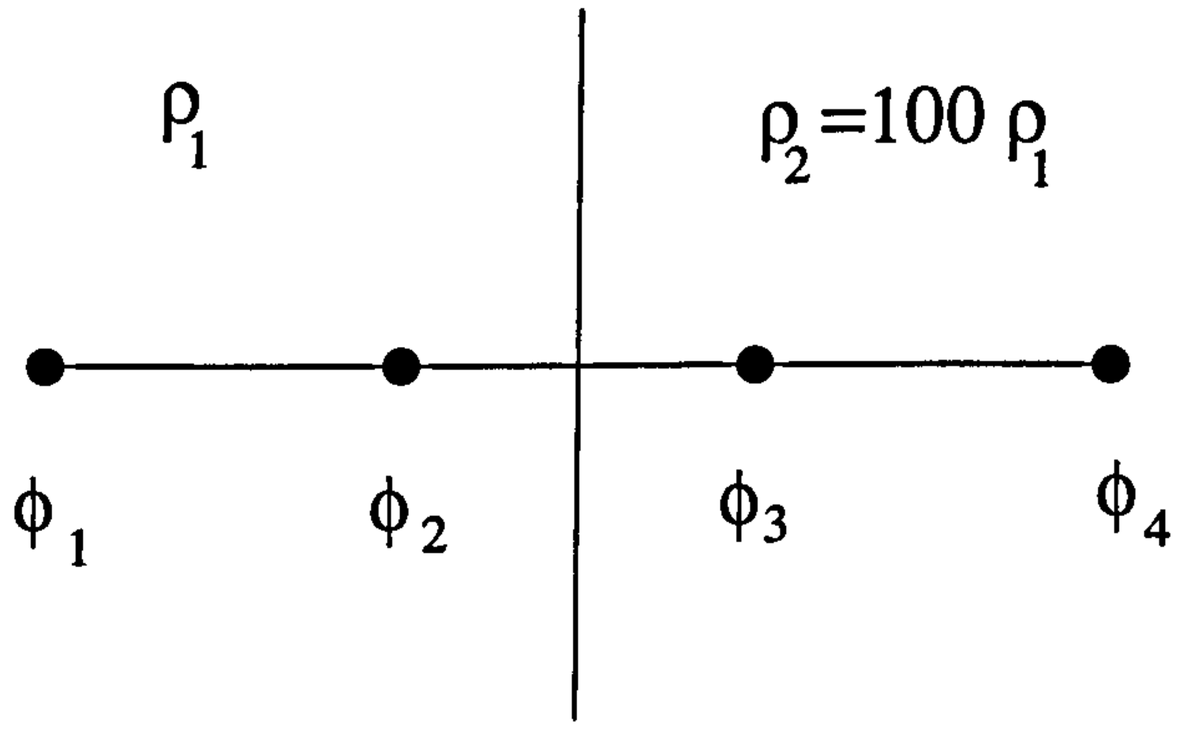

Figure 3.11: Boundary between low resistivity (left hand side) and high resistivity (right hand side).

right it will be fast. This is because the node on the right hand side of the boundary is dominated by the node on the other side of the boundary. The node on left hand side is dominated the nodes in that region and not the node on the other side of the boundary. However, if the current was flowing from right to left then the nodes on both sides of the boundary will be inhibiting the current flow as both the nodes are dependent on the node to which the current is flowing to rather than the node from which the current is flowing.

The nature of point iteration is that at each iteration the current flows away from the source. Therefore if the source is in a resistive material compared to the region to which it is flowing, then the point iteration method will be very slow because of the difference in the resistivity values. It was also noticed that the conjugate gradient method was using very small α values. Referring to figure 2.8, the effect is to make the update of $\mathbf{x_k}$ smaller, thereby making the method slower by reducing the effectiveness of each iteration. The reason that the α value is small that is the denominator is large, in fact, it must be three or four orders of magnitude larger than the modulus of $\mathbf{r_{k-1}}$ (which is not small at the beginning).

The problems caused by boundaries in the resistivity distribution also

extend to the iterative directions of the two compound methods. However, the solving directions break down these barriers so that the current flows in the same way as it would in the field but is immediately is spread across the boundary so that the iterative is useful and the fast areas can be utilised.

This hypothesis has not been proven but is useful in showing why test 8 takes so long for all the iterative schemes. Test 8 consists of a very conductive plate being put between the electrodes and is in the iterative directions of both the compound methods. This hypothesis would also explain the reason why the methods take larger to converge when the sizes of the grid cells are increased around the boundaries of the surveys. The increase in size of the grid cell is analogous to reducing the resistivity value in those cells.

3.3 The effect of the initial conditions

This section investigates the how three of the methods perform calculations analogous to those which are used to calculate the perturbation method Jacobian[6]. As far as the forward problem is concerned, the initial condition is the solution of the forward problem before the resistivity of one of the zones is perturbed. The perturbation tends to be very small. There are two reasons for this, the first is it improves the accuracy of the method, and the second is that it is quicker to calculate. However, the perturbation cannot be too small otherwise the volume becomes effected by machine accuracy.

The three methods chosen were point iteration, line iteration and panel iteration. There is little point in using the complete inversion method as it does not use an initial condition and therefore throws away a very important piece of information, since its starting point is always in the neighbourhood of the solution. The conjugate gradient method was not included but there is very little reason to suppose that it would not produce similar results to the other iterative methods.

The resistivities for each test number are the same as those in the previous section with a zone within the grid having its resistivity value increased by one percent. These perturbations are defined in appendix B.3. Even far from the perturbed zone, the effect of the perturbations is not in doubt, although it can be very small: the task is obviously related to the size of the change to the particular zone. The effect of these perturbations even far from the zone is not in doubt but can be very small as seen in chapter 7. The time taken is obviously related to the

[6]The perturbation method Jacobian is defined in section 6.3.1

Table 3.2: Results of starting close to the solution.

Test	Point Iteration	Line Iteration	Panel Iteration
1	0.33	0.83	2.09
2	0.06	0.21	1.04
3	0.88	10.22	12.85
4	0.17	0.33	1.04
5	0.17	0.33	0.98
6	0.17	0.49	1.04
7	0.05	0.33	0.99
8	0.72	11.09	12.85
9	1.04	4.06	7.25
10	0.33	2.03	3.63

effect of the change.

The values given in the table 3.2 below are in seconds. Rather than concentrating on the size of the change, table 3.2 concentrates on comparing the performance of each individual method. The results show that point iteration appears to be the most efficient at dealing with this particular type of problem. The reason for this is likely to be that point iterations can carry out a number of iterations very quickly. The other interesting point to note about the results are that all the methods seem to follow the same tend. This latter observation is not particularly surprising since the zones with the greatest change are likely to be the ones which take longest to calculate.

Comparing the table in this section with the one in the last section it is possible to see that the time taken to calculate the original problem is not related to the time taken to calculate the perturbed problem. A good example of this is test 9 where the time for point iteration to calculate the perturbed problem is nearly as long as the original (the difference being 0.11 seconds). In most cases the time saving of starting near the solution is considerable.

Chapter 4

Review of Literature on Inverse Methods

4.1 Introduction

This chapter will review the techniques used for solving the inverse problem. The first part is a review smoothness-constrained least-square inversion schemes which includes Occam's method. The second part of the chapter reviews other techniques that have been used to interpret ERS.

Section 4.2 will concentrate on smoothness-constrained inversion schemes. Smoothness-constrained least-squares inversion schemes are now the method of choice for 2D and 3D resistivity inversion (Constable, Parker & Constable [1987], Sasaki [1992], Sasaki [1994], Loke & Barker [1995] & Loke & Barker [1996*b*]). This type of scheme is also used in other fields for similar Inverse Problems.

A number of methods have been used for solving this particular inverse problem. Some of these techniques were developed specifically for the field of geophysics others have been used in other fields. These include methods from "simulated annealing" to the "maximum likelihood inversion method" used by Park & Van [1991] and Zhang et al. [1995]. There are interesting comparisons of these techniques in Yorkey & Webster [1987] and Tsourlos, Dittmer & Szymanski [1995]. The latter contains the formulas for the updates[1] and shows a number of methods which depend heavily on the calculation of the Jacobian.

[1]The formulas for updating the resistivity values in each iteration.

4.2 Smoothness-constrained least-squares inversion techniques

This section will give an explanation of the various parts of the smoothness-constrained least-squares inversion algorithm used, together with the constants and variables referred to in later chapters. This type of scheme used is widely in solving inverse problems and as a consequence it goes under various names and forms, for example, linear regularisation (Press, Teukolsky, Vetterling & B.P.Flannery [1992]), Marquardt Method (Ridge Regression) (Tsourlos et al. [1995] & Narayan, Dusseault & Nobes [1994]) and Occam's Method (Constable et al. [1987]). The differences are in the form of the smoothness constraint.

There are various methods which rely on least-squares (the following are taken from the appendix in Narayan et al. [1994]). The simplest least-squares methods only use the Jacobian and the difference between the observed and the calculated measurements at each iteration. The update and misfit for this least-squares solution are as follows.

$$\Delta \mathbf{x} = \left(\underline{\mathcal{J}}^T \underline{\mathcal{J}}\right)^{-1} \underline{\mathcal{J}}^T \Delta \mathbf{d} \tag{4.1}$$

$$\mathbf{e} = \Delta \mathbf{d}^T \Delta \mathbf{d} = \sum_{i=1}^{N} \left(\mathbf{d}_i - \mathbf{d}_{i,data}\right)^2 \tag{4.2}$$

A more advanced version described in Narayan et al. [1994] uses a weight matrix $\underline{\mathbf{W}}$ and is called the weighted least-squares (WLS) (or Gauss-Newton) method. The WLS also involves the use of an estimate of the model misfit.

$$\Delta \mathbf{x} = \left(\underline{\mathcal{J}}^T \underline{\mathbf{W}}\, \underline{\mathcal{J}}\right)^{-1} \underline{\mathcal{J}}^T \underline{\mathbf{W}} \Delta \mathbf{d} \tag{4.3}$$

$$\chi_R^2 = \frac{1}{N-M} \sum_{i=1}^{M} \frac{\left(\mathbf{d}_i - \mathbf{d}_{i,data}\right)^2}{\sigma_i^2} \tag{4.4}$$

The technique adopted is basically the Marquardt method but with the inclusion of a constraint.

$$\Delta \mathbf{x} = \left(\underline{\mathcal{J}}^T \underline{\mathbf{W}}\, \underline{\mathcal{J}} + k\underline{\mathbf{I}}\right)^{-1} \underline{\mathcal{J}}^T \underline{\mathbf{W}} \Delta \mathbf{d} \tag{4.5}$$

(Note that this is different from the definition in Tsourlos et al. [1995] even though they both quote from the same source. The $\underline{\mathcal{J}}^T$ is $\underline{\mathbf{W}}\underline{\mathcal{J}}^T$ in Tsourlos et al. [1995].)

$$\Delta ln(\mathbf{x}) = \left(\underline{\mathcal{J}}^T \underline{\mathbf{W}}\, \underline{\mathcal{J}} + k\underline{\mathbf{I}}\right)^{-1} \underline{\mathcal{J}}^T \underline{\mathbf{W}} \Delta ln\left(\mathbf{d}_{data} - \mathbf{d}\right) \tag{4.6}$$

This logarithmic form allows for a uniform weighting of data and model parameters. A drawback to this method is that to avoid negative values the modulus of the

measurements (or difference between modelled and data measurements) is taken, which means losing a sign.

"Occam's method" derives its name from the "razor" of William of Occam[2]:

Entia non sunt multiplicanda praeter necessitatem.[3]

This method was proposed for resistivity inversion by Constable et al. [1987]. It has become the successor to the Marquardt method as a technique for solving this particular inverse problem. This is the method that has been used in chapters 5, 6 and 7 below. Constable et al. set out with the intention of interpreting the solution with an arbitrary initial condition on the resistivity within the zones. The aim was to be able to pick out the main structures from a smoothed solution. The authors believed that sharp structural changes would not be found because "the diffuse nature of energy propagation 'smears out' the real structure of the ground." If this is true, then using any technique means that only the most noticeable structures will be found and that these would have 'smudged' edges. There is some justification for the view of Constable et al. but certainly for test problems it is possible to identify sharp changes in the resistivity (see section 6.3 below) although some of the best results may well appear to have 'smudged' edges especially those far from the electrodes. Furthermore, the stiff smoothness constraint may be smudging the edges. Constable et al.'s view is consistent with Occam's razor as it means that only the major structural changes are found, i.e. "no more" structure is "presumed to exist than" is "absolutely necessary".

Constable et al. suggest that successive iterates of the scheme $\mathbf{x_{k+1}}$, are found by choosing λ (the value of the smoothness constraint parameter) in such a way that the linear approximation to the misfit is arranged to match the desired tolerance. This form rarely converges, as a consequence of the large distance between the initial starting and end points. However Constable et al. suggest a modified form which is effective, namely supposing the kth iterate has been computed then the vector is defined by

$$\left[\lambda \underline{\mathbf{H}}^T \underline{\mathbf{H}} + \left(\underline{\mathbf{W}}\underline{\mathcal{J}}_k\right)^T \underline{\mathbf{W}}\underline{\mathcal{J}}_k\right] \mathbf{x}_{k+1}(\lambda) = \left(\underline{\mathbf{W}}\underline{\mathcal{J}}_k\right)^T \underline{\mathbf{W}}\mathbf{d}_k \tag{4.7}$$

where $\underline{\mathcal{J}}_k$ and $\mathbf{d}_k$ are function $\mathbf{x}_k$. Constable et al. then sweep through values of λ

[2]William of Occam c.1285-1349, English Franciscan friar and philosopher

[3]No more things should be presumed to exist than are absolutely necessary.

computing the true misfit of the model $\mathbf{x}_{k+1}(\lambda)$

$$X_{k+1}(\lambda) = \|\underline{\mathbf{W}}\mathbf{d} - \underline{\mathbf{W}}\mathbf{F}[\mathbf{x}_{k+1}(\lambda)]\| \tag{4.8}$$

where $\underline{\mathbf{W}}$ is the diagonal $M \times M$ matrix

$$\underline{\mathbf{W}} = diag\left\{\frac{1}{\sigma_1}, \frac{1}{\sigma_2}, \ldots, \frac{1}{\sigma_M}\right\}$$

and $\| \cdot \|$ denotes the usual[4] Euclidean Norm.

The data are contained within a vector $\mathbf{d} = (d_1, d_2, \ldots, d_M)^T$. These data can be either measurements from an actual survey or synthetic measurements produced from a test problem. There are M measurements. Each of these measurements has an associated error estimate σ_j.

The generally accepted method for modelling the subsurface is to divide the ground into discrete zones. The resistivity value for each of these zones makes up the model (the cross section of the model used is figure 6.1). The zones are usually in the shape of boxes, mainly for convenience. The model $\mathbf{x} \in \mathbf{F}$ is a vector a in Euclidean space of N dimensions, as are the measurements $\mathbf{d} \in \mathbf{F}^M$. Hence the forward problem can be expressed as

$$d_j = F_j[\mathbf{x}], \; j = 1, 2, \ldots, M$$

where F_j is the non-linear forward function associated with the jth datum, and could be expressed as

$$\mathbf{d} = \mathbf{F}[\mathbf{x}]$$

$\underline{\mathbf{H}}$ is an $N \times N$ matrix given by

$$\underline{\mathbf{H}} = \begin{bmatrix} 0 & & & & 0 \\ -1 & 1 & & & \\ & -1 & 1 & & \\ & & \ddots & \ddots & \\ 0 & & & -1 & 1 \end{bmatrix}$$

$\underline{\mathbf{H}}^T\underline{\mathbf{H}}$ is the initial guess which is the homogeneous case. Therefore, the solution produced is dependent on λ as to the extent to which the homogeneous case is allowed to smooth the solution.

[4]The Euclidean norm is the root of the sum of the squares (Pythagoras) i.e. a measure of distance.

$\underline{\mathcal{J}}$ is the $M \times N$ Jacobian or gradient matrix.

$$\underline{\mathcal{J}} = \nabla_x \mathbf{F}$$

or

$$\underline{\mathcal{J}}_{q,r} = \frac{\partial F_q[\mathbf{x}]}{\partial x_r}$$

The rows of $\underline{\mathcal{J}}$ are the discrete equivalents of the Fréchet derivatives in the continuous profile problem.

The method for calculating the Jacobian is the subject of chapter 5 and its effect on this technique will be shown in chapters 6 and 7. However, the dependence of equation (4.7) upon the Jacobian should be noted.

Equation (4.7) is derived from a non-linear equation, which contains a set of simultaneous non-linear equations which must be solved for $\mathbf{x}$. Two methods of solving the problem were given in Constable et al. The first was "to attack [the non-linear] equation directly and solve the system by Newton's method". But to do this required differentiation of $\underline{\mathcal{J}}$ to find the second derivative of $\mathbf{F}$, which the authors describe as "a very tedious piece of algebra". Newton's method appears very attractive, but it may swing wildly while providing only a very small reduction in mismatch. Press et al. [1992], (section 9.6 page 379) state that "there are *no good* general methods for solving systems of more than one nonlinear equation. Furthermore, it is not hard to see why (very likely) there *never will be* any good, general methods"(the italics is that of Press et al.). This seems to contradict the views of Constable et al., as their paper implies that it is possible (but that they could not do it).

Constable et al. state that (if convergent), equation 4.7 will solve the minimisation and that the limit should therefore be independent of the starting point. The problem with this method is that a straightforward minimisation scheme is very likely to diverge from the 'required' solution.

Constable et al. discuss the Marquardt method, which modifies the matrix $\underline{\mathcal{J}}^T\underline{\mathcal{J}}$ by adding a constant value to the diagonal, thus decreasing the size of the computed perturbation. The constant is chosen to decrease the misfit at each iteration for a fixed Jacobian. This is used to bring the misfit down to an acceptable level, and not to the minimum possible value. The problem with this is that the solution lies close to the initial guess since the changes are kept small. The model is thus strongly influenced by the initial choice. Sometimes the misfit can not be reduced sufficiently, requiring the introduction of more parameters. Also large-amplitude oscillations may develop with no real means of controlling the Marquardt

scheme.

Constable et al. found that their method met two of their criteria. Firstly, the method does not depend on the number of layers used. There are various methods which are dependent on the number of layers being set before the inversion is started. Secondly, the success of the method does not depend on the initial guess, although it works better if the solution is close to the initial guess. In the example they choose the method converged after six iterations. The reason for this rapid convergence is that the smoothness constraint is very strict, yielding a very smooth solution. The major feature of the algorithm given by Constable et al. is that the actual value is calculated rather than the change in the value which is customary. The effect of this is that the method smoothes the values and not the change in the values.

An example of Occam's method being used for medical imaging can be found in an unpublished paper Binley, Ramirez & Daily [c. 1993]. This a much simpler task than a geophysical survey as there is access to all the boundaries.

Binley et al. [c. 1993] look at practical problems associated with carrying out and interpreting ERT. Most of these problems are associated with reduction noise and errors. The smoothness constraint also helps to overcome some of the noise but it remains the fact that as in all non-linear problems a small amount of noise can have a large effect.

There are other smoothness-constrained least-squares inversion schemes: these are similar to Occam's method and contain similar parameters. Sasaki [1992] investigates how the size of the zone, the damping factor, the choice of electrode array and an outside anomaly affects the result of using a smoothness-constrained least-squares inversion routine, in the case of borehole-borehole-surface surveys.

The inversion routine used is similar to Occam's method although not identical to it: they would be identical if $\underline{\mathbf{W}}$ were the identity matrix. The update $\Delta\mathbf{x}$ is given by

$$\left(\lambda\underline{\mathbf{H}}^T\underline{\mathbf{H}} + \underline{\mathcal{J}}^T\underline{\mathcal{J}}\right)\Delta\mathbf{x} = \underline{\mathcal{J}}^T\Delta\mathbf{d} \tag{4.9}$$

where λ which may be regarded as either a Lagrange multiplier or a damping factor and $\underline{\mathbf{H}}$ is a 2D Laplacian operator.

Given that the surveying technique used involves placing electrodes down boreholes the results could be expected to be more accurate. Although this method is robust under Gaussian noise, one of the most striking results is that dipole–dipole surveys appear to be more robust vis-à-vis this noise than pole–dipole. There is a

strong argument against adding a fixed amount of noise to each measurement, as the noise will in reality be at such a level that for large measurements its effect will be very small while for a small measurements it will form a significant fraction of the measured value.

The effects of introducing inhomogeneities outside the volume of interest are revealing and should encourage study of the result of surrounding the volume of interest by sacrificial zones.

Sasaki [1994] uses exactly the same inversion algorithm as in his 1992 paper except that an equivalent system has been found. This equivalent system can be solved using single value decomposition or modified Gram-Schmidt methods.

Sasaki's model is interesting, as the 3D finite element mesh used allows for surface contours. However, this form would not take well to anisotropy. This could also mean, if not very carefully applied, that some electrodes may have much larger grid cells than is necessary (or wise) for accurate modelling. On the other hand, this method could be altered in such a way as to place large numbers of extra grid cells near the sources and in regions of particular interest. This would involve highly non-uniform grids as are occasionally used in computational fluid dynamics.

The results in Sasaki [1994] for a flat surface distinguished the features on the surface. However, the calculated apparent resistivities were not particularly close to the actual values. The non-flat surface example produces a worse result but this could have been caused by the size of those grid cells that contain electrodes.

Sasaki's conclusions appear sensible: in particular his comment that an improvement in the modelling of the forward problem would increase the accuracy of the solution.

Loke and Barker have been trying to perform very fast inversions which produce reasonable results with structure but not with the actual resistivity values. Loke & Barker [1995] look at 2D surveys comprising rectangular zones which are infinitely long in the y direction. The inversion scheme used is almost identical to the one used in Sasaki [1992] and Sasaki [1994], the only difference being that the update equation (4.9) for $\Delta\mathbf{d}$ is "the discrepancy vector containing the logarithmic differences between the measured and calculated apparent resistivity values".

The main part of Loke & Barker [1995] deals with the calculation of the Jacobian. It is very similar to the results in section 5.5.2 below except that it is restricted to 2D. Loke & Barker [1995] is a useful approach as it produces a fairly accurate homogeneous isotropic Jacobian. The results are what can be expected from a method that uses just the homogeneous Jacobian. The results do reveal

some simple structure. It is perhaps better to regard these solutions as the results of a first iteration rather than as a solution.

In Loke & Barker [1996*b*] the same update formula for the resistivities is used. However, equation (4.9) is then solved using two different methods: the Gauss - Newton method and the quasi - Newton method. The first is described as the "conventional method", whilst the second is referred to in Press et al. [1992] as Broyden's method although they are in essence two variants of the same method. Boyden's method produces an approximation to update the Jacobian.

The reasons for using such an update are to reduce the work considerably and to obtain a Jacobian which is rather closer to the actual Jacobian than is the homogeneous Jacobian. The results of Loke & Barker [1996*b*] are some of the best yet published but they are still (for example) 50% too small for the simple problem of a block in a homogeneous medium. The method is also quite fast and not particularly "memory-hungry". This method would be good for pre-processing the data so that the initial condition for a more accurate method might be gained quickly thereby reducing the number of iterations required.

Loke & Barker [1996*a*][5] contains much of the work published in their previous two papers. It basically puts the two methods together for pole–pole surveys on a small surface grid. The main thrust of the paper concentrates on the method of conducting the surveys rather than the interpretation of the results.

4.3 Other methods

A large variety of methods have been used and developed to solve the inverse problem, in addition to the smoothness-constrained least-squares inversion technique. Three review papers (Narayan et al. [1994], Tsourlos et al. [1995] and Yorkey & Webster [1987]), between them cover the field comprehensively. The last paper actually deals with ERT applied to medical imaging, but this is also relevant to geophysical problems. Narayan et al. [1994] review mainly least-square methods. Other methods published include some which use the conjugate gradient and approach some which use other nonlinear techniques.

The Yorkey & Webster [1987] paper contains a comparison of methods used for medical imaging. Unfortunately, the paper does not actually define the algorithms, but does compare the following techniques:-

- The *Newton - Raphson* algorithm, which uses the Newton - Raphson technique

[5]Note that this is published in the same volume as Loke & Barker [1996*b*].

modified by Yorkey to reconstruct the resistivity distribution, allowing a finite element method to reproduce the observed potentials as closely as possible. This method is "guaranteed to converge to the optimal solution" and is defined in Yorkey, Webster & Tompkins [1987]. This assertion may be true for the limited range of resistivities and boundary conditions in medical applications of ERT, but (as we observed in section 4.2 above) this is unlikely to be the case for geophysical tomography as such linearisation would not hold where the variations in resistivity are not so small.

- The *sensitivity* method, which was developed by Murai and Kagawa and is based on Geselowitz's Sensitivity Theorem.

- The *perturbation* method developed by Kim, Webster & Tompkins [1983]. This method produces a perturbation matrix (the same as the Jacobian discussed in chapter 5 below). This uses Gilbert's Simultaneous Iteration Reconstruction Technique.

- The *equipotential lines* and *iterative equipotential line* method which are based on a method proposed by Barber, Brown & Freeston [1983]. These methods compare their survey measurements with the measurements for the homogeneous case: they then use the resistivity measured between the equipotential lines at the measurement electrodes. This may work well in the neighbourhood of the homogeneous case but calculating the equipotential lines in a medium with large variations in the resistivity would not be a simple matter.

- The *double constraint* technique was proposed by Wexler et al [1985]. This constrains the finite element method with the measured potentials and the current source value. The calculated potential gradient in each element is used to determine the resistivity of each element.

The results for the Newton - Raphson and sensitivity methods produce the most accurate answers. The Newton - Raphson method is computationally intensive but the most accurate (but only for medical ERT's in general).

A further group of methods include Monte Carlo methods and genetic algorithms. Both types rely on a degree of randomness.

Chunduru, Sen, Stoffa & Nagendra [1995] looked for three types of structure, namely the "outcropping vertical dike, hemispherical sink and sphere models." If geological structures consisted of simple mathematical shapes in a homogeneous medium then this approach would have been more fruitful. If the methods discussed

by Chunduru et al. [1995] were general rather than specific, they could be tested on more complex problems.

The Monte Carlo methods use an energy function which is an L_2-norm misfit function, which is the same as the least squares criterion. One of the approaches is called "simulated annealing" (SA), which is essentially an optimisation technique. The algorithm (this version is Metropolis simulated annealing) is:

1. Perturb $\mathbf{x}_i$ to produce a new value $\mathbf{x}_j$ and calculate $E(\mathbf{x}_i)$

2. Calculate $\Delta E = E(\mathbf{x}_j) - E(\mathbf{x}_i)$

3. If $\Delta E < 0$ then $\mathbf{x}_j$ is accepted.

   Else the new model is accepted with a probability $P = e^{-\frac{\Delta E}{T}}$

where $E(\mathbf{x})$ is the energy of the model and T is a control parameter which is called the "temperature" (by analogy with solutions of the heat equation).

The second approach is called very fast simulated annealing (VFSA). This is basically the same as SA except that the temperature T is given by

$$T_i(K) = T_{0,i} e^{-C_i K^{\frac{1}{N}}}$$

where $T_i(K)$ is the temperature of the Kth iteration, $T_{0,i}$ are the initial values of the temperature, C_i is defined by the user (called the decay factor) and N is the number of model parameters. This is a possible method for choosing the zone that is to be updated.

Both approaches avoid the calculation of a Jacobian matrix, but they do process objective functions with arbitrary constraints. The algorithm is simple and most SAs are very likely to find an optimal solution. Unfortunately, SAs are generally very computationally intensive (although the VFSA is not).

The third method described in Chunduru et al. [1995] is a genetic algorithm. This method was developed a model of Darwinian evolution. Genetic algorithms are to evolution what neural networks are to the brain. Genetic Algorithms widely used in machine learning and similar areas.

The results show that VFSA is better than the Genetic Algorithm and much better than SA. The authors also note that VFSA can be used to perform inversions on "data from geologically complex media."

An improvement to VFSA is given in Chunduru, Sen & Stoffa [1996]. This uses cubic splines to reduce the number of model parameter from 450 to 24

(or 72 using the 2D splines). The results given are not particularly impressive. The effect of the splines is to give a drastic smoothing effect.

Another method for solving inverse problems is to use Fourier transforms. This is not a widely used. Molyneux & Witten [1994] tackle the inverse problem from an analytical prospective. They recognise that the process is nonlinear and proceed to linearise it "by assuming that the conductivity variations to be imaged are a small perturbation on the constant background value." This means that the inversion procedure will not necessarily be stable (or produce correct results) for wide ranges in resistivity.

The inversion formula is based on relating the Fourier transform of the measurements taken, to the Fourier-Laplace transform of the conductivity variations. Also some *a priori* knowledge of the conductivities is assumed. The DC electrical resistivity is taken to be considered as the limit as the frequency tends to zero.

Two interesting questions are posed at the end of this paper. The first concerns the "limits of resolution" and the importance of the "signal to noise ratio". The second is the validity of the small perturbation assumption which holds for other applications of ERT, although not necessarily in the field of geophysics.

It is possible to use an approximate inversion method, for example as stated in Li & Oldenburg [1994],where an iterative algorithm for inverting 3D pole–pole DC resistivity data was produced. The algorithm used was an AIM (approximate inversion mapping), which updates both model space (AIM-MS) and data space (AIM-DS). AIM uses Fourier transforms and avoids both the generation and inversion of 3D sensitivity and the use of a Jacobian matrix, which makes the method fast since only one forward problem needs to be solved per iteration.

Li & Oldenburg [1994] show that good results have been produced by using this method. However, there is smoothing of the structures far from the electrodes and quite a lot of noise near the surface. Although this method is very fast it is unlikely to produce a more accurate result as it uses approximate inversion.

Another paper which investigates the subject of approximations is Dabas, Tabbagh & Tabbagh [1994]. The inversion scheme used in this paper is an unweighted version of the Marquardt method. the authors also tested the Born and localised non-linear approximations. The conclusions drawn in this paper were that even if the computational time could be drastically reduced, these "cannot be used in the inversion process." The results of the inversions are good, but it should be borne in mind that this is not a complicated structure even though it is 3D (there are an upper and a lower level of zones).

Other criteria can be used apart from smoothness, for example as discussed in Park & Van [1991]. This paper is split into two parts. The first, proves that the adjoint to the forward problem is of the same form as the forward problem. This is explained in detail in appendix C below. The second part deals with an inversion scheme, namely the maximum likelihood inversion (MLI). This was developed by Tarantola & Valette [1982] and is the same method as used in Zhang et al. [1995].

The MLI method may be regarded as a variant of a least-squares method with a constraint other than smoothness: however the precise nature of the constraint is not explicitly defined in either Park & Van [1991] or Zhang et al. [1995]. MLI is designed to find the values which provide the best fit to the data observed minimising a function:

$$\begin{aligned}&(\underline{\mathbf{D}}\mathbf{x}+\underline{\mathcal{J}}\delta\mathbf{x}-\mathbf{d})^H\,\underline{\mathbf{R}}_{dd}^{-1}\,(\underline{\mathbf{D}}\mathbf{x}+\underline{\mathcal{J}}\delta\mathbf{x}-\mathbf{d})\\&\quad+(\mathbf{x}+\delta\mathbf{x}-\mathbf{x_0})^H\,\underline{\mathbf{R}}_{mm}^{-1}\,(\mathbf{x}+\delta\mathbf{x}-\mathbf{x_0})\end{aligned}\tag{4.10}$$

where

$\underline{\mathbf{D}}$ = operator for the forward problem,

$\underline{\mathcal{J}}$ = sensitivity matrix,

$\delta\mathbf{x}$ = perturbations in the model,

$\mathbf{x_0}$ = a priori model,

$\mathbf{d}$ = observed data,

$\mathbf{x}$ = current model,

$\underline{\mathbf{R}}_{dd}$ = data covariance matrix,

and

$\underline{\mathbf{R}}_{mm}$ = model covariance matrix.

The superscript H denotes the Hermitian. $\underline{\mathcal{J}}$, the sensitivity matrix, is defined by

$$\underline{\mathcal{J}}\Delta\mathbf{x}=\Delta\mathbf{d}\tag{4.11}$$

Equation (4.10) was differentiated and the result set to zero. This gave the following equation with a matrix problem produced for $\delta\mathbf{x}$:

$$\left[\underline{\mathcal{J}}^H\underline{\mathbf{R}}_{dd}^{-1}\underline{\mathcal{J}}+\underline{\mathbf{R}}_{mm}^{-1}\right]\delta\mathbf{x}=\underline{\mathcal{J}}^H\underline{\mathcal{J}}+\underline{\mathbf{R}}_{dd}^{-1}\,(\mathbf{d}-\underline{\mathbf{D}}\mathbf{x})+\underline{\mathbf{R}}_{mm}^{-1}\,(\mathbf{x_0}-\mathbf{x})\tag{4.12}$$

By substituting into equation (4.12) $\mathbf{x} = \mathbf{x}_k$ and $\delta\mathbf{x} = \mathbf{x}_{k+1} - \mathbf{x} - k$, we obtain

$$\mathbf{x}_{k+1} = \mathbf{x}_k + \left[\underline{\mathcal{J}}^H \underline{\mathcal{J}} + \underline{\mathbf{R}}_{mm}^{-1} + \epsilon^2 \underline{\mathbf{I}}\right]^{-1} \times \left[\underline{\mathcal{J}}^H \Delta\mathbf{d} + \underline{\mathbf{R}}_{mm}^{-1} (\mathbf{x}_0 - \mathbf{x})\right] \qquad (4.13)$$

where

$\mathbf{x_k}$ = k^{th} estimate of model,

$\mathbf{x_{k+1}}$ = $(k+1)^{\text{th}}$ estimate (update) of model,

$\epsilon^2\underline{\mathbf{I}}$ = damping,

and

$\Delta\mathbf{d}$ = the vector of differences between modelled responses and observed data.

This method updates under the dual constraints of fitting the observed data and of not deviating far from the *a priori* model. It should be noted that Park & Van assumed that $\underline{\mathbf{R}}_{dd}$ is the product an "average standard deviation" times the identity matrix, and also that $\underline{\mathbf{R}}_{mm}$ in equation (4.13) is divided by the average standard deviation of the observed data.

Park & Van [1991] say that least-squares inversion "may result in more complicated models than are necessary" and suggest an alternative constraint to that of smoothness. Such constraints may be applied to the total inverse of the model covariance matrix, $\underline{\mathbf{R}}_{mm}^{-1}$. This is generated before the iterations start and can be used to weight various model parameters. $\underline{\mathbf{R}}_{mm}^{-1}$ can be used to smooth the model or to hold parameters constant. Park & Van use a diagonal matrix with uniform weights. Also, Park & Van state that "linearisation of a nonlinear problem in which the material properties vary over several orders of magnitude ... will result in a very slowly converging solution". To get around this, Park & Van compute $\Delta \ln \rho$ and $\Delta \ln \mathbf{d}$ by recasting equation (4.11) into a logarithmic form:

$$\Delta \ln \mathbf{d} = \underline{\mathcal{J}} \Delta \ln \mathbf{x} \qquad (4.14)$$

The elements of the sensitivity matrices are calculated in different ways in these two papers. $\underline{\mathcal{J}}$ defined in equation (4.11) as same to the $\underline{\mathcal{J}}$. Park & Van use equation (5.8) to calculate this matrix. In equation (4.14) it is unfortunately not always possible to take the logarithm of the measurements. In this case (pole–pole) the values will all be positive but this is not necessarily true for difference measurements (pole–dipole, etc.). The rest of the paper basically shows a simple test case and an actual application, though neither is particularly accurate. This is worrying in the test case but wholly predictable, since the real observed data for a

pole–pole survey, usually contain large errors in the measurements, which are mostly unavoidable.

Apart from using maximum likelihood inversion, Zhang et al. [1995] use an interesting method for calculating the sensitivity matrix. The major point of this paper is to use the conjugate gradient technique for both the forward and inverse problem. The former of these is a useful pointer to a method which deserves wider application. The use of the technique for the inversion part of the problem is interesting however if the matrix (which corresponds to $\underline{\mathbf{A}}$ in $\underline{\mathbf{A}}\mathbf{x} = \mathbf{b}$) is nearly singular, then this inversion technique is less reliable. The elements of the sensitivity matrix are defined as

$$\underline{\mathcal{J}}_{q,r} = -\mathbf{a}_q^T \underline{\mathbf{K}}^{-1} \frac{d\underline{\mathbf{K}}}{d\rho} \mathbf{v} \tag{4.15}$$

where $\mathbf{a}$ is a vector that picks out the node at the potential electrode, $\mathbf{v}$ is a vector of voltage at each node and $\underline{\mathbf{K}}$ is the matrix containing the conductivities.

The results of this method are similar to those in Park & Van [1991]. Zhang et al. [1995] show that the Park & Van method allows us to pick out simple structures, although unfortunately the methods have not been applied to a complicated structure.

Ellis & Oldenburg [1994] use a method which converts the inverse problem into an objective-function optimisation problem. The minimisation method used is conjugate gradients. The synthetic test case used by Ellis & Oldenburg [1994] is the most complex of all the problems used in the literature reviewed (i.e. the five prism model). The results show most of the structure of the test case. The lack of resolution is blamed on a global smoothness constraint. Ellis & Oldenburg [1994] point out that ERT is better at resolving low resistivity than high resistivity.

The second of the comparison papers which are reviewed in this section is Tsourlos et al. [1995]. The authors compare Marquardt's method (ridge regression), Occam's method, quasi-Newton and simulated annealing. This is a diverse set of methods which incorporate most methods (although not the MLI method).

The Marquardt method, proposed by Marquardt [1963], uses an iterative procedure to update the resistivity.

$$\Delta\mathbf{x}_{t+1} = \left[\left(\underline{\mathbf{W}}\,\underline{\mathcal{J}}_t\right)^T \left(\underline{\mathbf{W}}\,\underline{\mathcal{J}}_t\right) + k\underline{\mathbf{I}}\right]^{-1} \left(\underline{\mathbf{W}}\,\underline{\mathcal{J}}_t\right)^T \underline{\mathbf{W}}\Delta\mathbf{d}_t \tag{4.16}$$

$$\mathbf{x}_{t+1} = \Delta\mathbf{x}_{t+1} + \mathbf{x}_t \tag{4.17}$$

where k is a damping factor and $\underline{\mathbf{W}}$ is a weighted diagonal matrix.

The quasi-Newton method updates the Jacobian at each iteration without having to start from scratch each time. The updating formula given is

$$\underline{\mathcal{J}}_{t+1} = \underline{\mathcal{J}}_t + \frac{\left[(\mathbf{d}_{t+1} - \mathbf{d}_t) - \underline{\mathcal{J}}_t \Delta \mathbf{x}_t\right]}{\Delta \mathbf{x}_t^T \Delta \mathbf{x}_t} \Delta \mathbf{x}_t^T \tag{4.18}$$

As this depends on the change in $\mathbf{d}$ from the previous to the present measurements, there is room for a prediction part. This would take the form of replacing $\mathbf{d}_{t+1}$ with $\mathbf{d}_{t+1} + \epsilon(\mathbf{d}_{obs.} - \mathbf{d}_{t+1})$. The effect of this is not obvious but the idea is to use the Jacobian to push the method in the direction of the solution by making it contain a small part of the Jacobian of the solution. Equation 4.18 was also used to update the Jacobian in Occam's method with some success.

The results given by Tsourlos et al. [1995] plainly show Occam's method to be the best and while the quasi-Newton Jacobian produces a worse result it was four times quicker after the first iteration. The conclusions of this paper also included a comment on simulated annealing, which was "extremely slow (by several orders of magnitude)". This seems to agree with others who have published work on simulated annealing.

The third of the comparative papers by Narayan et al. [1994] looks at a number of different inversion schemes beginning with 1D and 2D problems which are interesting. However the paper goes on to discuss 3D inversions giving both comment and the form of the actual schemes themselves (in the appendix of the paper).

The early work done on 3D problems tended to use the alpha centres method for modelling the forward problem and ridge regression (Marquardt method) for the inversions. Unfortunately, the alpha centres method cannot be used to model complex resistivity distributions.

The parameters of this model depend on the size of "the eigenvalues of the matrix (i.e. transpose of the square of the coefficient matrix)", which also has an effect on the stability of the solution. "The large range of eigenvalues encountered in most resistivity problems cause oscillations in the model parameters". The single value decomposition method, shown in Tripp, Hohmann & Swift Jr. [1984], is based on this information but its calculation of the single value decomposition of the coefficient matrix is intensive.

The results produced by Narayan et al. [1994] are not particularly good. The resemblance between the result and actual test problems is not convincing. The models are more complicated than some that have been used in other papers. Some of the conclusions drawn are interesting, for instance, "the sensitivity of the mea-

surements at the surface is directly proportional to the amount of power dissipated across the heterogeneous region." Also, these methods require accurate solutions of the forward problem.

There are various assumptions made when using least-squares. Al-Chalabi [1992] was published because "there is a general lack of awareness among 'lay' professionals regarding the limitations of least-squares". Unfortunately this paper is full of destructive rather them constructive criticism. The basic thrust of the paper is that using the L_2-norm is popular but it is not suitable due to limitations on the error of the normal distribution. This paper does not mention what these errors may be, although they are unlikely to be Gaussian. Apart from such comments this paper is unlikely to yield constructive developments. Although there is no explanation for the errors referred to in the paper, these may include the presence of white noise at a certain value.

Despite this some conclusions contained in the paper would seem to give two pointers. First, if the central limit theorem is applicable then "such cases are amenable to a least-squares treatment" and even if it is close the effect is still present. Secondly, low norms are suggested "e.g. $L_{0.4}$, $L_{0.75}$" or other alternatives such as "curtailment" or "robust statistics".

Chapter 5

Calculating the Jacobian for Resistivity Inversion

5.1 Introduction

This chapter deals with a novel method for calculating the Jacobian matrix used in resistivity inversion. There are four basic ways of conducting ERS: pole–pole, pole–dipole, dipole–pole and dipole–dipole. Each of these methods requires a slightly different algorithm to calculate the Jacobian matrix; only one of these, pole–dipole, are described in this chapter, the others are presented in appendices. The same approach is used for the derivation of the analytic Jacobian. The reason for choosing the pole–dipole survey was given in chapter 1 above. The pole–dipole technique has the following advantages:

1. High lateral resolution, independent of the depth of the survey.

2. The data can be constructed from pole–pole data.

3. The measurement dipole allows external noise to be rejected.

Resistivity inversion was covered comprehensively in the last chapter therefore no further description of the method is presented here. We shall, however investigate the role of the Jacobian. A brief outline of the methods used at present to calculate the Jacobian is given in section 5.1.1. In section 5.1.2 and appendix C we discuss the method Park & Van [1991] used to prove the adjoint of the forward problem, which could be used to calculate the Jacobian in an accurate and efficient manner.

The remainder of the chapter is split into four parts:

- an extension to Park & Van's work so that their adjoint can be used in surveys other than pole–pole
- The derivation of a new method for pole–dipole surveys
- The practical implementation of this method, with a section on the use of more than one grid.
- The last section of the chapter concerns the derivation of the analytic Jacobian for the homogeneous case.

5.1.1 Methods for calculating the Jacobian

This section reviews methods which have previously been used to calculate the Jacobian matrix. Starting with the obvious way of calculating the elements of the Jacobian (the perturbation method). The Jacobian is defined as

$$\underline{\mathcal{J}}_{q,r} = \frac{\partial F_q(\mathbf{x})}{\partial x_r} \tag{5.1}$$

which is the change in the qth measurement caused by a perturbation in the resistivity of the rth zone. This means that in practice the potential difference is calculated between a pair of electrodes and then the resistivity of the zone is perturbed by a small positive or negative amount and the potentials are recalculated (for each of the directions if both are used). If the resistivity of the zone q is perturbed in one direction then the value is the difference divided by the size of the perturbation in x_r: this gives the (q, r) element of $\underline{\mathcal{J}}$. If the resistivity is perturbed in both directions, a parabola can be fitted and the derivative calculated more accurately as the value of the gradient for the original resistivity is the value of the element in the Jacobian.

There are various problems in calculating the Jacobian in this fashion. The first of these is choosing the size of the perturbation. This involves balancing the need for the perturbation to be small enough for the linear approximation to hold but large enough for the value to be easily measured without introducing large numerical errors. The second problem is the time taken to calculate this Jacobian. This arises from having to solve two or three forward problems for each element in the Jacobian. In practice it is possible to do slightly better than this. The time taken by this method is proportional to the product of the number of current sources and the number of zones. This is because the potential electrodes are measuring points and therefore have no effect on the actual calculation. The last problem, is

that of the zones which lie far from the electrodes. These zones are always going to create small values in the Jacobian that are usually close to the accuracy of the finite difference model and thus unlikely to be reliable; there is also an argument that they have very little effect on the solution. This point will be discussed in detail in chapter 7 below.

There are other ways of calculating (or avoiding calculating) the Jacobian. The first of these definitely comes under the latter description. It involves calculating the homogeneous Jacobian, as this is where almost everyone starts, and then merely re-using the homogeneous Jacobian without performing any further calculations. For example Loke & Barker [1995] looked at a 2D method for a pole–pole survey. Their practical procedure includes the following: "The Jacobian matrix $\underline{J}$ is calculated for the electrode array from the partial derivative values that have been precomputed and stored in a data file." Their model then uses this to calculate the solution. They do very well on the structure but not so well on the resistivity values. This is really fast as there is no need to recalculate the Jacobian thereby missing out the part which takes longest. This is legitimate only if it is assumed that the structure of the solution is close to the homogeneous case, or if one just ignores all the non-linear terms wherever they occur. The example in Loke & Barker [1995] involved a block of material of five times the resistivity of the surrounding space with a sharp change. The results of their tests show a smooth change in the resistivity. This is a good start for predicting geological structure but is unsuitable as an assessment of subsurface properties.

Another method used is Broyden's update (Loke & Barker [1996*b*]). This works by approximating the Jacobian matrix with a matrix $\underline{B}$. Several 'tricks' are needed in this method, as it requires a square matrix. Problems occur with this method: e.g. it could fail to converge as $\underline{B}$ is not the exact Jacobian and therefore "we are not guaranteed" the right "descent direction". "Thus the line search algorithm can fail to return a suitable step if $\underline{B}$ wanders far from the true Jacobian" Press et al. [1992]. There are also problems when $\underline{B}$ becomes nearly singular but this will also affect other methods. One great advantage of this method is that if it works it is very much faster. The results however are not nearly good enough to meet the objectives. Unfortunately, this method seems to suffer from a tendency to predict a resistivity value far from the actual resistivity values used. "The highest model resistivity value near the centre of the rectangular block is about $250\Omega m$, which is less than the true value of $500\Omega m$" Loke & Barker [1996*b*]. The structure obtained by this method is reasonable. Whether this could be improved is

an open question although it looks somewhat of a numerical art to get good results.

Loke & Barker [1996*b*] seem to be trying to get a good idea of structure with the actual value of the resistivity being less important. Whatever their aims their work is important in this area. The two papers by Loke & Barker and McGillivray & Oldenburg [1990] are typical of the approach of other workers in the field. The shortcomings of what has been done provide further motivation for the present project.

5.1.2 Adjoint of the forward problem

The adjoint of the forward problem as derived in Park & Van [1991] has been used to calculate sensitivity matrices e.g. Park & Van [1991] and the basis for the homogeneous Jacobian in Loke & Barker [1995]. The derivation of the adjoint in Park & Van [1991] is based on a pair of coupled equations derived from Poisson's equation (see appendix A for the connection between Poisson's equation and equations 5.2 and 5.3).

$$\rho \mathbf{J} + \nabla \phi = \mathbf{0} \tag{5.2}$$

and

$$\nabla . \mathbf{J} = I_s \tag{5.3}$$

where ρ = resistivity, $\mathbf{J}$ = current density, ϕ = electric potential and I_s = current source in current per unit volume. The two above equations can be rewritten as

$$\begin{bmatrix} \rho \underline{\mathbf{I}} & \nabla \\ \nabla . & 0 \end{bmatrix} \begin{bmatrix} \mathbf{J} \\ \phi \end{bmatrix} = \begin{bmatrix} \mathbf{0} \\ I_s \end{bmatrix} \tag{5.4}$$

where $\underline{\mathbf{I}}$ is a 3×3 identity matrix. Let us replace the matrix $\rho\underline{\mathbf{I}}$ with a more general form: a matrix $\underline{\mathbf{R}}$ of (not necessarily uniform) resistivity in Cartesian coordinates[1]. For the moment the only constraint on $\underline{\mathbf{R}}$ is that it is not the null matrix. For mathematical considerations, this definition is broader than is necessary; its geological significance is that it models most anisotropic rocks. Therefore if $\underline{\mathbf{R}}$ is substituted for $\rho\underline{\mathbf{I}}$ in (5.4) then

$$\begin{bmatrix} \underline{\mathbf{R}} & \nabla \\ \nabla . & 0 \end{bmatrix} \begin{bmatrix} \mathbf{J} \\ \phi \end{bmatrix} = \begin{bmatrix} \mathbf{0} \\ I_s \end{bmatrix} \tag{5.5}$$

[1]There is a precedent for describing anisotropy in this way, for example see section 1.17 of Carslaw & Jaeger [1959].

By perturbation of material properties and field quantities in equation (5.4) the following is obtained

$$\begin{bmatrix} \underline{\mathbf{R}} & \nabla \\ \nabla. & 0 \end{bmatrix} \begin{bmatrix} \delta\mathbf{J} \\ \delta\phi \end{bmatrix} = \begin{bmatrix} -\underline{\delta\mathbf{R}}\mathbf{J} \\ 0 \end{bmatrix} \tag{5.6}$$

where $\delta\mathbf{J}$ and $\delta\phi$ are first order quantities. Higher order perturbations are neglected. The 2nd order term neglected at this point is $\underline{\delta\mathbf{R}}\delta\mathbf{J}$. We shall return to this point in section 7.4 (see equations (7.1) and (7.2)) where the actual size of this term will be discussed. The term is assumed to be negligible for the rest of this chapter.

Following Park & Van [1991] from equation (5.6) (see appendix C)

$$\int_\tau (\underline{\delta\mathbf{R}}\mathbf{J}) .\mathbf{J}' d\tau = \int_\tau I'_s \delta\phi d\tau \tag{5.7}$$

If I'_s is a delta function at the receiver location (x_{P1}, y_{P1}, z_{P1}) then $\mathbf{J}'$ is the current from a point at the receiver location (i.e. a Green's function).

$$\delta\phi\,(x_{P1},\ y_{P1},\ z_{P1}) = \int_\tau (\underline{\delta\mathbf{R}}\mathbf{J}) .\mathbf{J}' d\tau \tag{5.8}$$

where $\mathbf{J}$ is the current density at any point due to a source at the current electrode, and $\mathbf{J}'$ is the corresponding current density for a source at the potential electrodes at location (x_{P1}, y_{P1}, z_{P1}). τ is the size of the zone. Equations (5.7) and (5.8) are the basis for the main part of this chapter.

However, this is only possible if (see appendix C)

$$\mathbf{J}'. (\underline{\mathbf{R}}\delta\mathbf{J}) = \delta\mathbf{J}. (\underline{\mathbf{R}}\mathbf{J}') \tag{5.9}$$

$\underline{\mathbf{R}}$ must be defined in such a way that equation (5.9) is true. The obvious choice of is that $\underline{\mathbf{R}}$ is a diagonal matrix. Equation (5.9) infact holds if $\underline{\mathbf{R}}$ being a symmetric matrix. $\underline{\mathbf{R}}$ will clearly be a positive matrix since its elements are resistivities, which are always positive.

As $\underline{\mathbf{R}}$ is a symmetric matrix it will have three real eigenvalues. The implication of this in the physical system is that there are three independent resistivities which are in mutually orthogonal directions. A practical example of such a system is the case of some sedimentary rocks and slate where anisotropy is significant. The general matrix $\underline{\mathbf{R}}$ is outside the scope of the work reported here.

The case of a diagonal matrix $\underline{\mathbf{R}}$, is of geological interest, modelling, as it does for more general systems than those with scalar resistivities.

$$\underline{\mathbf{R}} = \begin{pmatrix} \rho_x & 0 & 0 \\ 0 & \rho_y & 0 \\ 0 & 0 & \rho_z \end{pmatrix} \tag{5.10}$$

This problem can be modelled by the finite difference formulation used here. Angle and directions are set by restricting ρ to be dependent on the direction of the co-ordinates of the model. The restrictions on $\underline{\mathbf{R}}$ also apply to $\underline{\delta\mathbf{R}}$, which must therefore be symmetric for the most general case. If $\underline{\mathbf{R}}$ is diagonal, $\underline{\delta\mathbf{R}}$ can be one of the following.

$$\underline{\delta\mathbf{R}} = \begin{pmatrix} \delta\rho_x & 0 & 0 \\ 0 & 0 & 0 \\ 0 & 0 & 0 \end{pmatrix}, \begin{pmatrix} 0 & 0 & 0 \\ 0 & \delta\rho_y & 0 \\ 0 & 0 & 0 \end{pmatrix}, \begin{pmatrix} 0 & 0 & 0 \\ 0 & 0 & 0 \\ 0 & 0 & \delta\rho_z \end{pmatrix} \text{ or } \delta\rho\underline{\mathbf{I}} \tag{5.11}$$

The reason for using the particular definitions give above, is that the different directions of resistivity would each appear as zones in the inversion. This problem may be tackled by solving for an isotropic material i.e. $\rho_x = \rho_y = \rho_z = \rho$ (i.e. using the last of the four possible $\underline{\delta\mathbf{R}}$) which is the original method, then introducing the directional ρ when the method nears convergence. The reason for this is that using a diagonal $\underline{\delta\mathbf{R}}$ triples the number of unknowns in the problem, as each zone then has three components of resistivity. The time taken to calculate the Jacobian matrix will increase by at least a factor of three (for the perturbation method), while for the inversion routine the solution space will have more local minima to be avoided. There is the question of what is actually gained by this ability to solve for anisotropic materials. The effects measured would give an idea of the structure of the rock, etc. which is extremely useful, relevant information.

5.2 Extensions to current adjoint method

This section considers the extension to the adjoint method beyond pole–pole surveys. Loke & Barker [1995] use the adjoint method but apply it to the homogeneous and 2D case. Although they give an example using a dipole–dipole survey their derivation is incomplete, as their $\delta\phi$ is a change in potential at a point rather than the change in the measurement. These issues are discussed in more detail in section 5.5.2, when we deal with the calculation of an analytical Jacobian matrix for the homogeneous case.

Starting from equation (5.7), which takes account of the boundary conditions but does not restrict the form of $\mathbf{J}$, $\mathbf{J}'$ or I'_s.

$$\int_\tau (\underline{\delta \mathbf{R}}\mathbf{J}) \,.\mathbf{J}' d\tau = \int_\tau I'_s \delta\phi d\tau \tag{5.7}$$

where I'_s is the source at the receiver position. This equation is completely general and applicable to any electrode array that may be used to acquire data in the field. Re-stating equation (5.8) for the pole–pole survey.

$$\delta\phi_{P1} = \int_\tau (\underline{\delta \mathbf{R}}\mathbf{J}) \,.\mathbf{J}' d\tau \tag{5.8}$$

Now consider the case of a dipole–pole survey (two sources $C1$ and $C2$ and one receiver $P1$). Here, I'_s and $\mathbf{J}'$ will be the same as in the pole–pole case the only difference will be in $\mathbf{J}$. By the principle of superposition for point sources, equation (5.8) can be rewritten for the dipole–pole case as

$$\delta\phi_{P1} = \int_\tau (\underline{\delta \mathbf{R}} (\mathbf{J}_{C1} - \mathbf{J}_{C2})) \,.\mathbf{J}' d\tau \tag{5.12}$$

The surveys of most interest are those where a potential difference is measured using an electrode dipole.

If we consider a pole–dipole survey using current electrode $C1$ and potential electrodes $P1$ and $P2$. This problem can be considered as the difference between two pole–pole surveys where the electrodes are $C1$ and $P1$, and $C1$ and $P2$. Therefore, these can be written as

$$\delta\phi_{P1} = \int_\tau (\underline{\delta \mathbf{R}}\mathbf{J}_{C1}) \,.\mathbf{J}'_{P1} d\tau \tag{5.13}$$

and

$$\delta\phi_{P2} = \int_\tau (\underline{\delta \mathbf{R}}\mathbf{J}_{C1}) \,.\mathbf{J}'_{P2} d\tau \tag{5.14}$$

The change in the potential difference is

$$\delta (\phi_{P1} - \phi_{P2}) = \delta\phi_{P1} - \delta\phi_{P2} = \int_\tau (\underline{\delta \mathbf{R}}\mathbf{J}_{C1}) \,.\mathbf{J}'_{P1} d\tau - \int_\tau (\underline{\delta \mathbf{R}}\mathbf{J}_{C1}) \,.\mathbf{J}'_{P2} d\tau \tag{5.15}$$

Equation (5.15) can be rewritten as

$$\delta\phi_{P1} - \delta\phi_{P2} = \int_\tau (\underline{\delta \mathbf{R}}\mathbf{J}_{C1}) \,.\, (\mathbf{J}'_{P1} - \mathbf{J}'_{P2}) \, d\tau \tag{5.16}$$

Similarly for the case of a dipole–dipole survey, if $\mathbf{J}$ is the current density of a dipole rather than a pole, it can be split into $\mathbf{J}_{C1}$and $\mathbf{J}_{C2}$. Applying the arguments stated above and equation (5.12) it follows that:

$$\delta\phi_{P1} - \delta\phi_{P2} = \int_{\tau} \left(\underline{\delta\mathbf{R}}\left(\mathbf{J}_{C1} - \mathbf{J}_{C2}\right)\right).\left(\mathbf{J}'_{P1} - \mathbf{J}'_{P2}\right) d\tau \tag{5.17}$$

We now examine equations (5.8), (5.12), (5.16) and (5.17). First, the change in the measurement is equal to the change in the resistivity multiplied by the product of actual and adjoint current densities in the zone. Secondly, the actual and adjoint parts are summed to give the total current densities for an elemental volume. The implication of this is that however many current sources there are, the solution would take the same form. There are no restrictions in the size or shape of the zone. There are also no restrictions on where the electrodes can be placed.

It follows that if the survey is carried out not on but near the surface the same boundary conditions can be used. However, if the survey is carried out between deep boreholes, then it can be assumed that the secondary field goes to zero below the surface, which means that all the boundary terms vanish for the same reason at the other five boundaries. This simplifies the problem because the volume modelled does not need to be as large as if the surface were included, thereby making it easier to solve.

5.3 Adjoint method for calculating the Jacobian

This section will show the connection between the Jacobian matrix and the adjoint described in section 5.2, for pole–dipole surveys. The derivations for pole–pole, dipole–pole and dipole–dipole will be found in appendices E, F and G respectively. Although $\underline{\delta\mathbf{R}}$ is more general than needed, it does enables us to see how the system develops for anisotropic zones.

As the title of this section suggests the aim is to calculate the Jacobian matrix using the adjoint of the forward problem. The intention is to use the equations developed in section 5.2. Before showing mathematically that there is a link between these equations, we shall explain the physical reasons for any link between the elements of the Jacobian and a perturbation in the resistivity, and a link between the Jacobian and the current densities of a zone.

Let us consider the elements of the Jacobian defined as

$$\underline{\mathcal{J}} = \nabla_{\boldsymbol{x}}\mathbf{F}$$

or, as in equation (5.1)

$$\underline{\mathcal{J}}_{q,r} = \frac{\partial F_q\left[\mathbf{x}\right]}{\partial x_r} \tag{5.1}$$

Of these two definitions, the second is more informative. $\mathbf{x}$ is the resistivity distribution, $F_q[\mathbf{x}]$ is the predicted measurement from such $\mathbf{x}$, q is a particular measurement and r is a particular zone. Therefore $\underline{\mathcal{J}}$ is the rate of change of the predicted measurements with respect to the rate of change of the resistivity of the zone. A value can be produced for this by perturbing the model slightly in each direction and finding the difference in the modelled measurements (Jackson, Gunn, Meldrum & Flint [1994]). The perturbation method helps us to understanding the physical implications of the Jacobian. The calculating of $\underline{\mathcal{J}}$ is very time consuming and the objective of this chapter is to investigate another method for doing this.

5.3.1 Physical significance of current density in calculating the Jacobian

Let us look at a single zone the resistivity of which we wish to perturb. In order to ascertain what is occurring we will reduce this to its simplest case. Let us look at the 2D case, since in 1D all the current would have to pass through the zone. Let us assume that the space is homogeneous, isotropic, and that the current is applied to this space so that it flows from one electrode to another electrode (in the pole–dipole case this electrode is assumed to be infinitely far away). The easiest case to understand is when the resistivity of the zone is the same as that of the surroundings.

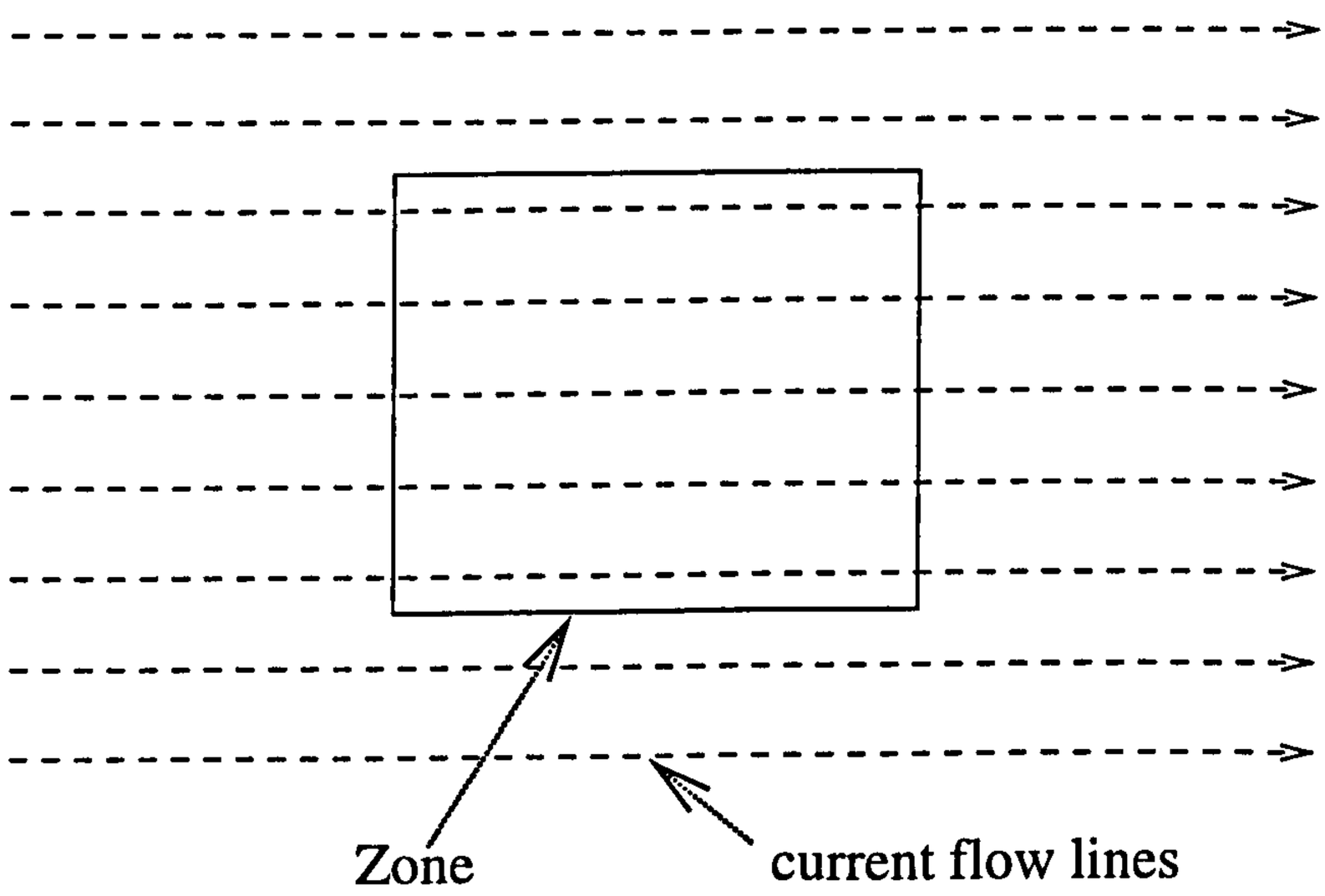

Figure 5.1: Current flow in homogeneous isotropic material.

In figure 5.1 there is no increase or decrease in the current density between

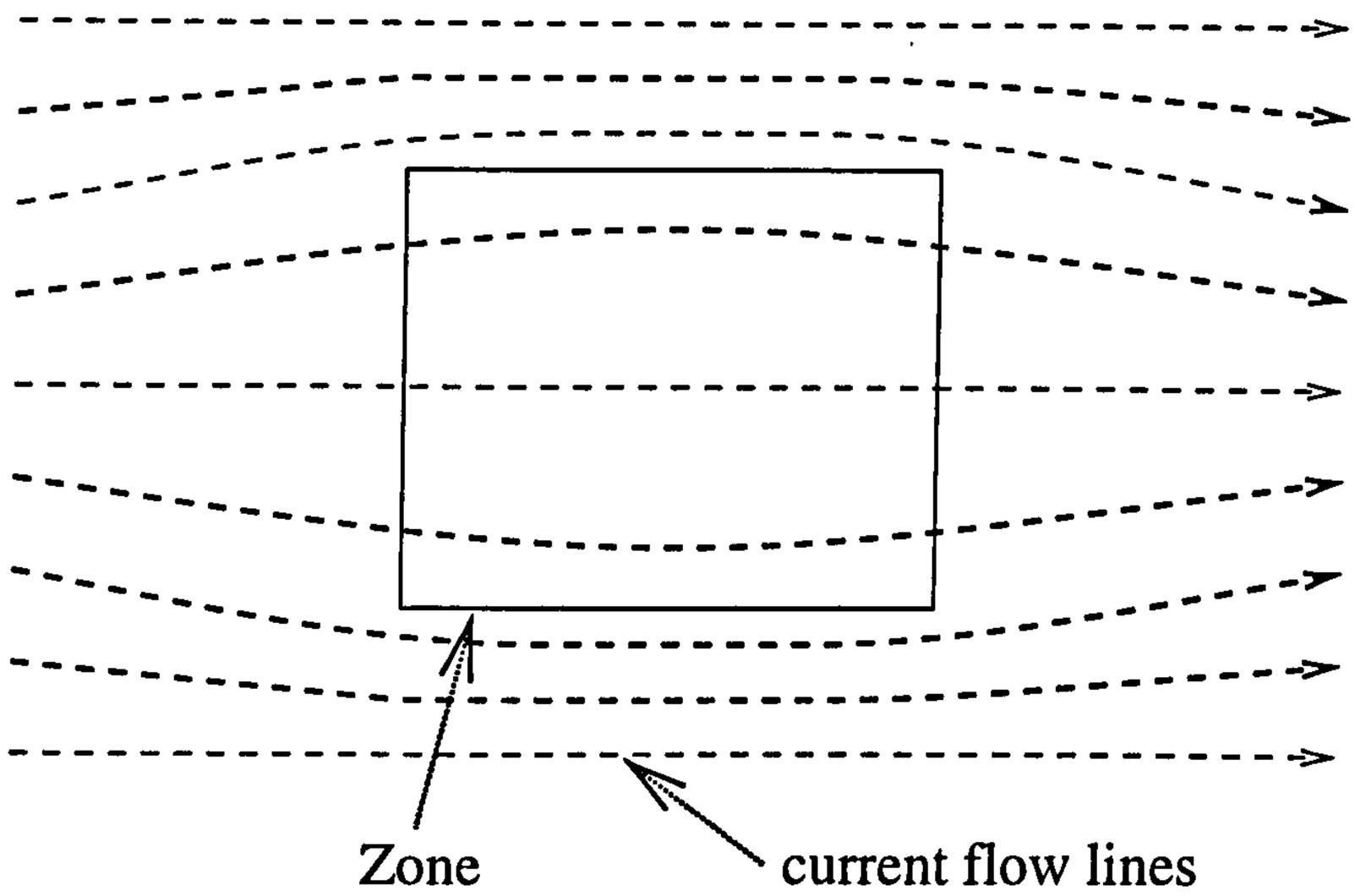

Figure 5.2: Current flow with a zone of higher resistivity than the surroundings.

the zone and its surroundings. This is the reference point for most of the other diagrams in this section. The first type of perturbation is where $\underline{\delta \mathbf{R}} = \delta\rho\underline{\mathbf{I}}$ which is the isotropic case. There are both positive and negative perturbations to the resistivity and which produce different flow patterns.

Let us give a positive perturbation to the resistivity zone in figure 5.1. The outcome, figure 5.2, shows that this reduces the current flowing through the zone. There are two implications of this: the first is that an increase in the resistivity means that less current will be flowing through the zone. Therefore the measurements will be higher, this is not likely to be a linear connection between the measurements and the change of resistivity in the zone. The second implication is that if the resistivity in the zone is much greater than the resistivity of the surroundings less current will flow in the zone: the accuracy of any measurements relating to the zone is then likely to be impaired. This may give a clue as to the reason for the occurrence of smearing during resistivity inversion (e.g. Sasaki [1992], Sasaki [1994], Loke & Barker [1996*b*]). This smearing is very common: in fact it is probably better to say that it is very rare for it not to occur. Smearing (i.e. an increase in resistivity) occurs at the side of the zone furthest from the electrode, as can be seen in 5.3.

The resistivity contours from the inversion are typically more spread out beneath the zone. This may be because the resistive zone directly above reduces the current flow beneath the zone, making the zone beneath harder to solve, because of a reduced current density. The current flow for this case would be similar to figure

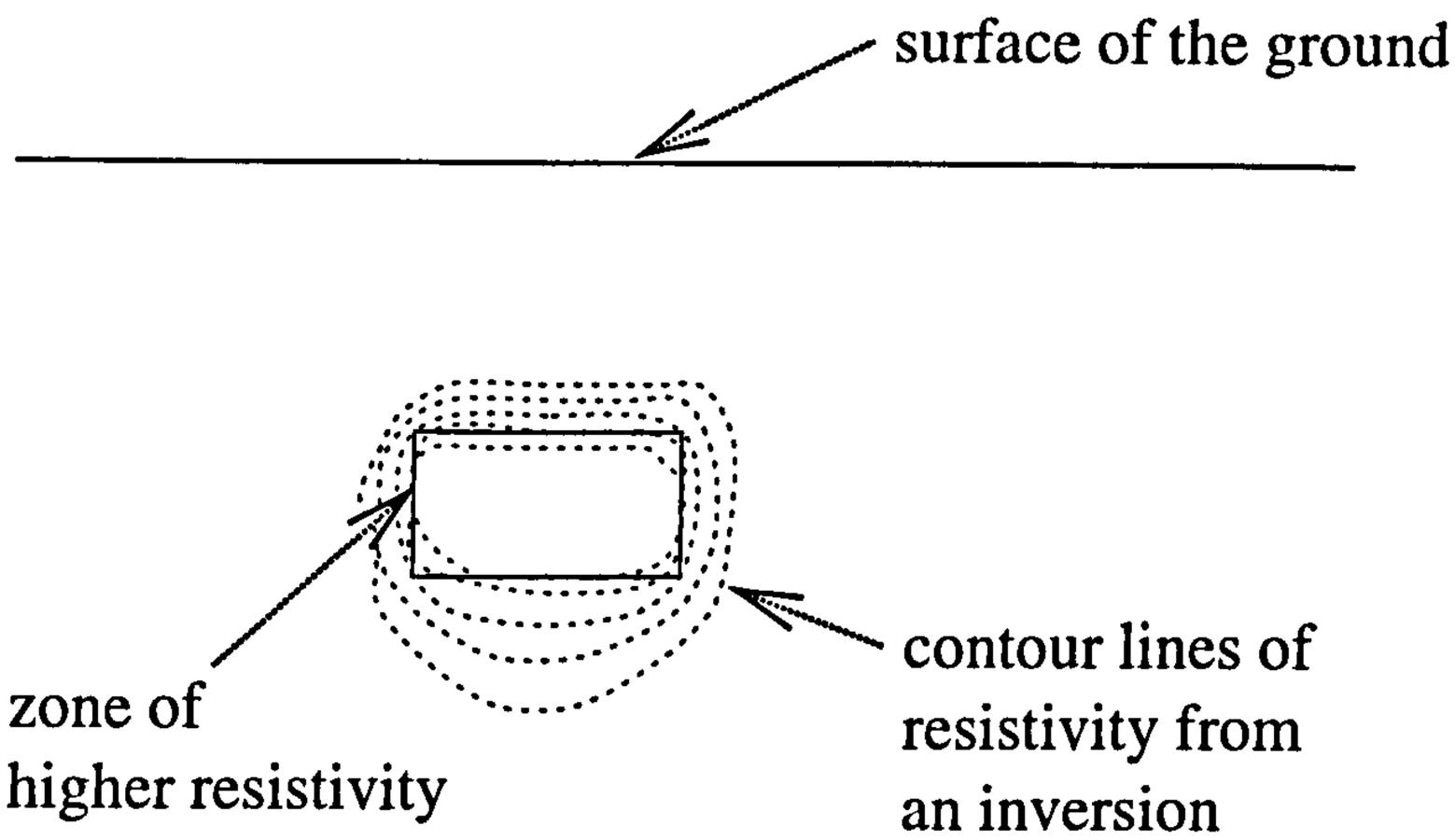

Figure 5.3: 'Smearing' of results beneath a zone of higher resistivity.

5.4.

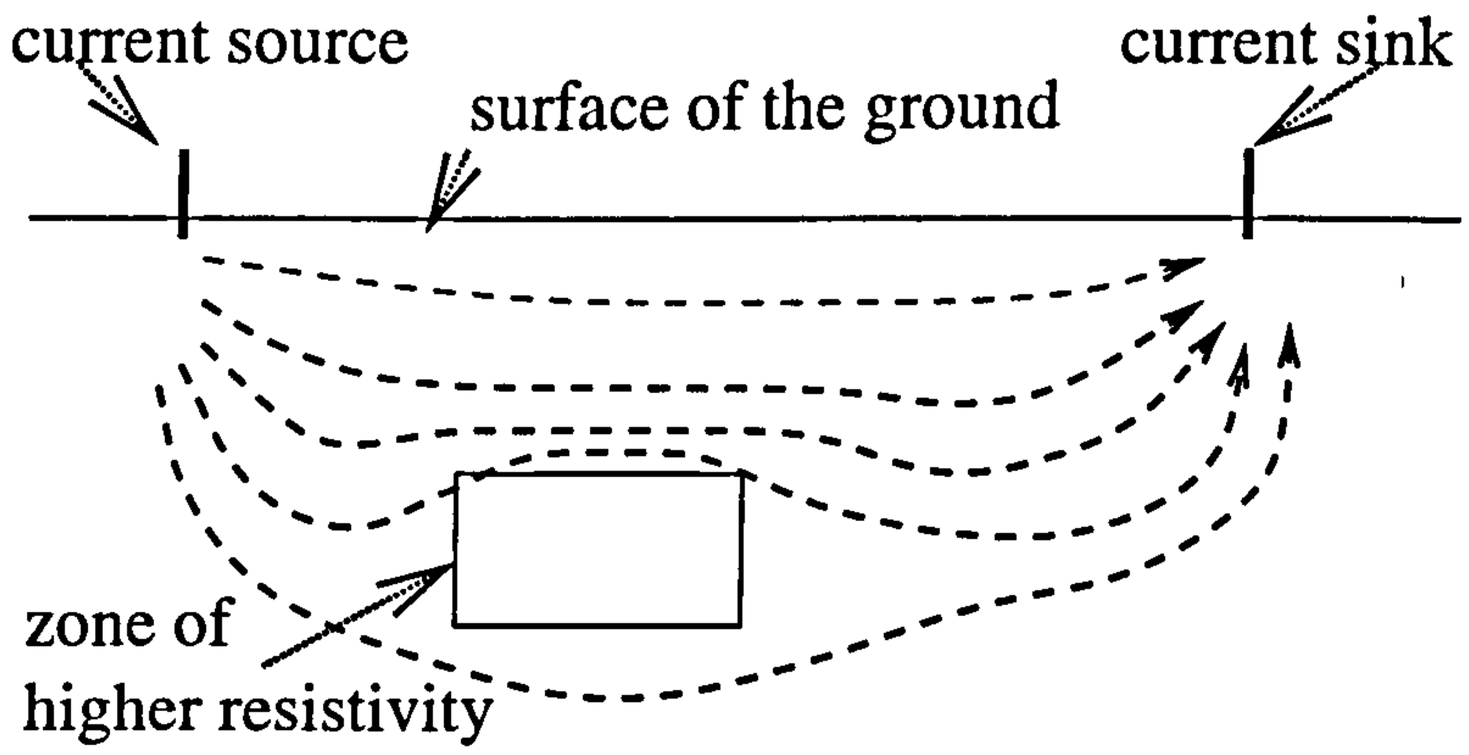

Figure 5.4: An example of reduced current flow beneath a zone of higher resistivity.

The effect of a decrease in resistivity is to encourage the current to flow through the zone, thereby increasing the zone's current density. This means that less current will be flowing through surrounding zones.

The current flow through an anisotropic zone is more complex. The ratio of the resistivities in the different directions will have the greatest effect, but there will also be an effect due to the angle of the anisotropy to the direction of current flow. The directions of these resistivities will be given by the eigenvectors of the matrix $\underline{\mathbf{R}}$. Figure 5.6 shows that the current will flow through an anisotropic zone. There is little doubt that the current around the zone will be affected by the anisotropic resistivity of the zone. If one of the directions inside the zone has a much larger resistivity than the rest, then locally, within the zone, the effect will be to allow us to treat the divergence of the current as one-dimensional.

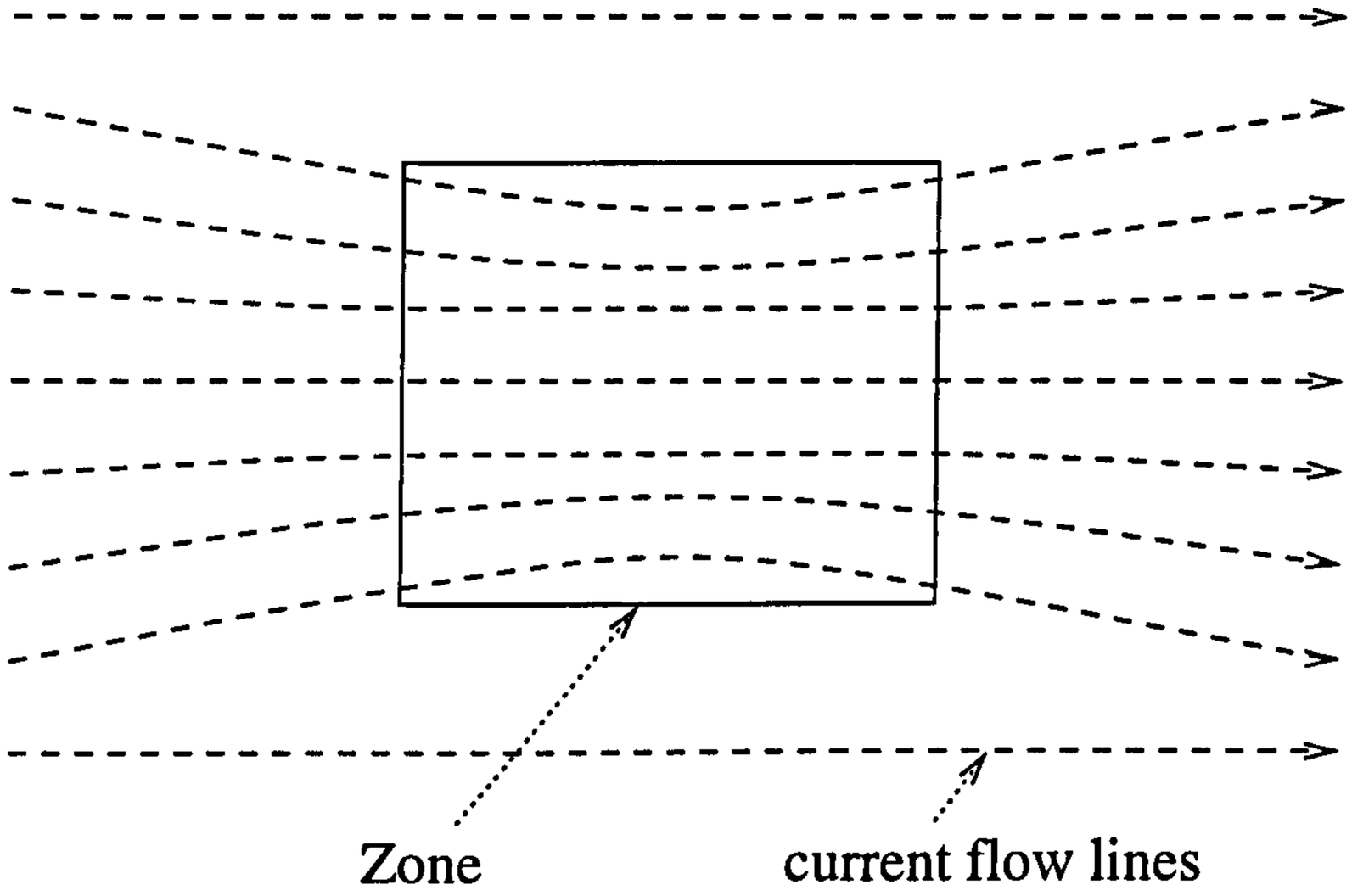

Figure 5.5: Current flow with a zone of higher resistivity than the surroundings.

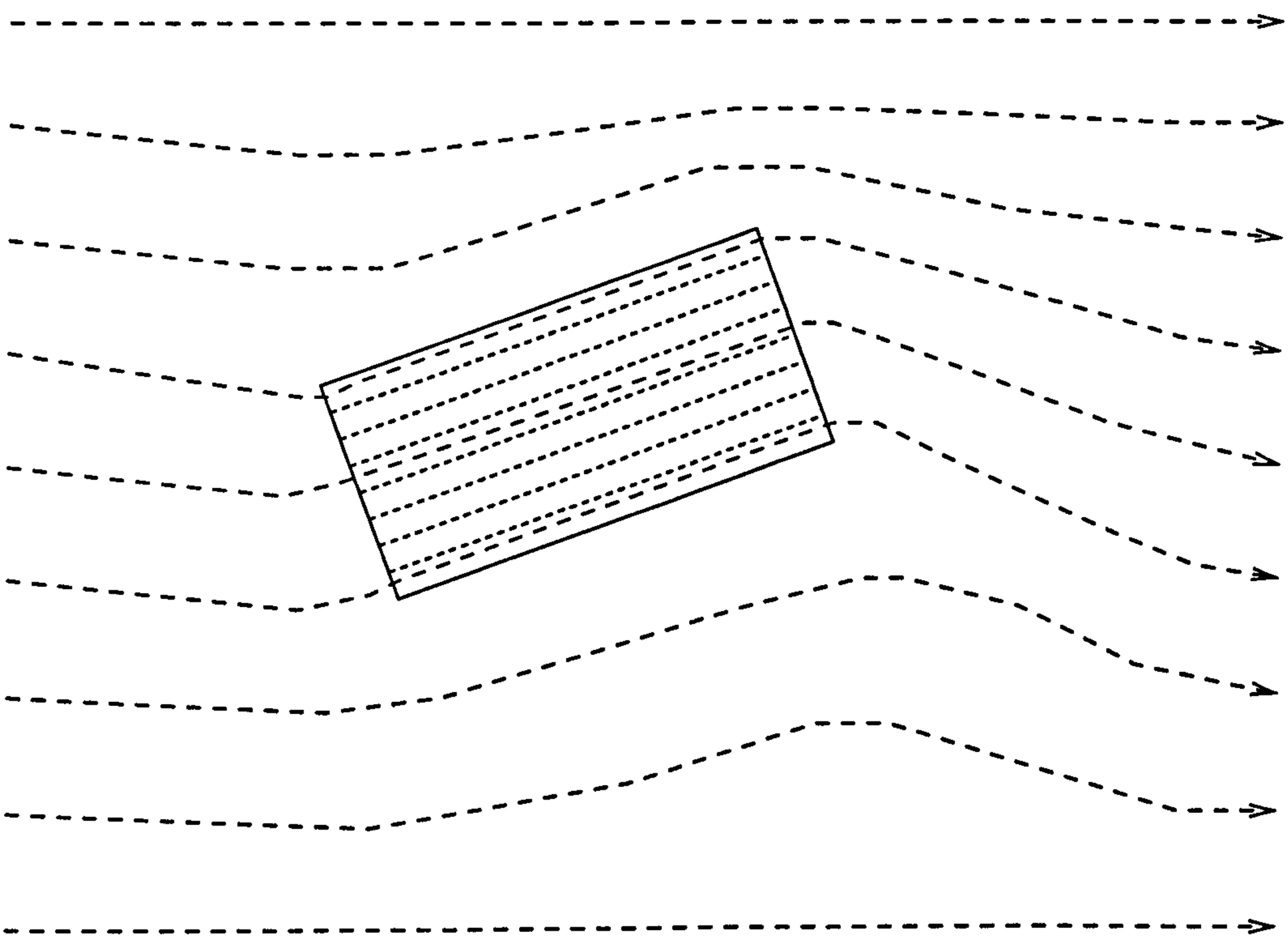

Figure 5.6: Current flow with a strong anisotropy.

5.3.2 Derivation of a method for pole–dipole surveys

This section will concentrate on pole–dipole surveys. Derivations for the other types of surveys will be found in the appendices E, F and G. In all four derivations a general form is given which allows for anisotropy.

Below is a schematic diagram (figure 5.7) of a pole–dipole survey, where the positive current source is at electrode C1 with a value i, the measurement v is the difference in the potentials at electrodes P1 and P2. All the electrodes are on the surface but there is no requirement for them to be on the surface.

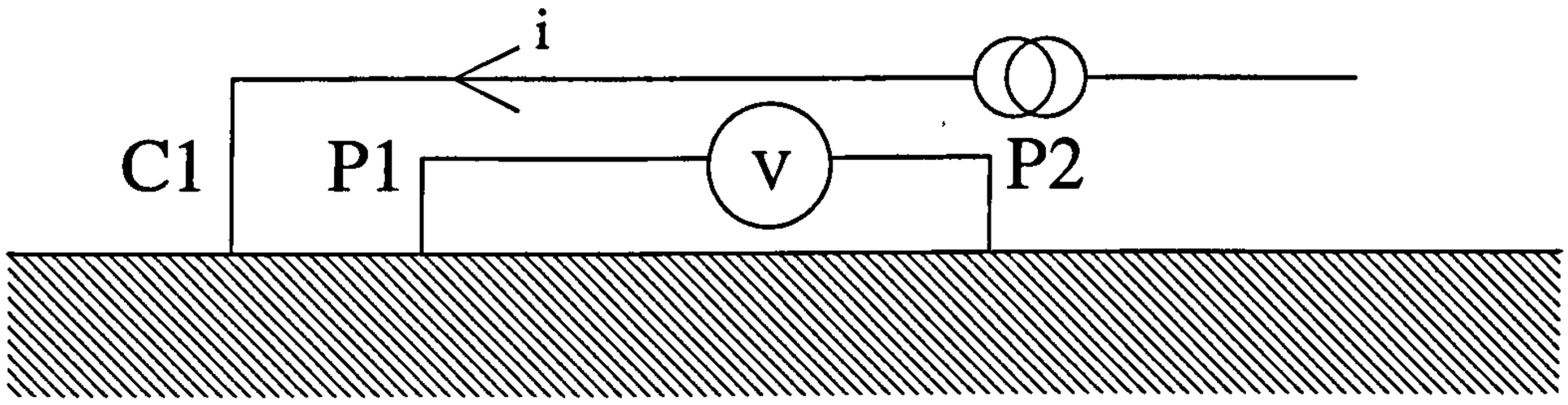

Figure 5.7: An example of a pole–dipole measurement.

Hence the normalised measurement is given by the difference between the potential at $P1$ and $P2$ divided by the current i (the notation used is i_{C1}).

$$v = \frac{\phi_{P1} - \phi_{P2}}{i_{C1}} \tag{5.18}$$

It follows from this that if there is a positive perturbation in the resistivity of a block r, this will give

$$v^+ = \frac{(\phi_{P1} + \delta\phi_{P1,r}) - (\phi_{P2} + \delta\phi_{P2,r})}{i_{C1}} \tag{5.19}$$

and the result of a negative perturbation on block r is

$$v^- = \frac{(\phi_{P1} - \delta\phi_{P1,r}) - (\phi_{P2} - \delta\phi_{P2,r})}{i_{C1}} \tag{5.20}$$

From the three equations above it is possible to produce three forms of δv.

$$\delta v^+ = v^+ - v = \frac{\delta\phi_{P1,r} - \delta\phi_{P2,r}}{i_{C1}} \tag{5.21}$$

$$\delta v^- = v - v^- = \frac{\delta\phi_{P1,r} - \delta\phi_{P2,r}}{i_{C1}} \tag{5.22}$$

$$\delta v = v^+ + v^- = \frac{2\delta\phi_{P1,r} - 2\delta\phi_{P2,r}}{i_{C1}} = \frac{2\left(\delta\phi_{P1,r} - \delta\phi_{P2,r}\right)}{i_{C1}} \tag{5.23}$$

Equation (5.23) is the central difference formula and has twice the perturbation of the other two. Also δv^+ is the same as δv^-, this is not necessarily true when using the perturbation approach but it is roughly true.

This gives us a formula for calculating the change in the measured voltage due to the change in resistivity of a block using the adjoint outlined above. To

relate this to the Jacobian $\underline{\mathcal{J}}$, equation (5.1), let us choose δv^+ as the change due to the perturbation of $\delta\rho_r$ and define $\delta v^+_{q,r}$ to be the change in the voltage of the q^{th} measurement due to a change in the resistivity of the r^{th} zone. It follows from this that

$$\underline{\mathcal{J}}_{q,r} = \frac{\partial F_q\left[\mathbf{x}\right]}{\partial x_r} = \frac{\delta v^+_{q,r}}{\delta\rho_r} \tag{5.24}$$

By substituting equation (5.21) into equation (5.24) we see that

$$\underline{\mathcal{J}}_{q,r} = \frac{\delta\phi_{P1,q,r} - \delta\phi_{P2,q,r}}{\delta\rho_r i_{C1}} \tag{5.25}$$

Now substituting equation (5.16) into equation (5.25),

$$\underline{\mathcal{J}}_{q,r} = \frac{\int_{\tau_r}\left(\underline{\delta\mathbf{R}}_r\mathbf{J}_{C1,q}\right).\left(\mathbf{J}'_{P1,q} - \mathbf{J}'_{P2,q}\right)d\tau_r}{\delta\rho_r i_{C1}} \tag{5.26}$$

At the end of section 5.1.2 some examples were given as to the forms $\underline{\delta\mathbf{R}}$ could take. To simplify equation (5.26) choose $\underline{\delta\mathbf{R}}$ such that

$$\underline{\delta\mathbf{R}} = \delta\rho\underline{\mathbf{S}} \tag{5.27}$$

where $\underline{\mathbf{S}}$ is a symmetric matrix of only 1's and 0's. Examples of $\underline{\mathbf{S}}$ could be as follows:-

$$\underline{\mathbf{S}} = \begin{pmatrix}1&0&0\\0&1&0\\0&0&1\end{pmatrix}, \begin{pmatrix}1&0&0\\0&0&0\\0&0&0\end{pmatrix}, \begin{pmatrix}0&0&0\\0&1&0\\0&0&0\end{pmatrix}, \text{ etc}$$

By substituting equation(5.27) into equation (5.26) the result is

$$\underline{\mathcal{J}}_{q,r} = \frac{\int_{\tau_r}\left(\delta\rho_r\underline{\mathbf{S}}_r\mathbf{J}_{C1,q}\right).\left(\mathbf{J}'_{P1,q} - \mathbf{J}'_{P2,q}\right)d\tau_r}{\delta\rho_r i_{C1}} \tag{5.28}$$

As $\delta\rho_r$ is merely a scalar constant, which is set to a certain value when using the perturbation method, it can be taken out of the integral. It can also be cancelled to give

$$\underline{\mathcal{J}}_{q,r} = \frac{1}{i_{C1}}\int_{\tau_r}\left(\underline{\mathbf{S}}_r\mathbf{J}_{C1,q}\right).\left(\mathbf{J}'_{P1,q} - \mathbf{J}'_{P2,q}\right)d\tau_r \tag{5.29}$$

However, if this is the isotropic case then $\underline{\mathbf{S}}_r = \underline{\mathbf{I}}$, and equation (5.29) becomes

$$\underline{\mathcal{J}}_{q,r} = \frac{1}{i_{C1}}\int_{\tau_r}\left(\mathbf{J}_{C1,q}\right).\left(\mathbf{J}'_{P1,q} - \mathbf{J}'_{P2,q}\right)d\tau_r \tag{5.30}$$

Let us now consider

$$\underline{\mathbf{S}} = \begin{pmatrix} 1 & 0 & 0 \\ 0 & 0 & 0 \\ 0 & 0 & 0 \end{pmatrix}$$

which is the anisotropic case for the x direction. Substituting then $\underline{\mathbf{S}}$ into equation (5.29)

$$\underline{\mathcal{J}}_{q,r} = \frac{1}{i_{C1}} \int_{\tau_r} \left(\begin{pmatrix} 1 & 0 & 0 \\ 0 & 0 & 0 \\ 0 & 0 & 0 \end{pmatrix} \mathbf{J}_{C1,q} \right) . \left(\mathbf{J}'_{P1,q} - \mathbf{J}'_{P2,q} \right) d\tau_r \tag{5.31}$$

To simplify equation (5.31), the current density vectors may be written as vector components. Therefore equation (5.31) becomes

$$\underline{\mathcal{J}}_{q,r} = \frac{1}{i_{C1}} \int_{\tau_r} \left(\begin{pmatrix} 1 & 0 & 0 \\ 0 & 0 & 0 \\ 0 & 0 & 0 \end{pmatrix} \begin{pmatrix} J_{C1,q,x} \\ J_{C1,q,y} \\ J_{C1,q,z} \end{pmatrix} \right) . \left(\begin{pmatrix} J'_{P1,q,x} \\ J'_{P1,q,y} \\ J'_{P1,q,z} \end{pmatrix} - \begin{pmatrix} J'_{P2,q,x} \\ J'_{P2,q,y} \\ J'_{P2,q,z} \end{pmatrix} \right) d\tau_r$$

which can be simplified to

$$\underline{\mathcal{J}}_{q,r} = \frac{1}{i_{C1}} \int_{\tau_r} J_{C1,q,x} \left(J'_{P1,q,x} - J'_{P2,q,x} \right) d\tau_r \tag{5.32}$$

The implications of this are that the change in the measurement due to a change in the resistivity in the x direction is dependent on the current densities in the x direction from both the current and potential electrodes. This is a useful result as it implies that one only needs to know the current densities in the direction in which the resistivity is being perturbed. It follows that it is possible to calculate the Jacobian for anisotropic problems using the adjoint method.

The adjoint current density is calculated in an identical way to that for the actual current density. The proof for the adjoint is in appendix C. Equation (5.30) becomes

$$\underline{\mathcal{J}}_{q,r} = \frac{1}{i_{C1}} \int_{\tau_r} (\mathbf{J}_{C1,q}) . (\mathbf{J}_{P1,q} - \mathbf{J}_{P2,q}) \, d\tau_r \tag{5.33}$$

Equation (5.33) gives us a means of calculating the Jacobian that does not depend on choosing a perturbation of the resistivity of a zone. All that is needed to calculate the value is the current density within the zone from each electrode used in the particular measurement. In this case they are the three electrodes $C1$, $P1$ and $P2$.

5.4 Practical implementation

This section describes the implementation of the adjoint method for calculating the Jacobian. It contains a description of the algorithm used to calculate the values in the Jacobian and the theoretical advantages and disadvantages of the particular method chosen. A particular problem arises in marrying the potentials from two finite difference meshes used to calculate the forward problem. The problem involves the question of how the potentials are used and the effect of errors in these potentials. A solution using overlapping grids of different sizes (but with some common nodes) is presented.

5.4.1 The method as implemented

Equation (5.33) as derived in section 5.3.2 is in itself not particularly useful as it is not possible to derive an analytic function for current densities in 3D heterogeneous space. However, the forward problem calculates potentials and not current densities. Equation (5.33) is

$$\mathcal{J}_{q,r} = \frac{1}{i_{C1}} \int_{\tau} (\mathbf{J}_{q,C1}) \,.\, (\mathbf{J}_{q,P1} - \mathbf{J}_{q,P2})\, d\tau \tag{5.33}$$

where the r zone is made up of a number of cells of the finite-difference mesh. Hence, equation (5.33) can be rewritten as a sum over all the cells in the τth zone where δx, δy and δz are the dimensions of the cells in the zone.[2]

$$\mathcal{J}_{q,r} = \frac{1}{i_{C1}} \sum_{\tau} \mathbf{J}_{q,C1} \,.\, (\mathbf{J}_{q,P1} - \mathbf{J}_{q,P2})\, \delta x \delta y \delta z \tag{5.34}$$

If the number of cells is very large, equation (5.34) tends to equation 5.33. This is a good approximation, except where there are rapid changes in current density, which occurs only in the region around the electrodes. Equation (5.34) is then a good approximation to the true value of an element of the Jacobian.

There are three methods that could be used to improve this. First, we could increase the number of grid cells in each zone, particularly near the electrodes, since this would either mean that the zones were bigger and fewer in number or that the mesh would be finer. Neither of these options is helpful. Secondly, we could use a numerical integration scheme such as the trapezium rule or Simpson's rule. Both would be an improvement on the current method but neither is particularly good at interpolating near the electrode source; but neither is equation (5.34) for

[2] δx, δy and δz can vary from cell to cell.

the same reason. The error arises due to the finite-difference approximation of a point source. Using a better numerical integrating package on an approximation is not necessarily going to be beneficial. Thirdly, we could use a correction factor. Correction factors are used widely in this field (e.g. Dey & Morrison [1979]). They are used in correcting the modelled measurements using a comparison with analytic potentials, and are, therefore, an integral part of any direct perturbation method.

It is possible to write current density in terms of potential: using the vector form of Ohm's Law

$$\mathbf{E} = -\nabla\phi = \rho\mathbf{J} \tag{5.35}$$

where $\mathbf{E}$ is the electrical field. This approach will be used as one of the methods of calculating an analytic homogeneous Jacobian in section 5.5.2. However this is not a particularly practical way forward as differentiating at discrete points leads to an increase in errors and the likelihood of singularities. Therefore a different route is necessary. As $\mathbf{J}$ is a vector, taking the x component in $\mathbf{J}$ is:-

$$J_x = \frac{i_x}{\delta y.\delta z} \tag{5.36}$$

Equation (5.36) gives the current density in the x direction in terms of I_x, the current in the x direction can be calculated directly from the 3D forward finite difference model.

Let us consider the 1D case, with three nodes, and in particular the current density of the middle node:

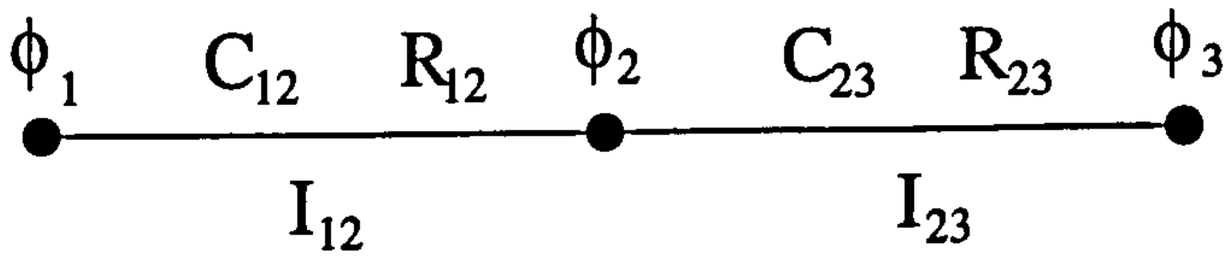

Figure 5.8: 1D case for calculating current at node 2

C is the value of conductance between the nodes and ϕ is the potential at each node. Applying Ohm's Law to this case produces

$$I_{12} = \frac{\phi_2 - \phi_1}{R_{12}} = (\phi_2 - \phi_1)\, C_{12} \tag{5.37}$$

If the above is repeated between nodes 2 and 3,

$$I_{12} = \frac{\phi_3 - \phi_2}{R_{23}} = (\phi_3 - \phi_2)\, C_{23} \tag{5.38}$$

From equations (5.37) and (5.38) the total current at node 2 can be found:

$$total\ current = I_{12} + I_{23} \tag{5.39}$$

This is a very useful check of the method since it is effectively applying Kirchoff's Law at node 2, which means that the total should equal zero unless there is a current source at that node. We shall now define a direction (the x direction in this case) of the current density **J** as :-

$$J_2 = \frac{(I_{12} + I_{23})}{2} \frac{1}{\delta y \delta z} = \frac{I_2}{\delta y \delta z} \tag{5.40}$$

where I_2 is the average current flowing in the cell. The fact that this is an average and not a derivative means that it smoothes rather than roughens the solution.

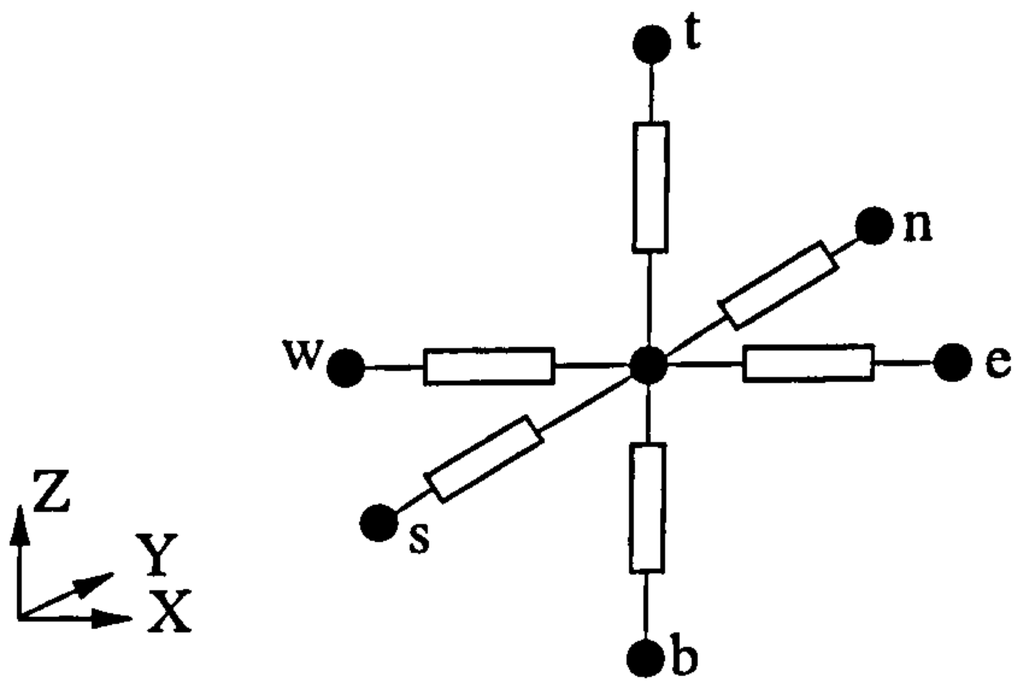

Figure 5.9: Labelling scheme in 3D.

Using figure 5.9 equation (5.40) would become a series of equations in 3D, which are

$$J_x = \frac{(I_{xw} + I_{xe})}{2\,(\delta y \delta z)} = \frac{I_x}{\delta y \delta z} \tag{5.41}$$

$$J_y = \frac{(I_{yn} + I_{ys})}{2\,(\delta x \delta z)} = \frac{I_y}{\delta x \delta z} \tag{5.42}$$

$$J_z = \frac{(I_{zt} + I_{zb})}{2\,(\delta x \delta y)} = \frac{I_z}{\delta x \delta y} \tag{5.43}$$

These substitutions would express the Jacobian in terms of the currents. Let us consider a node (k, l, m) in the finite-difference grid. Using the left-hand side of equation (5.37) a template is provided for all three directions, for converting current into potential. Then equations (5.41), (5.42) and (5.43) become

$$J_{x,k,l,m} = \frac{(\phi_{k-1,l,m} - \phi_{k,l,m})\, C_{w,k,l,m} + (\phi_{k,l,m} - \phi_{k+1,l,m})\, C_{e,k,l,m}}{2\delta y_{k,l,m} \delta z_{k,l,m}} \tag{5.44}$$

$$J_{y,k,l,m} = \frac{(\phi_{k,l-1,m} - \phi_{k,l,m})\, C_{n,k,l,m} + (\phi_{k,l,m} - \phi_{k,l+1,m})\, C_{s,k,l,m}}{2\delta x_{k,l,m}\delta z_{k,l,m}} \tag{5.45}$$

$$J_{z,k,l,m} = \frac{(\phi_{k,l,m-1} - \phi_{k,l,m})\, C_{t,k,l,m} + (\phi_{k,l,m} - \phi_{k,l,m+1})\, C_{b,k,l,m}}{2\,(\delta x_{k,l,m}\delta y_{k,l,m})} \tag{5.46}$$

Expanding equation (5.34),

$$\underline{\mathcal{J}}_{q,r} = \frac{1}{i_{C1}} \sum_{p=1}^{no.cells} \begin{pmatrix} J_{C1,x,q,p}.\,(J_{P1,x,q,p} - J_{P2,x,q,p})\,\delta x_p.\delta y_p.\delta z_p \\ +J_{C1,y,q,p}.\,(J_{P1,y,q,p} - J_{P2,y,q,p})\,\delta x_p.\delta y_p.\delta z_p \\ +J_{C1,z,q,p}.\,(J_{P1,z,q,p} - J_{P2,z,q,p})\,\delta x_p.\delta y_p.\delta z_p \end{pmatrix} \tag{5.47}$$

By substituting equations (5.44), (5.45) and (5.46) into equation (5.47), it is possible to obtain an algorithm for the adjoint method for calculating the Jacobian from the finite-difference potentials produced by solving the forward problems. This algorithm is given in equation (D.2) of appendix D.

This method requires the potentials for all cells of the finite-difference grid within the zones plus a layer cells around the outside of the zones, for all the electrodes that are current electrodes and/or potential electrodes. Even for a reasonable-sized array of electrodes very large numbers of potentials need to be accessed. Consequently, large amounts of RAM are required or the program is run with excessive disk access.[3]

5.4.2 The two grid problem

This section describes the method that was developed to solve a problem encountered during the development of the adjoint method. The solution provided an insight into the constraints on calculating the Jacobian using this method.

The problem was caused by the fact that two grids are used Jackson et al. [1997]. A coarse grid (L) is used to calculate the boundary potentials for the fine grid (S) [4]. This arrangement is satisfactory as long as all the zones are within a fine grid. However this is not always the case (see figure 5.10). The fine grid could be increased in size to encompass the zones, however this was rejected as it would take too long to calculate.

---

[3]For the test problem used in Chapter 6 it was nearly possible to run it in RAM, but as this was only a 2D array of 3D zones it was decided to use a set of temporary files on the hard disk. Large problems could be tackled, but at the expense of slower running. After a large amount of memory was assigned to disk caching, it was found that the computational speed was increased dramatically and the disk access reduced. It is now becoming possible to move to a completely RAM based approach, since 128MBytes of RAM, or more, is widely accessible. This can be easily incorporated into the program.

[4](L) and (S) stand for large and small which is the definitions used in the inversion program.

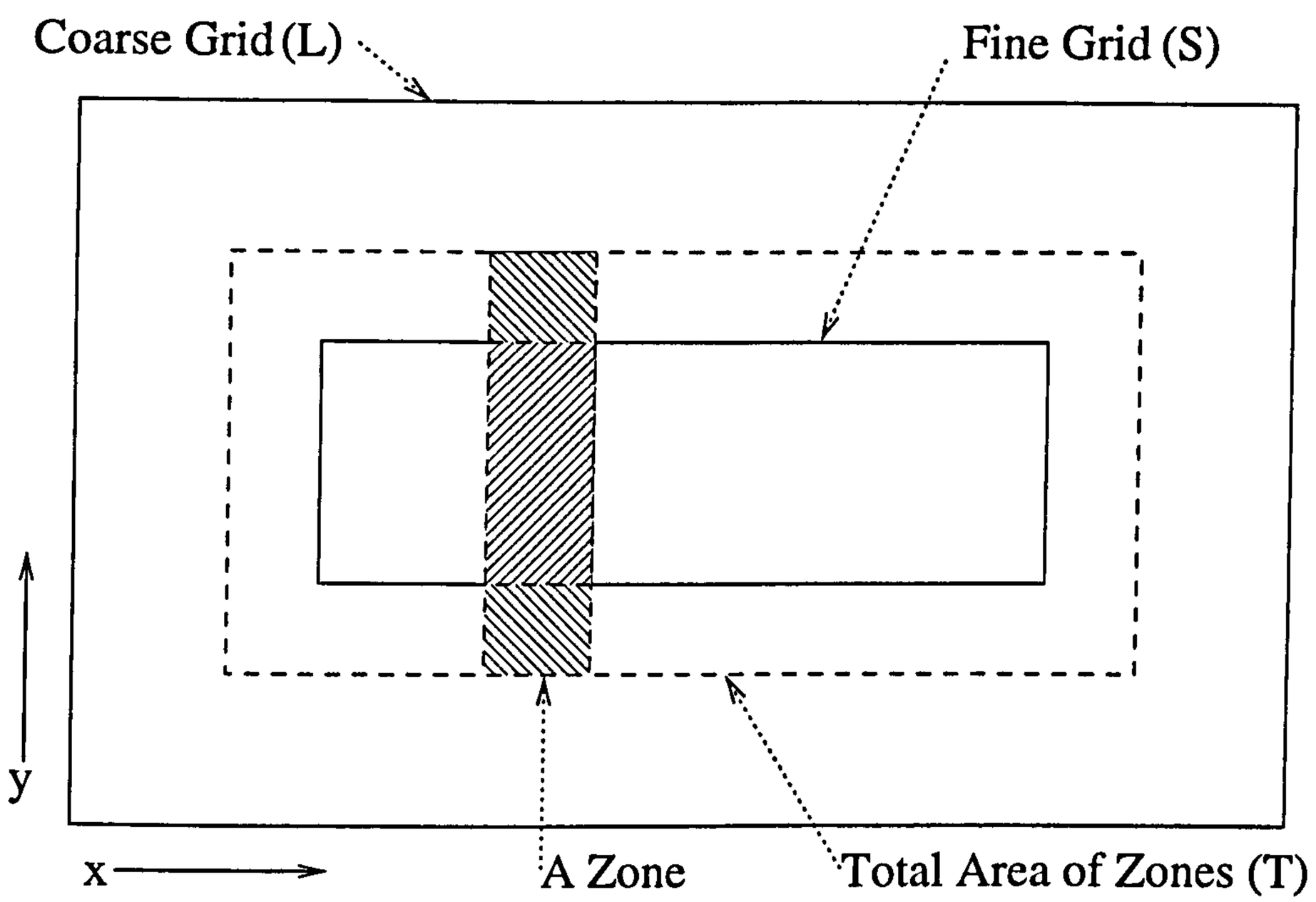

Figure 5.10: Plan view of the two grids and zones

A third grid (T) was developed using the same size cells as the fine grid but covering the whole of the volume of the zones. Onto this third grid (T) interpolated coarse grid potentials were placed. Then the potentials calculated using the fine grid (S) were used to define the potentials in the 'fine grid region' of the third grid (T). These potentials were then used to calculate the current densities for the values of the Jacobian. The result of this was to produce a Jacobian with values that did not always correspond to those that had been calculated to test the adjoint method. This was a surprise, as the potentials were the same as those used for the test case, and since the code used to calculate the values of current density and the Jacobian had not been changed, the only difference was that previously the zones where totally within the fine grid. It was found that the total current flowing into each node was not always close to zero. This test defines the finite-difference error at each node. The interpolated nodes and those of the original fine mesh were largely 'error free' but on the boundary between the two there were substantial errors. These errors were of similar magnitude to the potentials at these nodes, resulting in errors of three or four orders of magnitude greater than the elements of the Jacobian.

The obvious answer to this problem was to make the fine grid bigger. This was not really practical as the time to calculate each of the sources became vastly greater. During the search for an answer various interpolation schemes were

investigated but the 3D nature of the of the boundary meant that some sort of iterative solver was required. One solution was to use the same code as the forward problem to recalculate this boundary, but this entailed calculating a much larger fine mesh.

The solution that was chosen and eventually developed, evaded these problems by joining the grids together at the last stage rather than superimposing them at the first stage as follows:

1. the value of the Jacobian $\underline{\mathcal{J}}_1$ is calculated using potentials on the coarse grid (L) and then interpolated on to an extended finer grid (T) which includes the whole of each zone.

2. the value of the Jacobian $\underline{\mathcal{J}}_2$ is calculated using the interpolated potentials in 1.(above) but now over the portion of the zone that lies within the fine grid (s).

3. the value of the Jacobian $\underline{\mathcal{J}}_3$ in 2 above is calculated using the potential calculated on the fine grid (s).

The Jacobian is calculated as $\underline{\mathcal{J}} = \underline{\mathcal{J}}_1 - \underline{\mathcal{J}}_2 + \underline{\mathcal{J}}_3$, as shown in figure 5.11, solving the problem of the different sized grids. To calculate the adjoint Jacobian the grids must be set up so that the coarse grid (L) interpolates correctly onto the extended fine grid (T) otherwise parts of the program which rely on the nodes being in the same place will fail.

The main conclusion arising from this section is that the adjoint method for calculating the Jacobian depends on the calculation of accurate potentials to produce accurate current densities. Accuracy is important because a potential difference is being used and the potentials can be of similar magnitude. [5]

[5]Fortran variables were used which stored sixteen significant figures and the convergence criterion for iterative forward problem solvers is set at 1×10^{-14}. This allows the potential difference between neighbouring nodes to be at least three orders of magnitude larger than the error in the potentials.

However there is a disadvantage to the method, namely the need to store both the fine grid (S) potentials and the ones interpolated coarse grid (L) for all the electrodes used, in addition to the conductivities for the extended fine mesh. The test survey had 41 electrodes each of which had associated coarse and fine grids. The fine grid (S) takes up 96K and the extended fine grid (T) takes up 384K. It was possible to store these in 64Mb of memory but the PC was only able to run a very basic operating system and did not always load the program. A version of the

(*continued on p78*)

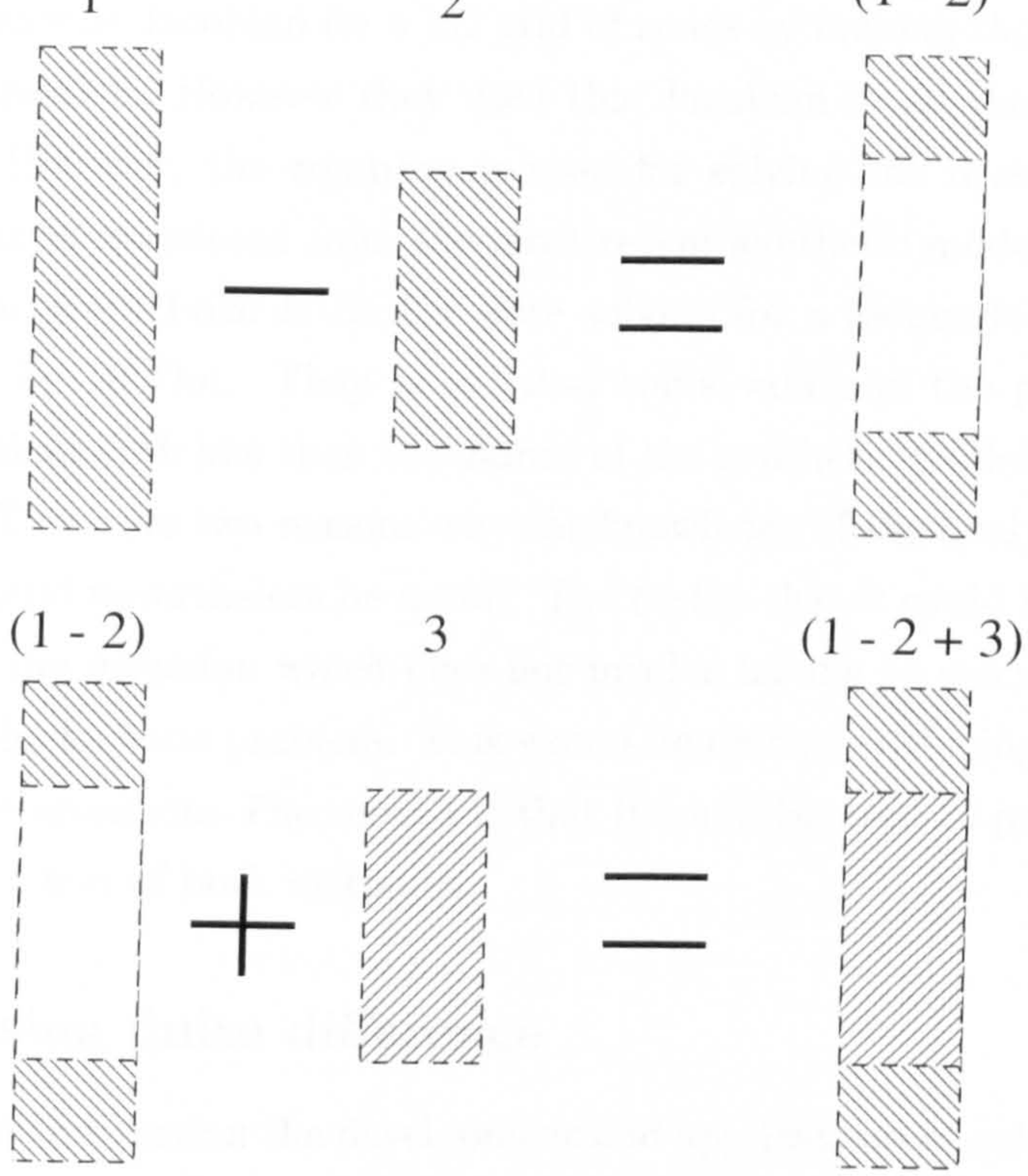

Figure 5.11: plan view of $1 - 2 + 3$ method

5.5 Analytic methods for calculating the homogeneous Jacobian

The homogeneous Jacobian is calculated using a homogeneous resistivity for the whole of the volume of the survey. The Jacobian is also the starting point for the inversions. Loke & Barker [1995] showed that it was possible to calculate the homogeneous Jacobian for a 2D grid of zones by making the zone infinitely long in the y direction. However they used this Jacobian in all the iterations for their inversion. However, the equation is used for solving the inverse problem only if the Jacobian is calculated from the most recent synthetic model. This is obviously not the case, since Loke & Barker were solving for a rectangle of zones of $500\Omega m$ surrounded by $100\Omega m$. They noted that some values of the predicted resistivity were more than 50% less than the values of the synthetic model.

There are two reasons why the knowledge of the analytical homogeneous Jacobian would nevertheless be useful. The first is that it could be used for the first iteration of the inversion which does not involve having to calculate the potentials by solving the forward problem. This would be quicker, reducing the time taken to calculate the inversion. The second is that it could be used to produce a correction factor or as a test of both methods.

5.5.1 Using finite difference

In this section the development and applications of a Jacobian calculated from analytic potentials are described, extending the method developed in section 5.4 above.

This method is the similar to equation (D.2), in that the same equation is used to calculate the Jacobian. The difference lies in the method used for calculating the potential, namely a half-space for a point source. If the source is at the origin, then the potential is calculated by

(*continued from p76*)

program which calculates the adjoint Jacobian using potentials read from files has been developed (there are two per electrode). These files are pre-processed so that the files contain only the potentials in a structure that is known by the program. During the calculation of the Jacobian in the program, the appropriate six files were loaded so that all the zones for each particular measurement could be calculated. While this approach is disk intensive and slower, it is generally applicable to full 3D surveys using 220 electrodes.

$$\phi = \frac{\rho I}{2\pi \mathcal{R}} \tag{5.48}$$

where $\mathcal{R}$ is the distance from the source, using Cartesian co-ordinates where the source is not necessarily at the origin. Equation(5.48) can be written as

$$\phi = \frac{\rho I}{2\pi \sqrt{(x-x_0)^2 + (y-y_0)^2 + (z-z_0)^2}} \tag{5.49}$$

where x_0, y_0 and z_0 are the co-ordinates of the electrode.

This is used to calculate all the nodes in the grid except the source node. This has to be calculated differently as the potential would of course be infinite, as would the value of the Jacobian for the zone including the electrode. This is neither realistic nor particularly practical. The method used for calculating this is to use the finite-difference equations at the source (i.e. using Kirchoff's Law).

Our purpose in calculating this approximation was to provide a simple method for checking the algorithm from equation (D.2). [6] This method was not developed to be used as a correction but it could be used as a computationally cheap method for calculating the first iteration of an inversion. The time saving comes from not reading any potential files during the calculation of the Jacobian.

5.5.2 Using numerical integration

This section produces an good approximation to the 'analytic homogeneous' Jacobian for the pole–dipole survey in 3D. This is similar in some ways to the work done by Loke & Barker [1995]. They started from an isotropic form of equation (5.8), except with the current densities substituted by the divergence of the potential. Loke & Barker were primarily interested in 2D zones where the zones were infinitely long in the y direction. They also forced the electrodes to be at the ground surface.

As with section 5.4 the solution of equation (5.33) is to be calculated from potential values.

$$\underline{\mathcal{J}}_{q,r} = \frac{1}{i_{C1}} \int_{\tau_r} (\mathbf{J}_{C1,q}) \,.\, (\mathbf{J}_{P1,q} - \mathbf{J}_{P2,q})\, d\tau_r \tag{5.33}$$

In section 5.4.1 the use of

$$-\nabla\phi = \rho\mathbf{J}$$

[6] This proved a much better method for spotting mistakes in the code than comparison with the perturbation method Jacobian although this was also used.

was rejected because numerical differentiation inherently increases errors in this case enough to affect the results significantly. However this limitation does not apply to an analytic method. Therefore, substituting for **J** in equation (5.33) produces

$$\underline{\mathcal{J}}_{q,r} = \frac{1}{i_{C1}} \int_{\tau_r} \left(\frac{-\nabla \phi_{C1,q}}{\rho} \right) . \left(\frac{-\nabla \phi_{P1,q}}{\rho} - \frac{-\nabla \phi_{P2,q}}{\rho} \right) d\tau_r. \tag{5.50}$$

The value of the current source is i_{C1}. Using equation (5.49), assuming the current source is at the origin the value of $\nabla \phi$ is,

$$\nabla \phi = -\frac{\rho i_{c1}}{2\pi} \begin{pmatrix} \frac{x}{(x^2+y^2+z^2)^{\frac{3}{2}}} \\ \frac{y}{(x^2+y^2+z^2)^{\frac{3}{2}}} \\ \frac{z}{(x^2+y^2+z^2)^{\frac{3}{2}}} \end{pmatrix} \tag{5.51}$$

The locations of the three electrodes $C1$, $P1$ and $P2$ are (x_{C1}, y_{C1}, z_{C1}), (x_{P1}, y_{P1}, z_{P1}) and (x_{P2}, y_{P2}, z_{P2}). we se that

$$\mathbf{J}_{C1,q} = \frac{i_{C1,q}}{2\pi} \begin{pmatrix} \frac{(x-x_{C1,q})}{\left((x-x_{C1,q})^2+(y-y_{C1,q})^2+(z-z_{C1,q})^2\right)^{\frac{3}{2}}} \\ \frac{(y-y_{C1,q})}{\left((x-x_{C1,q})^2+(y-y_{C1,q})^2+(z-z_{C1,q})^2\right)^{\frac{3}{2}}} \\ \frac{(z-z_{C1,q})}{\left((x-x_{C1,q})^2+(y-y_{C1,q})^2+(z-z_{C1,q})^2\right)^{\frac{3}{2}}} \end{pmatrix} \tag{5.52}$$

Equation (5.52) and the versions for $\mathbf{J}_{P1,q}$ and $\mathbf{J}_{P2,q}$ can be substituted into equation (5.33).

$$\underline{\mathcal{J}}_{q,r} = \frac{1}{i_{C1}} \int_{\tau_r} \left(\frac{i_{C1,q}}{2\pi} \begin{pmatrix} \frac{(x-x_{C1,q})}{\left((x-x_{C1,q})^2+(y-y_{C1,q})^2+(z-z_{C1,q})^2\right)^{\frac{3}{2}}} \\ \frac{(y-y_{C1,q})}{\left((x-x_{C1,q})^2+(y-y_{C1,q})^2+(z-z_{C1,q})^2\right)^{\frac{3}{2}}} \\ \frac{(z-z_{C1,q})}{\left((x-x_{C1,q})^2+(y-y_{C1,q})^2+(z-z_{C1,q})^2\right)^{\frac{3}{2}}} \end{pmatrix} \right)$$

$$\cdot \left(\frac{i_{C1,q}}{2\pi} \begin{pmatrix} \frac{(x-x_{P1,q})}{\left((x-x_{P1,q})^2+(y-y_{P1,q})^2+(z-z_{P1,q})^2\right)^{\frac{3}{2}}} \\ \frac{(y-y_{P1,q})}{\left((x-x_{P1,q})^2+(y-y_{P1,q})^2+(z-z_{P1,q})^2\right)^{\frac{3}{2}}} \\ \frac{(z-z_{P1,q})}{\left((x-x_{P1,q})^2+(y-y_{P1,q})^2+(z-z_{P1,q})^2\right)^{\frac{3}{2}}} \end{pmatrix} \right)$$

$$-\frac{i_{C1,q}}{2\pi}\left(\begin{array}{c}\dfrac{(x-x_{P2,q})}{\left((x-x_{P2,q})^2+(y-y_{P2,q})^2+(z-z_{P2,q})^2\right)^{\frac{3}{2}}}\\ \dfrac{(y-y_{P2,q})}{\left((x-x_{P2,q})^2+(y-y_{P2,q})^2+(z-z_{P2,q})^2\right)^{\frac{3}{2}}}\\ \dfrac{(z-z_{P2,q})}{\left((x-x_{P2,q})^2+(y-y_{P2,q})^2+(z-z_{P2,q})^2\right)^{\frac{3}{2}}}\end{array}\right)d\tau_r \qquad (5.53)$$

Equation (5.53) can be simplified by expanding out the dot product. This splits the problem into the difference between two pole–pole surveys. τ_r is the volume over which the integration is performed. τ_r be a rectangular box defined by the opposite corners $(x_{b,r},\ y_{b,r},\ z_{b,r})$ and $(x_{e,r},\ y_{e,r},\ z_{e,r})$ (b is the "beginning" and e is the "end" of the box).

$$\underline{\mathcal{J}}_{q,r}=\frac{i_{C1,q}}{4\pi^2}\int_{z_{b,r}}^{z_{e,r}}\int_{y_{b,r}}^{y_{e,r}}\int_{x_{b,r}}^{x_{e,r}}$$
$$\left(\frac{\left((x-x_{C1,q})(x-x_{P1,q})+(y-y_{C1,q})(y-y_{P1,q})+(z-z_{C1,q})(z-z_{P1,q})\right)}{\left((x-x_{C1,q})^2+(y-y_{C1,q})^2+(z-z_{C1,q})^2\right)^{\frac{3}{2}}\left((x-x_{P1,q})^2+(y-y_{P1,q})^2+(z-z_{P1,q})^2\right)^{\frac{3}{2}}}\right.$$
$$\left.-\frac{\left((x-x_{C1,q})(x-x_{P2,q})+(y-y_{C1,q})(y-y_{P2,q})+(z-z_{C1,q})(z-z_{P2,q})\right)}{\left((x-x_{C1,q})^2+(y-y_{C1,q})^2+(z-z_{C1,q})^2\right)^{\frac{3}{2}}\left((x-x_{P2,q})^2+(y-y_{P2,q})^2+(z-z_{P2,q})^2\right)^{\frac{3}{2}}}\right)$$
$$.dx.dy.dz \qquad (5.54)$$

At the current electrode the two terms in the integral both tend to ∞ therefore the triple integral becomes $\infty-\infty$, which is not particularly useful. At the first potential electrode, the first term becomes infinity, and at the second potential electrode, the second term becomes infinity.

To gain a better understanding of the integrand, it has been plotted using "Maple". For this $C1$ is at $(5,0,0)$, $P1$ is at $(10,0,0)$ and $P2$ is at $(15,0,0)$. The z value has been fixed for both of the diagrams the layout of the electrodes means that the solution will be rotationally symmetric about the x axis.

From figures 5.12 and 5.13 we see that apart from the vicinity of the electrodes (discontinuities). the values of this function are very close to zero. This means that most of the zones will involve an integral over small values. The implications of this are that for zones not close to the electrodes the function will be flat and also close to zero. The further the zone is from the electrode, the smaller will be the value. The implication is that the method of calculating the value of the Jacobian (by summing the values of the function) is not too bad for most values of the

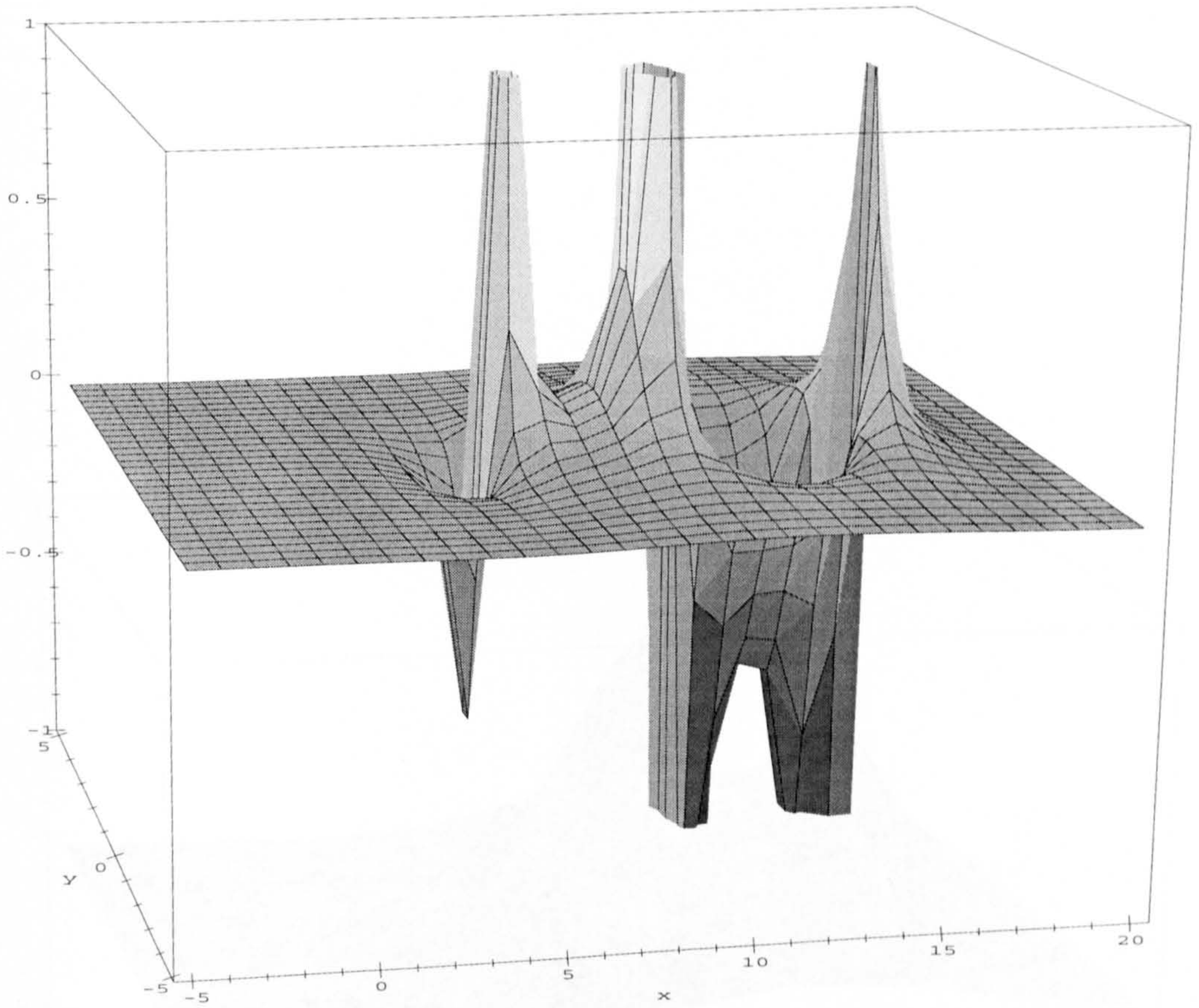

Figure 5.12: Plot of function multiplied by 10^3 for $z = -0.1$

Jacobian. The errors will be large near the electrodes as this is where the function becomes very steep. However, near the discontinuities, any numerical integration method will run into difficulties.

As we know the location of the electrodes and the zones of interest are known, it would be useful to gain an understanding by comparing the numerical evaluations of the integral with the other methods which is the subject of chapter 7 below.

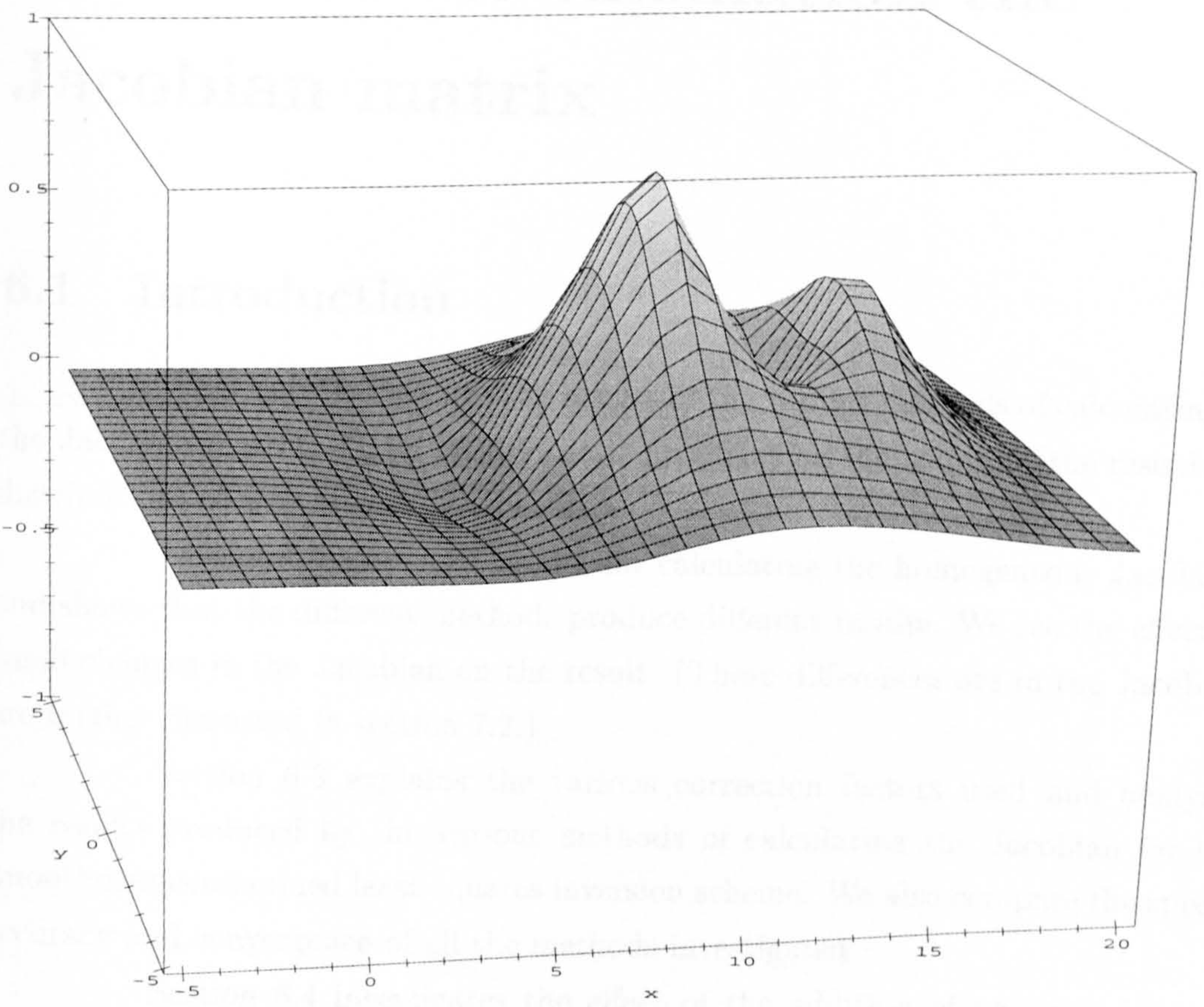

Figure 5.13: Plot of function multiplied by 10^5 for $z = -2.5$

Chapter 6

Results of the calculation the Jacobian matrix

6.1 Introduction

This chapter contains the results of the various methods of calculating of the Jacobian matrix. These results show the effects on the solution (the resistivity distribution) of a particular test problem.

Section 6.2 gives the results for calculating the homogeneous Jacobian, and shows that the different methods produce different results. We see the effect of small changes in the Jacobian on the result. (These differences are in the Jacobian are further discussed in section 7.2.)

Section 6.3 explains the various correction factors used and analyses the results produced by the various methods of calculating the Jacobian for the smoothness-constrained least-squares inversion scheme. We also compare the speed, accuracy and convergence of all the methods investigated.

Section 6.4 investigates the effect of the addition of an extra layer of nodes in the coarse grid near the surface. This is designed to improve the accuracy of the current density near the surface, which should not improve the results not only near the surface but also generally. However, this method of improving the results is very computationally expensive.

The inverse problem used as a test for this chapter uses 112 zones with 352 measurements. Using such a test problem means that the Jacobian is a matrix of 112 columns $\times$ 352 rows, (a selection of the matrices are shown in chapter 7). The resistivity distribution of the test case i.e. the solution of the inversion, is shown in figure 6.3.

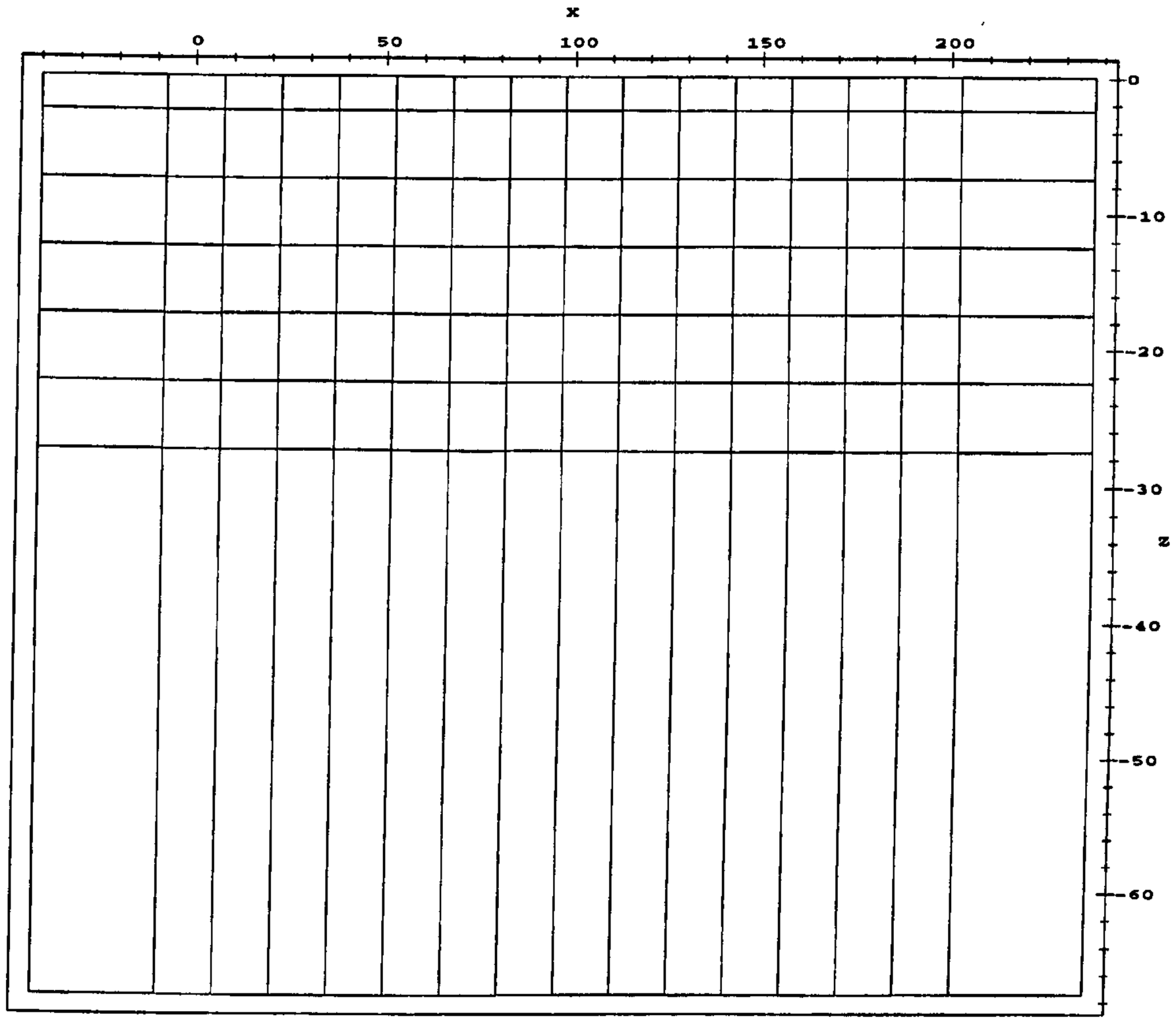

Figure 6.1: The zones of the test survey

The survey that has been used to calculate these results relies on electrodes that are only on the surface. They are spaced at $5m$ intervals along the x axis between the origin and $x = 195m$. This makes the survey effectively 2D. The zones, as shown in figure 6.1, form a grid in the xz plane and go from $-75m$ to $40m$ in y. The zones are in 7 layers of 16 and are numbered from left to right and from top to bottom. The zones in the columns on either side and the row at the bottom[1] are there so that the space outside these can be modelled, thus taking into account variance in the resistivity outside the region of the survey (although these external zones are not specifically needed in our test problem).

[1]These zones in the bottom row will only be partially displayed (e.g. see figures 6.2 and 6.3) as otherwise they tend to dominate the images.

6.2 Results of calculating non-analytic homogeneous Jacobian

There are two ways in which the Jacobians can be compared. The first is a comparison of their output from the first iteration of the inversion[2]. This is shown in figure 6.2. The second method (see chapter 7) will be to compare the elements of the Jacobian.

The starting point for this research was the perturbation method (see section 6.3.1) for calculating Jacobian. This was compared with all the other Jacobians produced. The perturbation method is a way of producing the Jacobian for this inversion scheme.

The first of the homogenous Jacobians produced was that of the uncorrected adjoint method. This is the direct output of equation (D.2) using the finite-difference potentials. Even though the adjoint methods are different from the perturbation method, this does not mean that the results will be different, just that they are likely to suffer from different problems.

The images in figure 6.2 are the resistivity distributions produced after the first iteration by all the methods used. All the images are similar. Comparing the perturbation method with the uncorrected adjoint method, the area of orange (high resistivity) is not as deep as, but wider than that given by the uncorrected adjoint method. The top layer of zones of the perturbation method has a higher value than the adjoint method, although the lower zones of the adjoint method have higher value than those of the perturbation method. This can be seen also by looking at the first pages in appendices H.3 (perturbation method) and H.4 (adjoint method) below, where the actual values are displayed. The values are different but it can be seen that the structures are similar which suggests that neither is wildly incorrect.

The other three images in figure 6.2 are the measurement-corrected adjoint method, potential-corrected adjoint method and hybrid method: these are very similar in their structure, although the values are subtly different. The values for the measurement-corrected adjoint are generally smaller than the other adjoint methods below the second layer of zones and greater in the top two layers. It should be noted that small changes in the values of the Jacobian have quite an effect on the result of the iteration and these are best seen by looking at the actual values which are in

[2]The measurements will effected the results of the first iteration but since the effect is the same for all methods.

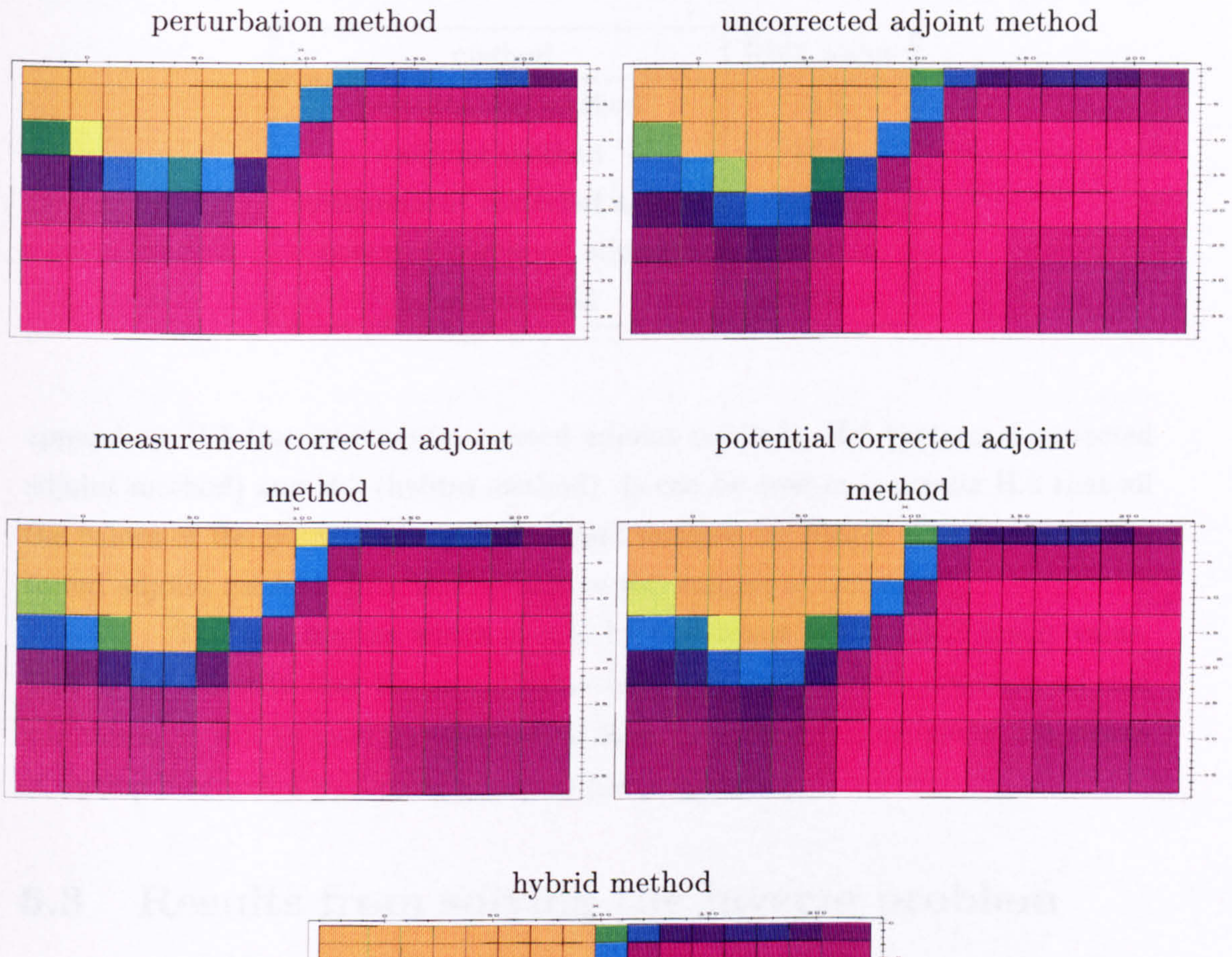

Figure 6.2: The resistivity values of the zones after the first iteration of all five methods used for calculating the Jacobian.

Table 6.1: Comparison of the RMS value after the first iteration.

method	RMS Value
perturbation method	13.9
adjoint method	14.9
measurement corrected adjoint	14.7
potential corrected adjoint	15.0
hybrid method	18.0

appendices H.5 (measurement-corrected adjoint method), H.6 (potential-corrected adjoint method) and H.7 (hybrid method). It can be seen in appendix H.6 that all the values of the potential-corrected adjoint method are bigger than in the uncorrected adjoint method. (We shall return to this subject in chapter 7.

The last matter which should be mentioned is the RMS misfit value. This is the quantity that the smoothness-constraint least-squares inversion scheme minimises: it will be used for comparison later, in section 6.3, as one of the means of testing how well a particular inversion has progressed.

6.3 Results from solving the inverse problem

This section contains the results of the inversions run on a test problem. The results from the three adjoint method Jacobians and the hybrid Jacobian will be compared with the perturbation method Jacobian.

To compare the results of these techniques some measures of convergence are needed. The three chosen were:

1. The RMS misfit between the actual measurements and the calculated potential differences generated from the present resistivity distribution.

2. A measure of difference between the present model and the test model used to calculate the actual measurements.[3].

3. The comparison of the structure of the present resistivities with those of the solution.

[3]This is defined this measure of the difference between logs of the test model and the result. $value = \frac{1}{no.\ zones} \sum \frac{log_{10}(\rho_{res}) - log_{10}(\rho_{mod})}{log_{10}(\rho_{mod})}$

The first two comparisons produce a value; the third is a much more subjective question. The comparison of structure will reveal the existence of a feature and whether its location is correct. A feature will be either a group of zones which have the same (or similar) resistivity or boundaries between such groups of zones. All three comparisons tend to give similar results but there do exist cases where the difference between the measurements is negligible but the actual difference in the values is quite large. This can also apply to the structure, but it does not follow that the other two measures of convergence will produce a good result.

The first two means of comparison rely on a knowledge of the test case. The typical test case used contains a rectangular volume of zones of a higher resistivity than the surrounding area. The one chosen in this case is more complex (see figure 6.3). The resistivity values of the test model are shown in appendix H.2. The

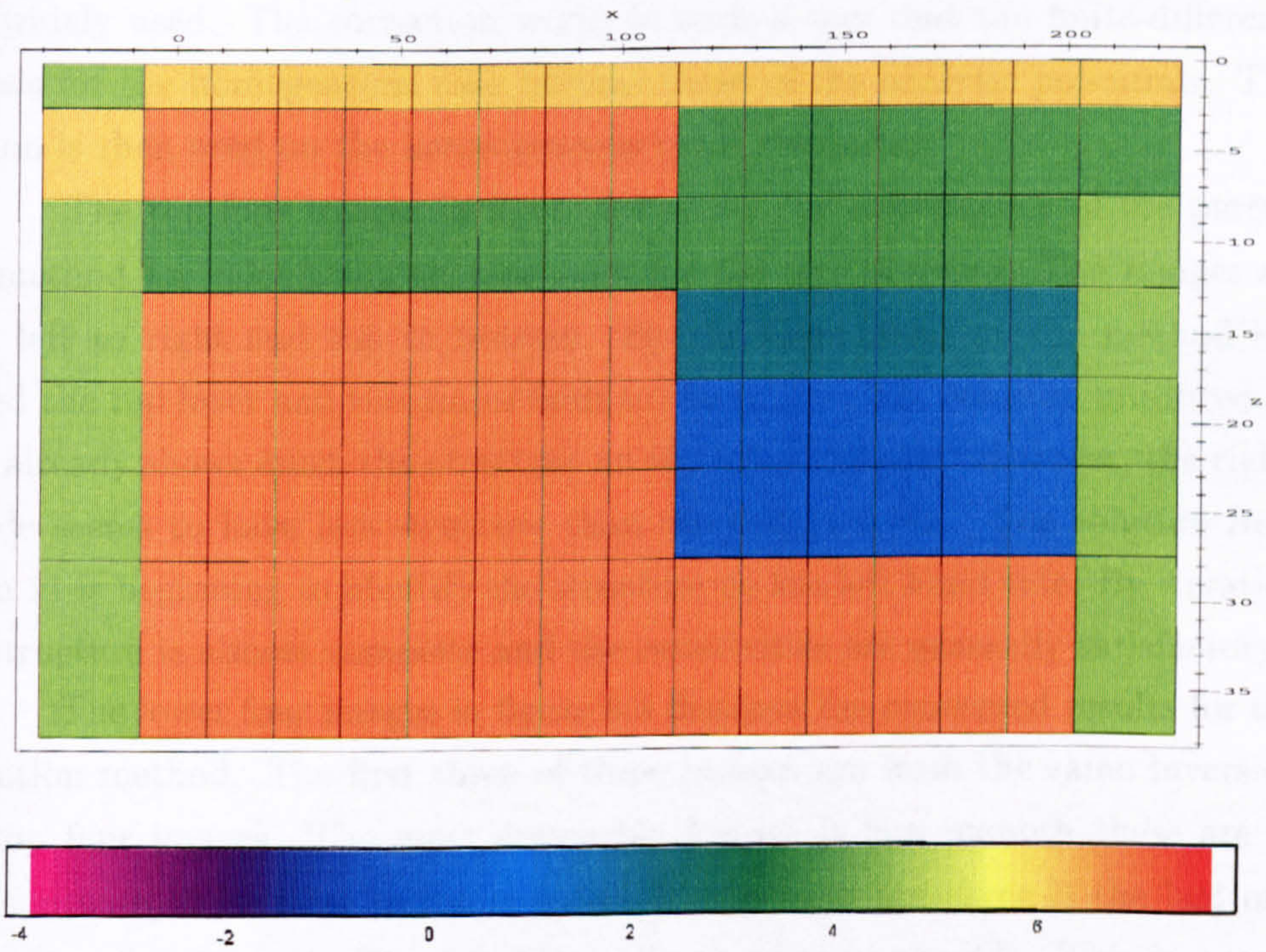

Figure 6.3: The natural logarithm of resistivity values of the test case (solution). (The realistic model "data" was kindly supplied by B.G.S..)

natural logarithm is used to compress the wide range of resistivity values. Otherwise the lower values tend to be amalgamated even if they differ from each other by a factor of 10. In common with accepted practice (Jackson et al. [1997]), during each iteration of these inversions the smoothness constraint is reduced, automatically improving the results.

6.3.1 Perturbation method

In this section the results of using the perturbation method to calculate the Jacobian for the test problem are shown, to provide a 'yard stick' to comparing the other methods developed. The actual values calculated are displayed in appendix H.3.

The perturbation method used is a method of producing the Jacobian for the inverse problem as described in section 5.1.1. A correction is used on the measurements, which for the purpose of this chapter will be called the *measurement correction*. This correction has been applied to all the measurements used in all the inversions described in this chapter, but since only the perturbation Jacobian uses the measurements, only the perturbation Jacobian will be affected by the measurement correction. This correction was developed by Dey & Morrison [1979] and is now widely used. The correction works in such a way that the finite-difference potentials for the homogeneous case become those of the analytic potentials. This correction is then used on the heterogeneous cases thereafter.

The top four images in figure 6.4 shows the convergence of the perturbation method for calculating the Jacobian for the test problem. The images are ordered left to right and top to bottom. By the third iteration the method has identified the top layer and the major fault in the centre. The solution produced by the 7th already shows much the structure on the left-hand side. However, the right-hand side seems to have less structure than the test problem. The solution from iteration 11 is beginning to identify the structure on the left hand side. By iteration 17 the structure is almost complete and the resistivities are generally satisfactory.

The lower four images in figure 6.4 displays the converged results for the perturbation method. The first three of these images are from the same inversion as the top four images. The most noticeable feature is how smooth these are in comparison with those later in the chapter. The best of the three is the last one which is from iteration 21. The last image shows what is possible. This is one of the best results obtained. It has a far lower λ (smoothness-constraint, see section 4.2) value than the rest and has a faster reduction in the stiffness in the value of λ.

The convergence, shown in figure 6.5, of the perturbation method is steep to begin with, then levels off and descends very slowly. It is possible to keep this method descending quickly by having a much faster rate of slackening of λ, this being the method used to produce image 8 in figure 6.4. Figure 6.6 shows a measure of the difference between the test model and the current solution. This has a minimum at iteration 11, showing non-optimal values of λ have been used.

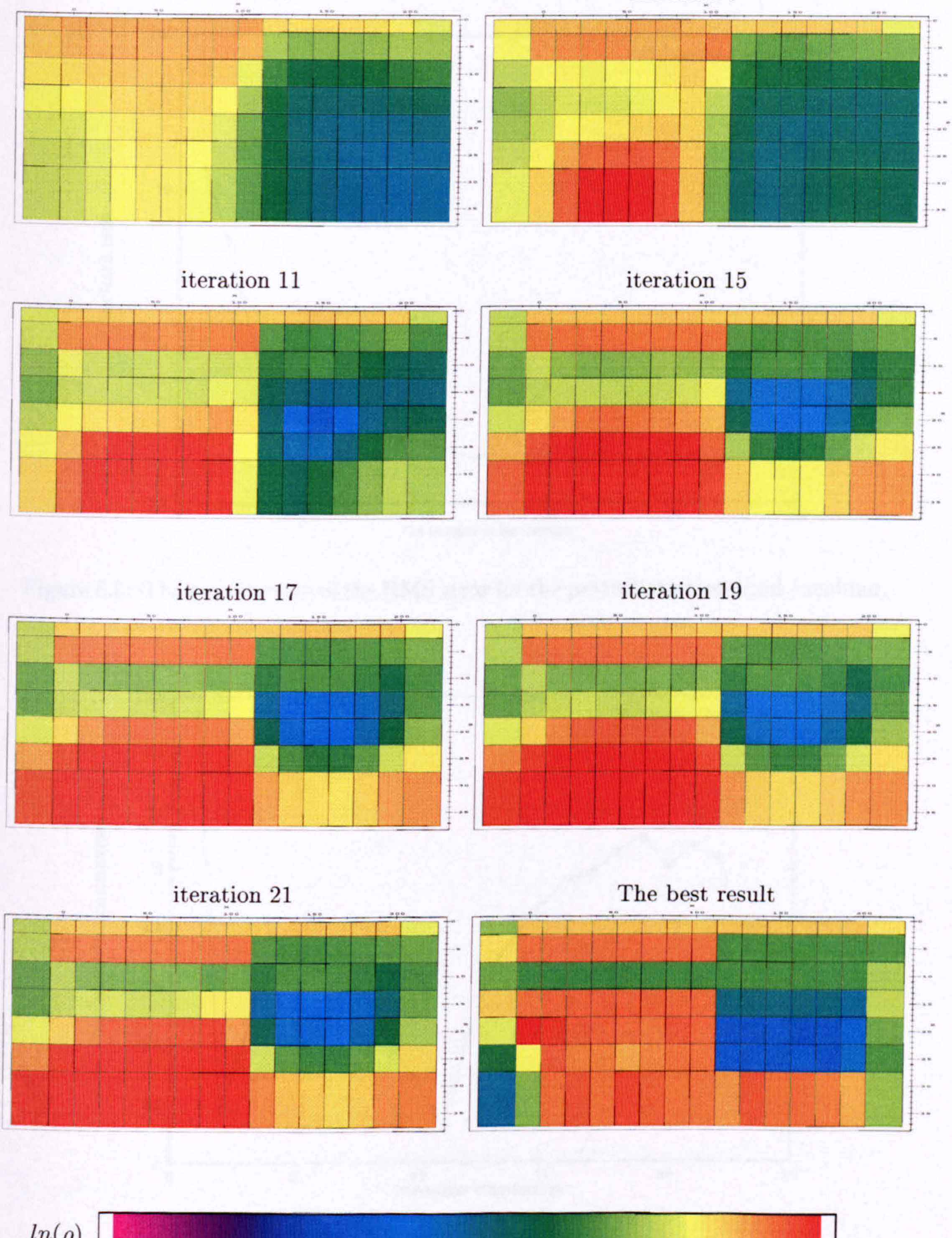

Figure 6.4: The natural logarithm of the resistivity values of the zones using the perturbation method Jacobian.

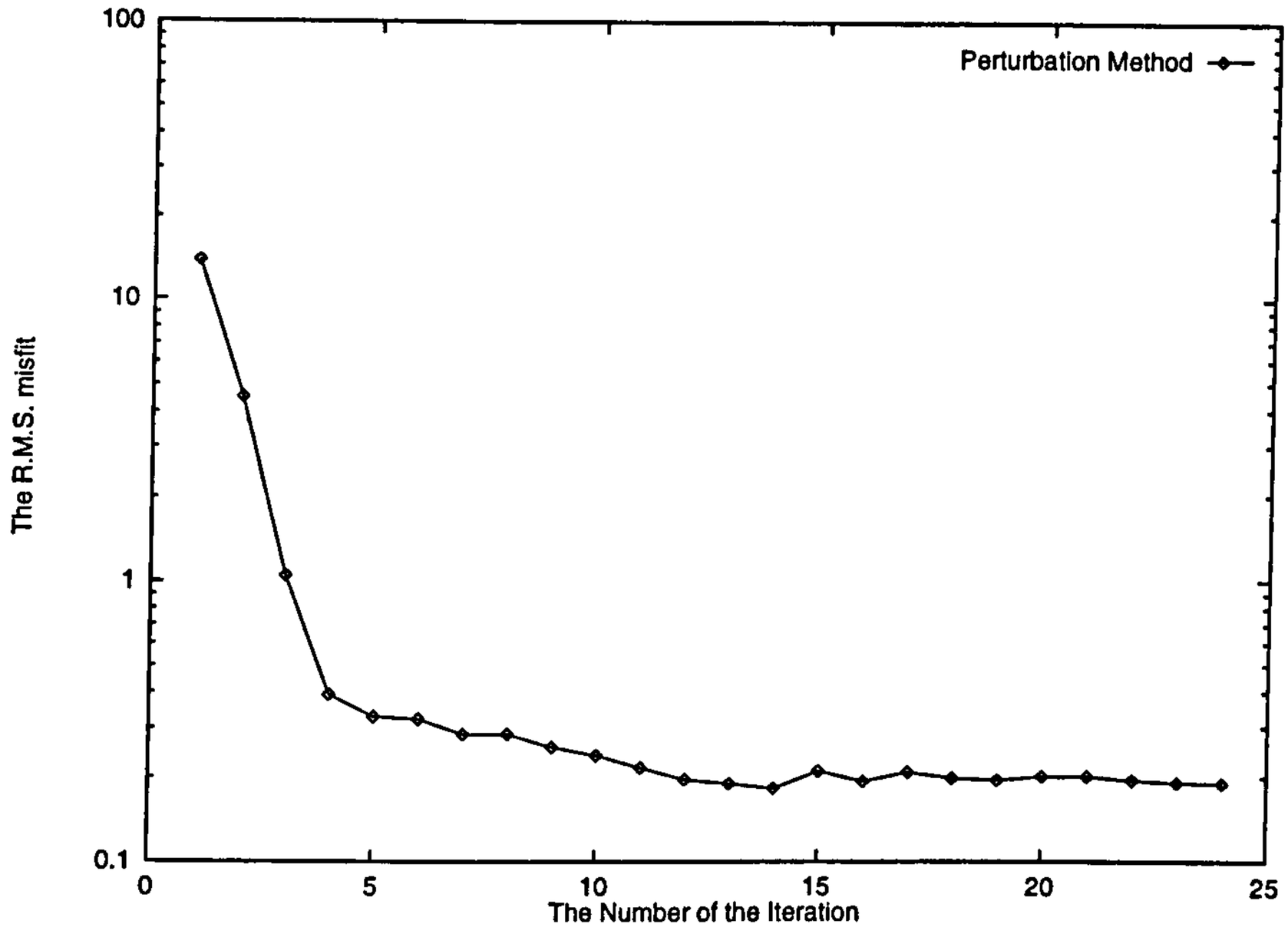

Figure 6.5: The convergence of the RMS error for the perturbation method Jacobian.

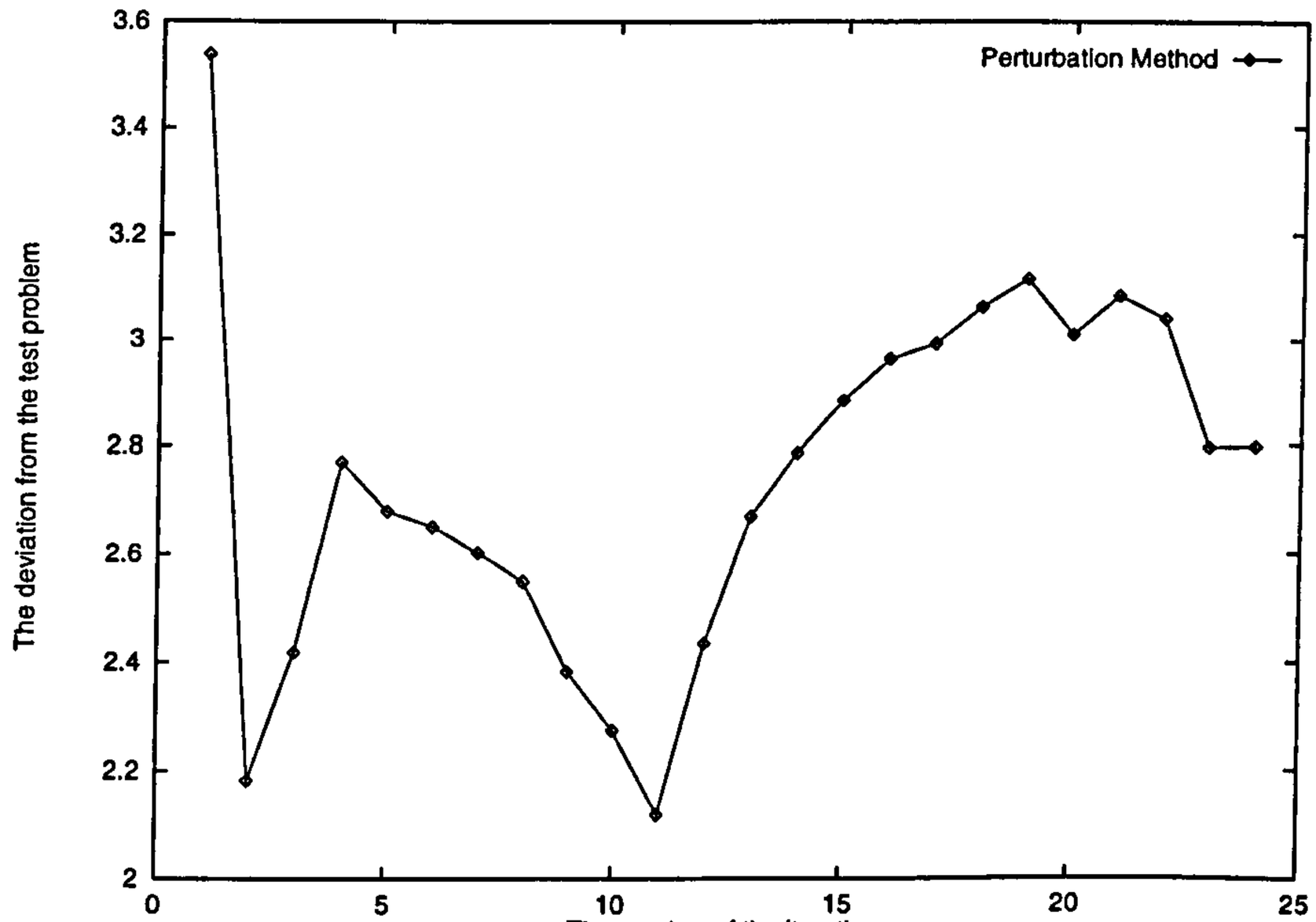

Figure 6.6: A measure of the deviation between the result of each iteration and the test model for the perturbation method Jacobian.

The time[4] taken to perform one iteration of the perturbation method is about 5 hours[5]. Unlike the adjoint methods of calculating the Jacobian only the current source needs to be calculated, which for the test problem is one third of the electrodes. Virtually all the time taken by this method is to calculating the Jacobian. The time taken, directly depends on the product of the number of zones, the number of current sources and the time taken to compute the Forward Problem. The rest of the calculation takes about 10 minutes, i.e. insignificant compared with that for calculating the Jacobian. This time is not dependent on the method of calculating the Jacobian as will appear in the adjoint method timings.

6.3.2 Adjoint method

This section shows the way in which the uncorrected adjoint method affects the solution of the test inverse problem. The values of the resistivity at each iteration are given in appendix H.4.

The top four images in figure 6.7 shows the way in which the solution develops using the adjoint method to calculate the Jacobian. In general, the method detects a major change in resistivity in the middle of the survey volume. There is also a strip along the surface of the ground which has a resistivity similar to that of the left hand side. We thus see that some of the major features of the solution have been found. As the method develops, the left-hand side begins to display more structure and is where the reduction in the smoothness constraint has its greatest effect. The values in the top layers gradually become more accurate. This is to be expected as all the current must first pass through the top layer.

By the time the method reaches iteration 15 there is a good reproduction of the top three layers in structure and some of the value of resistivity. However, there is definite blurring of the structure below this level. In particular, the right-hand side, where there are the lowest resistivities, the block of zones with very low resistivities are almost completely masked by the zones above. On the left-hand side the third layer is not distinct from the fourth layer but shows evidence of a low resistivity region. The method has not identified many of the features in the lower layers and seems to have created a spurious area of very high resistivity. This area is slightly less than twice the resistivity of the solution.

The lower four images in Figure 6.7 show what happens to the solution once it arrives at the minimum values of the RMS error as shown in figure 6.8. Also

[4]Time taken on a Pentium Pro 200MHz PC with $64Mb$ of RAM.

[5]This can be reduced by a factor of three if all the potentials are stored in memory.

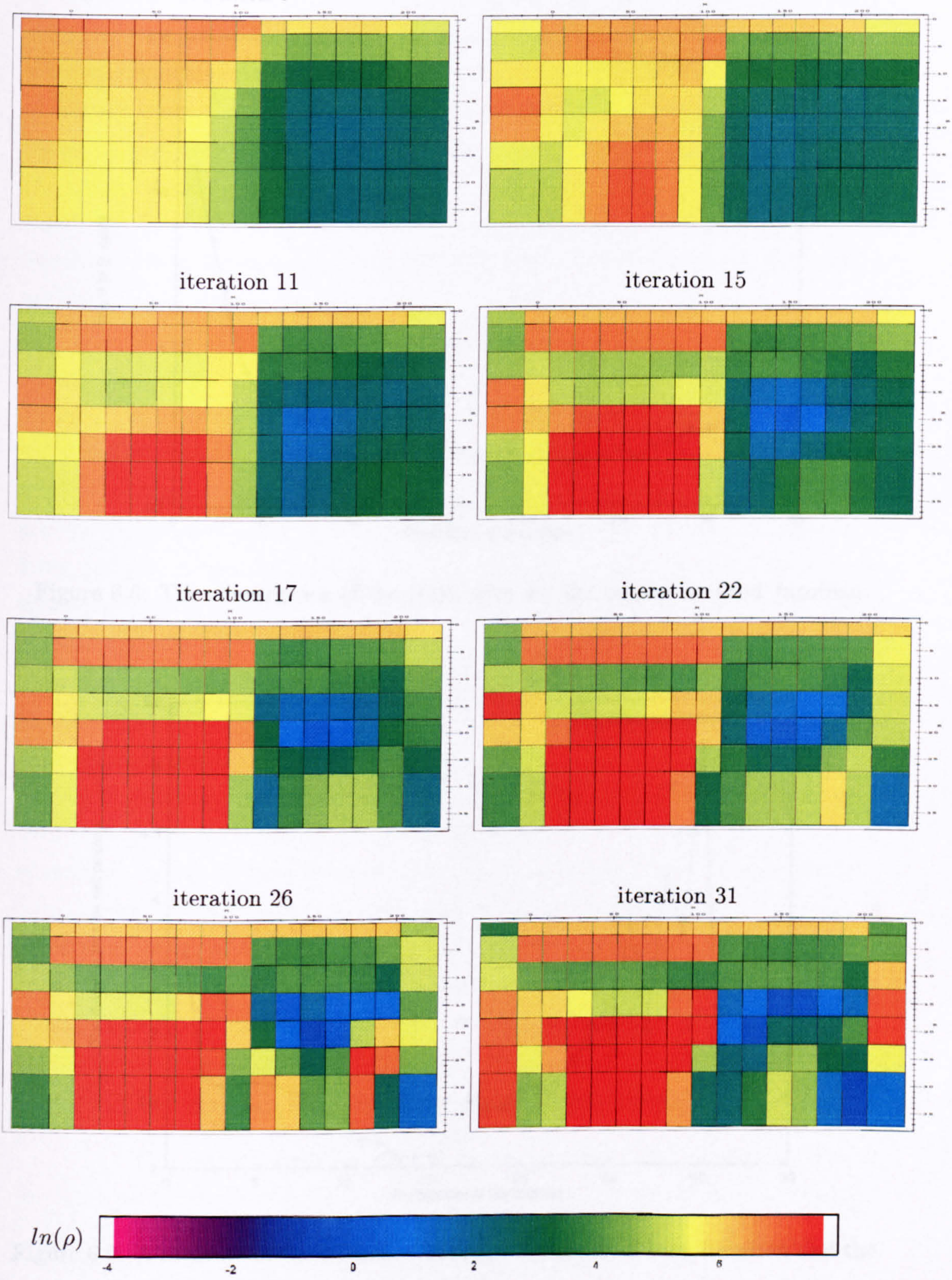

Figure 6.7: The natural logarithm of the resistivity values of the zones using the adjoint method Jacobian.

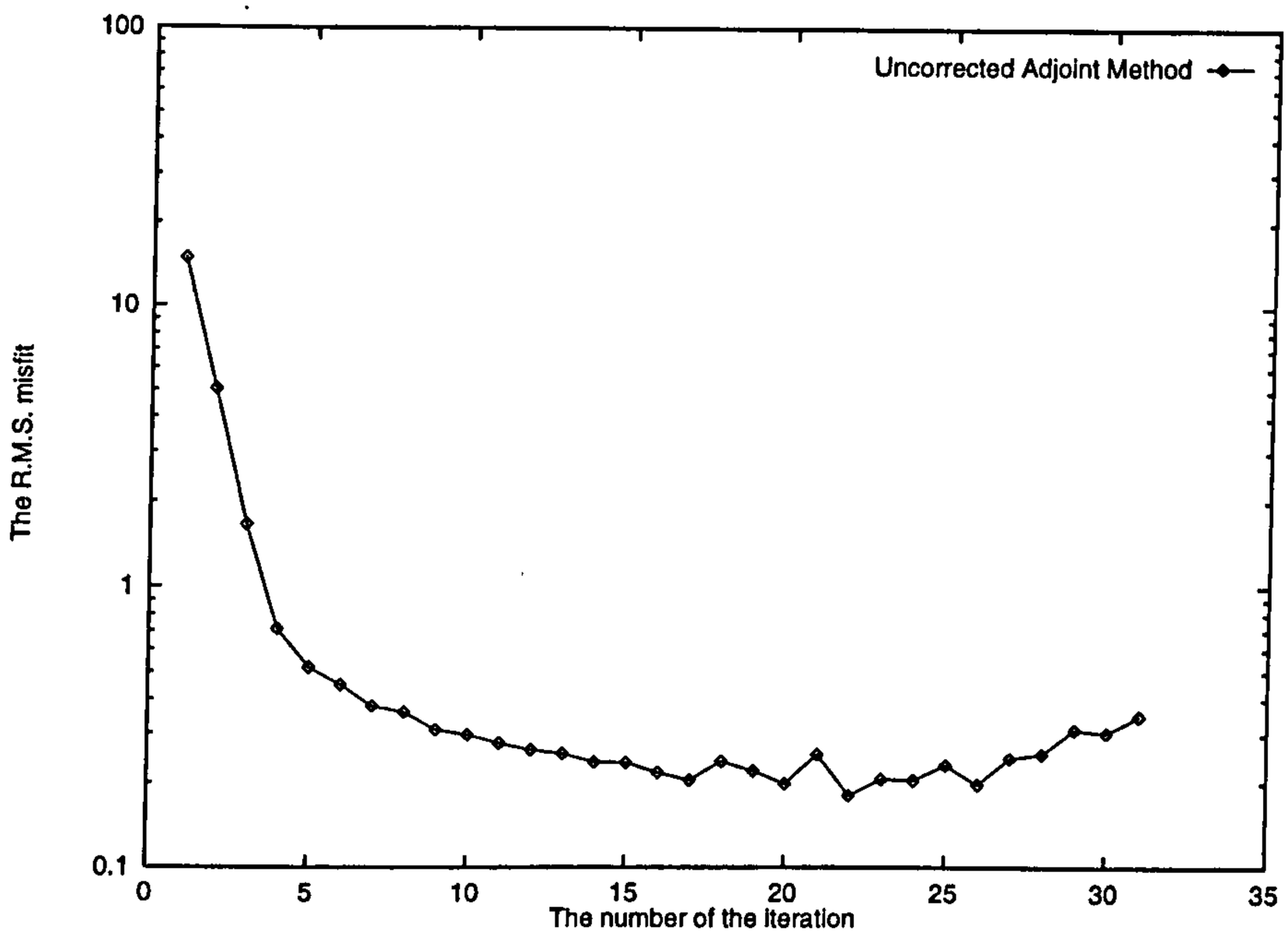

Figure 6.8: The convergence of the RMS error for the adjoint method Jacobian.

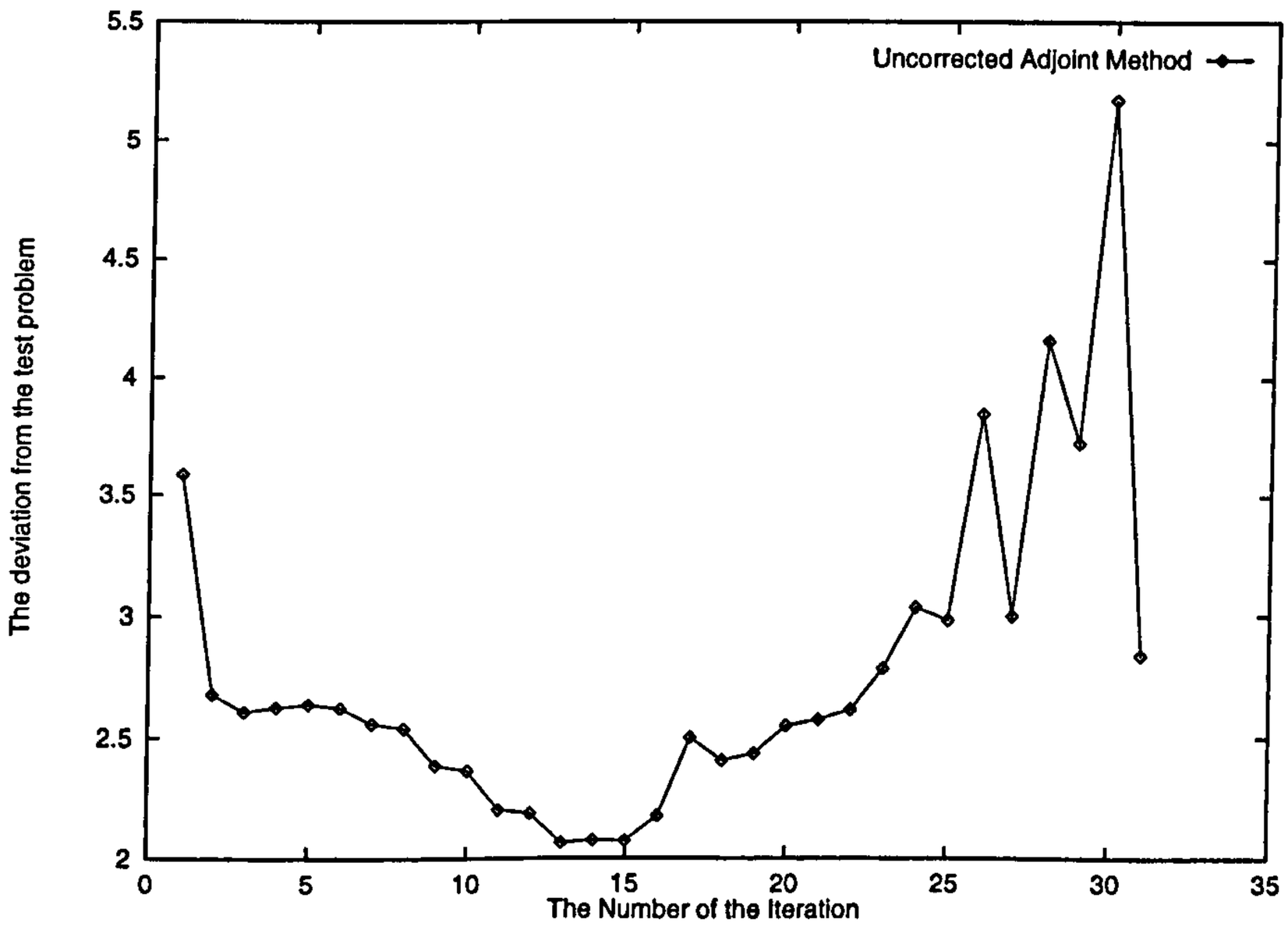

Figure 6.9: A measure of the deviation between the result of each iteration and the test problem for the adjoint method Jacobian.

shown in figure 6.7 is the result of the final iteration (no. 31). This last image shows how coarse the solution has become. There are some sharp changes in the value of the resistivity but the lower half and the boundaries reveal some elements of the structure, though these are not particularly close to the correct resistivity values. The other three images are possible solutions which are the first minimum, the lowest[6] minima and the last minimum of the RMS misfit in figure 6.8. Of these three, the first two are similar and both are "smoother" solutions than the third. The image from iteration 22 would be chosen as the best solution as it is the one with the lowest RMS error.

Initially, the convergence of the method (as shown in figure 6.8) is relatively fast. The error reduces, at a less steep, but nearly constant rate until iteration17. The method continues more or less uniformly until to iteration 26, after which point the RMS misfit starts to diverge.

Figure 6.9 shows a measure of how the result from each iteration compares with the test model. The solution is closest to the results of iterations 13-15. Even at these points the solution still has a reasonably large error in both the resistivities and the structure. The method then diverges from the test model until it reaches iteration 25. The divergence occurs in the lower zones first, because these from large errors compared with their small values in the Jacobian. The last part of the plot shows a wildly-varying function. This is probably caused by the slackness of the smoothness constraint.

The time[7] to complete one iteration is 60 minutes, of which 45 minutes is used to calculate the Jacobian. This is a fixed overhead and depends on the number of measurements and cells in the region containing all the zones. It is possible to write a more efficient program which will fit into the memory[8] but if the size of problem is increased the present program would be able to cope with it without a great increase in time. The most of the other 15 minutes is spent calculating the potentials and depends on the size of the changes in resistivity values.

6.3.3 The measurement-corrected adjoint method

This method is similar to the adjoint method. The correction factor is the same as for the perturbation method. There are differences in the results as

[6]This is not necessarily the global minimum of either this minimisation or of the whole problem.

[7]Time taken on a Pentium Pro $200MHz$ with $64Mb$ of RAM.

[8]The effect of storing all the potentials in memory would reduce the time to calculate the Jacobian down to about 15 minutes.

compared with the adjoint method although these are not easily seen in the top half of figure 6.10. These are best seen by comparing the values in appendices H.4 and H.5. Noticeable differences occur in the other layers.

These differences tend to be near the lower resistivity values and, in particular the third layer down, where the values are lower. This is also true for the blue patch on the right hand side, which is both deeper and bigger than in the adjoint method. The results are similar to those generated by the adjoint method especially in the upper layers. In the lower layers there is less than a 10% difference.

The lower four images in figure 6.10 display the results for increasing iterations. These are ordered in the same way as section 6.3.2. Of these only iteration 17 is similar to that of the adjoint method. The solution from iteration 31 is still becoming coarser and does not correctly predict the lower layers. The solution from iteration 20 would be chosen because of the lower RMS error. This method, like the adjoint method, has reproduced most of the features. The errors are again largest in the neighbourhood of the lower resistivity values.

The convergence of the method is similar in form to that of the adjoint method (see figure 6.11). It converges faster for the first five iterations than does the adjoint method. After the method has reached the lowest minimum it appears not to diverge as quickly as the uncorrected adjoint method. It is not clear by iteration 31 whether or not the RMS error value has in fact reached its global minimum. However, this method is unlikely to lead to a better solution than one of images 5-7 in figure 6.10.

Figure 6.12 shows a measure of how the result of each iteration compares with the test model. The result at iteration 13 is the closest to the solution. At this point the smoothness constraint is still reasonably stiff. Even at this point the solution still has a reasonably large error in both the resistivities and structure. After this point the method diverges from the test model fairly rapidly. As in section 6.3.2, this divergence is caused by the inaccuracies in the lower zones.

The time taken by this method is the same as for the adjoint method. The correction is performed just before the Jacobian is written to a file. Each value undergoes one floating point multiplication with the correction. The time taken to do this is negligible in comparison with the time taken to calculate the Jacobian. Therefore, for all practical purposes the correction has no effect on the time taken.

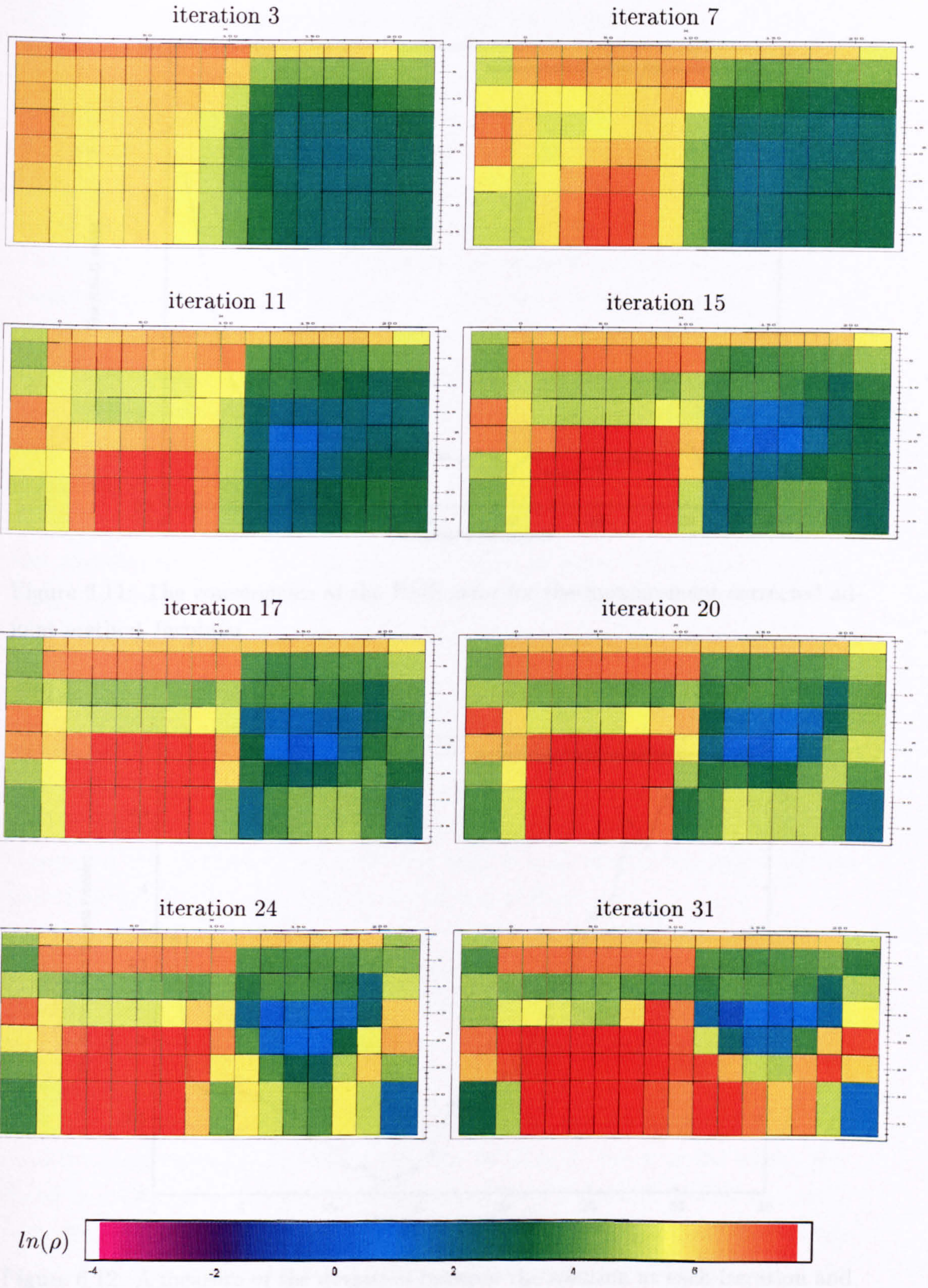

Figure 6.10: The natural logarithm of the resistivity values of the zones using the measurement corrected adjoint method Jacobian.

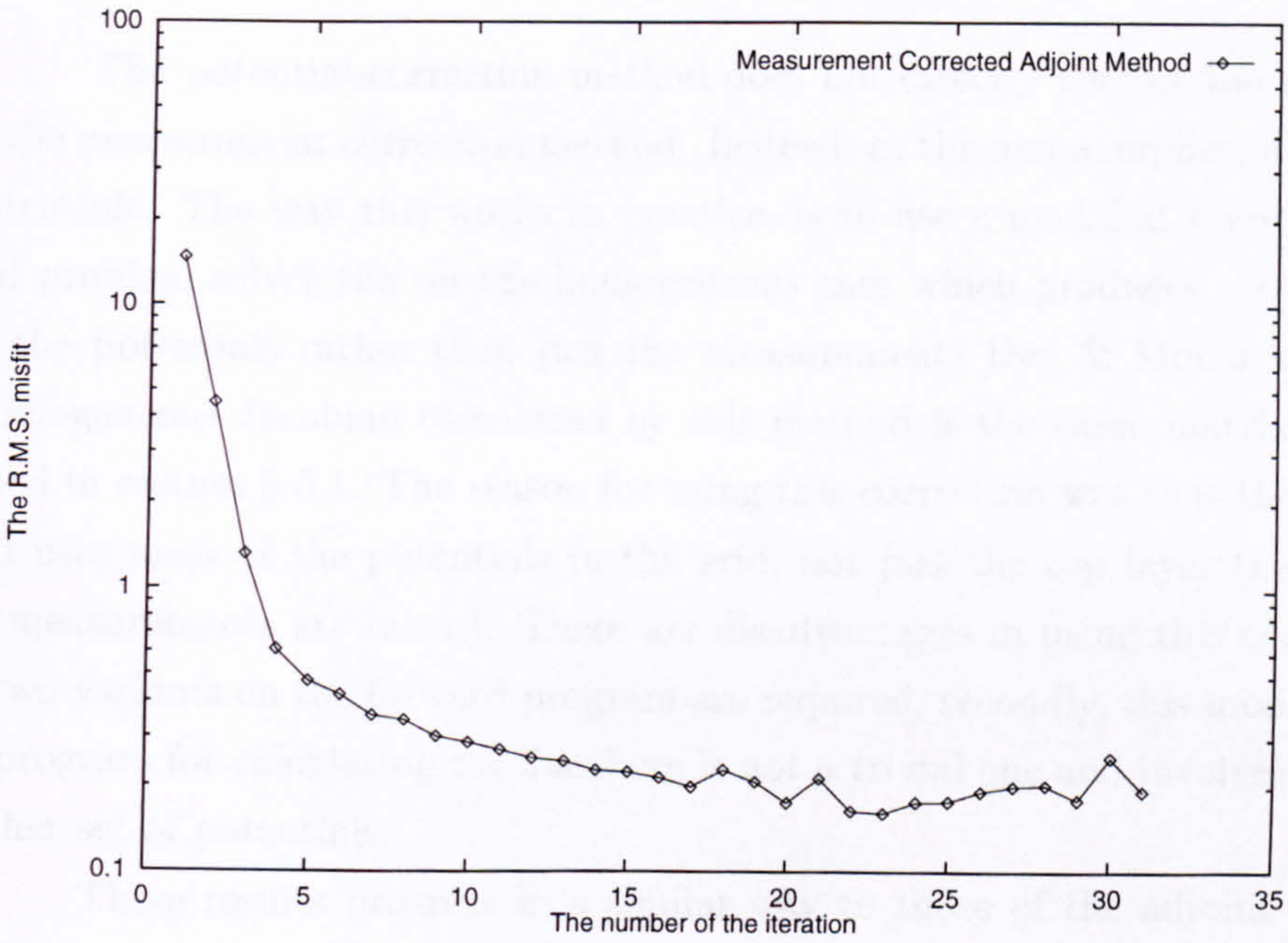

Figure 6.11: The convergence of the RMS error for the measurement-corrected adjoint method Jacobian.

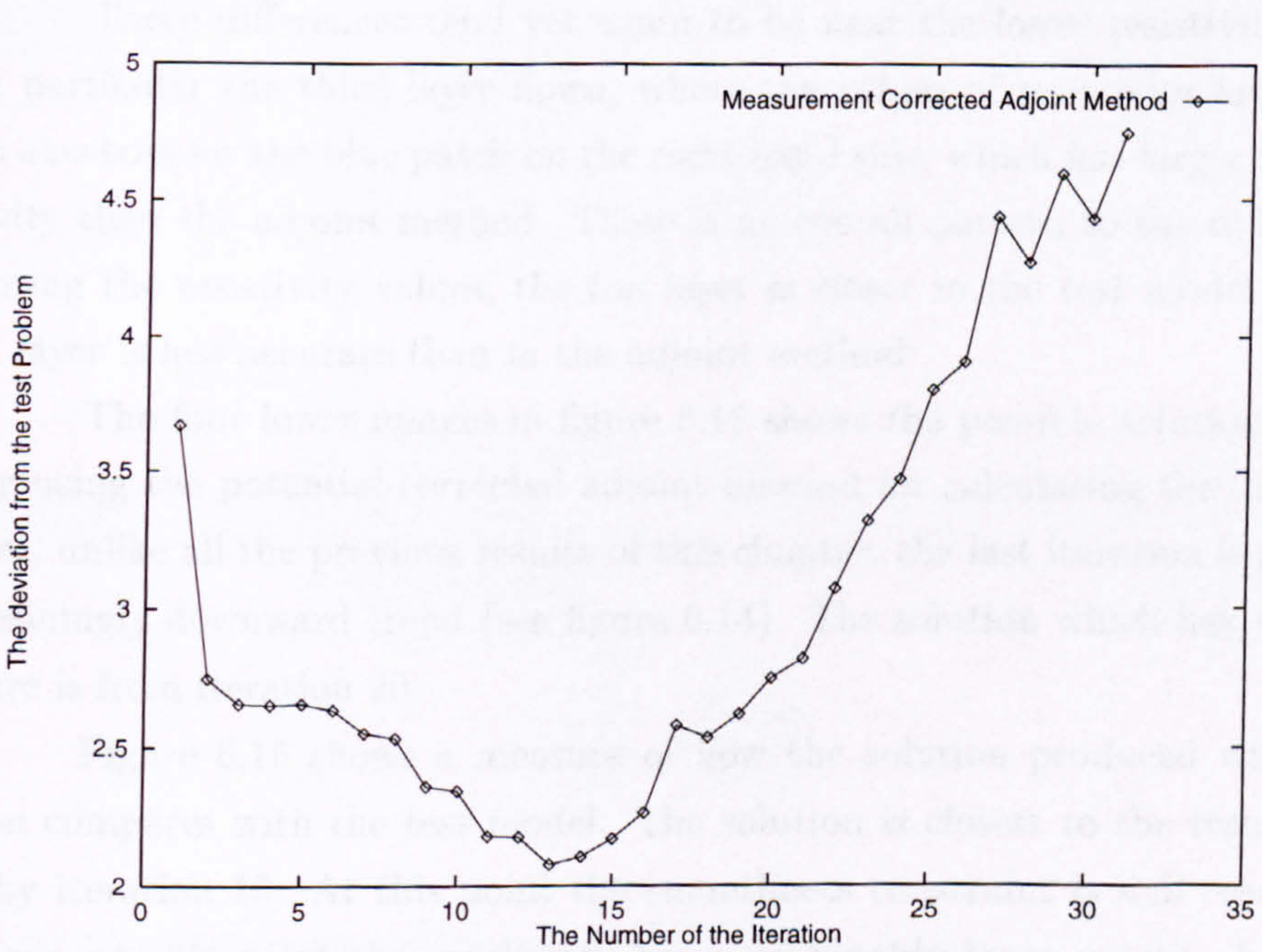

Figure 6.12: A measure of the deviation between the solution at each iteration and the test problem for the measurement-corrected adjoint method Jacobian.

6.3.4 Potential-corrected adjoint method

The potential-correction method does not directly correct the Jacobian unlike the measurement correction method. Instead, as the name implies, it corrects the potentials. The way this works in practice, is to use a modified version of the forward problem solver run on the homogeneous case which produces a correction for all the potentials rather than just the measurements Dey & Morrison [1979]. The homogeneous Jacobian calculated by this method is the same matrix as that described in section 5.5.1. The reason for using this correction was that the adjoint method uses most of the potentials in the grid, not just the top layer (i.e. where all the measurements are taken). There are disadvantages in using this correction, firstly two variants on the forward program are required; secondly, this modification to the program for calculating the Jacobian is not a trivial one and involves loading in another set of potentials.

These results progress in a similar way to those of the adjoint method and measurement corrected adjoint method (see in figure 6.13). There are some small differences on the top layers but these are best seen by comparing the values in appendices H.4 and H.6. The differences that are noticeable occur in the lower layers.

These differences tend yet again to be near the lower resistivity values and in particular the third layer down, where the values of resistivity are higher. This is also true for the blue patch on the right-hand side, which has larger values of resistivity than the adjoint method. There is no overall pattern to the differences. Comparing the resistivity values, the top layer is closer to the test model but the second layer is less accurate than in the adjoint method.

The four lower images in figure 6.13 shows the possible solutions generated by using the potential-corrected adjoint method for calculating the Jacobian. However, unlike all the previous results of this chapter, the last iteration is actually on a seemingly downward trend (see figure 6.14). The solution which has the best structure is from iteration 20.

Figure 6.15 shows a measure of how the solution produced with each iteration compares with the test model. The solution is closest to the results produced by iteration 13. At this point the smoothness constraint is still reasonably stiff. Even at this point the result still has a reasonably large error in both the resistivities and structure. After this point the method diverges from the test model more rapidly than the other two adjoint method variants. This demonstrates that the method with the lowest RMS error is not necessarily the one that produces the

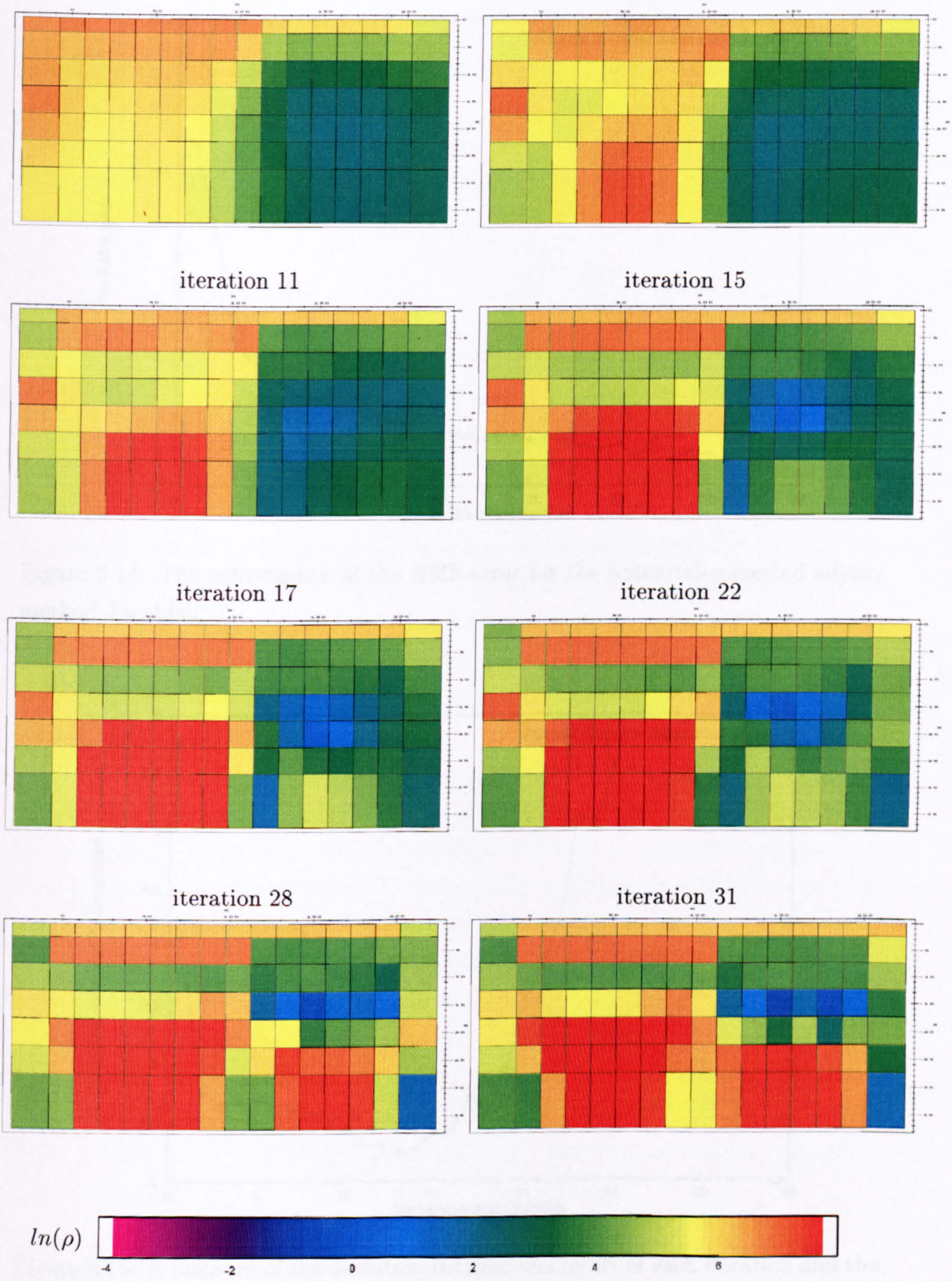

Figure 6.13: The natural logarithm of the resistivity values of the zones of the potential-corrected adjoint method Jacobian.

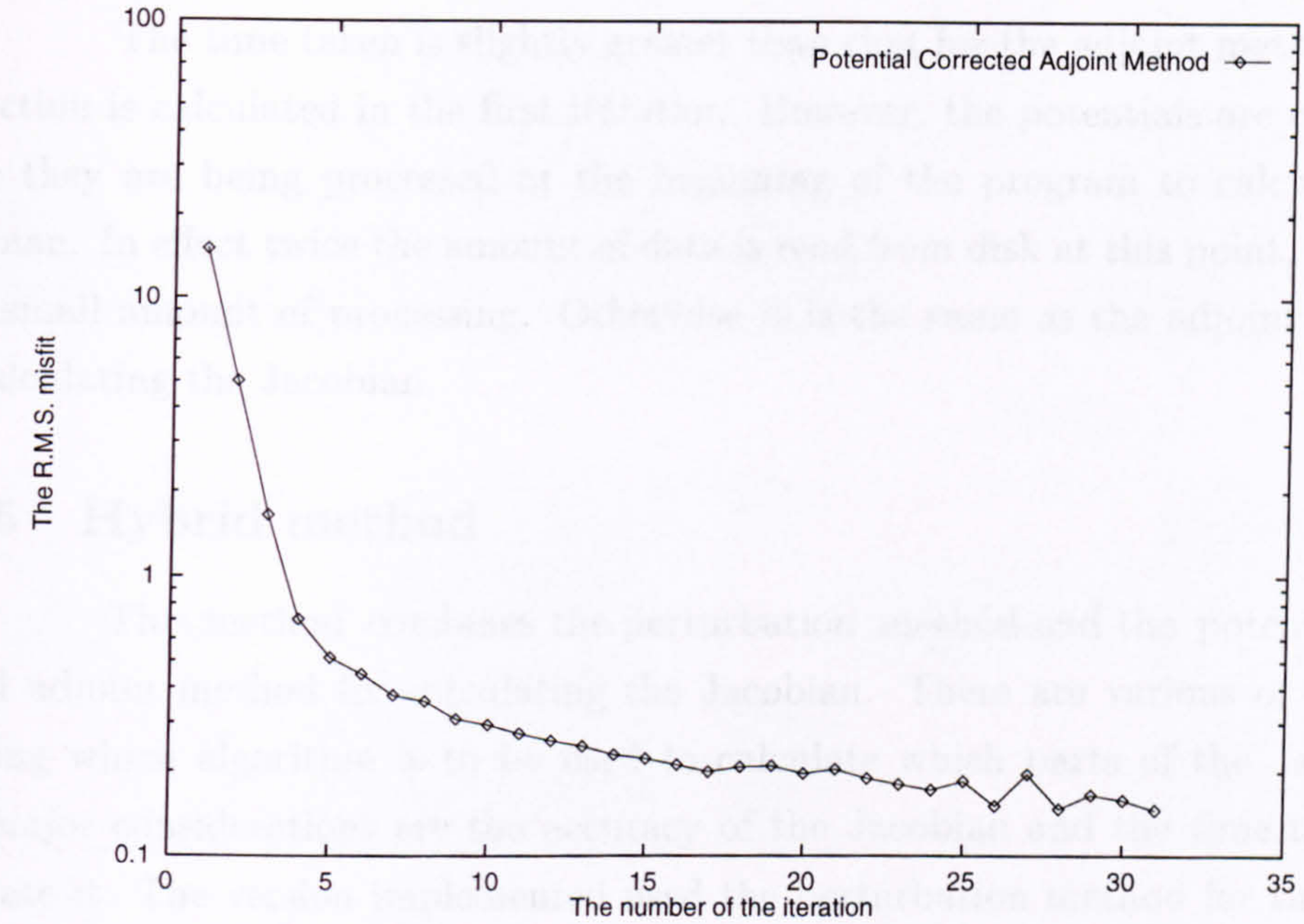

Figure 6.14: The convergence of the RMS error for the potential-corrected adjoint method Jacobian.

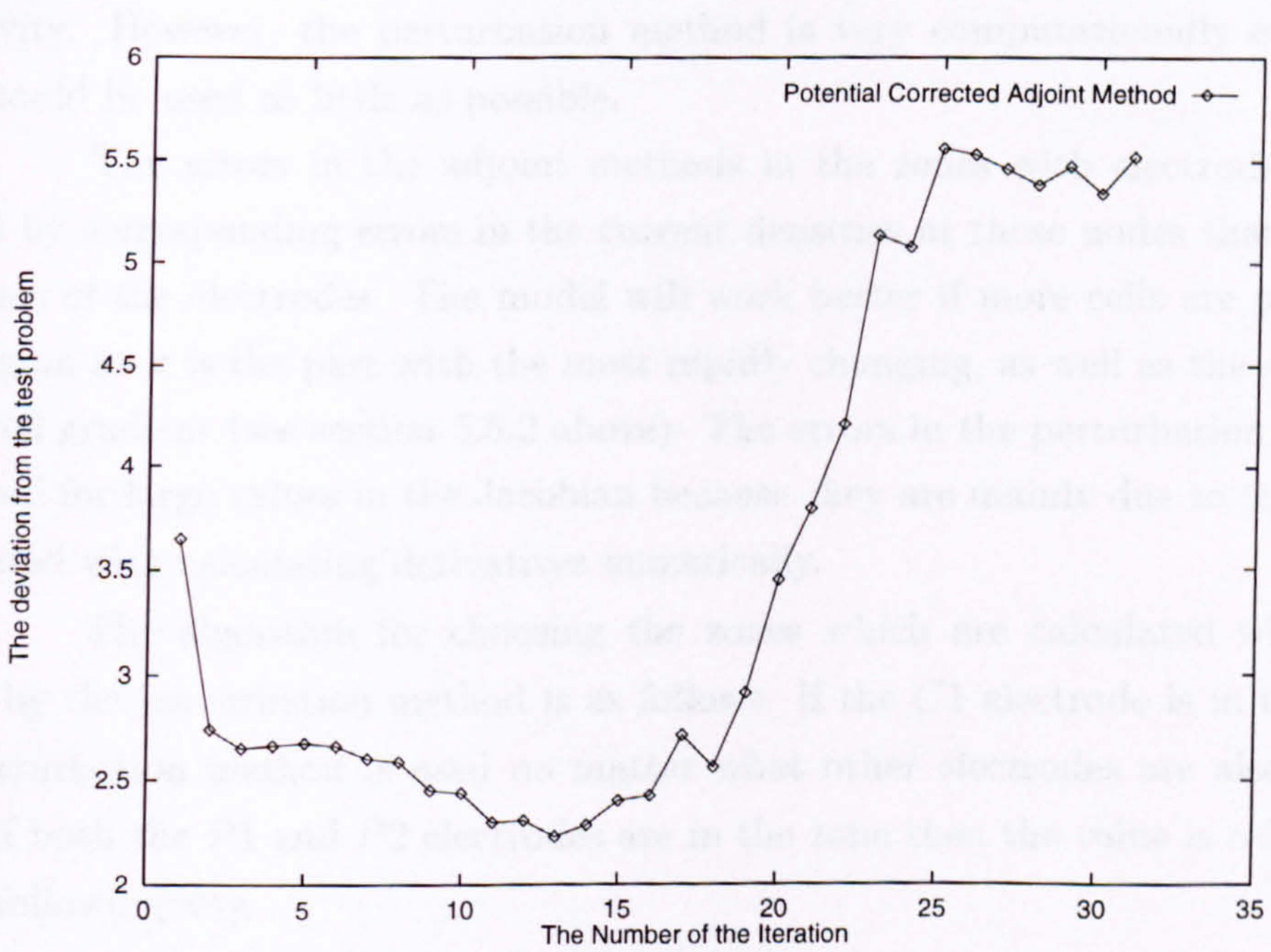

Figure 6.15: A measure of the deviation between the result of each iteration and the test case for the potential corrected adjoint method Jacobian.

best result.

The time taken is slightly greater than that for the adjoint method. The correction is calculated in the first iteration. However, the potentials are corrected while they are being processed at the beginning of the program to calculate the Jacobian. In effect twice the amount of data is read from disk at this point, followed by a small amount of processing. Otherwise it is the same as the adjoint method for calculating the Jacobian.

6.3.5 Hybrid method

This method combines the perturbation method and the potential-corrected adjoint method for calculating the Jacobian. There are various of ways of deciding which algorithm is to be used to calculate which parts of the Jacobian. The major considerations are the accuracy of the Jacobian and the time taken to calculate it. The version implemented used the perturbation method for the zones containing electrodes, and the potential-corrected adjoint method for the rest. The reasoning is as follows: the adjoint methods differ widely in the zones with electrodes in them. Therefore we use the perturbation method for these zones because it does not suffer from the same errors and is accurate when the calculating value is large resistivity. However, the perturbation method is very computationally expensive and should be used as little as possible.

The errors in the adjoint methods in the zones with electrodes in are caused by corresponding errors in the current densities at those nodes that are the locations of the electrodes. The model will work better if more cells are placed in this region as it is the part with the most rapidly changing, as well as the steepest, potential gradient (see section 5.5.2 above). The errors in the perturbation method are small for large values in the Jacobian because they are mainly due to the errors associated with calculating derivatives numerically.

The algorithm for choosing the zones which are calculated wholly or partly by the perturbation method is as follows. If the $C1$ electrode is in the zone the perturbation method is used no matter what other electrodes are also in the zone. If both the $P1$ and $P2$ electrodes are in the zone then the value is calculated in the following way.

Starting with equation (5.25)

$$\underline{\mathcal{J}}_{q,r} = \frac{\delta\phi_{P1,q,r} - \delta\phi_{P2,q,r}}{\delta\rho_r i_{C1}}$$

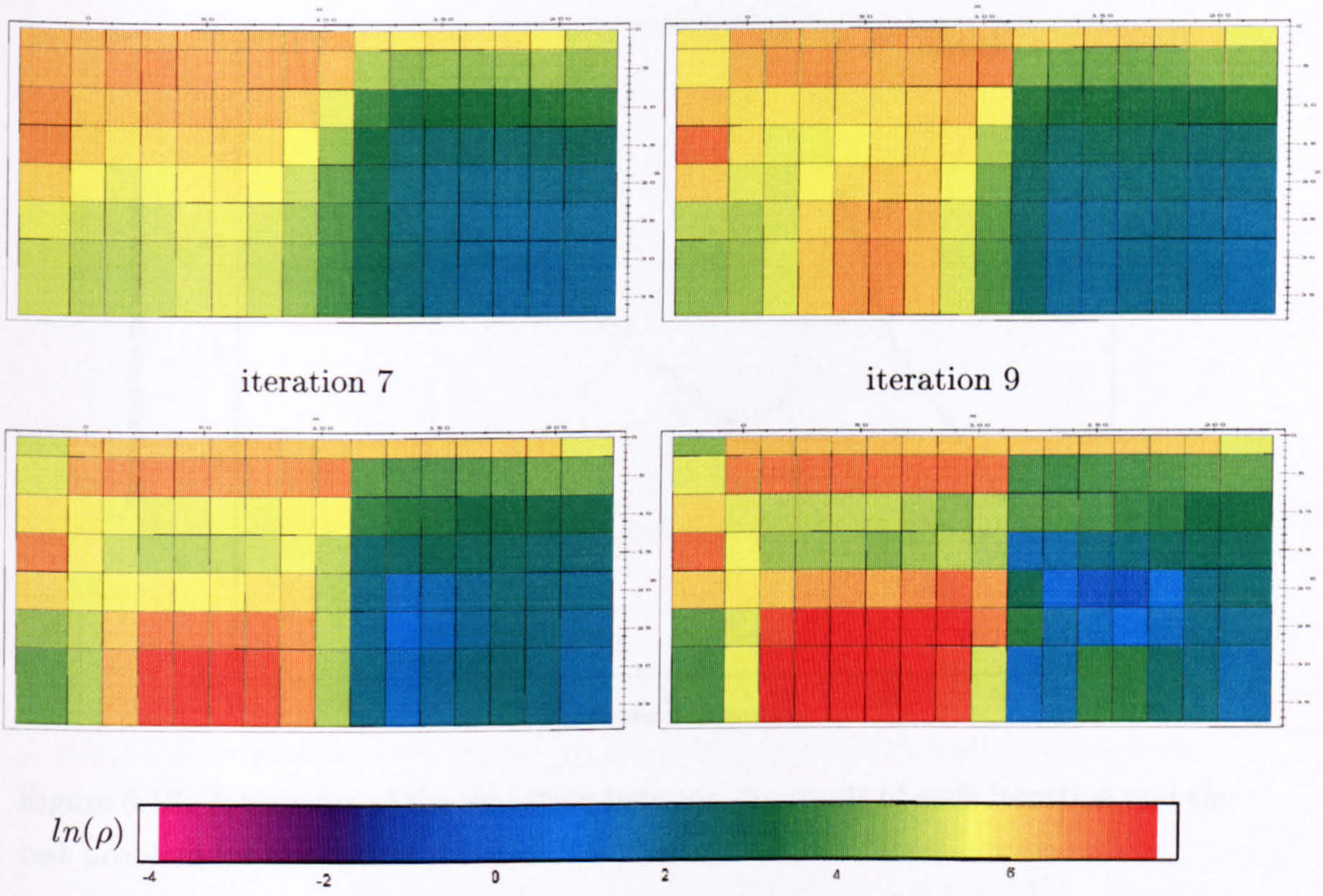

Figure 6.16: The natural logarithm resistivity values of the zones of hybrid method Jacobian.

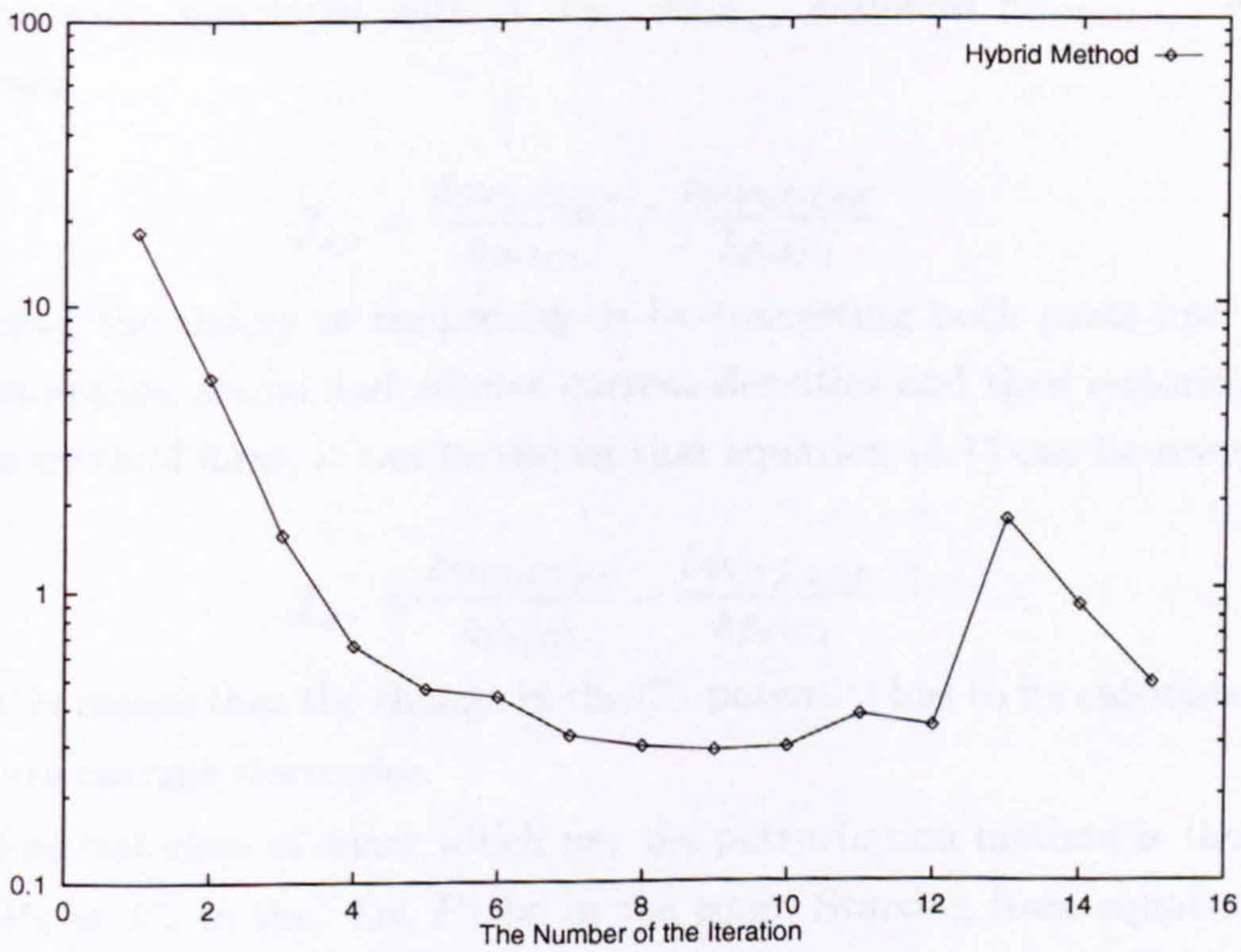

Figure 6.17: The convergence of the root mean squared error for the hybrid method Jacobian.

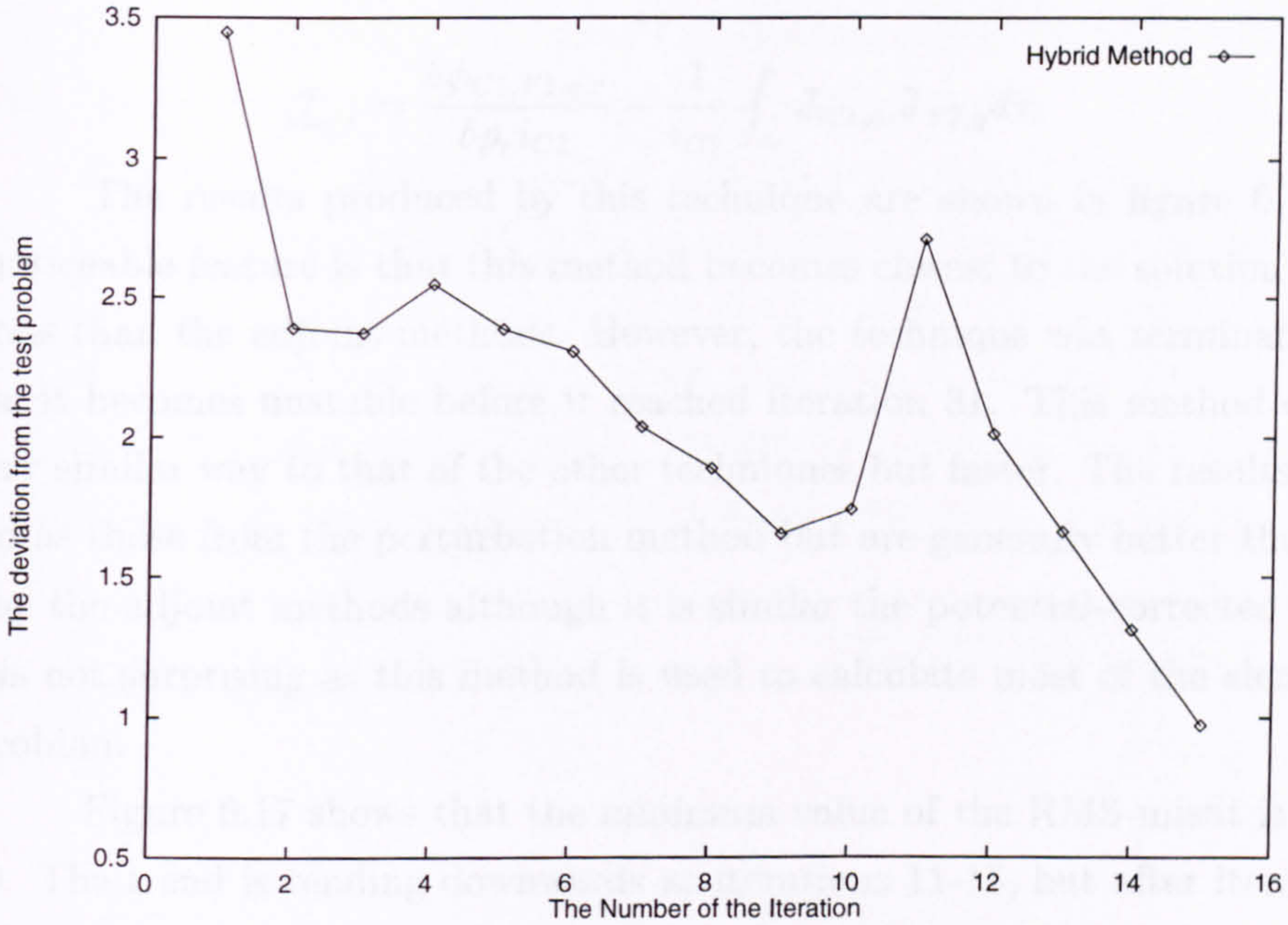

Figure 6.18: A measure of the deviation between the result of each iteration and the test problem for the hybrid method Jacobian.

This shows that the problem can be split into two parts, one for each potential electrode. Changing the notation so that each potential has both a source and potential electrode associated with it, i.e. $\delta\phi_{P1,q,r}$ becomes $\delta\phi_{P1,C1,q,r}$, equation (5.25) becomes

$$\underline{\mathcal{J}}_{q,r} = \frac{\delta\phi_{P1,C1,q,r}}{\delta\rho_r i_{C1}} - \frac{\delta\phi_{P2,C1,q,r}}{\delta\rho_r i_{C1}} \tag{6.1}$$

By either using the theory of reciprocity or by converting both parts into the adjoint form, swapping actual and adjoint current densities and then restoring to the perturbation method form, it can be shown that equation (6.1) can be rewritten as

$$\underline{\mathcal{J}}_{q,r} = \frac{\delta\phi_{C1,P1,q,r}}{\delta\rho_r i_{C1}} - \frac{\delta\phi_{C1,P2,q,r}}{\delta\rho_r i_{C1}} \tag{6.2}$$

In practice this means that the change in the $C1$ potential has to be calculated when $P1$ and $P2$ are current electrodes.

The last class of zones which use the perturbation method is those with just one of $P1$ or $P2$ in the. Let $P1$ be in the zone. Starting from equation (6.1), the $P1$ part becomes the P1 part of equation (6.2) and the P2 part uses the adjoint method (or a variant). Therefore the element of the Jacobian is calculated from

$$\underline{\mathcal{J}}_{q,r} = \frac{\delta\phi_{C1,P1,q,r}}{\delta\rho_r i_{C1}} - \frac{1}{i_{C1}} \int_{\tau_r} \mathbf{J}_{C1,q}.\mathbf{J}_{P2,q} d\tau_r \tag{6.3}$$

The results produced by this technique are shown in figure 6.16. The most noticeable feature is that this method becomes closest to the solution in fewer iterations than the adjoint methods. However, the technique was terminated early because it becomes unstable before it reached iteration 31. This method develops in a very similar way to that of the other techniques but faster. The results are not so good as those from the perturbation method but are generally better than those given by the adjoint methods although it is similar the potential-corrected adjoint, which is not surprising as this method is used to calculate most of the elements in the Jacobian.

Figure 6.17 shows that the minimum value of the RMS misfit is at iteration 9. The trend is tending downwards at iterations 11-15, but after iteration 15 it becomes unstable. A similar trend occurs when the solutions are compared with the test model in figure 6.18.

Even though only one zone is being perturbed for each current source this takes about 15 to 20 minutes[9] to calculate 14 values. This may be worth the extra time taken, even though the method appears to "blow up" after a certain length of time, as the result is produced more quickly but the value of λ is much larger than any of the other results.

6.4 The effect of increasing the number of nodes

Increasing the number of nodes does not invariably produce a straightforward increase in accuracy (see section 7.2.2 below) this may not always be the case. The test problem was changed by adding an extra layer of coarse grid nodes at $z = -5$m which introduced three new layers in the fine grid. The small grid lost its uniformity in the z direction. This means that the number of nodes was increased near the surface and the electrodes. The extra nodes should be well positioned because this is the region where the steepest changes in current density occur. It should also improve the accuracy of the model for the same reason.

The first and most obvious effect is to increase the time (and number of iterations) taken to solve the related forward problems. This does not appear to have the same effect on the time taken to calculate the Jacobian, which did not increase greatly. This would not be true for the perturbation method, where a small increase

[9] On a Pentium Pro PC $200MHz$

in the time taken to calculate the forward problem would be greatly magnified as it is heavily due to its dependent on the forward problem.

The adjoint method Jacobian and the potential-corrected adjoint Jacobian were calculated using the new grids, as were the measurements for the test case. The convergence (as shown in figure 6.19) is similar to the convergence of the methods without the extra nodes until the lowest minimum is reached, after which both of the methods start diverging. However, the potential-corrected adjoint reaches its lowest minimum later and reaches a smaller value does than the adjoint method.

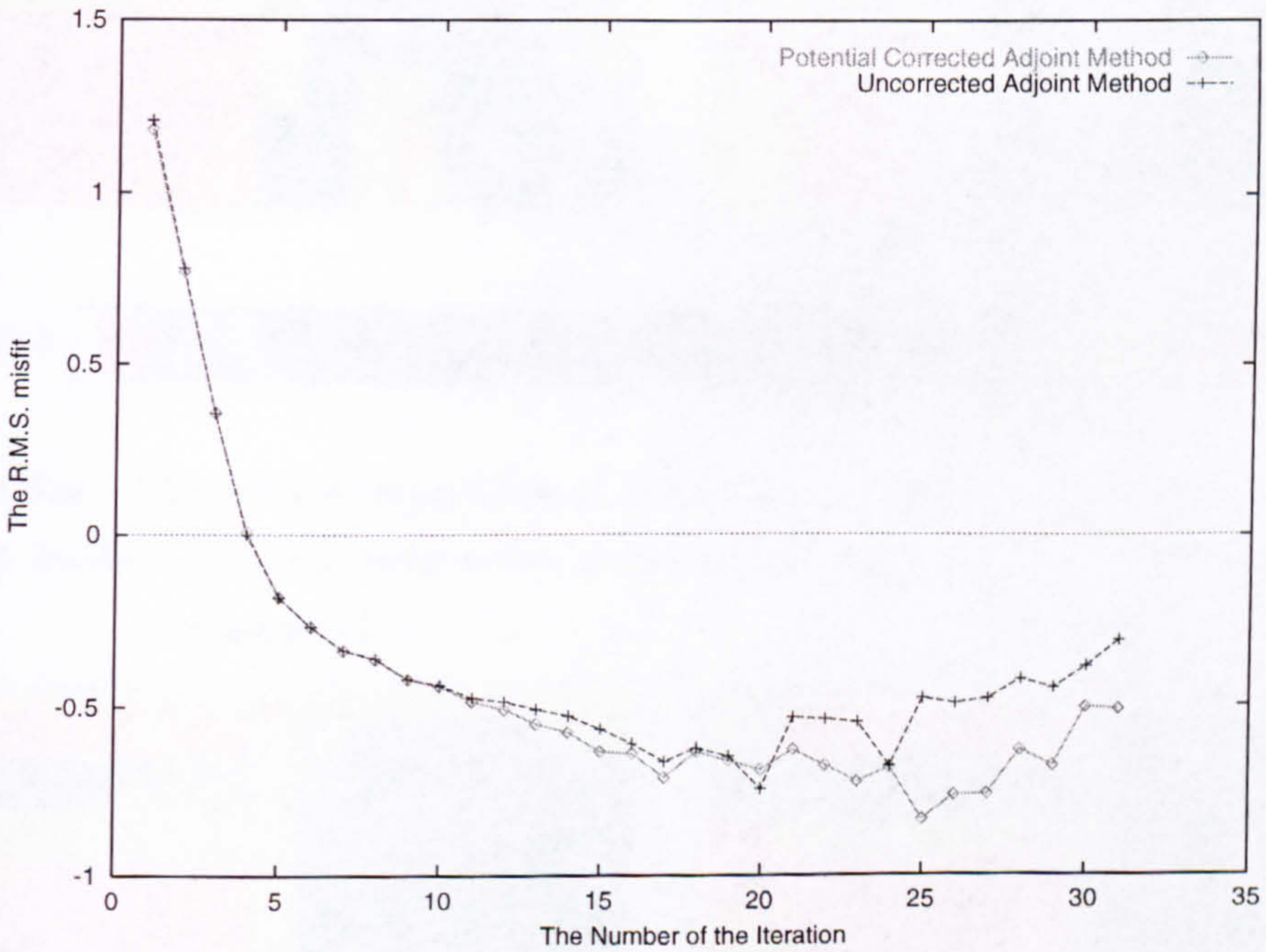

Figure 6.19: The convergence of the RMS error for the adjoint method Jacobian and the potential-corrected adjoint method Jacobian with extra nodes at the surface.

The results of the two solutions are shown in figures 6.20 and 6.21. It can be seen that iteration 31 of both methods is beyond where the inversion should have ended. At the bottom left-hand corner of each there appears to be a very poor solution. The structure below the third layer is beginning to disappear. The results from iterations 17 & 20, have a greater RMS error than when the extra nodes are not included. The results appear to show the patch of low resistivity on the right-hand side more accurately than any of the other adjoint methods used, without the extra nodes. Therefore, although the RMS error is large, the solutions appear to be closer to the true values.

Figure 6.22 shows how the results of each iteration deviate from the solution. As can be seen the best agreement is produced by the potential-corrected

iteration 17

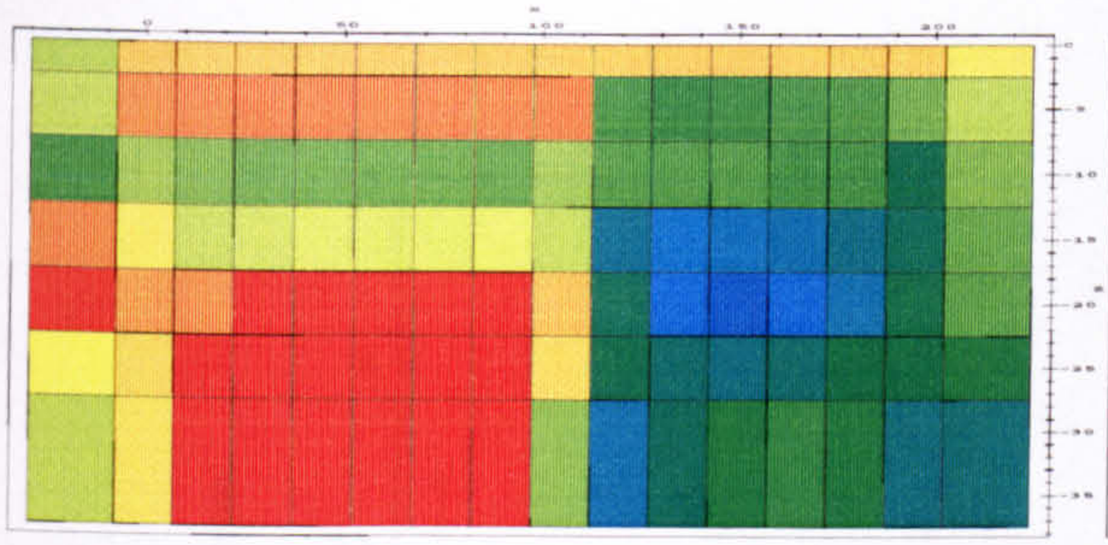

iteration 20

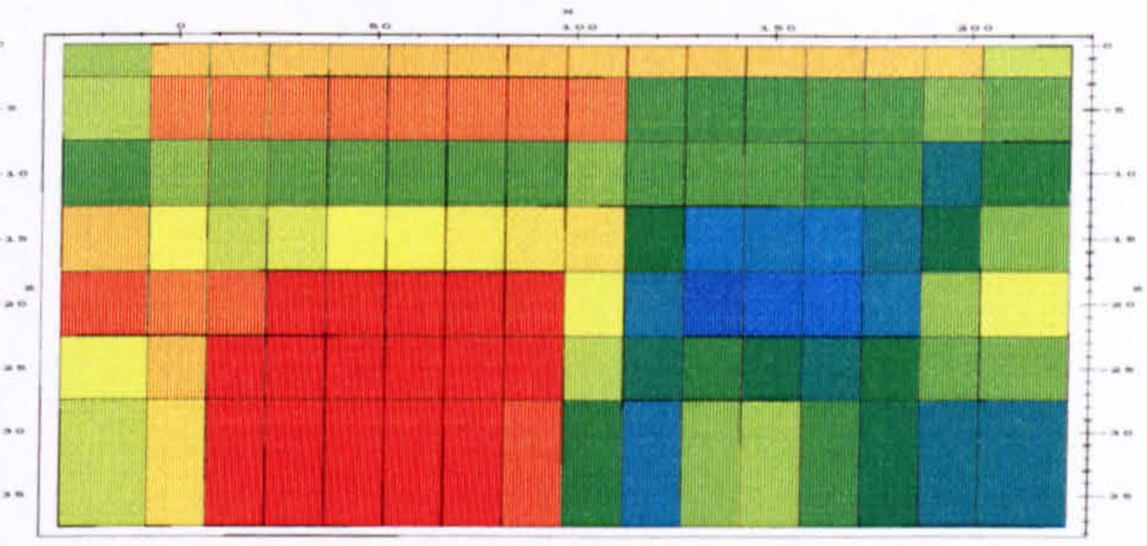

iteration 24

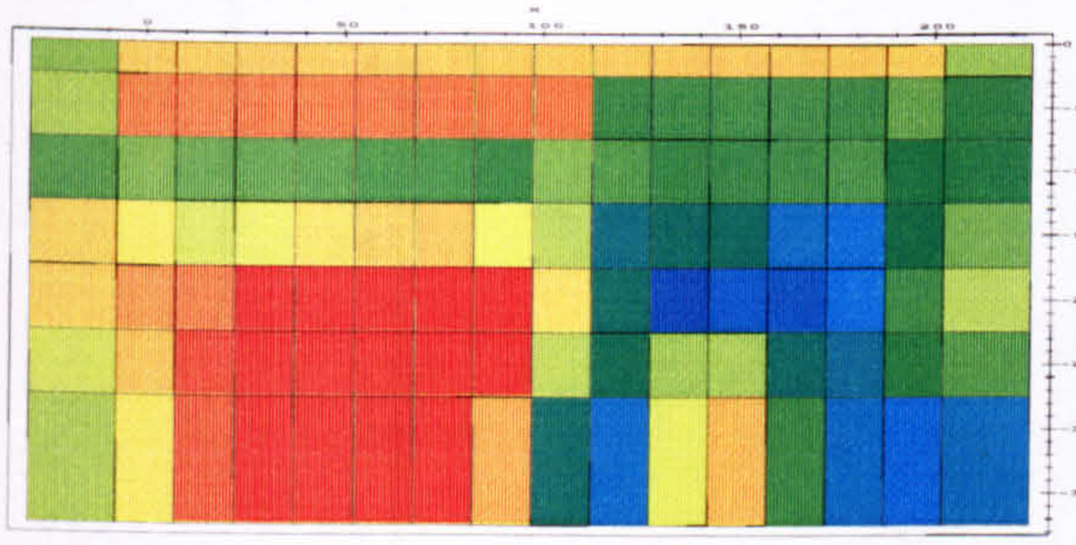

iteration 31

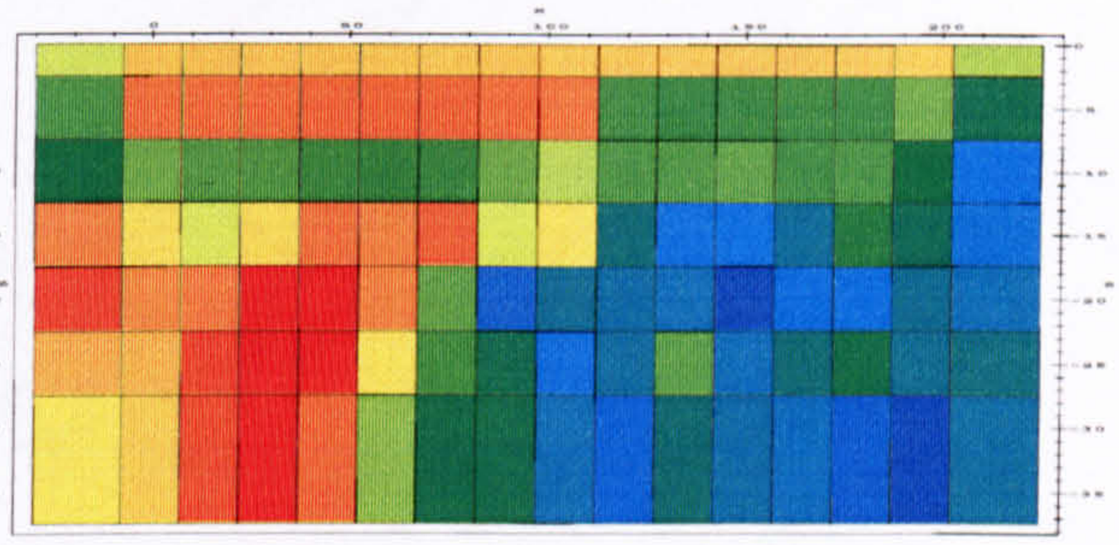

Figure 6.20: The natural logarithm of the resistivity values of the zones using the adjoint method Jacobian with extra nodes at the surface.

iteration 17

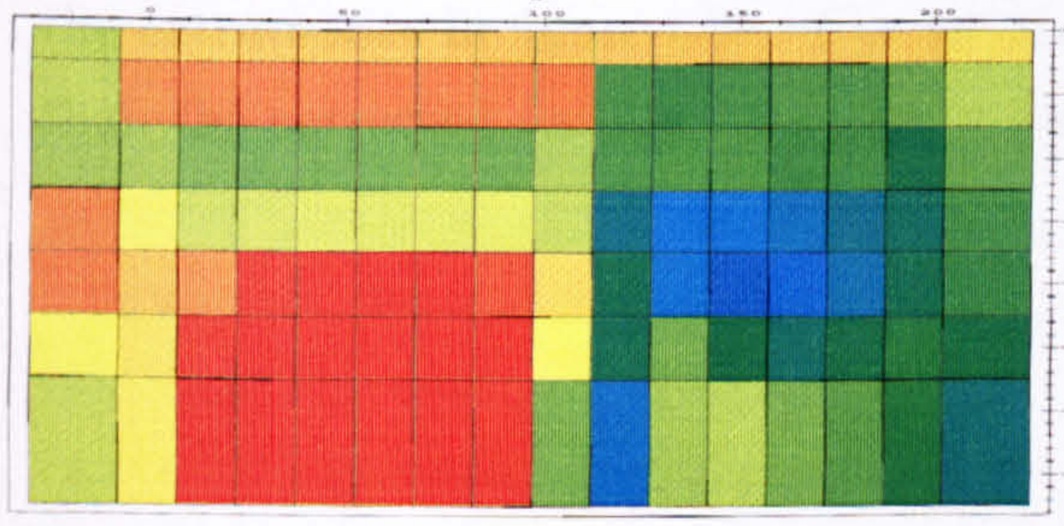

iteration 20

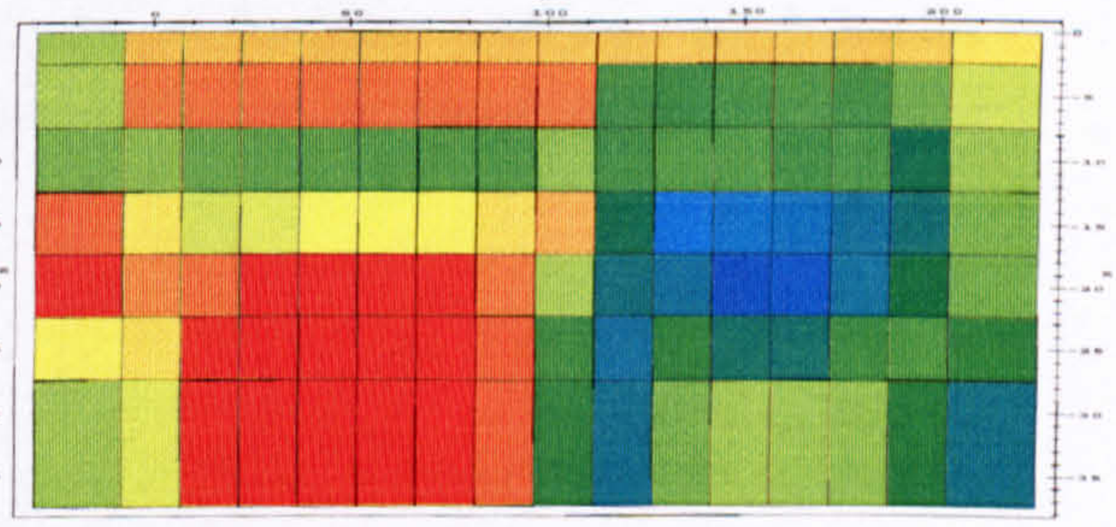

iteration 25

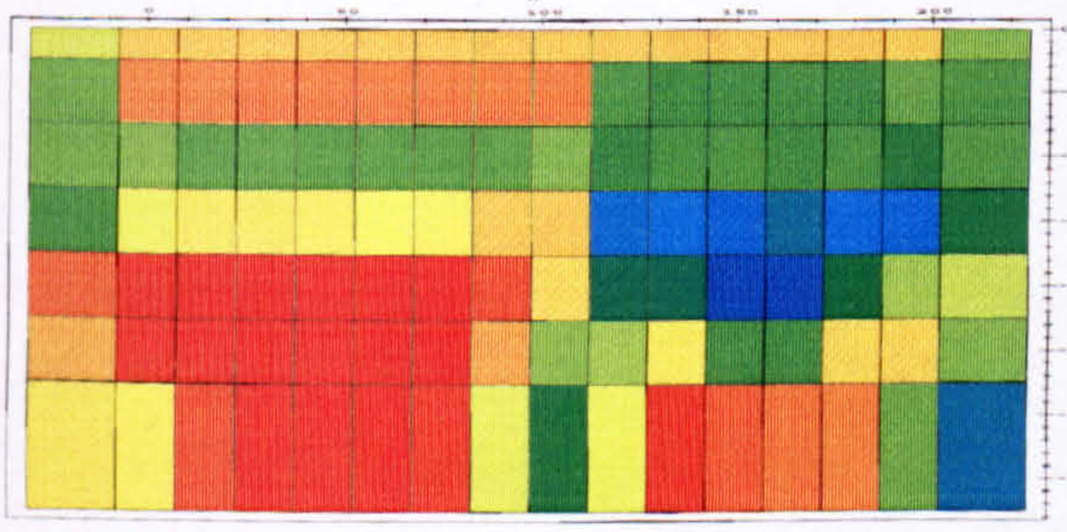

iteration 31

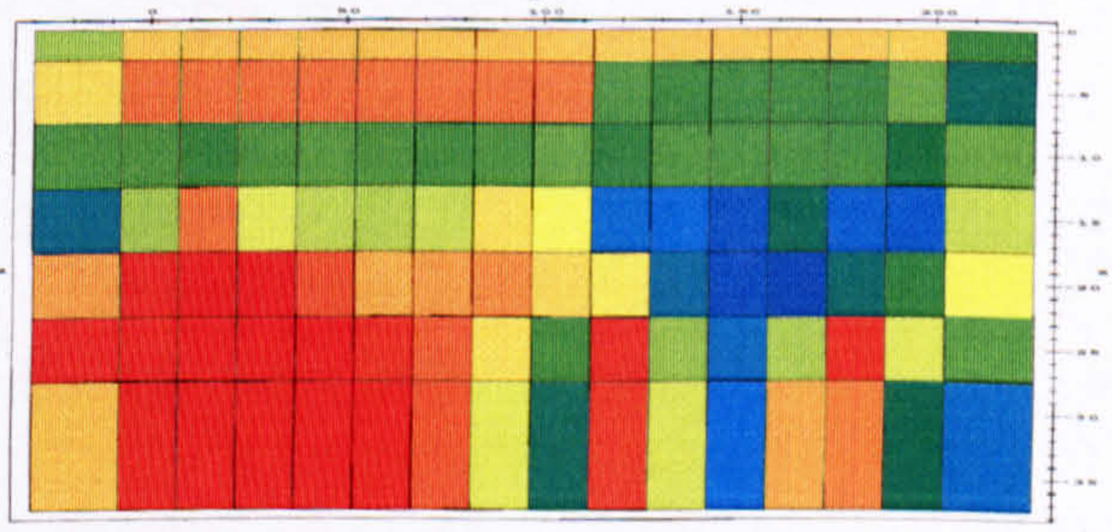

Figure 6.21: The natural logarithm of the resistivity values of the zones using the potential-corrected adjoint method Jacobian with extra nodes at the surface.

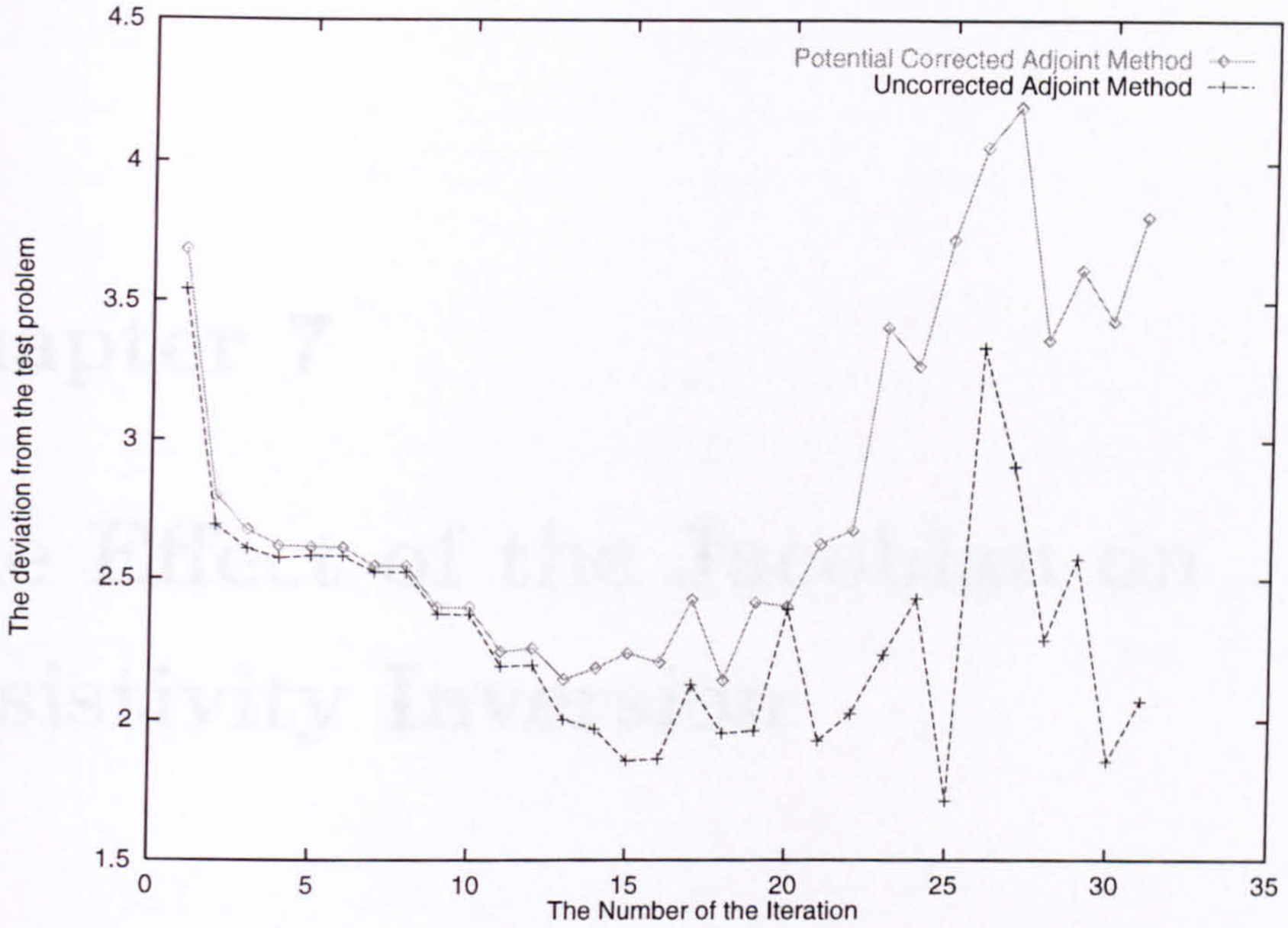

Figure 6.22: A measure of the deviation between the result of each iteration and the test problem with an increased number of nodes.

adjoint method is in iteration 25 and follows roughly the same shape as it did without the extra nodes in figure 6.15. The adjoint method Jacobian performs much better than the corrected version[10] and has it lowest difference at iteration 25.

[10]This is not true when the extra nodes are not included.

Chapter 7

The Effect of the Jacobian on Resistivity Inversion

7.1 Introduction

This chapter looks in detail at the Jacobians used in calculating the results in chapter 6. Its purpose is to show that the calculation of the Jacobian is an important part of the inversions. Being able to view the Jacobians is an important part of assessing which method is most likely to produce a Jacobian matrix close to the analytic Jacobian for both the homogeneous case (for which an actual comparison can be produced) and the heterogeneous case. It will highlight errors occurring which would otherwise go unseen in such a large matrix where the elements vary over several orders of magnitude.

The Jacobians discussed and displayed in this chapter are split into two types. The first are the homogeneous Jacobians produced for each of the different methods. These Jacobians contain patterns, which are not affected by variations in resistivity, such as "striping" (see figures 7.2, 7.3) etc.) which runs in every case from bottom left to top right of each "block". It should however be borne in mind when examining the Jacobian, that the patterns may not be immediately evident from the matrix. The second are the heterogeneous Jacobians. Three different resistivity distributions are compared:

1. The uses of the measurements to calculate a better starting point for the iterations than the homogeneous case.

2. The best result calculated (a perturbation method Jacobian).

3. The actual solution.

The comparisons reveal the effect of the resistivity distributions on the Jacobian and how close the best result is to the solution. These Jacobians, when compared with the homogeneous case, show why it is necessary to spend enough time on these calculations.

Section 7.4 looks at the structure of the solution, which can be seen in Jacobian and discusses whether the Jacobian leads the resistivity distributions or trails them. The effect of a stiff smoothness-constraint on damping errors in the Jacobian is also discussed.

To be able to display these Jacobians, the values must be transformed to reduce the seven orders of magnitude between the largest and smallest values. After a period of trial and error the following mapping was applied:-

$$function = \begin{cases} log_{10}(a) + 10 & a > 1 \times 10^{-10} \\ -log_{10}(-a) - 10 & a < -1 \times 10^{-10} \\ 0 & -1 \times 10^{-10} < a < 1 \times 10^{-10} \end{cases}$$

This allows the parameter a to be both positive and negative and allows for large variations in magnitude. It should be noted that the magnitude of the parameter is in the range $10^{-9} < |a| < 10^{-1}$.

As well as looking at images of the whole Jacobian, four different measurements will be used. These are measurements 1, 169, 189 and 352. (Measurement 1 contains one of the largest values in the Jacobian (under the electrodes). Measurement 189 is the mirror image of measurement 1. Measurement 169 has the electrodes placed far apart, and its the mirror image is measurement 352.) A table of the first two measurements of the computed homogeneous Jacobian can be found in appendix H.1.

The measurement correction adjoint method is not discussed in this chapter since it is very similar to the other adjoint methods. The corrections produced by the measurement and potential-correction methods are small. This means that the major differences between the uncorrected adjoint method and the perturbation method still hold for these two. The measurement correction is constant at 0.922 as shown in figure 7.1 which relates to the first measurement and is thus represented by a straight line. The potential correction tends only to correct by $\pm 3\%$. This is not true for the zones on the left hand boundary (i.e. zones 1 and 17) where the correction is slightly less than a 15% reduction in the size of the original value. It also increases the value of the Jacobian far more than it decreases it, making the values closer to that of the perturbation method.

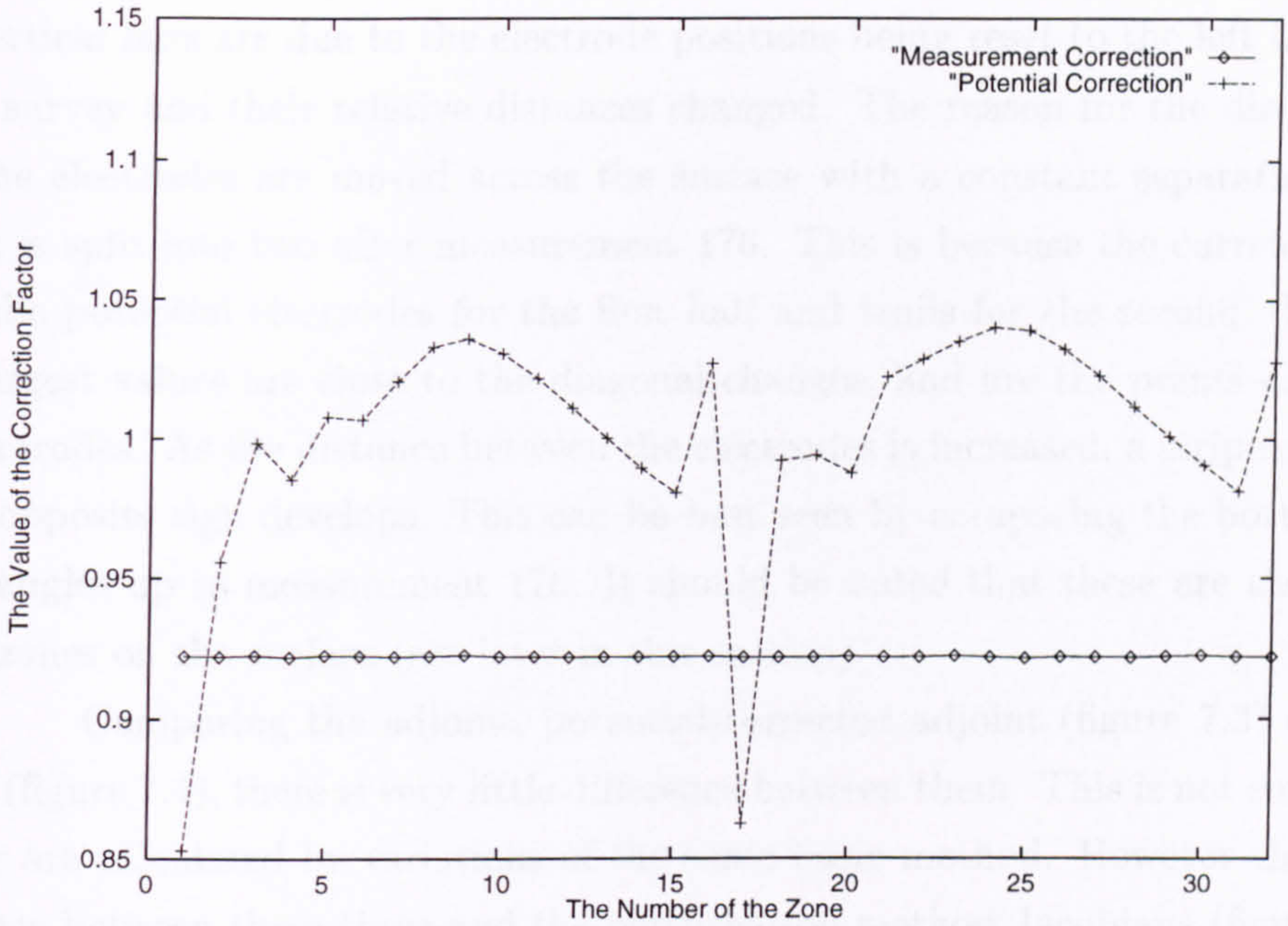

Figure 7.1: A Comparison of the values of measurement and potential correction factors.

7.2 Homogeneous Jacobian

There are two types of homogeneous Jacobian, firstly those calculated from the potentials from the finite difference model and secondly the one that implicitly calculates the potentials. The former type uses methods that are the results we have seen in chapter 6. These will be described in section 7.2.1. The second uses the analytic method derived in section 5.5.2 will be found in section 7.2.2

7.2.1 Results of the calculated homogenous Jacobians

Comparing the results for the first iteration for all the methods, in section 6.2, shows that slightly different results are produced. This must be caused by differences between the Jacobians, as all the other parameters remain the same for all the inversions. However, before discussing the differences, the structure of the Jacobians must be explained.

Taking the homogeneous adjoint Jacobian, shown in figure 7.2, as an example, the most noticeable structure is that the matrix seems to be divided up into a number of rectangles which are split by a diagonal which runs from the bottom left to top right of each rectangle (not necessarily from corner to corner). The horizontal bars are caused by changes in the layers of zones (every 16 zones).

The vertical bars are due to the electrode positions being reset to the left hand end of the survey and their relative distances changed. The reason for the diagonals is that the electrodes are moved across the surface with a constant separation. The matrix is split into two after measurement 176. This is because the current source leads the potential electrodes for the first half and trails for the second. We note that largest values are close to the diagonal changes, and are the points closest to the electrodes. As the distance between the electrodes is increased, a stripe of values of the opposite sign develops. This can be best seen by comparing the bottom row of rectangles up to measurement 176. It should be noted that these are the values in the zones on the surface (see later in this section).

Comparing the adjoint, potential-corrected adjoint (figure 7.3) and the hybrid (figure 7.4), there is very little difference between them. This is not surprising as they are calculated by variations of the same basic method. However there is a difference between these three and the perturbation method Jacobians (figure 7.5). These differences are in zones 49 to 80, where zones 49 to 64 appear to have a positive constant added to that of the adjoint. The zones 65 to 80 appear to have had a negative value added to them.

It is easier to see the difference by comparing measurements 1, 169, 189, and 352. These form two pairs (1, 189 and 169, 352) which are reflections of the other in the pair. The values of the Jacobian are laid out in the same way as the zones. Comparing the first measurement of the adjoint (figure 7.6) to the hybrid (figure 7.7), it can be seen that zone 2 changes sign. This is one of the zones where the hybrid calculation uses the perturbation method. Zone 2 for the first measurement also happens to be associated with one of the largest values in the Jacobian. This phenomenon is repeated where the electrodes are close together (e.g. measurements 2 and 3).

Comparing the adjoint with the perturbation Jacobian, some distinct differences can be noted. These are, like the hybrid Jacobian, at zone 2 for the first measurement and also show large discrepancies in the fourth and fifth layers. The major difference is at zone 2 where there is not only a change of sign but also an order of magnitude difference. From the relevant lines in the table in appendix H.1 it can be seen that this occurs only for the surface zones. The two zones shown here are both on the surface and contain the $P2$ electrode. They both have some of the largest values in their respective rows. The implication of this is that this difference may have a large effect on the result.

Considering measurement 169 in figures 7.6 and 7.8, as a good example,

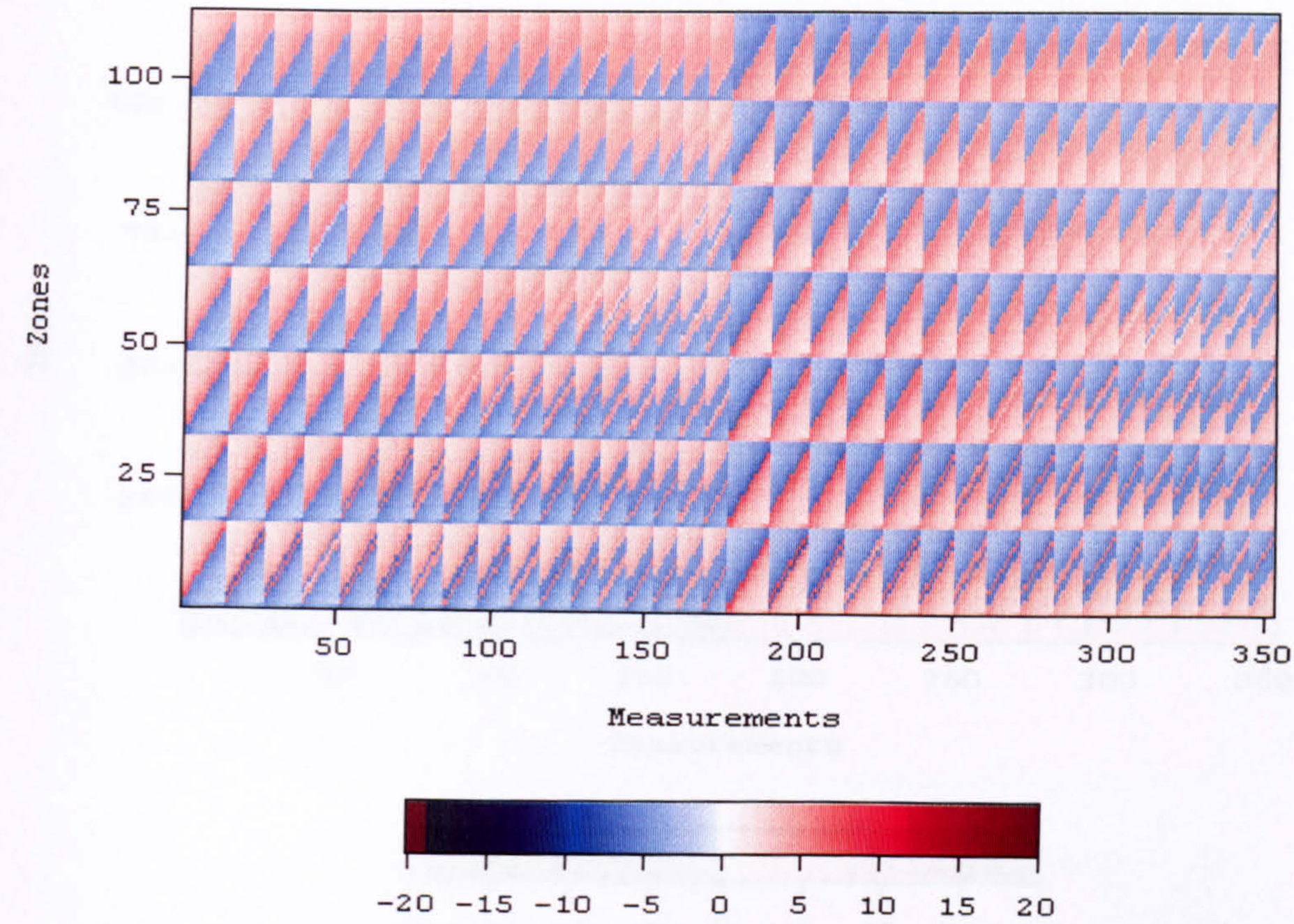

Figure 7.2: Homogeneous Jacobian calculated by the adjoint method.

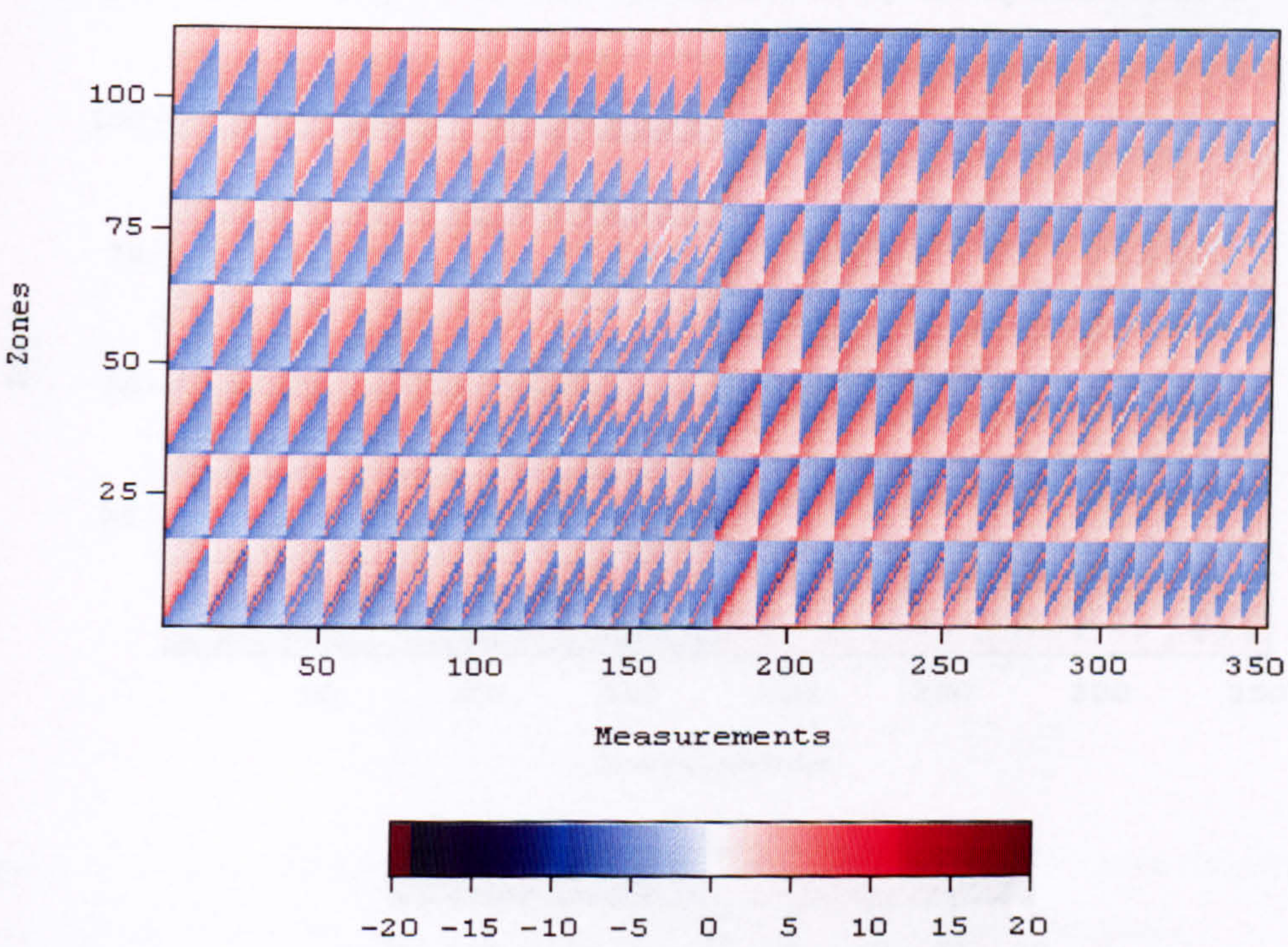

Figure 7.3: Homogeneous Jacobian calculated by the potential corrected adjoint method.

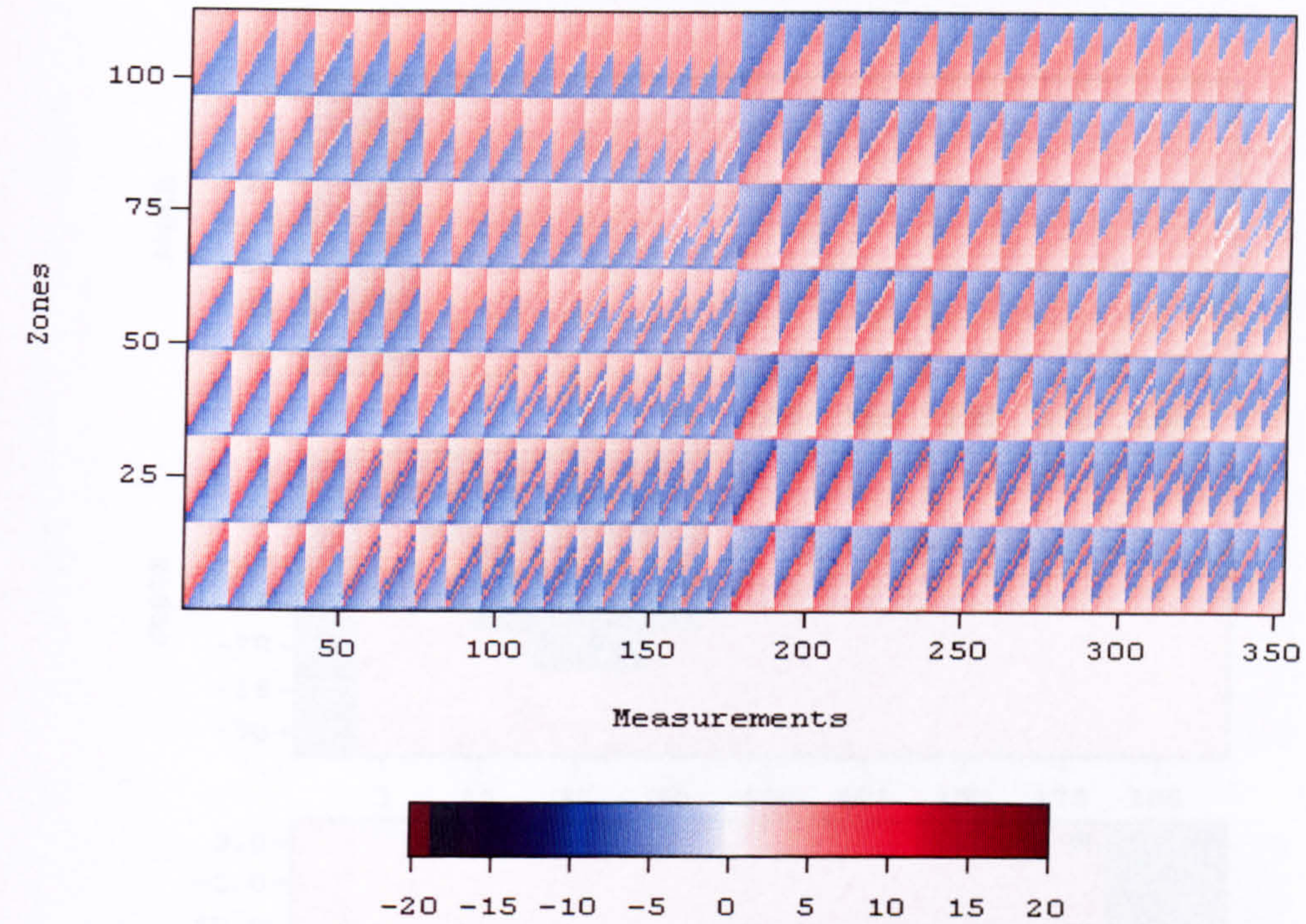

Figure 7.4: Homogeneous Jacobian calculated by the hybrid method.

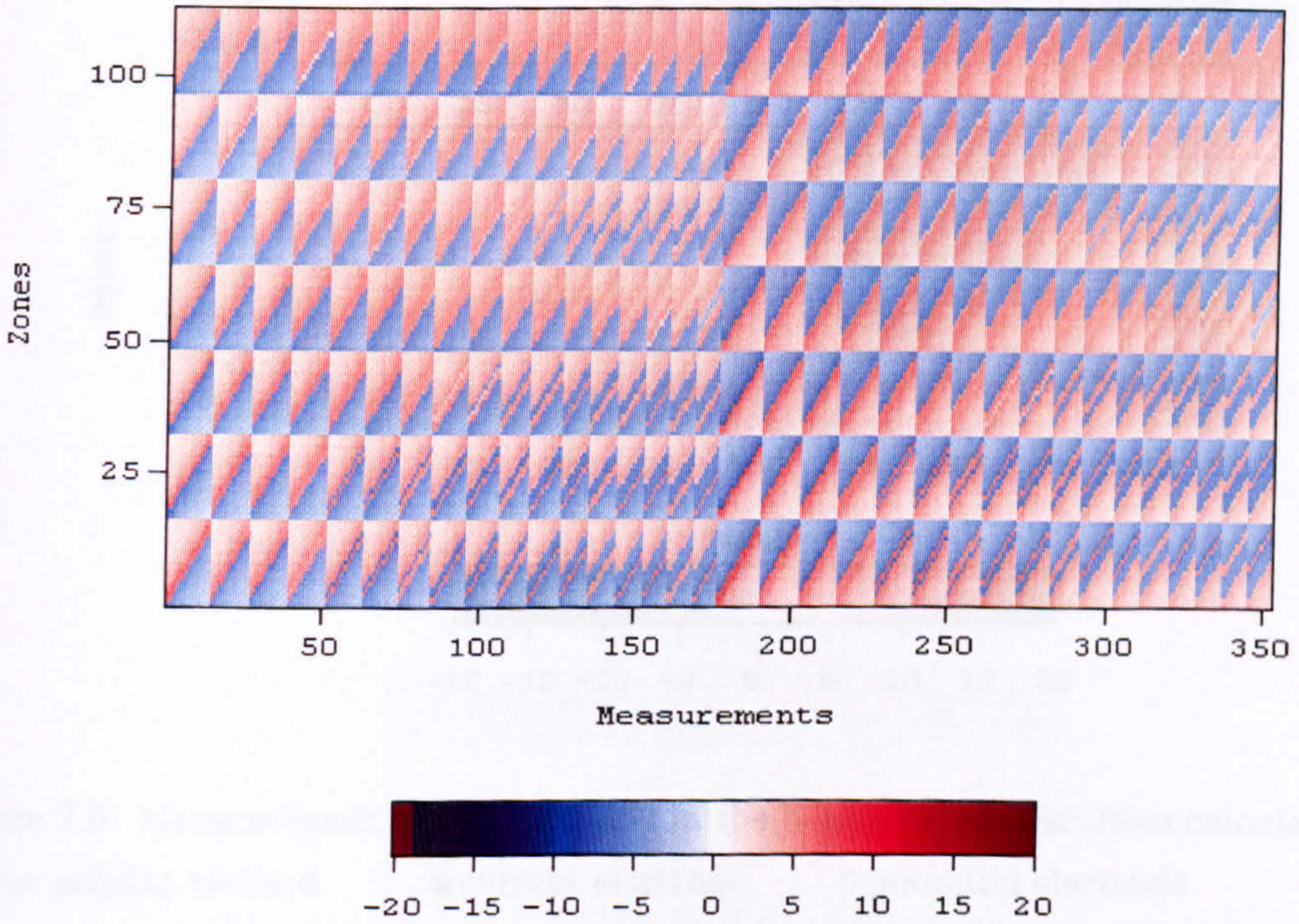

Figure 7.5: Homogeneous Jacobian calculated by the perturbation method.

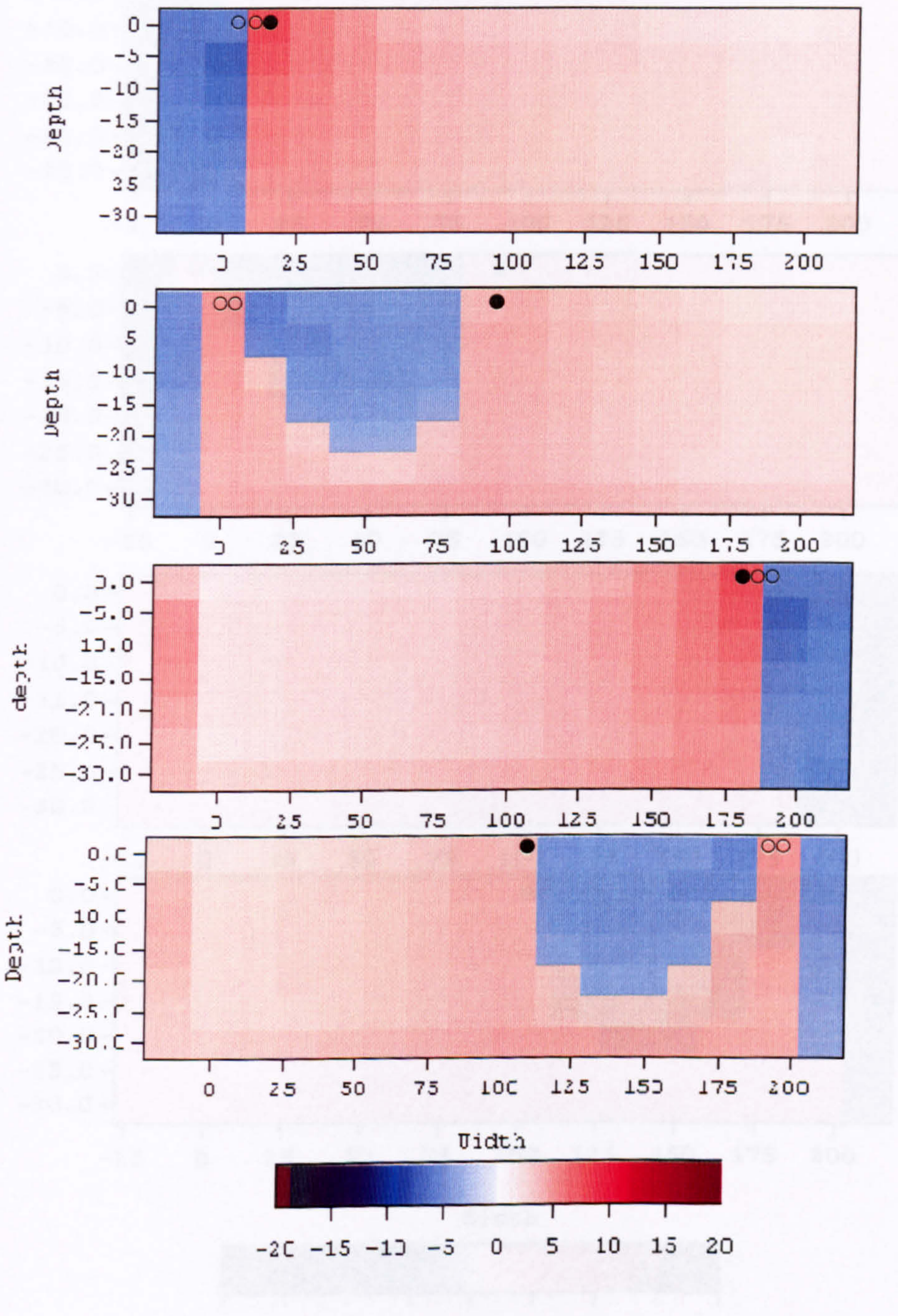

Figure 7.6: Measurements 1, 169, 189, 352 in the homogeneous Jacobian calculated by the adjoint method. ● current electrode ○ potential electrode

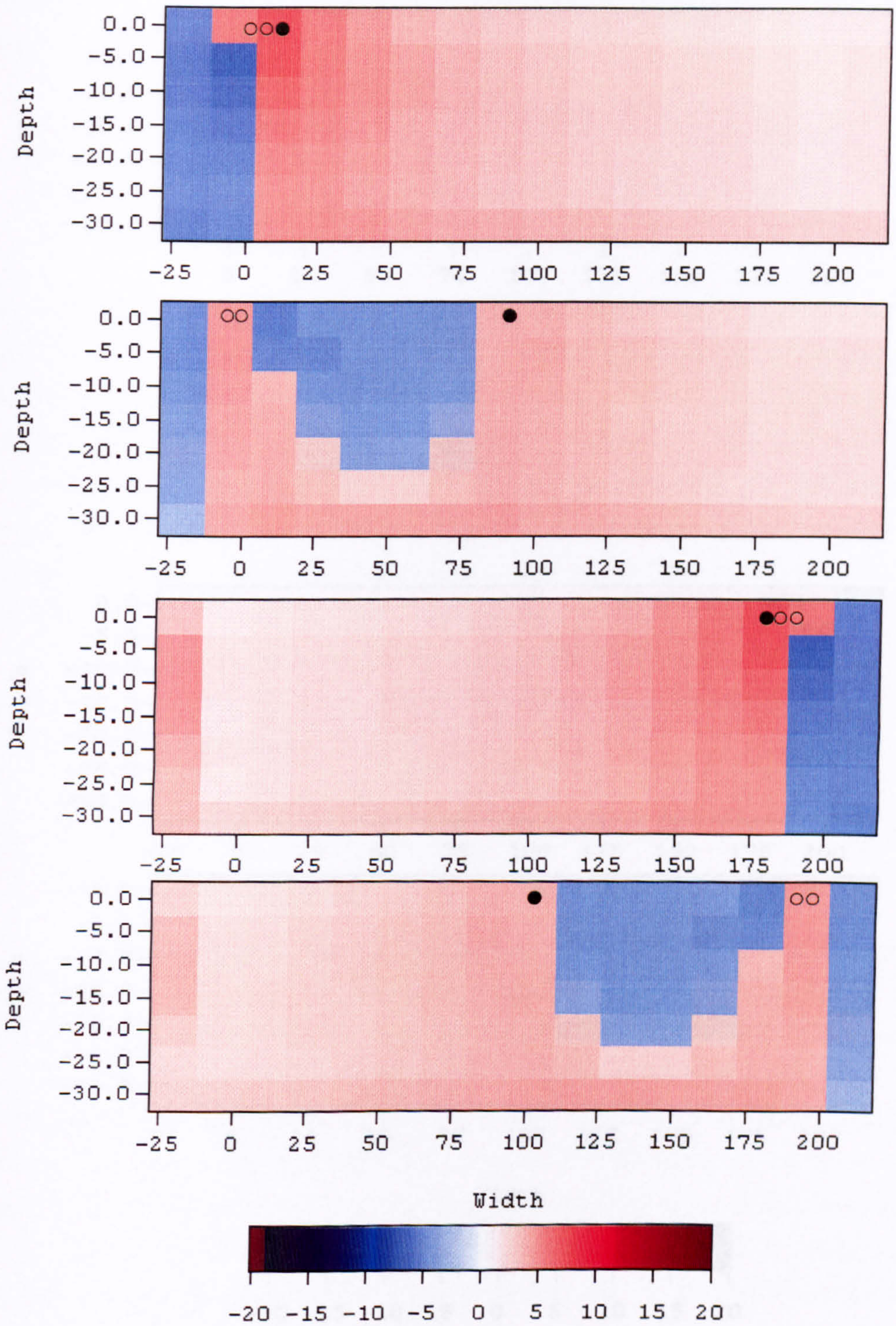

Figure 7.7: Measurements 1, 169, 189, 352 in the homogeneous Jacobian calculated by the hybrid method. ●current electrode ○potential electrode

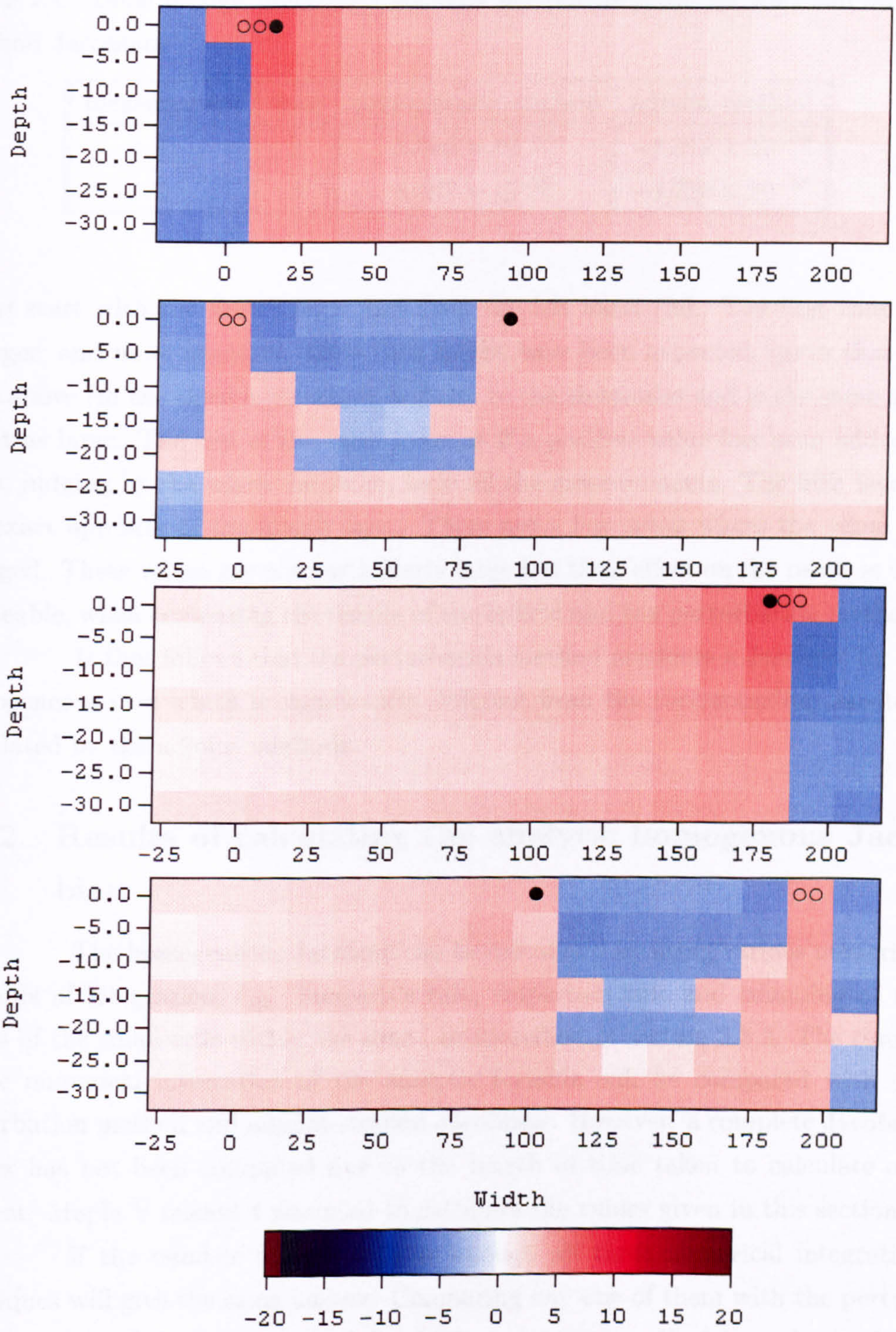

Figure 7.8: Measurements 1, 169, 189, 352 in the homogeneous Jacobian calculated by the perturbation method. ● current electrode ○ potential electrode

Table 7.1: Table of sign differences between the perturbation method and adjoint method Jacobians

measurement	zone	perturbation method	adjoint method
1	2	8.042×10^{-04}	-4.012×10^{-05}
2	3	8.047×10^{-04}	-4.220×10^{-05}

let us start with the fourth layer and from the left hand end. The first zone has a larger, and more negative, value than might have been expected, given that the zone above (in the third layer which is closer to the electrodes and is the same size) is not as large. The rest of the layer looks as if a positive value has been added to it, as, judging by the whole Jacobian, have all the measurements. The fifth layer is the exact opposite of the fourth layer. There are a few zones where the value has changed. These values are not particularly large but their effect on the result is very noticeable, when comparing the results of the hybrid and the perturbation methods.

It thus follows that the perturbation method produces a Jacobian for the homogeneous case which is significantly different from the corresponding Jacobian calculated by the adjoint methods.

7.2.2 Results of calculating the analytic homogenous Jacobian

The homogeneous Jacobian can be calculated by using various numerical methods of integration, e.g. Simpson's rule, trapezium rule and summing of the values of the small cells within the zone , as described in section 5.5.2. The results of the numerical integration of the analytic formula will be compared with the perturbation method and adjoint method Jacobians. However, a complete Jacobian matrix has not been computed due to the length of time taken to calculate one element. Maple V release 4 was used to calculate the values given in this section.

If the number of cells is large enough all three numerical integration techniques will give the same answer. Comparing any one of them with the perturbation method and adjoint method Jacobians is not necessarily fair, as both of the non-analytic Jacobians are calculated over a much coarser grid.

In figure 7.9 it can be seen that for most values the analytic Jacobian follows the adjoint method Jacobian. However, the analytic Jacobian is not defined in zones 2 and 3 since this is where the electrodes are located and the function is

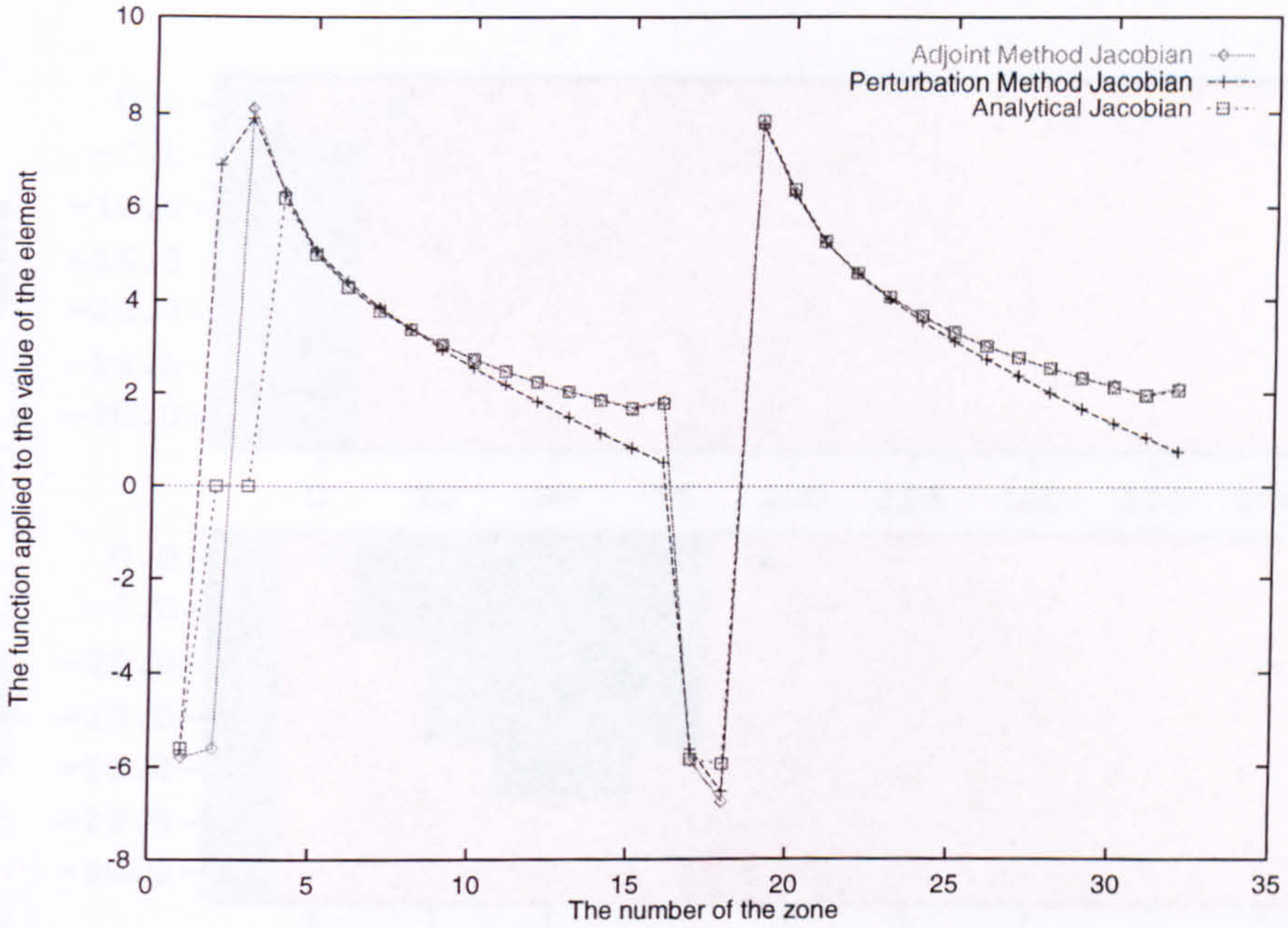

Figure 7.9: Comparing the element of the Jacobian given by the first measurement and zones 1 to 32.

discontinuous in these zones. As a consequence, the values have been set to zero. It differs from the adjoint method Jacobian in the value furthest from the electrodes, i.e. zone 16 is greater than zone 15 (this is also true for the zones 31 and 32 directly beneath 15 and 16).

The trapezium rule with 14 points in each direction in each zone was used to produce figure 7.10. Although the zones containing the electrodes have been calculated, these will contain errors due to the discontinuities in these zones. Comparing this with the non-analytic methods, we see that the structure is almost identical to that of the hybrid Jacobian. This is because to the zones with electrodes have the same sign as the hybrid method. This highlights the errors in the extended fine mesh caused by interpolating the coarse mesh potentials.

During the calculation of the most accurate values of the Jacobian, it was noticed that there was not always a smooth reduction in the error as the number of nodes in each direction was increased. This seemed to be contrary the results in section 6.4.

Let us consider the behaviour of the Simpson's rule output as the number of cells is increased. Values of two zones are shown in figures 7.11 and 7.12. The value taken as a reference was calculated by increasing the number of cells in each direction to 60. Both zones converge satisfactorily. The trapezium rule for 60 cells

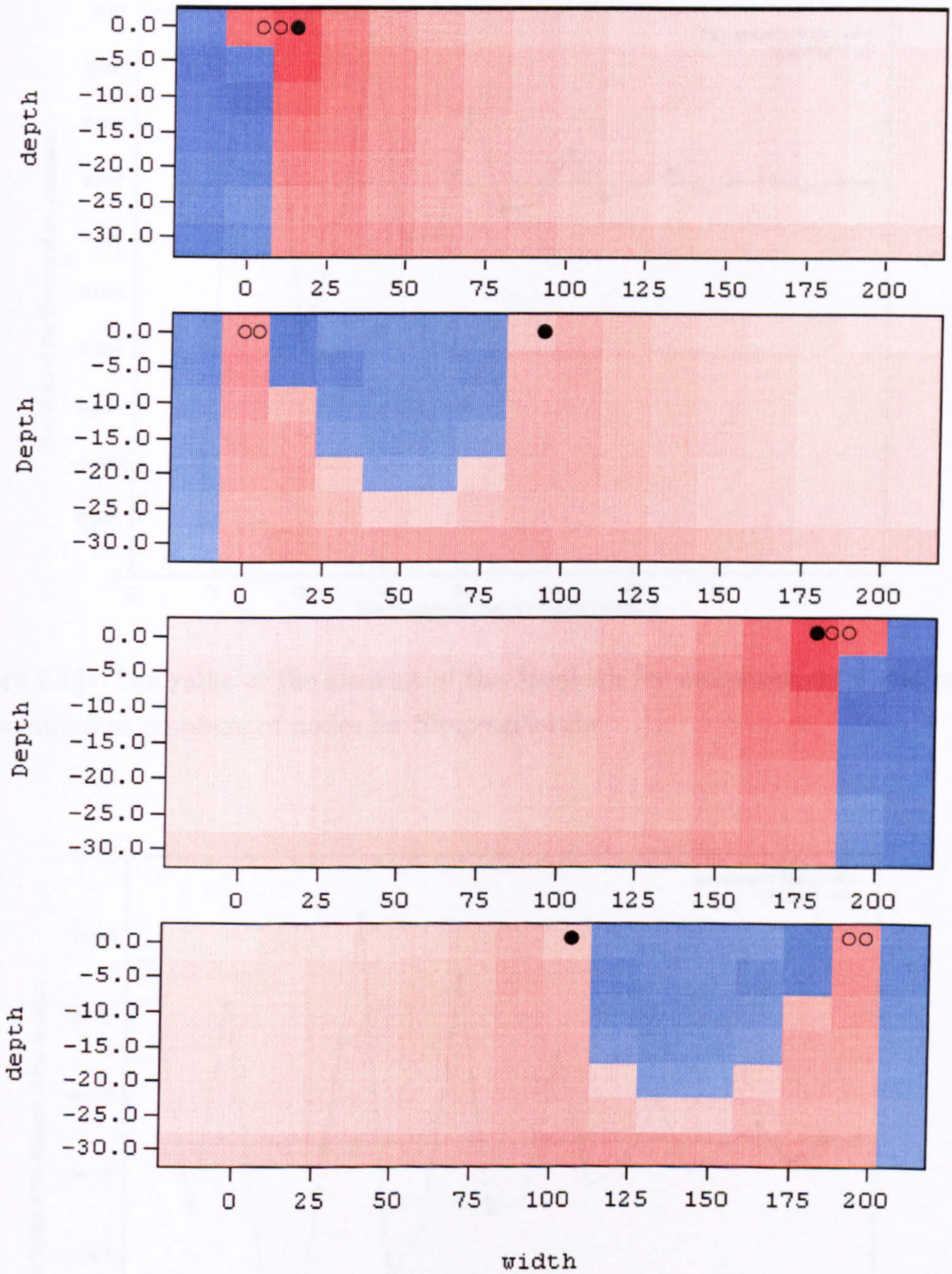

Figure 7.10: Measurements 1, 169, 189, 352 in the homogeneous Jacobian calculated from the analytic equation. ● current electrode ○ potential electrode

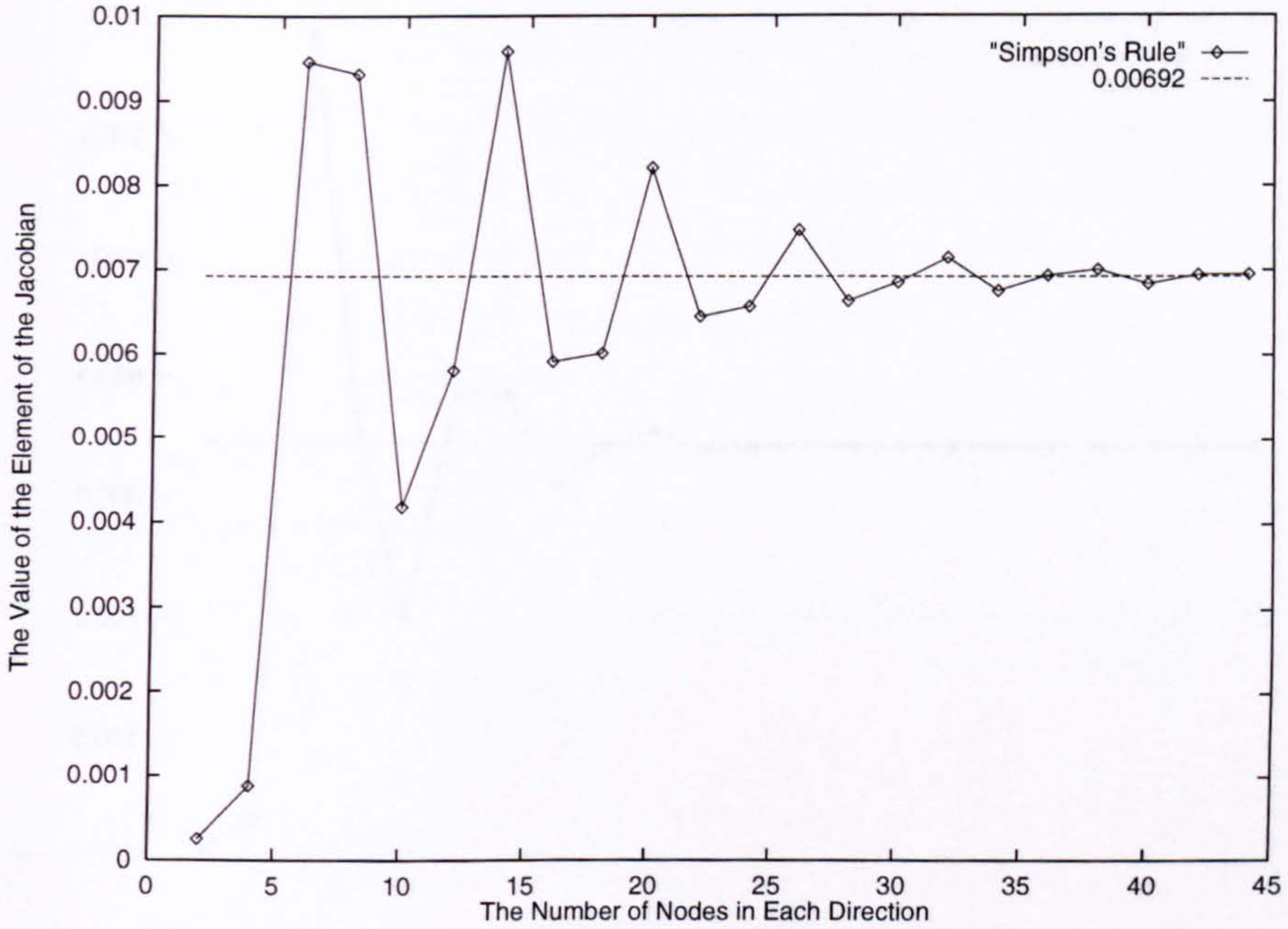

Figure 7.11: The value of the element of the Jacobian for measurement 1 and zone 19 for different numbers of nodes for Simpson's rule.

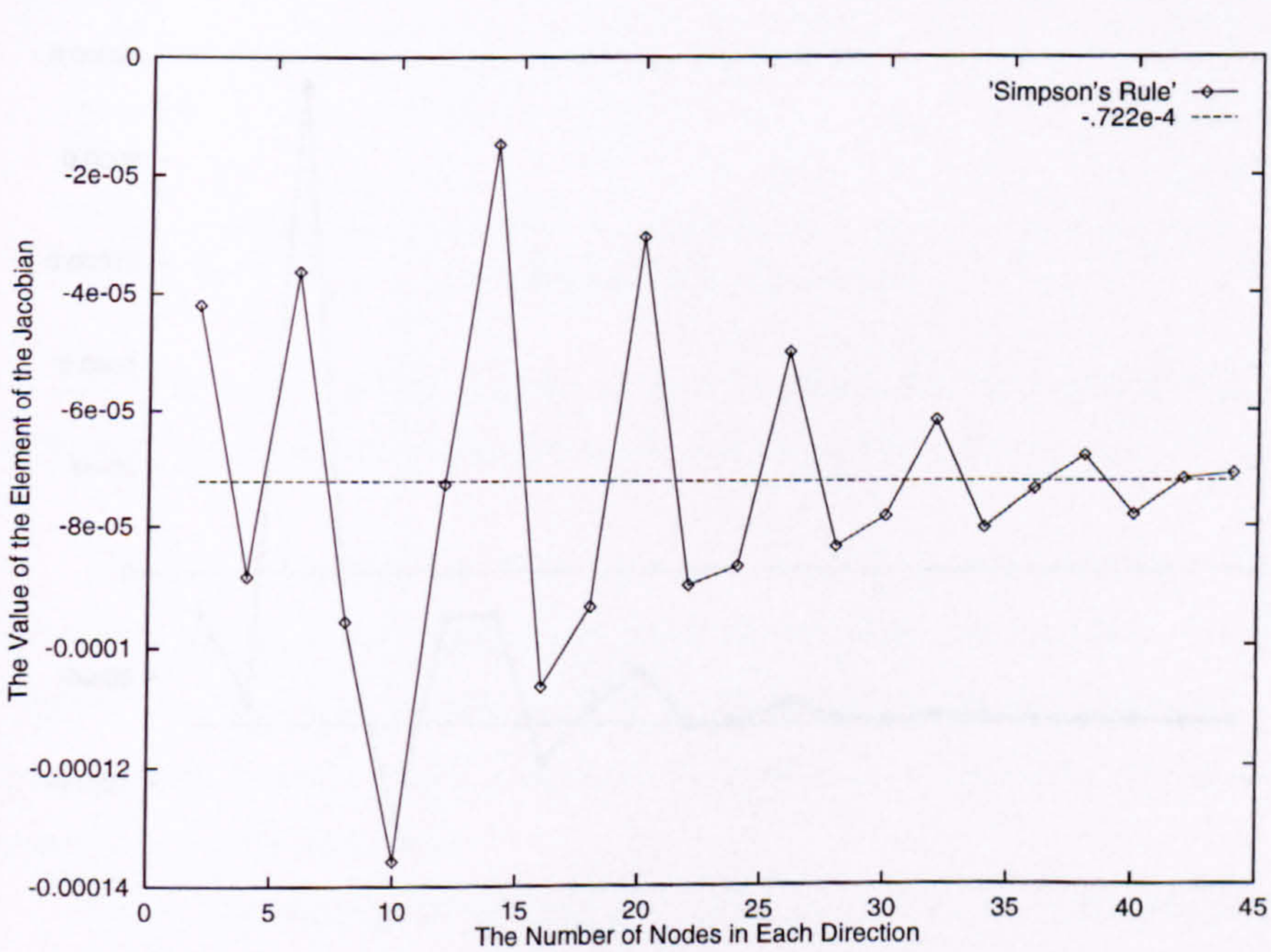

Figure 7.12: The value of the element of the Jacobian for measurement 1 and zone 18 for different numbers of nodes for Simpson's rule.

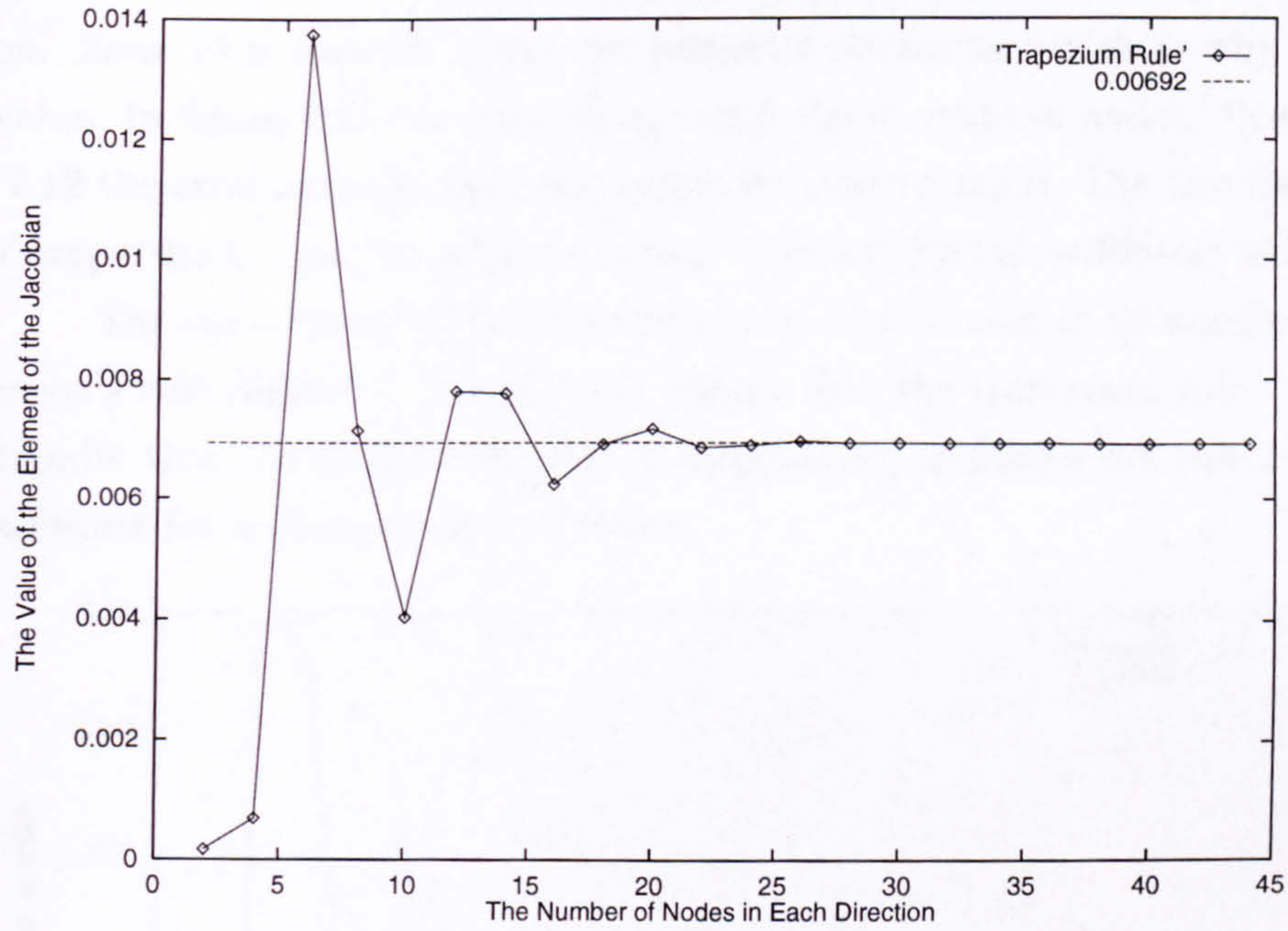

Figure 7.13: The value of the element of the Jacobian for measurement 1 and zone 19 for different numbers of nodes for trapezium rule.

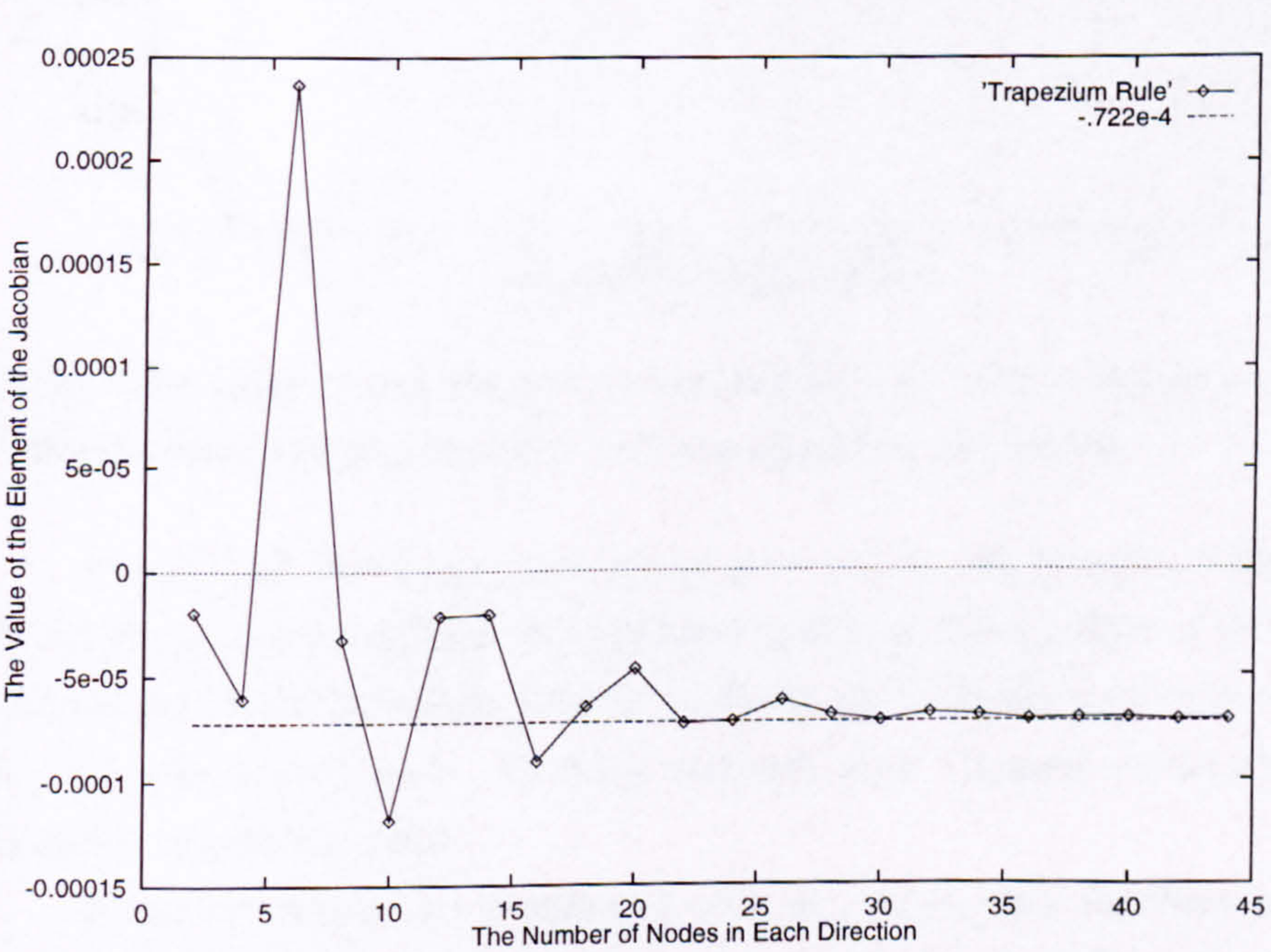

Figure 7.14: The value of the element of the Jacobian for measurement 1 and zone 18 for different numbers of nodes for trapezium rule.

gives the same results to 2 significant figures. This result is close that of analytical solution. Zone 19 is directly below the potential electrodes which is why it has a large value. In figure 7.11 the error decays with the increase in nodes. However, in figure 7.12 the error actually increases before decreasing again. The two figures are similar properties in that the graphs converge after a period of oscillatory behaviour.

The convergence of the trapezium rule can be seen to be similar to that of Simpson's rule (figures 7.13 and 7.14), except that the trapezium rule converges more rapidly than Simpson's rule, rather surprisingly, as Simpson's rule is usually more accurate for a given number of nodes.

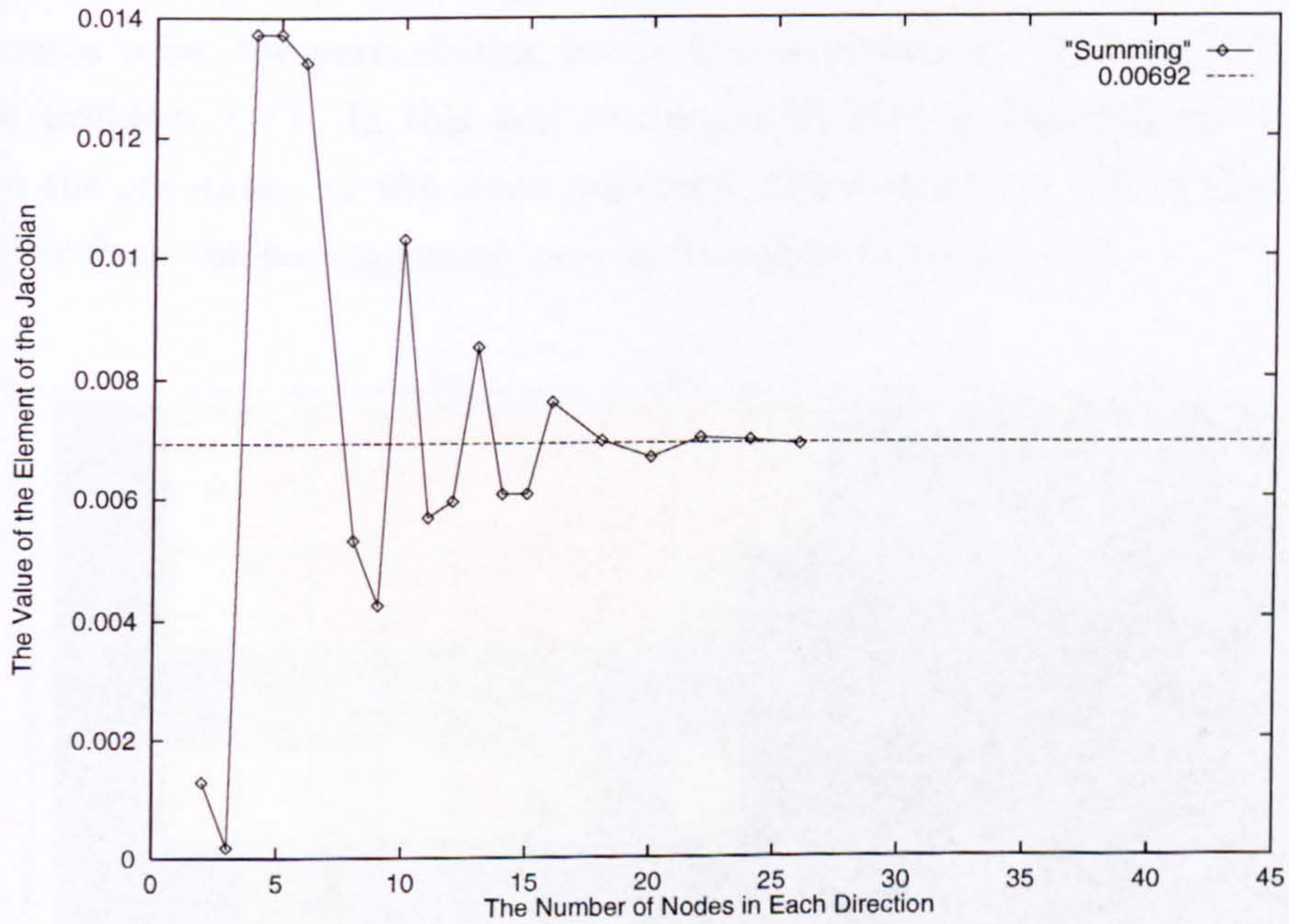

Figure 7.15: The value of the element of the Jacobian for measurement 1 and zone 19 for different numbers of nodes given by summing the cell values.

Figure 7.15 shows the convergence achieved by summing the values in all the cells within a zone as a function of the cell-size (i.e. the number of cells in the zone). Summing produces results similar to those given by the trapezium rule for $20 \times 20 \times 20$ cells in each zone. All three methods show damped oscillatory decay as the number of cells increases.

Thus, increasing the number of cells by one in each direction may not actually improve the value produced and moreover it may actually make it worse when there are only a small number of cells. However, for larger numbers of cells the value will be reasonably close to the value of the analytic Jacobian.

Changing to a "better" method (Simpson's rule or trapezium rule) for

numerical integration does not improve the calculation enough to warrant the extra time required.

7.3 Heterogeneous Jacobian

This section considers the Jacobians produced from heterogeneous resistivity distributions. Three different resistivity distributions are discussed. The first uses the output from the first iteration to estimate the resistivities. This was one of the original methods used for interpretation and was used as a starting point by Jackson et al. [1994]. The second uses one of the best results generated during an inversion using the perturbation method to calculate the Jacobian. The last, is the test problem itself. In this way we should be able to highlight the difference between the Jacobians for the same resistivity distributions as well as showing how they differ from the homogeneous case as described in section 7.2.

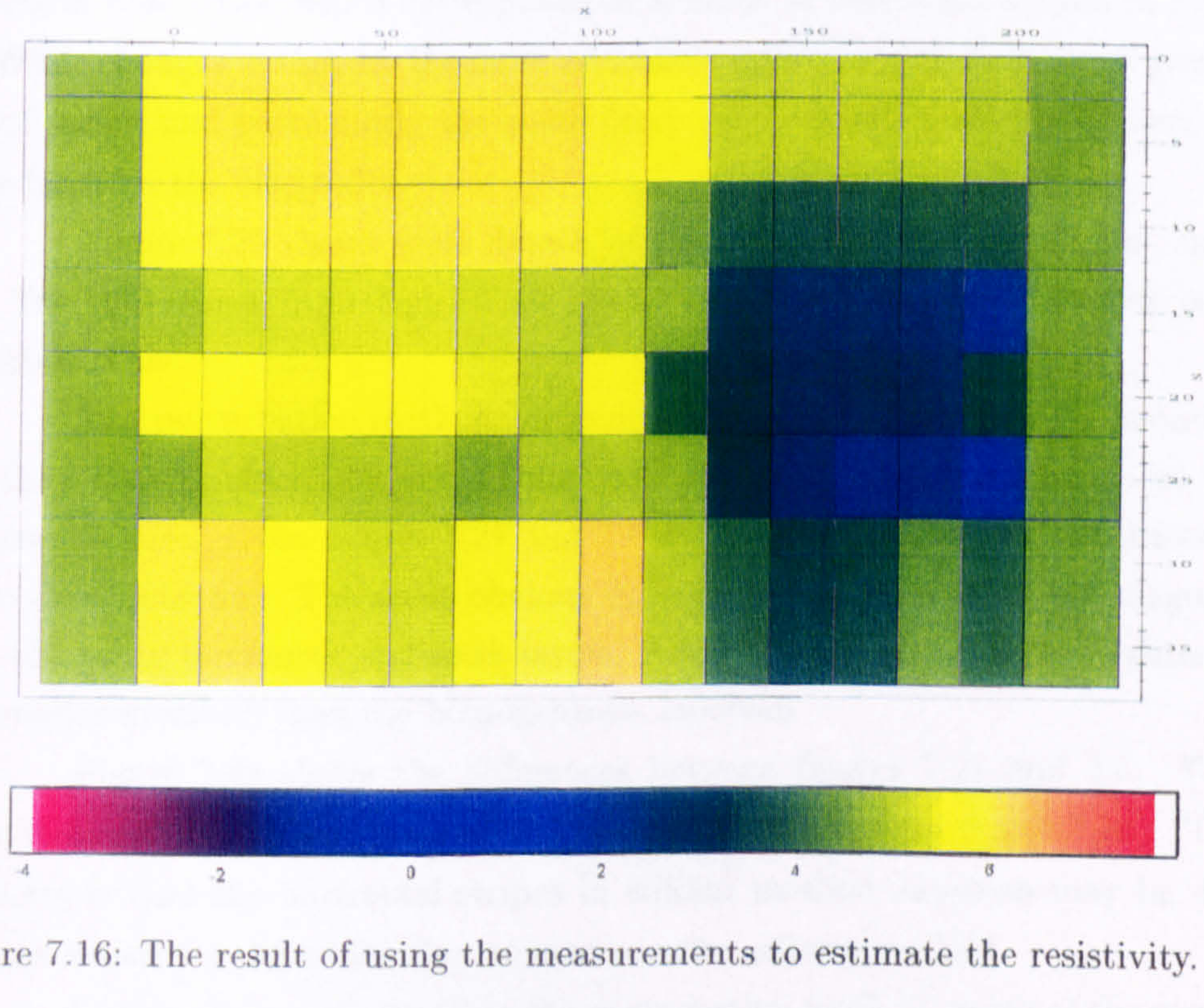

Figure 7.16: The result of using the measurements to estimate the resistivity.

The first resistivity distribution is shown in figure 7.16. This is actually closer to the solution than the first iteration of any of the methods which start from the homogeneous case. All the techniques for calculating the Jacobian used in section 7.2.1, have been tested on this set of resistivities.

The uncorrected adjoint method Jacobian, which is displayed in figure 7.17, has the same basic structure as the homogeneous Jacobian. The differences between them are seen in figure 7.18, which shows the loss of smoothness. The deepest zones have most of the brightest patches (the largest differences). There are two types: diagonal stripes and horizontal stripes. The blotches are a combination of the two types. There are many small changes which are generally the opposite sign to those in the same position in figure 7.17.

Looking in more detail at the Jacobian for the chosen measurements, (in figure 7.19), there is no symmetry between measurements 1 and 189 and between 169 and 352. In fact if figure 7.19 is compared with figure 7.6 it can be seen that there have been considerable changes in various regions of the grid. The general structure caused by the location of the electrodes is still a major influence on these images.

One of the changes in sign can be seen in measurement 169, where there is a vertical blue stripe which corresponds to a series of horizontal stripes in figure 7.17. While changes in sign are the most noticeable differences, there is also a greater range of values and particularly the small (very pale) values, particularly near the surface far from the electrodes.

Figure 7.20 shows some details of the potential-corrected adjoint Jacobian. The differences from figure 7.19 are so small that they are invisible on a logarithmic scale.

The perturbation method Jacobian (figure 7.21) shows a much smoother result than that produced by the adjoint methods: it is nearly as smooth as the homogeneous case. From figures 7.21 and 7.5 we see how similar the structures of the two Jacobians are. The most obvious differences can be seen in the diagonal stripes of blue in the fourth and sixth layers. Also the first two layers are lighter in tone (smaller in value) than the homogeneous Jacobian.

Figure 7.22 shows the differences between figures 7.21 and 7.5. This has the diagonal stripes but none of the horizontal ones (see in figure 7.18). The implication is that the horizontal stripes in adjoint method Jacobian may be due not to the resistivity differences but to errors in the adjoint method.

Looking in greater detail at the perturbation method, much of the structure seen in the homogeneous case is still evident (figure 7.23). However, the values have changed. It is possible to see the influence of the resistivity distribution on the Jacobian. The boundaries between the red and blue have moved, generally downwards, and have less smooth boundaries. The most severely affected is measurement

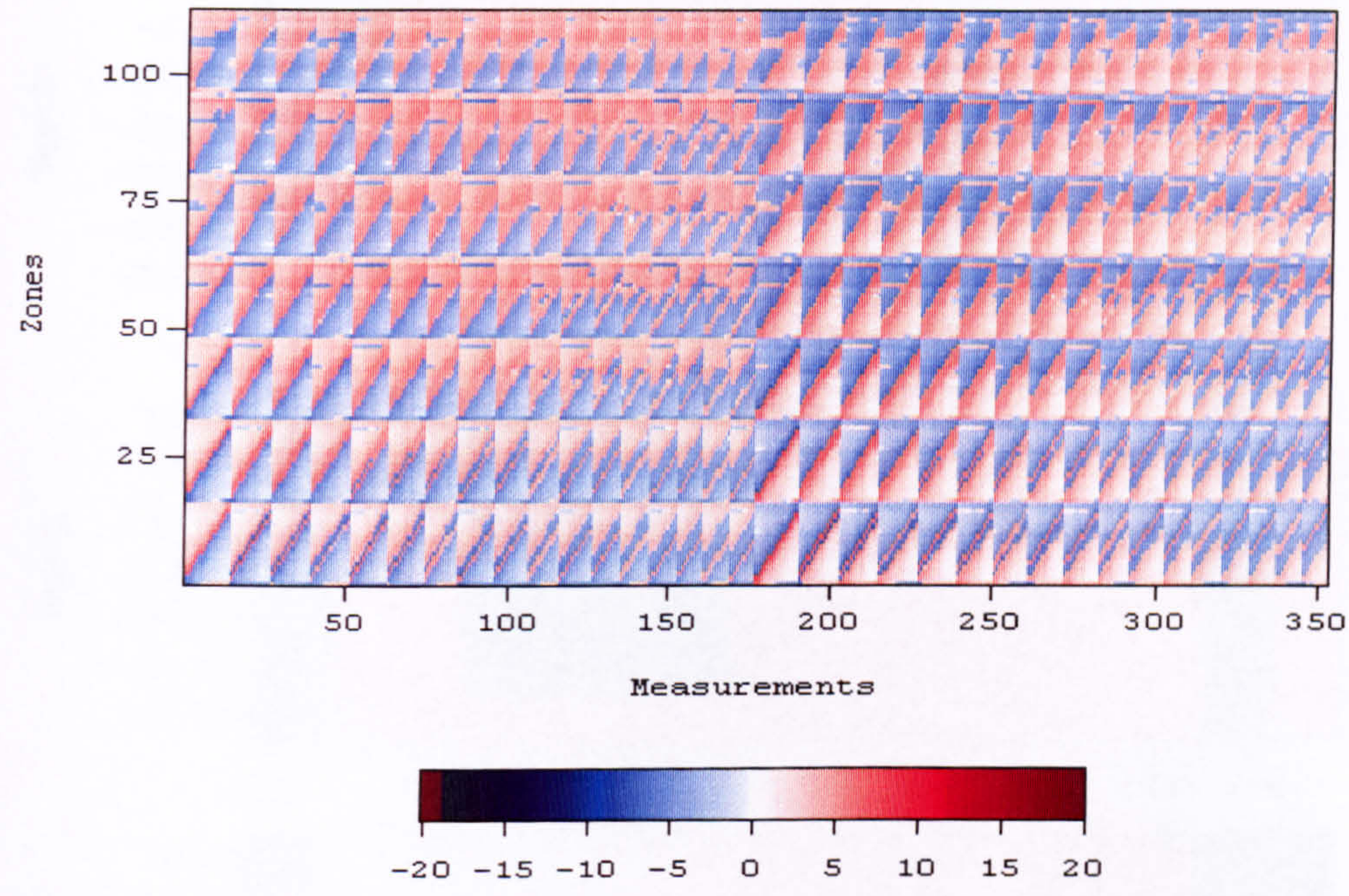

Figure 7.17: Jacobian calculated by the adjoint method on the resistivity distribution from the measurement start.

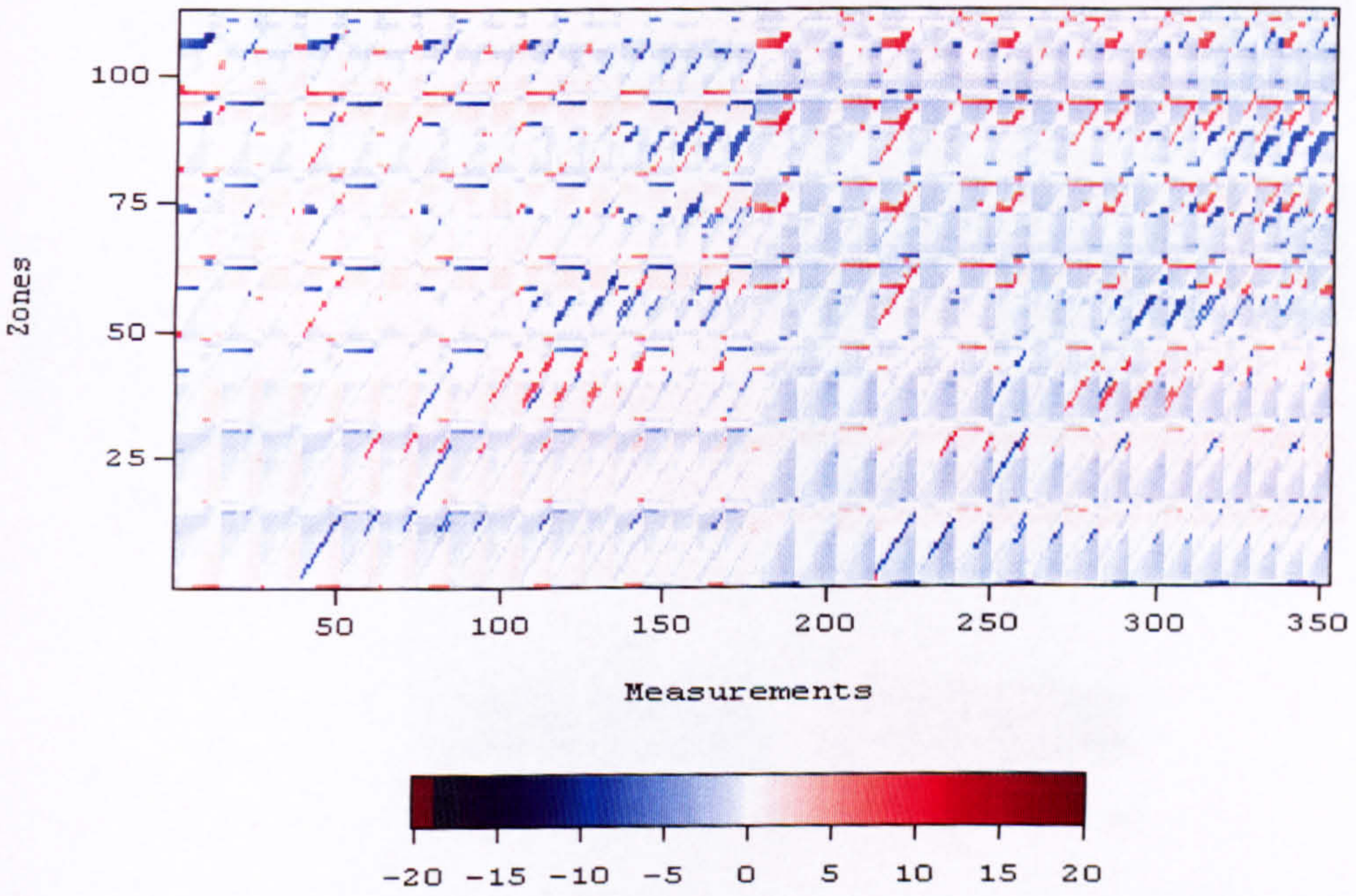

Figure 7.18: Difference between figures 7.17 and 7.2.

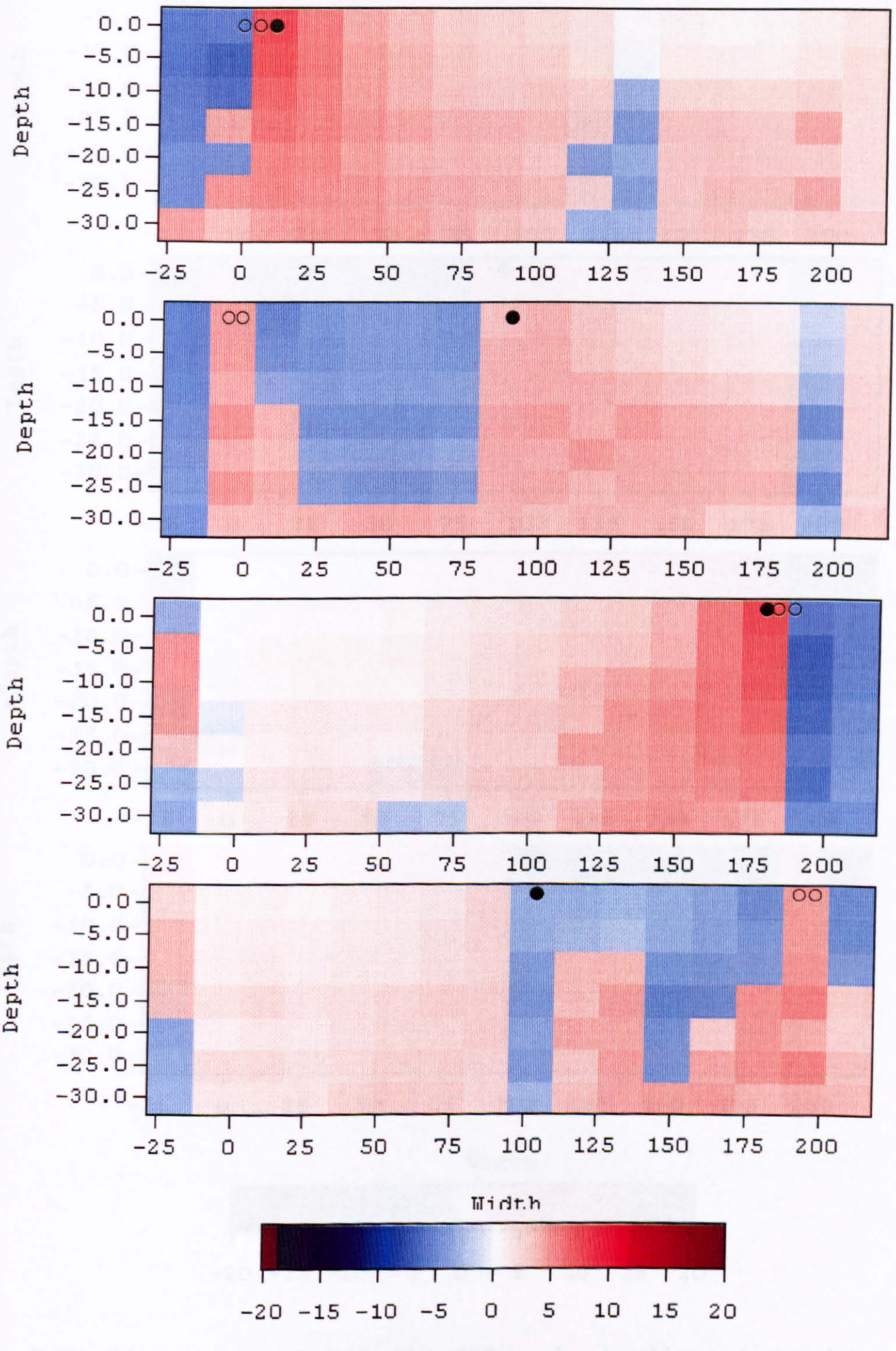

Figure 7.19: Measurements 1, 169, 189, 352 in the Jacobian calculated by the adjoint method. ● current electrode ○ potential electrode

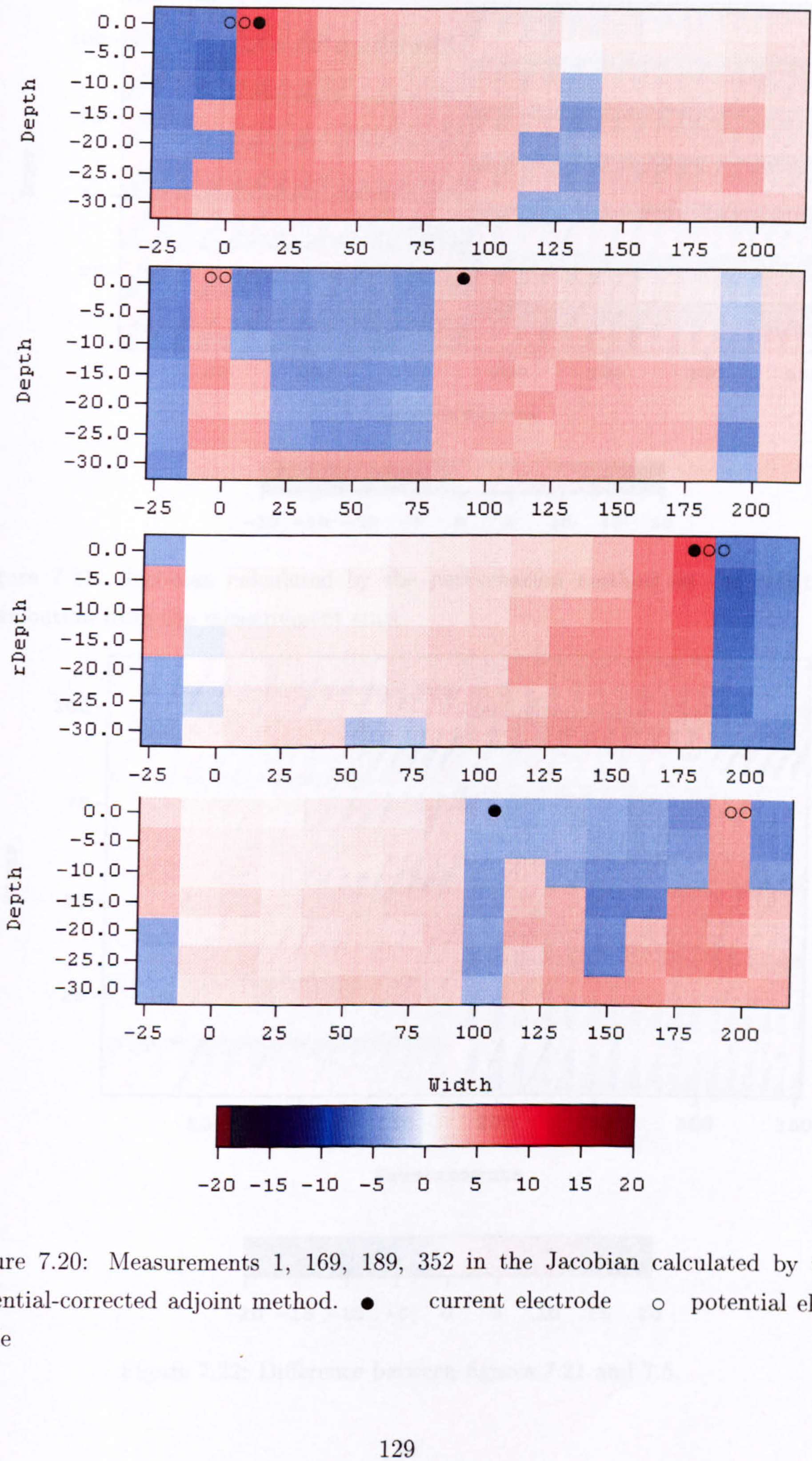

Figure 7.20: Measurements 1, 169, 189, 352 in the Jacobian calculated by the potential-corrected adjoint method. ● current electrode ○ potential electrode

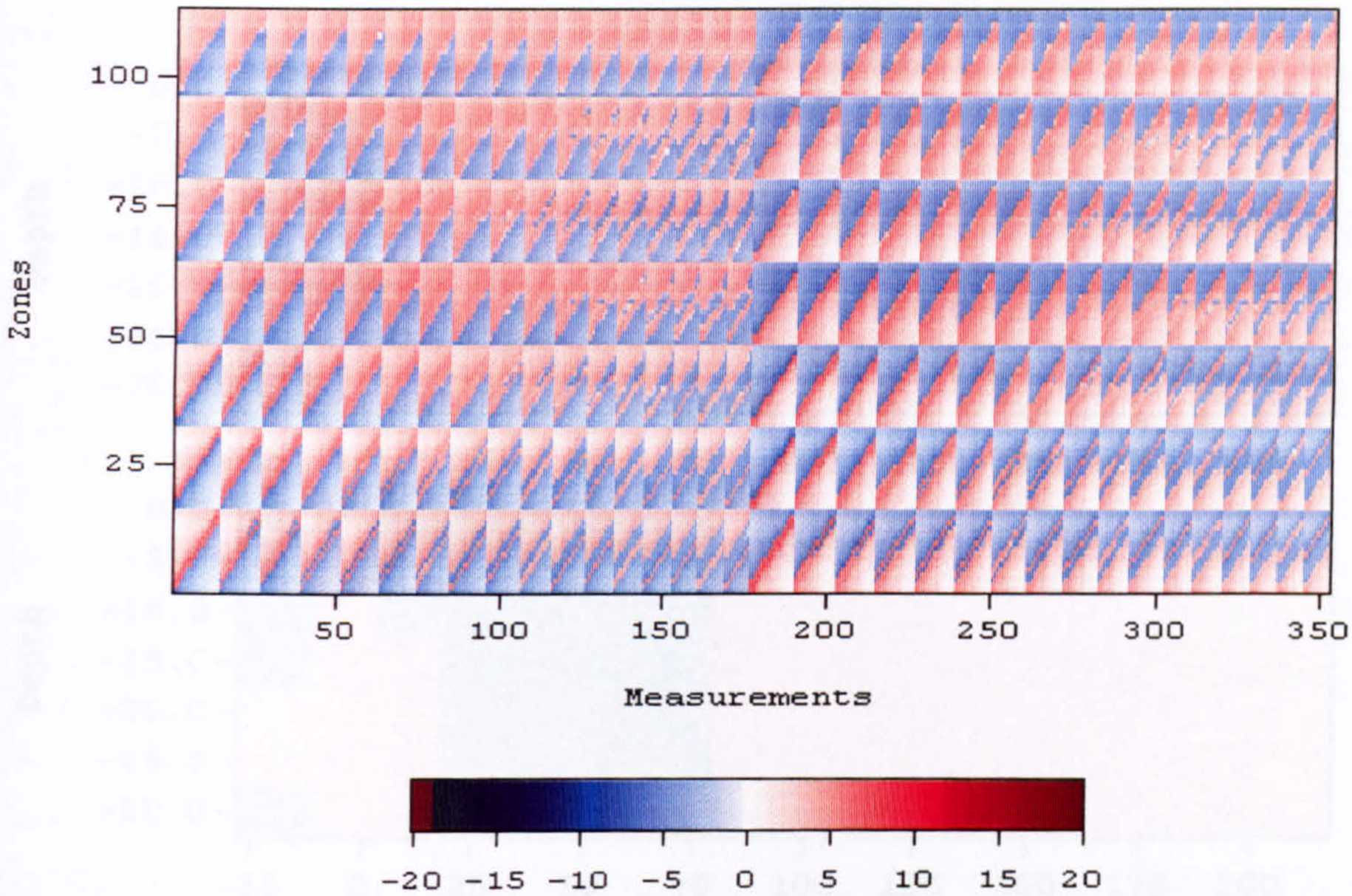

Figure 7.21: Jacobian calculated by the perturbation method on the resistivity distribution from the measurement start.

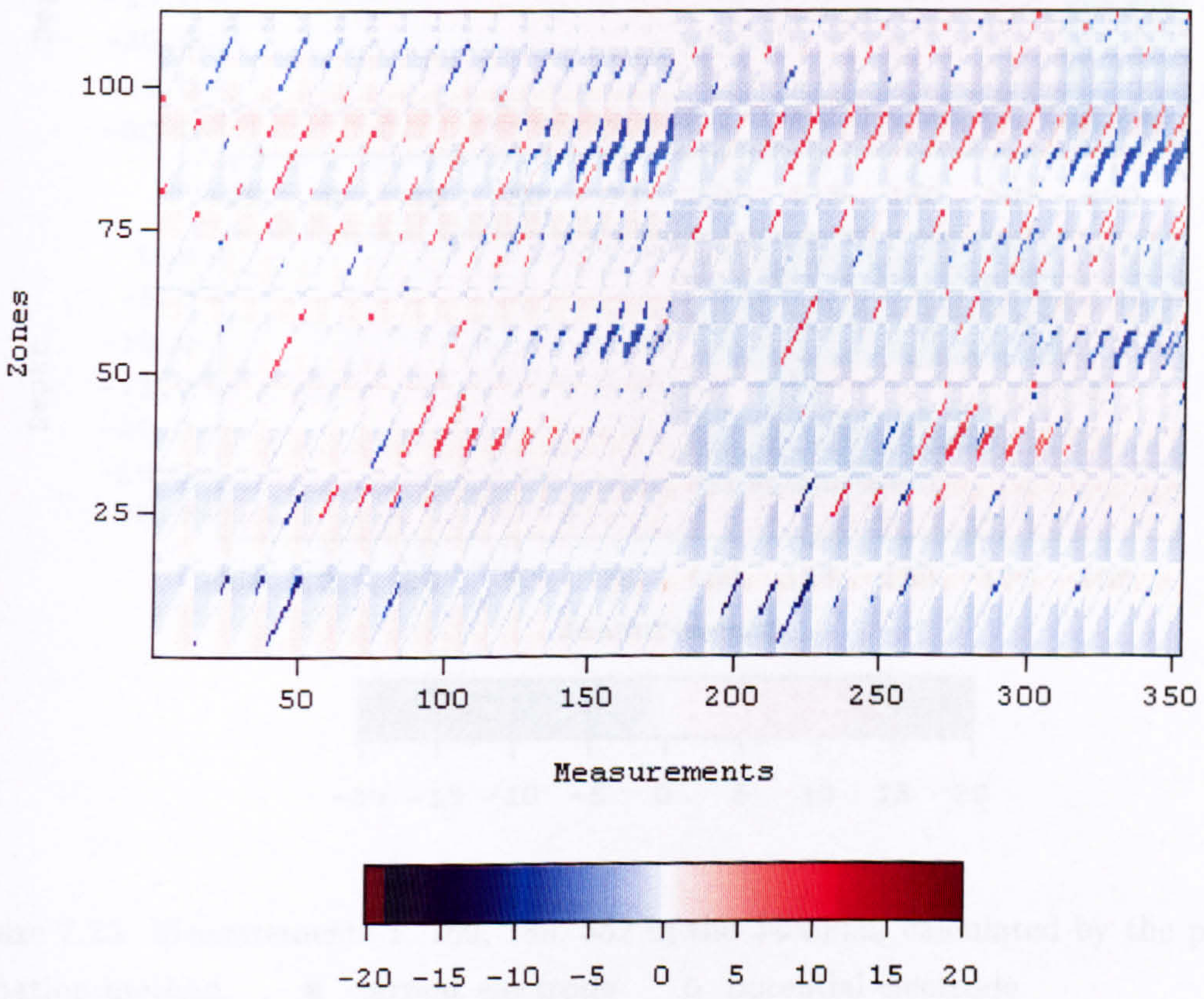

Figure 7.22: Difference between figures 7.21 and 7.5.

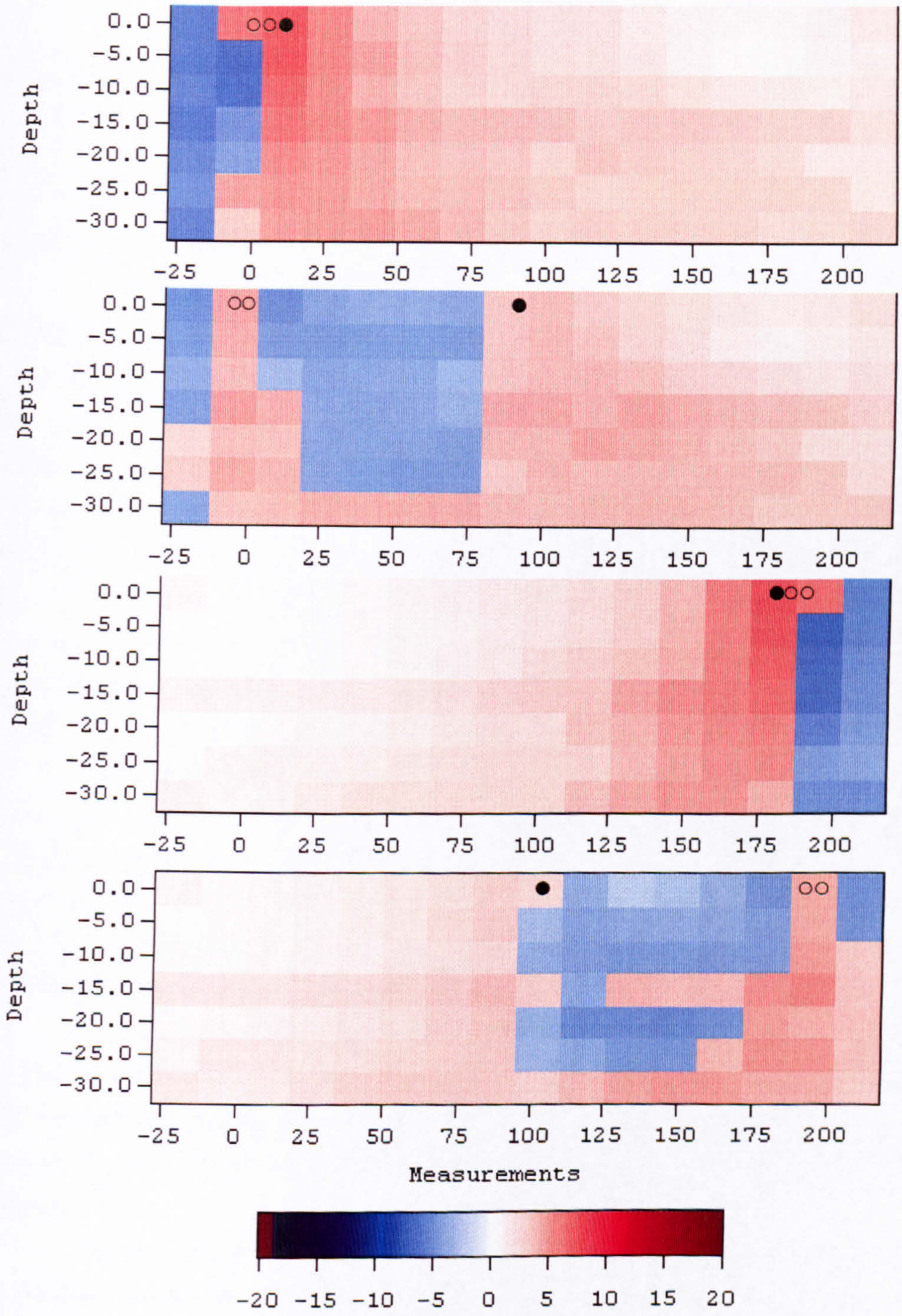

Figure 7.23: Measurements 1, 169, 189, 352 in the Jacobian calculated by the perturbation method. ● current electrode ○ potential electrode

352 where the blue region has changed shape and increased in area.

The hybrid Jacobian, shown in figure 7.24, is predictably similar to the adjoint method. This can also be seen in the measurements shown in figure 7.26. The hybrid method was used to improve the result by correcting the largest values. To a certain extent this was successful, as shown in section 6.3.5 but the problem remains that the method still has all the errors of the adjoint methods for other elements of the Jacobian.

The differences between the hybrid and perturbation methods are shown in figure 7.25 (and thus in effect the differences between the adjoint method and the perturbation method). The differences not included are in the largest values, in the layer of zones on the surface (zones 1 to 16). Most of the bright patches of figure 7.25 are the horizontal strips from the adjoint method. There are very few diagonal stripes most of which are concentrated below the third layer and in those parts of the Jacobian where the current source and potential electrodes are far apart. The last and least noticeable feature is uniformly a very pale shade of blue almost everywhere. This is different from all the other comparisons where the pale shades were evenly distributed between red and blue. The values are thus less than or equal to those given by the perturbation method.

The remainder of this section concentrates on the Jacobians calculated from the best available result and from the actual solution of the test problem. The first of these Jacobians is taken from one of the best solutions generated and its image is shown in figure 7.27. Comparing figure 7.27 with both figures 7.5 and figure 7.21 clear differences are evident. The structure has not changed greatly but the values of some of the elements have changed by several orders of magnitude.

The differences between figure 7.27 and figure 7.5 are shown in figure 7.28. The major changes are of the diagonal stripe type with no horizontal stripes: thus is consistent with the other perturbation method Jacobians. The values can be seen to be orders of magnitude different from the previous resistivity distribution (see figure 7.22).

Figure 7.29 shows some of the detail of the Jacobian displayed in figure 7.27. However, unlike the other images of the Jacobian the colour scale represents the actual values. Looking at the brightest parts of the Jacobian, on the left hand side the third layer is bright for all the measurements. On the right hand side the fourth and fifth layers are bright. These correspond to the bright parts of figure 7.27 and also to the lowest values of resistivity. The zones with reduced values of the elements of $\underline{\mathcal{J}}$ correspond to zones with higher resistivity. Thus, these 'Jacobian' images show

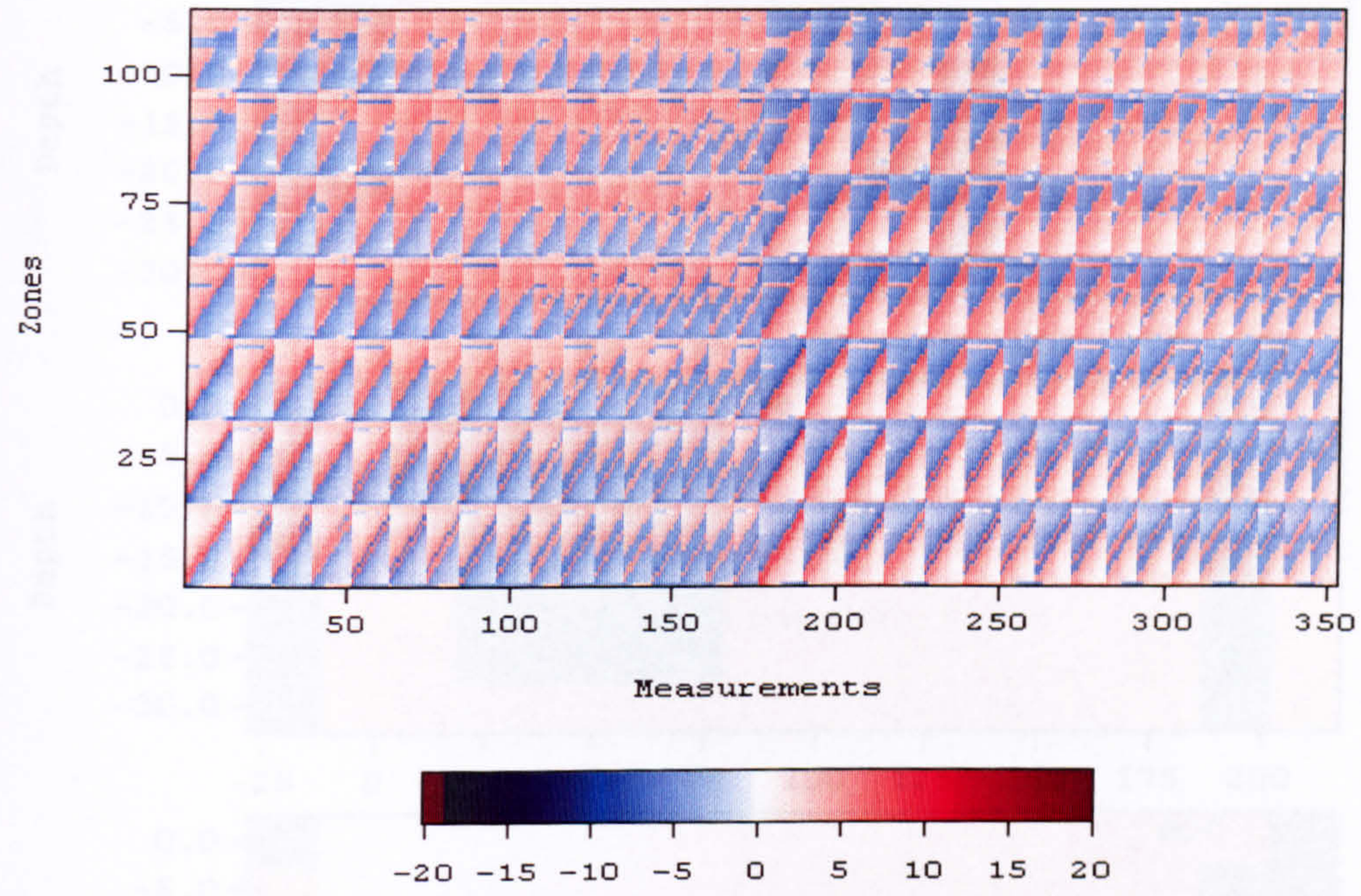

Figure 7.24: Jacobian calculated by the hybrid Method on the resistivity distribution from the measurement start.

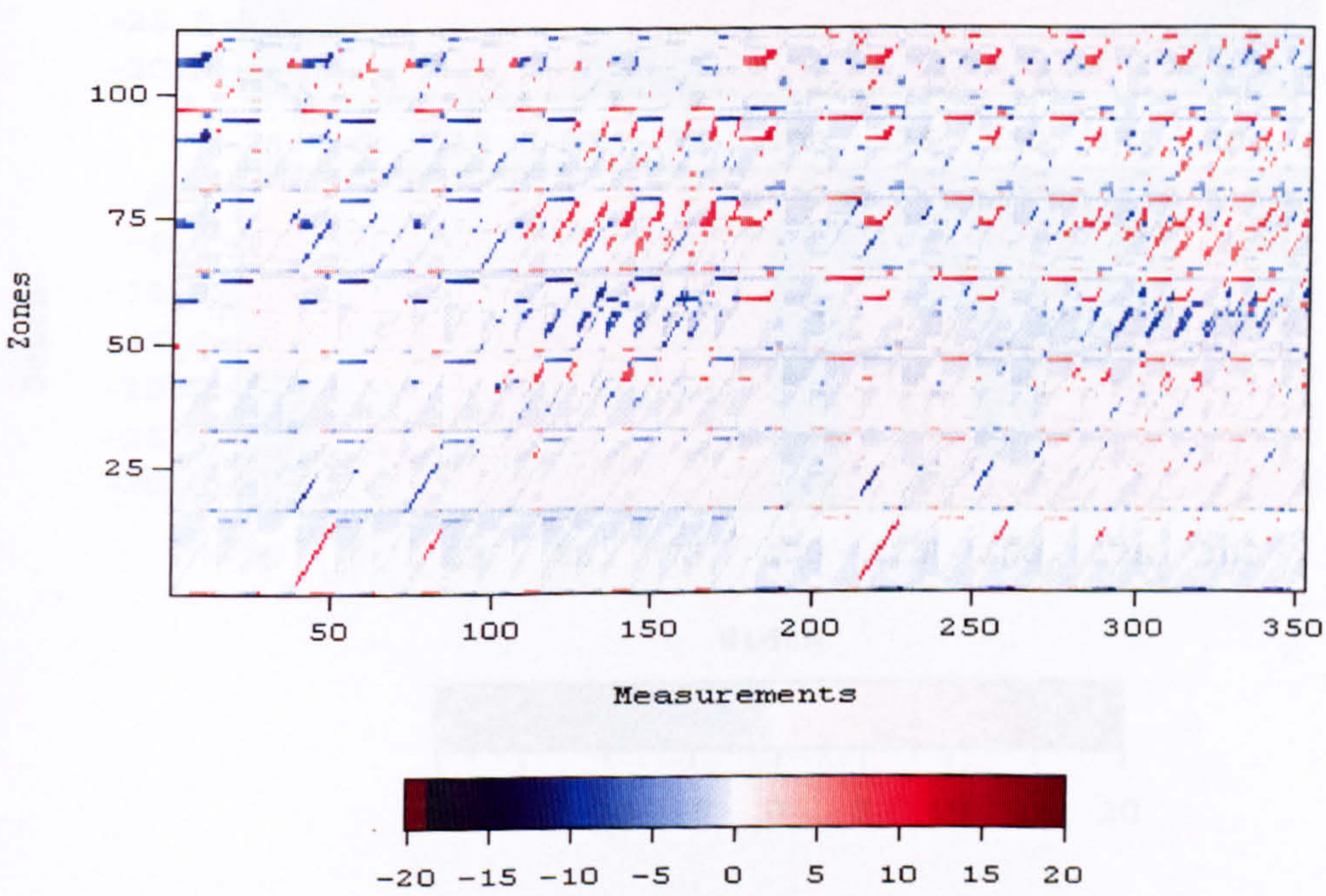

Figure 7.25: Difference between figures 7.24 and 7.21.

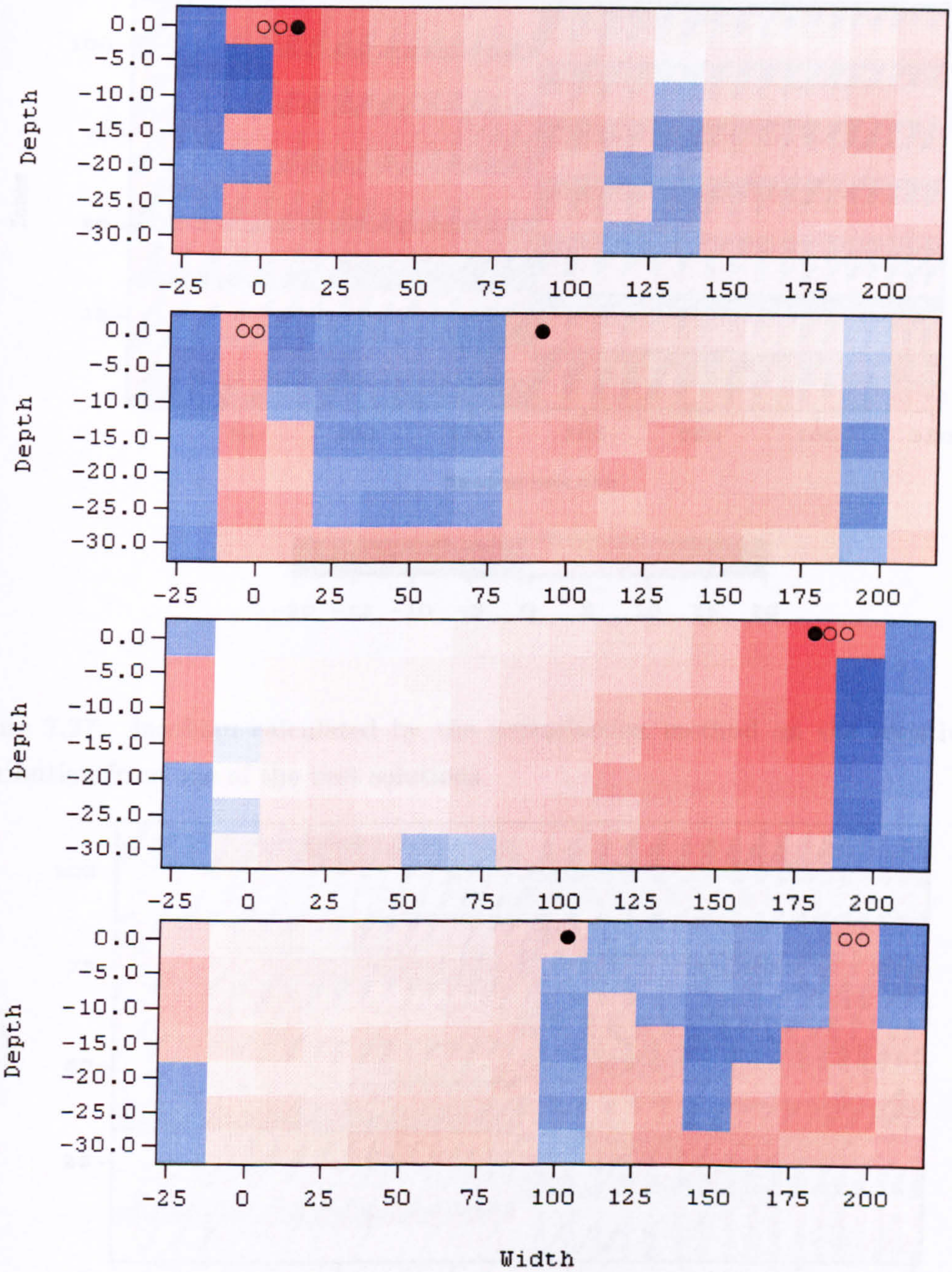

Figure 7.26: Measurements 1, 169, 189, 352 in the Jacobian calculated by the hybrid method. ● current electrode ○ potential electrode

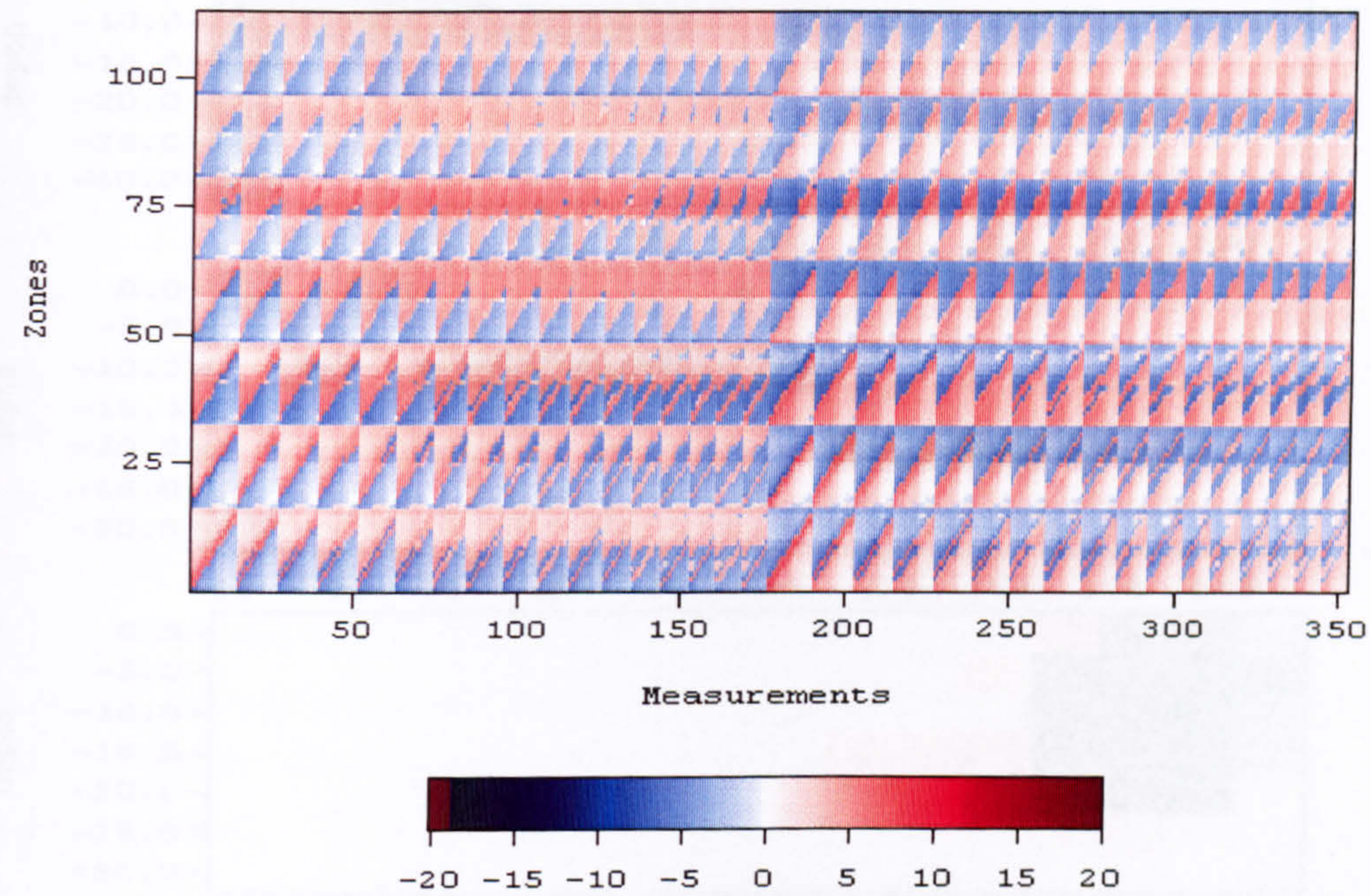

Figure 7.27: Jacobian calculated by the perturbation method on the resistivity distribution from one of the best solutions.

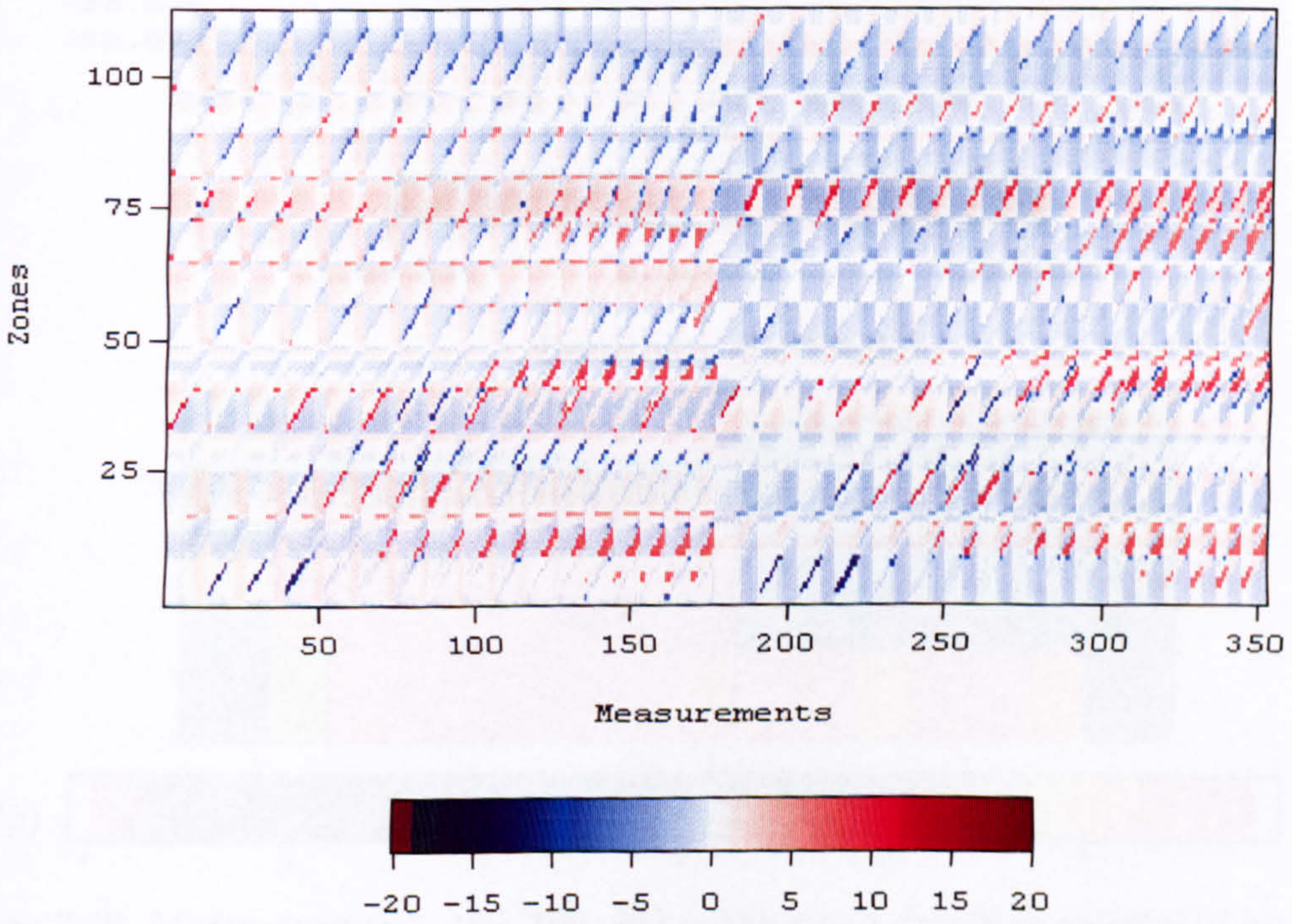

Figure 7.28: Difference between figures 7.27 and 7.5.

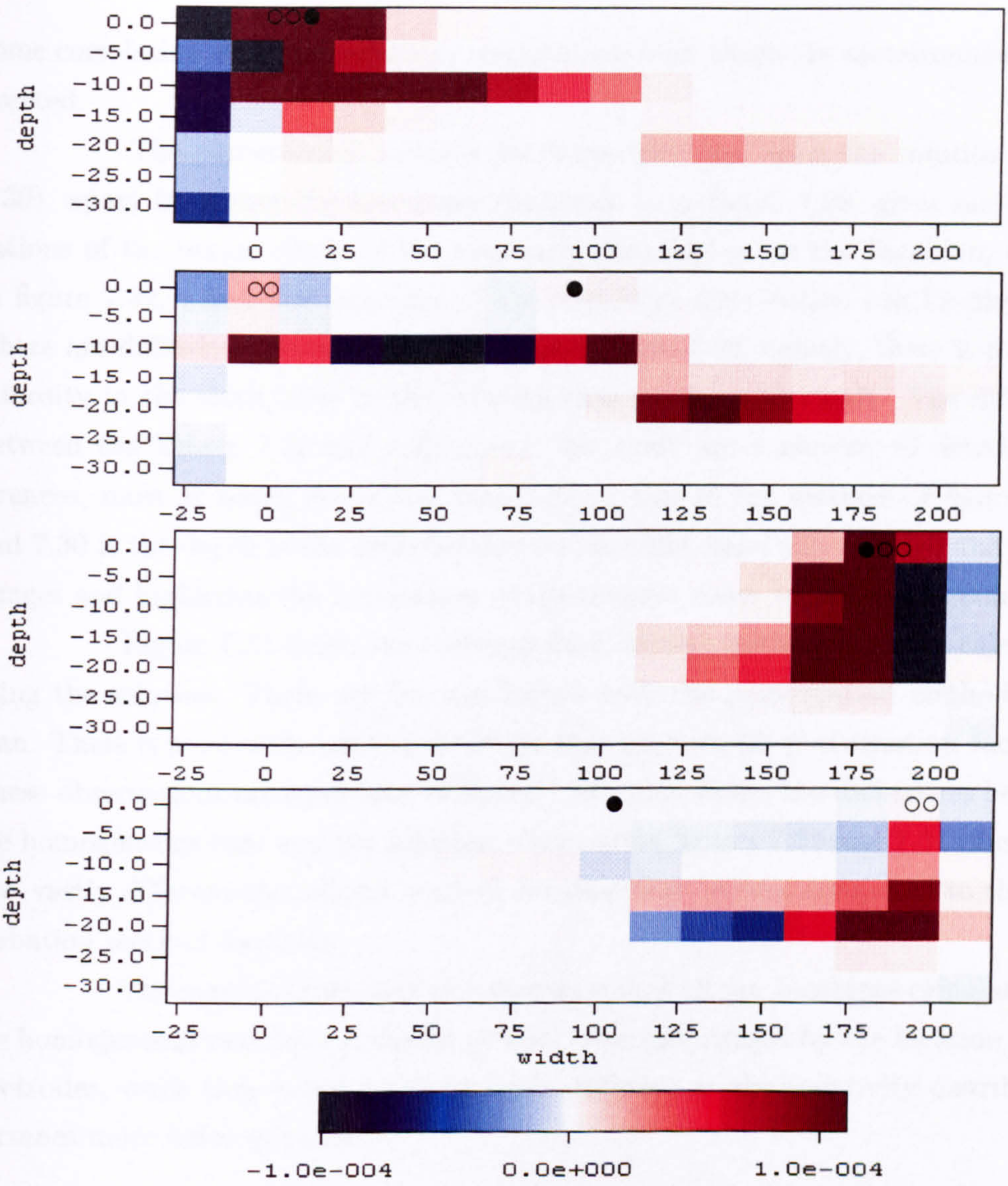

Resistivity distribution

Figure 7.29: Measurements 1, 169, 189, 352 in the result Jacobian calculated by the perturbation method for the best result produced. ● current electrode ○ potential electrode

some correlation with the resistivity distribution from which the measurements were created.

The perturbation method Jacobian calculated from the solution (figure 7.30), apart from showing how close the result is to figure 7.28, gives many indications of the major effects of the resistivity distribution on the Jacobian, as seen in figure 7.32, where the structure of the resistivity distribution can be discerned. There are differences between figure 7.27 and figure 7.30, namely, there is more luminosity in the sixth layer in the solution than in the best result. The difference between the figures 7.32 and 7.29 shows that there are a number of detailed differences, most of which are in the lower layers. One of the features of figures 7.27 and 7.30 is the depth of the investigation on the right-hand side in third and fourth images and highlights the importance of the deepest zones to the measurement.

Figure 7.33 shows the corresponding adjoint method Jacobian calculated using the solution. There are few similarities with the perturbation method Jacobian. There is none of the smooth structure that exists in the perturbation Jacobian. These observations are confirmed in figure 7.34 which shows the differences between the homogeneous case and the solution. Comparing figures 7.34 and 7.31 illustrates how vastly different the adjoint method Jacobian has become compared to the perturbation method Jacobian.

The main conclusion of this section is that all the Jacobians calculated for the homogeneous case have a similar general structure caused by the location of the electrodes, while they become progressively different as the resistivity distribution becomes more heterogeneous.

7.4 Effects of the Jacobian

This section discusses the importance of the Jacobian to the solution of the inverse problem and the effect of the smoothness constraint in reducing the effect of the errors in the Jacobian. The intention is to bring together the results from sections 6.3 and 7.3.

By comparing the results produced in chapter 6 with those in published papers it is possible to see that the general method used of trying to calculate an accurate Jacobian and a slackening smoothness-constraint produces better results. As image 8 in figure 6.4 shows, it is possible to produce results which are quite close to the solution by using a steeper descent in the value of λ (i.e. a quick slackening of the smoothness-constraint). This only worked when using the perturbation method

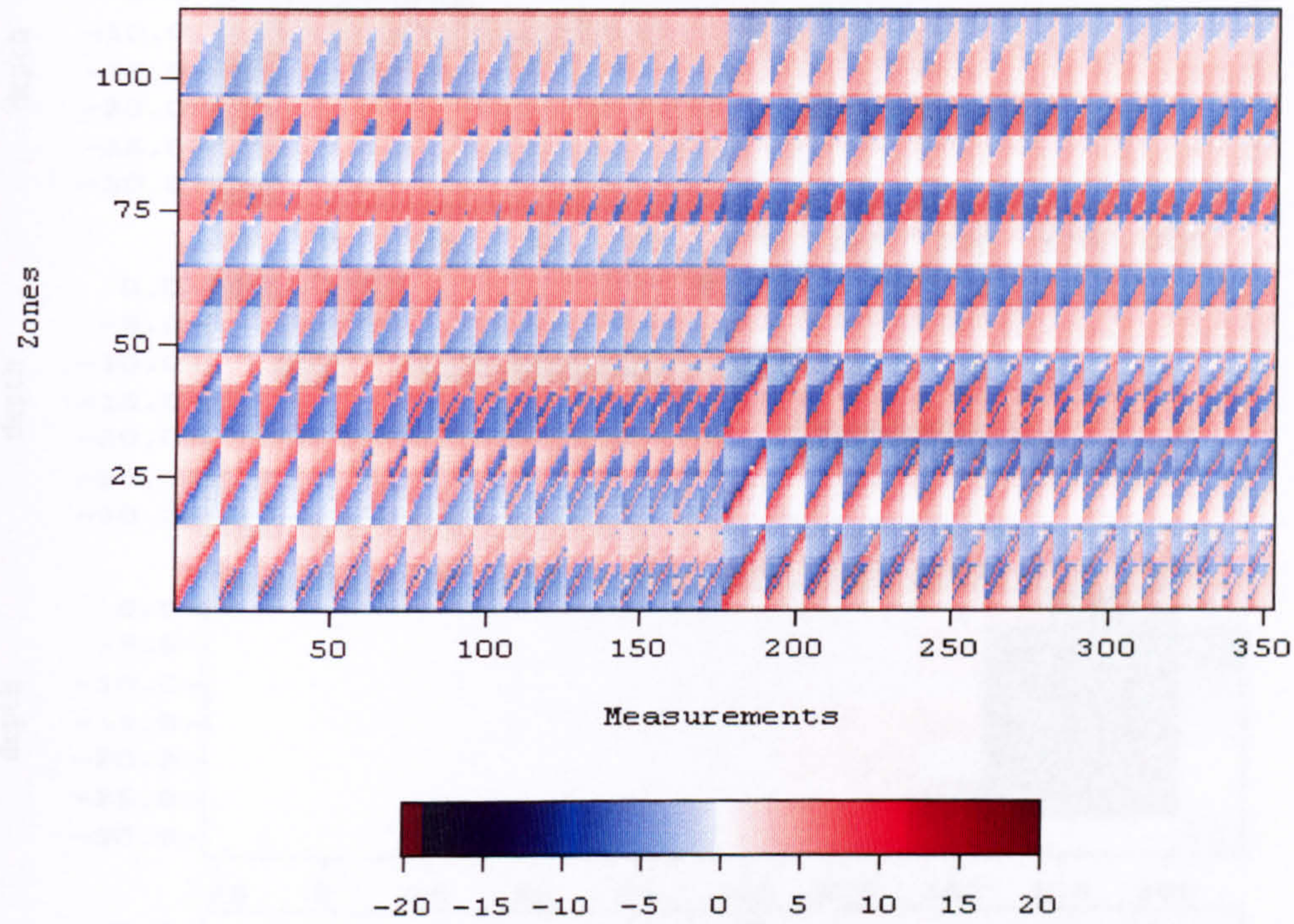

Figure 7.30: Jacobian calculated by the perturbation method on the resistivity distribution from the solution.

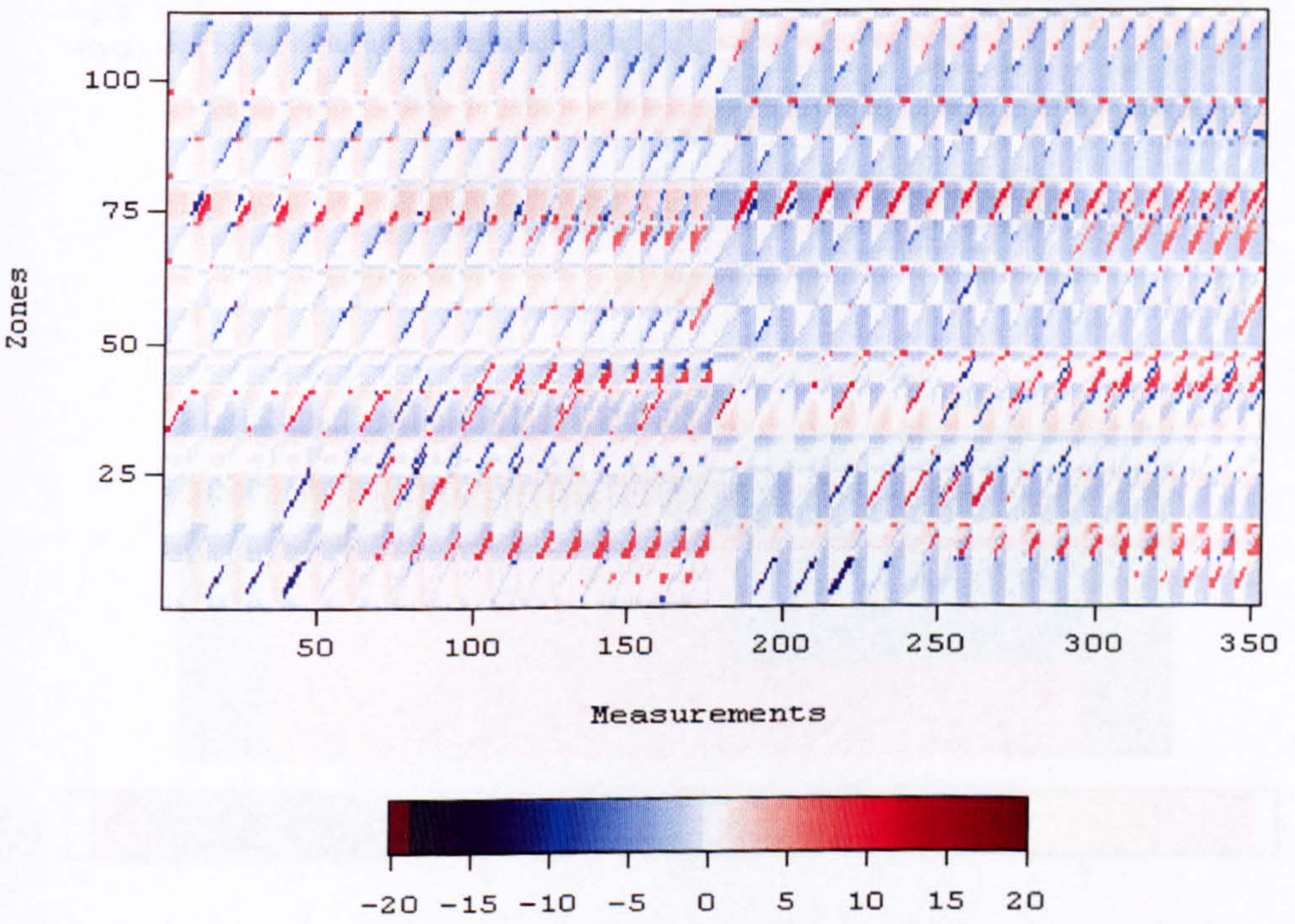

Figure 7.31: Difference between figures 7.30 and 7.5.

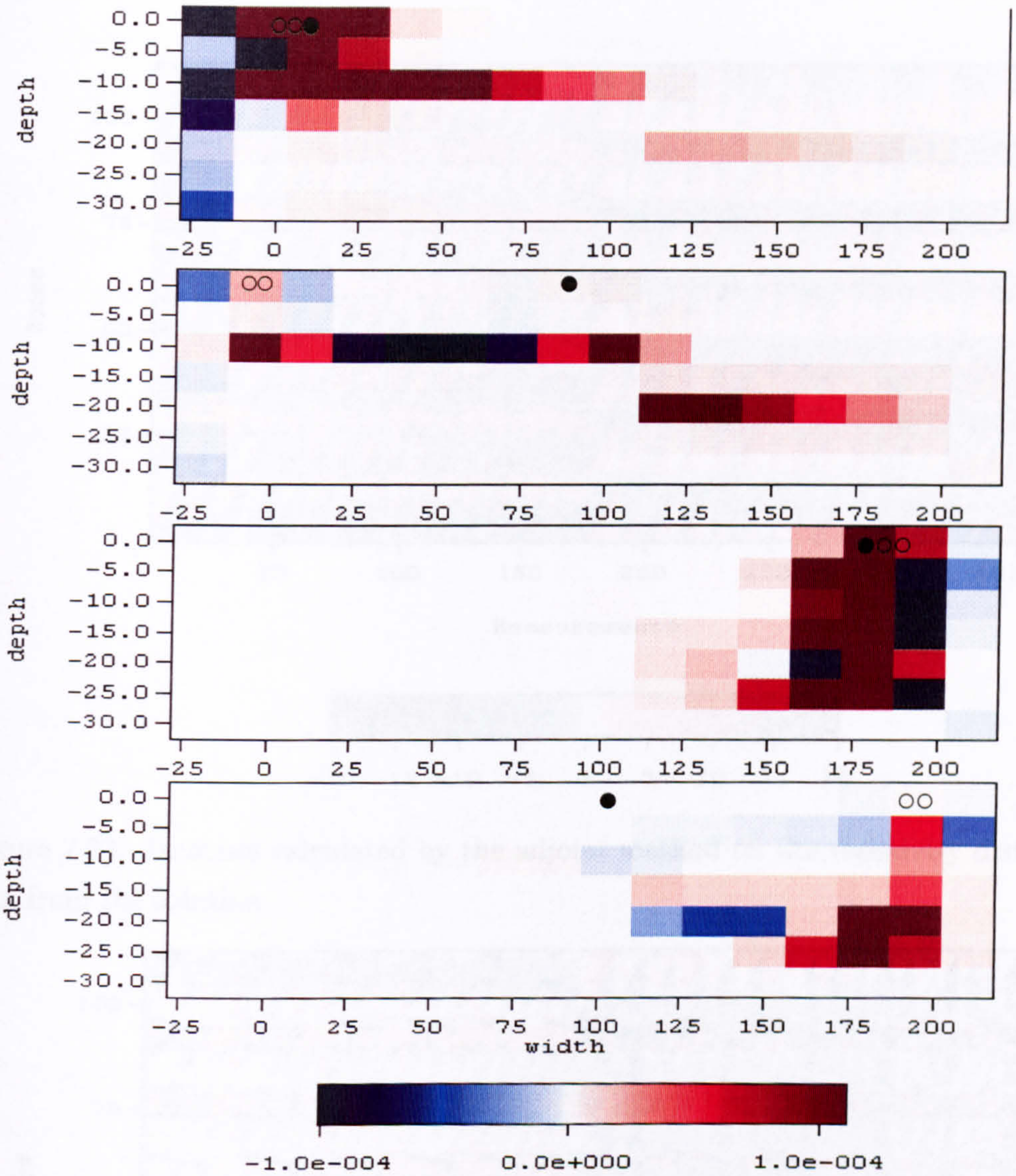

Resistivity distribution

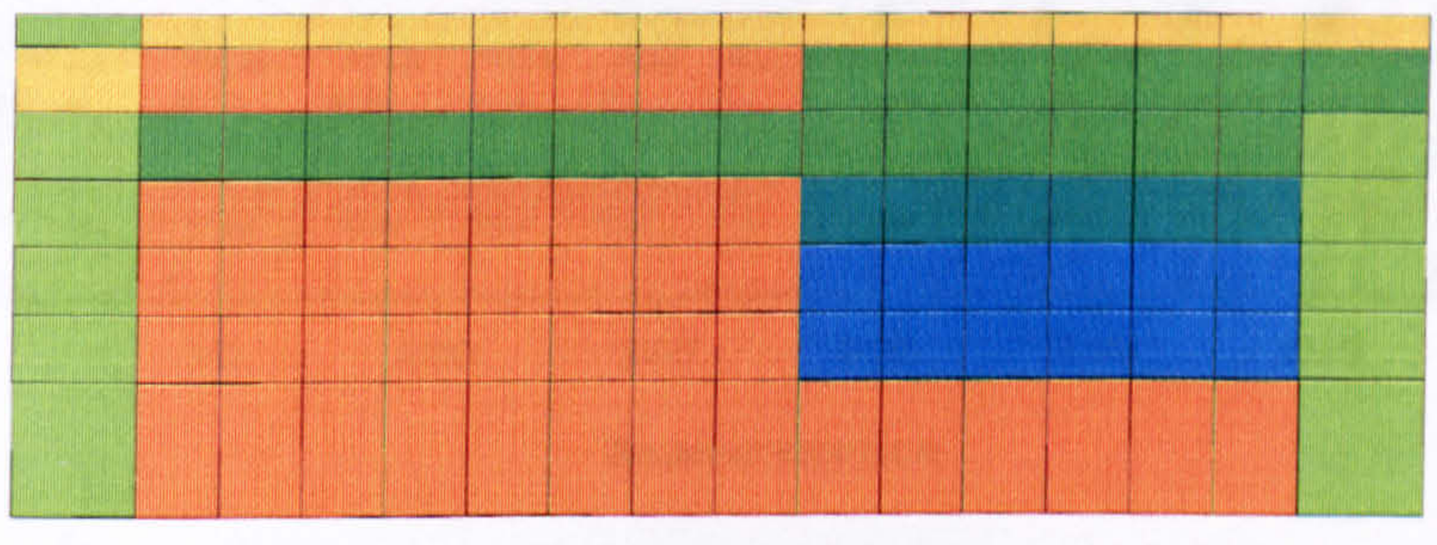

Figure 7.32: Measurements 1, 169, 189, 352 in the result Jacobian calculated by the Perturbation Method for the solution. ● current electrode ○ potential electrode

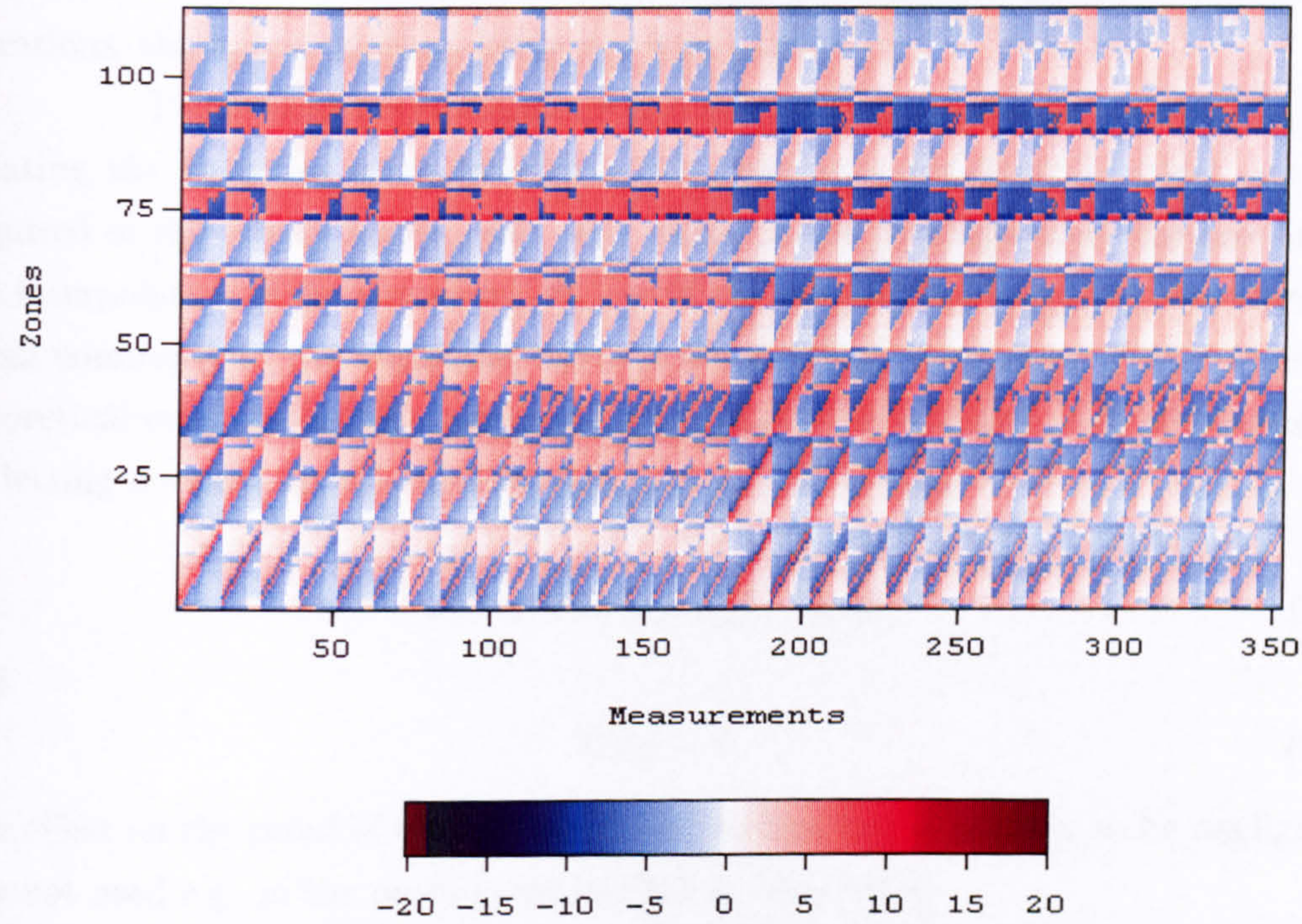

Figure 7.33: Jacobian calculated by the adjoint method on the resistivity distribution from the solution.

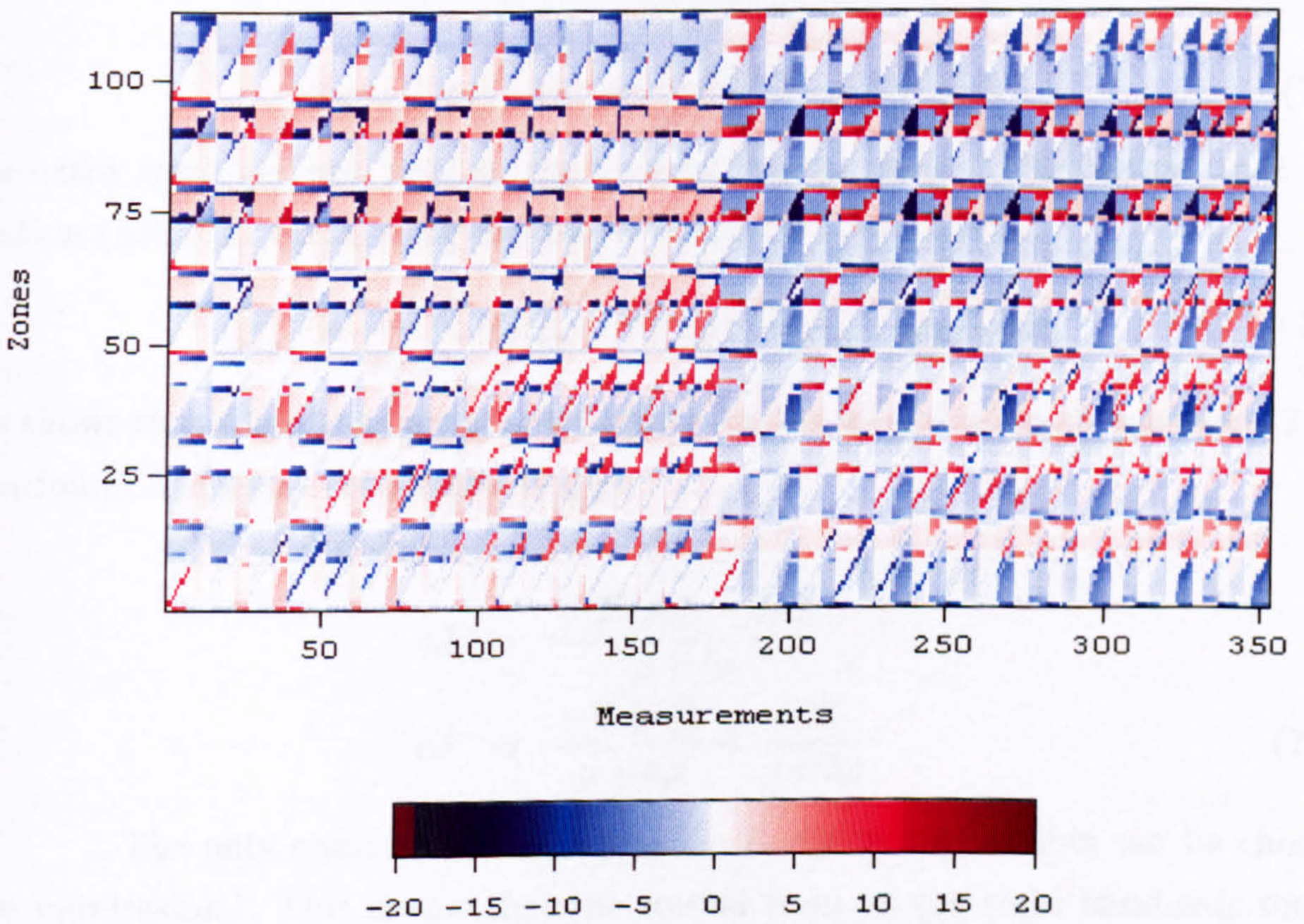

Figure 7.34: Difference between figures 7.33 and 7.2.

for calculating the Jacobian. The other techniques became unstable after a few iterations, the hybrid method being the least stable.

Theoretical approximations are required in the adjoint method for calculating the Jacobian using heterogeneous resistivity distributions which are not required in the homogeneous case. Any errors in the homogeneous case are due to the interpolation of the coarse grid (L) on to the extended fine grid (T), but they are small compared to the variability seen in the heterogeneous case. Let us consider theoretical errors in the heterogeneous case. Equations (5.2) and (5.3) are perturbed by letting $\rho \rightarrow \rho + \delta\rho$, $\phi \rightarrow \phi + \delta\phi$ and $\mathbf{J} \rightarrow \mathbf{J} + \delta\mathbf{J}$, giving

$$\rho\delta\mathbf{J} + \nabla\delta\phi = -\delta\rho\mathbf{J} - \delta\rho\delta\mathbf{J} \tag{7.1}$$

and

$$\nabla.\delta\mathbf{J} = 0 \tag{7.2}$$

The effect on the proof of the adjoint is not obvious but it is likely to be negligible: it is not used e.g. in the proof given in Park & Van [1991].

However, the right-hand sides of equations (7.1) and (7.2) are used in the derivation of the integral and appear in equation (C.11). If the extra term is added it follows through in such a way that equation (5.8) becomes

$$\delta\phi\left(x_{P1},\ y_{P1},\ z_{P1}\right) = \int_{\tau} \left(\delta\rho\left(\mathbf{J} + \delta\mathbf{J}\right)\right).\mathbf{J}'\mathbf{d}\tau \tag{7.3}$$

This extra term appears only in the current density term. This means that the equation (5.33) for calculating the Jacobian can be rewritten as

$$\underline{\mathcal{J}}_{q,r} = \frac{1}{i_{C1}} \int_{\tau_r} \left(\mathbf{J}_{C1,q} + \delta\mathbf{J}_{C1,q}\right).\left(\mathbf{J}_{P1,q} - \mathbf{J}_{P2,q}\right) d\tau_r \tag{7.4}$$

This shows that there is an extra term caused by the second order in equation (7.1). Equation (7.1) can be rearranged to give

$$\delta\mathbf{J} = \frac{-\nabla\left(\delta\phi\right) - \delta\rho\mathbf{J}}{\rho + \delta\rho}$$

$$\delta\mathbf{J} = \frac{-\nabla\left(\delta\phi\right)}{\rho + \delta\rho} - \frac{\delta\rho\mathbf{J}}{\rho + \delta\rho} \tag{7.5}$$

The only quantity which is small is $\delta\rho$ ($\rho \gg \delta\rho$), as this can be chosen to be infinitesimal. This means that the second term on the right hand side tends to zero. Equation (7.2) gives

$$\frac{\partial\delta J_x}{\partial x} + \frac{\partial\delta J_y}{\partial y} + \frac{\partial\delta J_z}{\partial z} = 0$$

This means that the components of $\delta\mathbf{J}$ are independent of x, y, and z for any given $\delta\rho$.

The first term on the right hand side of equation (7.5) does not obviously tend to zero. Also this term is likely to be largest when ρ is small. It is known that $\frac{\delta\phi}{\delta\rho}$ tends to a limit as these are related to the elements values in the Jacobian matrix. Taking the x direction as an example, this term is the change in $\delta\phi$ due to a change in x. Let us consider the case of two zones, a left and a right zone, where the left zone is of very low resistivity and the right is of high resistivity. Given that these two zones are neighbours, the distance to the electrodes is similar (assuming they do not have an electrode in either of them). Then $\frac{\partial\phi}{\partial x}$ will be very large in the region of the boundary and as a consequence so will $\frac{\partial J_x}{\partial x}$. Also the left-hand zone is likely to have a much larger value in the Jacobian than the right hand zone. The implication is that there is a change in $\delta\phi$ between the two zones. Therefore $\frac{\partial\delta\phi}{\partial x}$ is going to exist with a non zero, possibly large value. Considering just the left-hand side of the boundary where ρ is small and $\frac{\partial\delta\phi}{\partial x}$ is not small then it is possible for $\delta\mathbf{J}$ to be not small. The approximation in the adjoint theory may thus not be negligible.

It is possible to conclude that some (if not most) of the errors are due to small errors in the calculation of the gradient.

There are errors in the Jacobian, especially in the adjoint method and its variants for heterogeneous resistivity distribution. However, far from the solution (see section 6.3), the adjoint methods produced arguably better results than the Perturbation Method, using a set of large λ values which decreased slowly. It is known that a large λ value will smooth out errors in the measurements, especially those from field data. Given that the results from using the adjoint method were reasonably smooth but not so smooth as the results from the perturbation method, it could be hypothesised that the smoothness constraint smoothes out errors not only in the measurements but also in the Jacobian.

Assuming that the above hypothesis is true, then adjoint methods could be used in the solution of this inverse problem in such a way that most of the iterations could be performed in this way, subsequently using the perturbation method. This method would require λ to decrease slowly for the adjoint iterations and then to decrease faster for the iterations which use the perturbation method Jacobian. This would be faster than just using the perturbation method.

It may be worth observing that at various points in our work we have found that the simplest (least sophisticated) approach was not only the most robust but often the fastest. For example, the results of point iteration in chapter 3 (here

the saving was in CPU time), and the use of simple summation of values for the integration in section 7.2.2, where the integral actually converged faster for the simplest method. The moral[1] would seem to be:

1. That we should not despise, or worse discard, simple methods without revisiting them occasionally.

2. That we should not assume that methods devised to overcome the limitations of early, slow computers are necessarily still relevant in the context of the fast and powerful machines now available.

We have demonstrated that

1. It is possible to produce good results if the Jacobian is calculated accurately.

2. The Jacobian depends on the resistivity distribution (and therefore on the current density).

3. The errors in the Jacobian can be reduced by stiffening the smoothness constraint.

We should expect future research in this field to be underpinned by these conclusions.

[1]The credit for the moral must go to Gordon Reece.

Chapter 8

Conclusions

Solving the inverse problem to produce a fast and accurate solution involves the need for fast and accurate solution of the forward problem and the Jacobian. It must be noted that the forward problem is an integral part of the inverse problem since it is essential for both the calculation of the Jacobian and of the synthetic measurements, while the Jacobian is a fundamental part of algorithms used for solving the inverse problem.

8.1 Forward methods

The results in chapter 3 show that it is not possible to pick *a* method of choice as being superior in all circumstances. However, a set of rules emerges which can be used to choose the most suitable method for solving for a given set of conditions. The rules are flexible enough to choose the method best suited to the "new" conditions. All the methods considered converge to the solution for the finite difference discretisation and the results referred to in this section are derived mainly from chapter 3.

For solving homogeneous problems, the conjugate gradient method was shown to be the quickest and is not affected by the ratio of the number of nodes in differences directions. The number of iterations for a given size of grid is small. Point iteration, although slower than the conjugate gradient method is far quicker than the other methods and is also not affected by the orientation of the grid. The other three methods, line and panel iteration and complete inversion, were much slower and had a preference as to the orientation of the grid according to the ratio of the number of nodes in the different directions.

The results for the heterogeneous case show that all the iterative schemes

are greatly affected by the resistivity distribution. The tests were chosen to find the weaknesses of the methods and are a guide to how each method would perform in calculating the synthetic measurements used in the calculation of the inverse problem. The complete inversion method is oblivious of the resistivity distribution and will always produce an answer in the same time for a given size of grid. The reason that the conjugate gradient method took so long was because α (the size of the update) is very small. The other three iterative methods seem to follow the same trends, which is not surprising given that their iterative are effectively the same. Point iteration is the fastest method in most of the tests, while in most of the tests, line iteration appears to produce the most constant value of the time taken. This method can also be faster than point iteration.

Section 3.3 describes the ability of the three stationary iterative methods to solve forward problems, which are of a type akin to those solved when the perturbation method Jacobian is calculated. Point iteration seems to be the fastest, and is entirely satisfactory for our purpose, although there is no reason to suppose that the conjugate gradient method would not be quick at this type of problem equally quickly.

The test problems were run using a smaller grid than would normally be used in modelling surveys. This was to enable all the methods to be used, including complete inversion. The grids had a ratio of 1:1:1 of the number of nodes in each direction. The size of the grid would indicate that the results may be slightly biased against the conjugate gradient method which is less dependent on size of the grid than the other methods.

Of the two algorithms developed, complete inversion has the greatest potential, as it could be modified to permit repeated calculations over the same resistivity distributions. There are drawbacks in this, namely the need for large amounts of RAM in solving practical surveys. Panel iteration is similar to line iteration but can be very slow when the direct part of the calculation forms a large proportion, since this is computationally expensive.

The method of choice depends on the exact nature of the problem but the following rules can be used as a guide for choosing the appropriate method:-

- Small problems, particularly those with complicated resistivity distributions, are best solved by complete inversion.
- Homogeneous or nearly homogeneous problems should be solved by the conjugate gradient method.

- Strongly heterogeneous problems by point iteration or line iteration in some cases (see section 3.3)

- Problems starting near to the solution e.g. those involving small perturbations of the resistivities, should be solved using either point iteration or the conjugate gradient method.

We saw in chapter 5 how a two-grid system can be used to model the surveys. This drastically reduced the number of potentials to be calculated and stored, and thus the amount of time and memory used (Jackson et al. [1997]). A further refinement of such a system is an area for further research. As suggested in chapter 2, another future development may be by iterating radially from the source electrode to calculate the forward problem. We have also shown that some forms of anisotropy could be included in the forward model (and hence the inverse problem) enabling a very common geological situation to be addressed.

8.2 Inverse methods

The inverse problem associated with the interpretation of electrical resistivity tomography can be tackled with a number of different techniques. Most of these techniques require the calculation of a sensitivity or Jacobian matrix. The accurate calculation of this part is often overlooked, mainly because, for geophysical surveys, the matrix is large, difficult to display and time-consuming to calculate.

The adjoint Jacobian method derived in chapter 5 uses the knowledge of the adjoint of each measurement to the corresponding Jacobian. This method uses current densities originating from both the current and potential electrodes in the zones to calculate the value of the Jacobian. However, the actual scheme which was implemented did not explicitly calculate the current densities but took the potentials calculated from the forward problem to calculate the elements of the Jacobian. This method is much faster than the perturbation method and is does not depend on the number of zones, making it ideal for large surveys which have many zones. The adjoint method depends on the number of electrodes and the number of measurements. In section 5.5 we showed how to produce very close approximations to the analytic homogeneous isotropic Jacobian.

In any of the zones which had electrodes there was found to be a change of sign between the adjoint and perturbation Jacobians. The hybrid method was produced to alleviate this problem by using the perturbation method for the zones

with electrodes in them and the potential-corrected adjoint method[1] for the remainder.

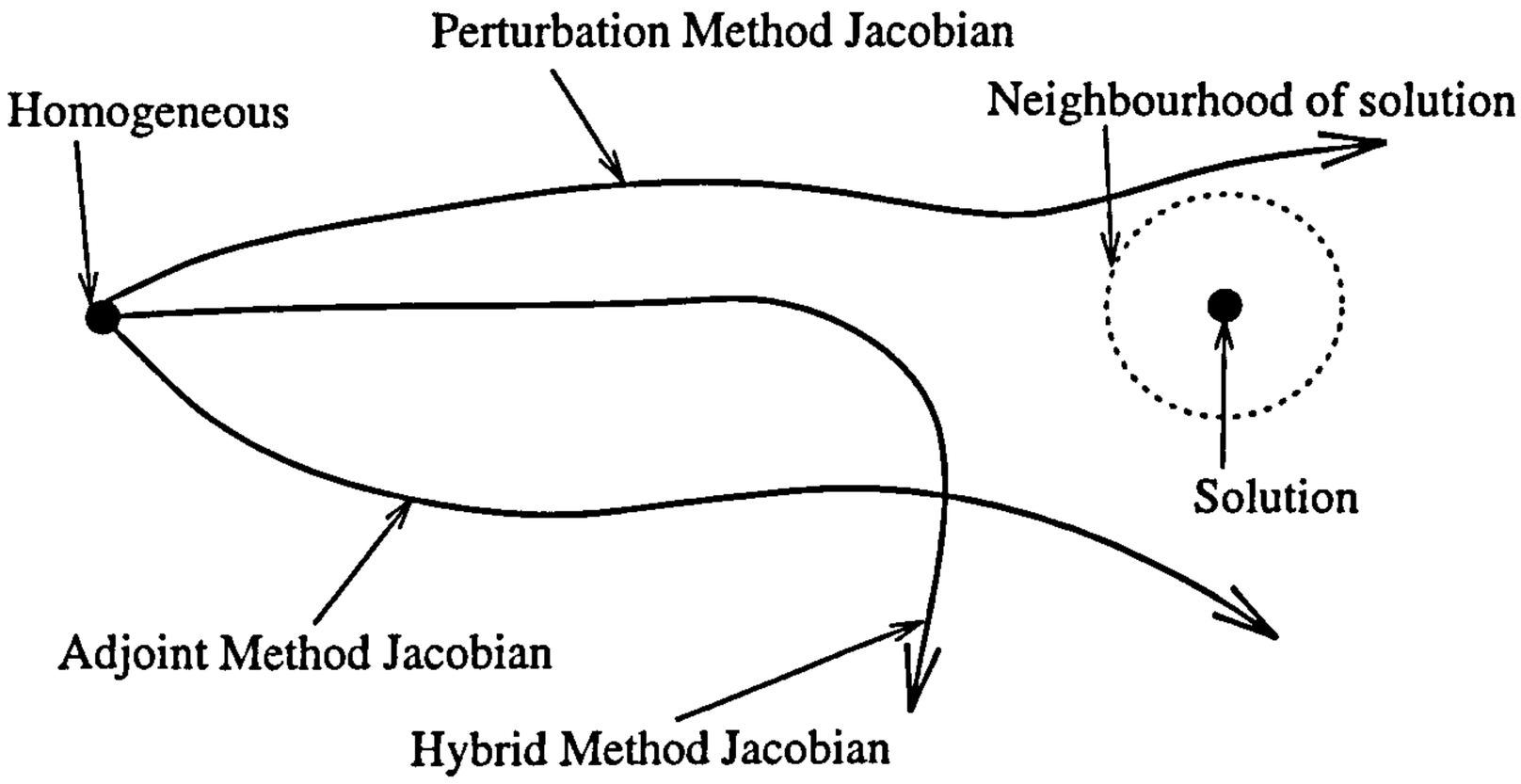

Figure 8.1: A representation of how the methods behave in solution space and how different methods of calculating the Jacobian affect Occam's method for calculating the inverse problem.

The results in chapter 6 use a smooth slowly slacking smoothness-constraint. The adjoint methods perform well in these conditions better than the perturbation method. The hybrid performs well at the beginning, but suddenly diverges. However, the best result was obtained by using a much steeper descent of the smoothness-constraint and using the perturbation method. Figure 8.1 gives a idea as to how the methods behave. None of them actually penetrating the neighbourhood of the solution though the perturbation method comes closest. Unfortunately, the perturbation method is the slowest, even if only a third of the electrodes were current electrodes. The perturbation method took seven times as long as the adjoint methods whilst the hybrid method took slightly more than twice as long as the adjoint methods.

Chapter 7 demonstrated the differences in the Jacobians. The techniques can be directly compared in both the homogeneous and heterogeneous cases. For the homogeneous case, the adjoint methods performed well but encountered a problem with the sign of the value in the zones with the electrodes. There were also a few problems in boundary zones caused by errors in the interpolation of potentials. The perturbation method has a pattern of small errors in the lower zones even for the homogeneous Jacobians. The hybrid method generates values closest to the result of numerical integration of the formula given in section 5.5.2 in x, y, and z.

[1]This is a variant on the adjoint method, see section 6.3.4.

The Jacobians produced by the heterogeneous cases were quite different from those produced by the homogeneous case. It follows that the use of the homogeneous Jacobian must introduce large errors in typical inversion schemes. It was found that there were three types of changes between the heterogeneous and homogeneous Jacobians:

- Diagonal stripes which occurred near large values in the Jacobian, which occurred in all the methods.
- Horizontal stripes which only occurred in the Adjoint and Hybrid methods.
- Smaller changes in the magnitude of the values.

The last being caused by the relative values of the resistivity. The diagonal stripes are major changes caused by the differences between the resistivity distributions. The horizontal stripes are errors likely to be caused by neglecting a term which is in fact negligible only when the resistivity distribution changes smoothly[2], which is not the case. The structure of the Jacobian is dependent on the location of the electrodes and the resistivity distribution, which is linked to the current flow and thus current density.

It was found that the adjoint method suffers from large errors for highly heterogeneous resistivity distributions. These errors can be explained in part by an approximation in the adjoint theory. It has been demonstrated (e.g. Sasaki [1992]) that if a set of measurements has errors then a stiffer smoothness-constraint will 'average' these errors during an inversion. The results in chapter 6 combined with the knowledge of errors in heterogeneous Jacobians calculated partly or wholly by using the adjoint, lead to the conclusion that a stiffer smoothness constraint will also smooth out these errors. This is consistent with the 'smoothed' nature of the tomograms presented in the literature (e.g. Sasaki [1992], Loke & Barker [1996*b*]) for test problems where the solution is known.

A common practice is to use 'approximate' and 'fast' methods for calculating the Jacobian. Our conclusion is that, on the contrary, greater emphasis should be placed on the accuracy of the Jacobian. Therefore a balance should be struck between the errors in the measurements and the errors in the Jacobian, we have demonstrated that the perturbation method is the most accurate numerical method for calculating the Jacobian. It follows that if a fast method, such as the

[2]The resistivity distribution used to model the ground is piecewise constant.

adjoint method, is used at the beginning of the inversion then the perturbation method should be used for the last few iterations.

The adjoint methods for calculating the Jacobian would work well on anisotropic survey data since effectively the number of zones is tripled. A method that is independent of the number of zones will thus have a considerable speed advantage in this type of problem.

Appendix A

Model

The ground is assumed to be a conducting (not necessarily particularly conductive) solid. Therefore given that Ohm's Law is

$$\mathbf{E} = \rho\mathbf{J} \tag{A.1}$$

where $\mathbf{E}$ is the electrical field and $\mathbf{E} = -\nabla\phi$, $\mathbf{J}$ is the current density and ρ is the resistivity. We occasionally need to consider anisotropic media, which we treat by replacing ρ with a matrix $\underline{\mathbf{R}}$ which is assumed to be positive definite[1] (resistivity is positive). The anisotropic version of Ohm's Law is

$$-\nabla\phi = \underline{\mathbf{R}}\mathbf{J} \tag{A.2}$$

Also the divergence of the current density over a particular volume is zero unless there is a current source/sink present i.e. $\nabla.\mathbf{J}$. However, if in the space being modelled there is a current source I_s, it can be shown that

$$\nabla.\mathbf{J} = I_s \tag{A.3}$$

By rearranging equation (A.2) to produce a formula for $\mathbf{J}$ and substituting into equation (A.3) a form of Poisson's equation is produced.

$$\nabla.(\underline{\mathbf{K}}\nabla\phi) = -I_s \tag{A.4}$$

where $\underline{\mathbf{K}} = \underline{\mathbf{R}}^{-1}$. In Poisson's equation $\underline{\mathbf{K}}$ would normally be a scalar conductivity k (or ρ^{-1}) and I_s would be a scalar source term.

As can be seen in figure A.1, the space being modelled is a 3D half-space. It is assumed that no current flows across the air/ground boundary which is thus a

[1] A matrix $\underline{\mathbf{A}} \in \Re^{n\times n}$ is *positive definite* if $\mathbf{x}^T\underline{\mathbf{A}}\mathbf{x} > 0$ for all nonzero $\mathbf{x} \in \Re^n$. Effectively, this means that all the eigenvalues are positive.

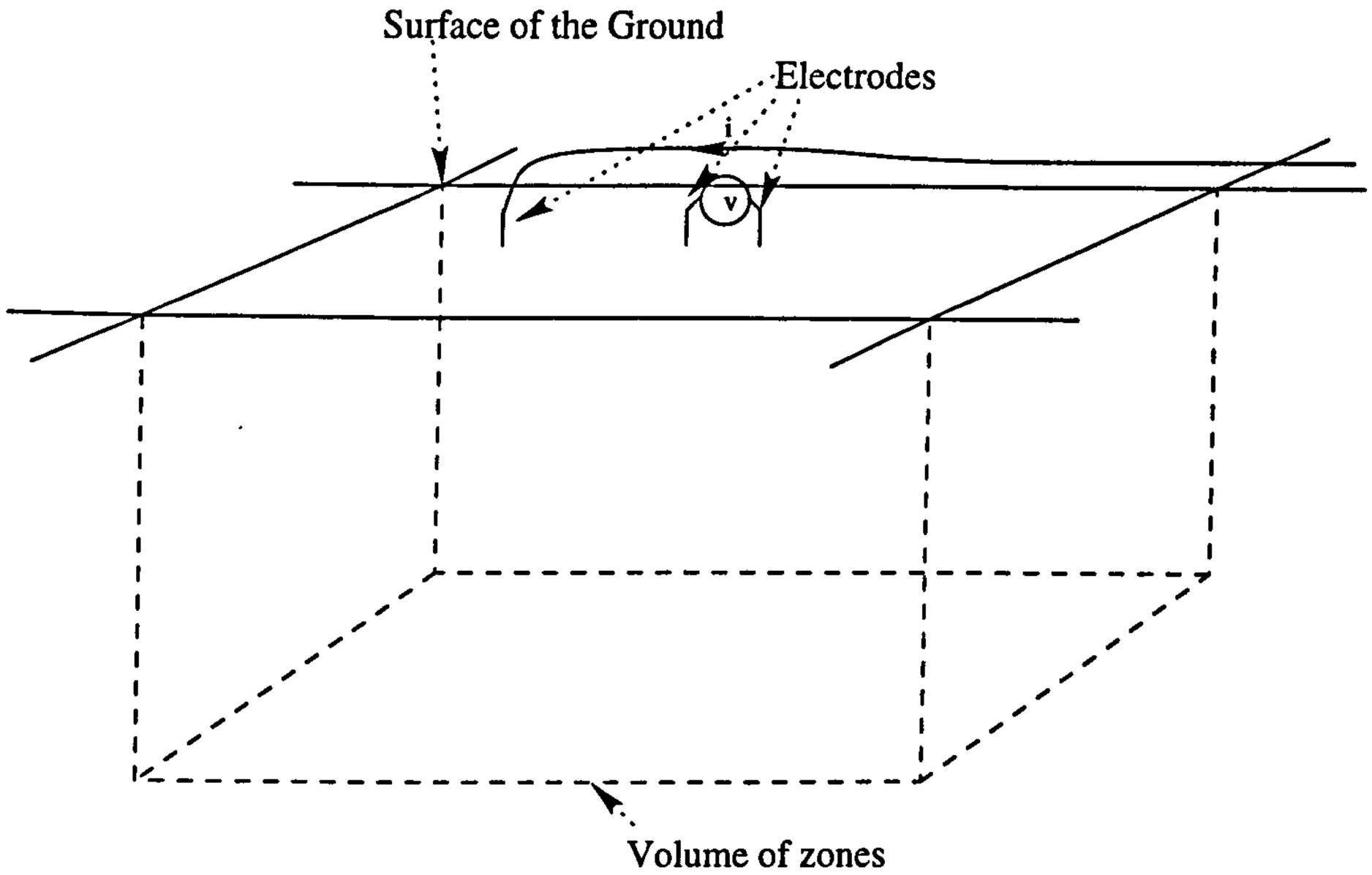

Figure A.1: Model of a measurement during an electrical resistivity survey

Neumann boundary, i.e. $\frac{\partial \phi}{\partial z} = 0$, analogous to an adiabatic boundary in the case of heat conduction.

As a half space is being modelled, the other five boundaries are infinitely far from the electrodes. This is not practicable for numerical modelling purposes and is overcome by setting the boundaries at a finite but comparatively large distance from the survey, and their potential set either at zero or at the analytic homogeneous potential value for that point.

The ground is assumed to be connected and a continuum. The latter assumption implies that the microstructure is not of interest. This is not totally true: the parts of the micro structure which are of interest are those which have noticeable macro effects, e.g. the contents of the pores, the alignment of grains to produce anisotropy[2]. The ground is assumed to be "connected", which is equivalent to assuming that there exists a non-arbitrary potential at every point.

The particular type of survey is used here is pole–dipole surveys. This means that the current sink electrode is said to be infinitely far from the other electrode. In practice this electrode is set a long way from the survey, and is often placed perpendicular to the line of the other electrodes.

There are various methods of discretising this problem of which a selection is given in Spitzer & Wurmstich [1995]. However, the version which has

[2]This is a similar sort of alignment as is found in liquid crystals.

been used, is a simple finite difference scheme which only uses the six nearest nodes Reece [1986], Williams [1996]. The more complex varieties mentioned by Spitzer & Wurmstich [1995] produce a better model but this is often outweighed by the storage space required. The type used is analogous to modelling the ground as a network of resistors.

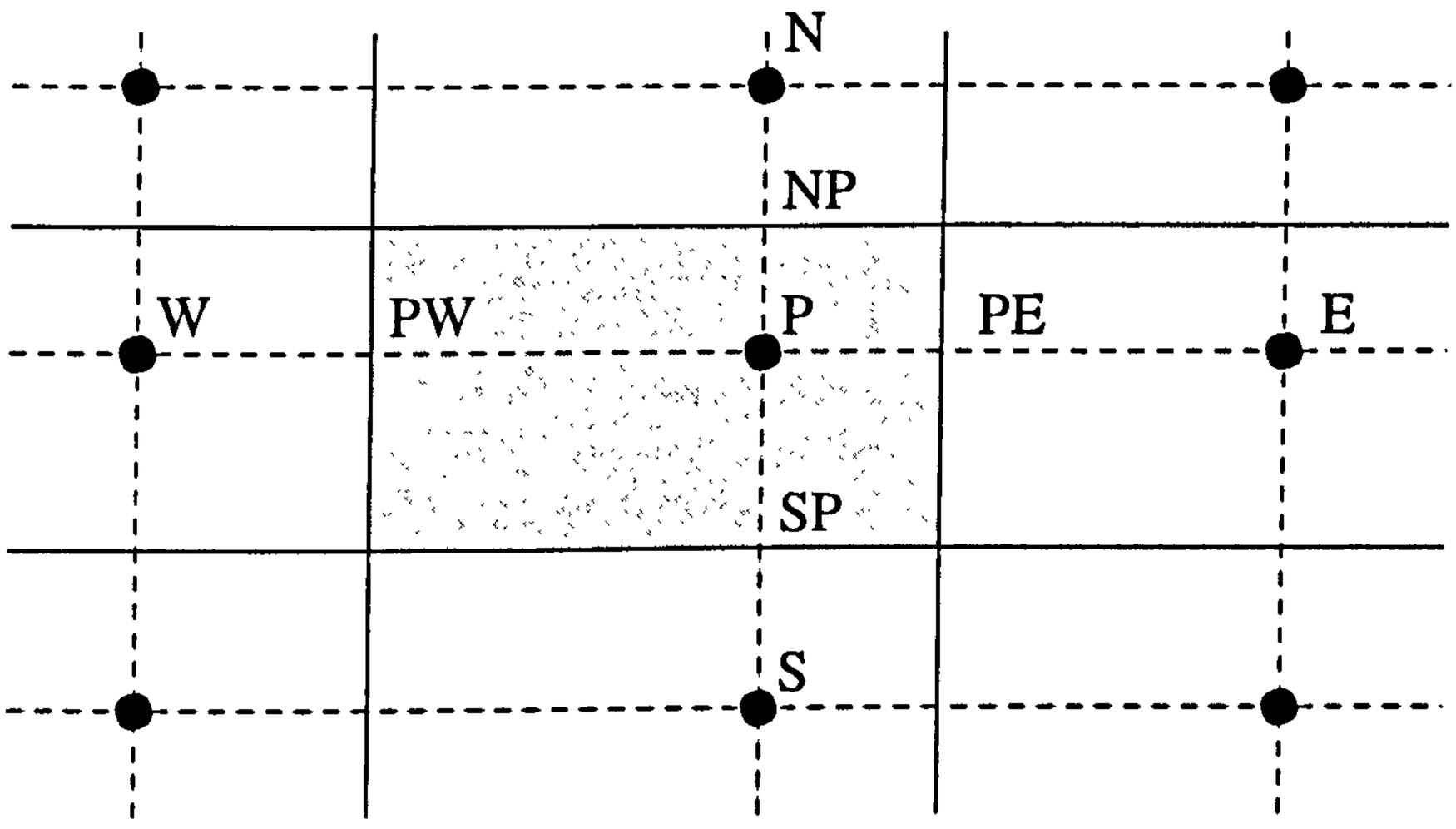

Figure A.2: One grid cell. This is figure 7.2 from [Reece 1986].

Figure A.2 shows a 2D grid cell (the shaded area) where P is the node in the node in the cell. If just the horizontal direction x is considered then the net flow of current across the cell is

$$\frac{k_{PE}\frac{\phi_E-\phi_P}{x_E-x_P} - k_{WP}\frac{\phi_P-\phi_W}{x_P-x_w}}{x_{PE}-x_{WP}}$$

quoted from Reece [1986]. In the above formula, ϕ_* is the potential at a point $*$, $x_{1*} - x_{2*}$ is the distance between x_{1*} and x_{2*} and k_{PE} is the conductivity between nodes P and E. From this, a set of simultaneous equations for the potential at each node in the grid can be produced and can be written as the matrix equation (equation(1.1))

$$\underline{\mathbf{A}}\mathbf{x} = \mathbf{b}$$

where the $\underline{\mathbf{A}}$ contains the conductivities (or relative conductivities), $\mathbf{b}$ contains the sources and boundary conditions and $\mathbf{x}$ the vector of values of ϕ.

The method used in modelling the measurements during the inversions uses two grids. The coarser one models the boundary conditions and the general structure and a finer grid to model more accurately the space where the electrodes

are positioned. The large grid produces the boundary conditions and the initial starting point for fine grid.

Appendix B

Results of Forward Problem

B.1 The results of the effect of size on the forward problem

The figures in this first part of this appendix relate to the first half of section 3.2. This related to the size and shape of the forward problems. The task was to solve a steady state heat conduction problem. In the task set the grid cells were uniform. The conductivity was set a at $1W/mK$ and the uniform source was set at 100 Joules per m^3. The size of the cube was set at $1m^3$. The boundaries were Dirichet and set at zero, whilst initially all nodes were zero.

For each method used for solving this problem on a finite difference grid there are two graphs. The first, concentrates on size alone, and the second on the shape. The lines, which have been fitted, were done to fit the highest order term and not the average. As a consequence, only the last four or five data points could be used due to the effect of lower order terms, but as can be seen from most of the images in section 3.2 the highest order term fits the data on a non log-log graph fairly well.

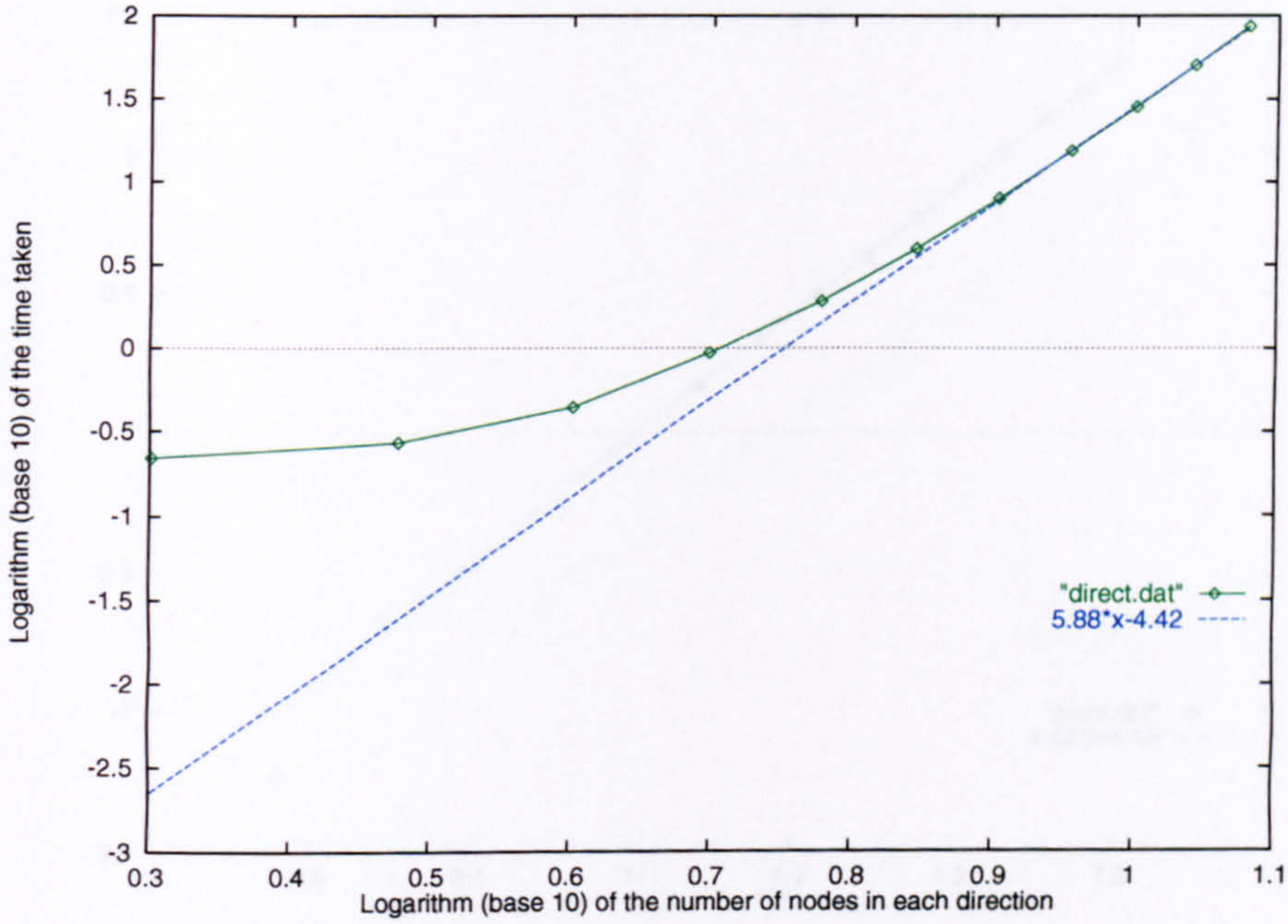

Figure B.1: Log-log plot for a cube of nodes for Complete Inversion.

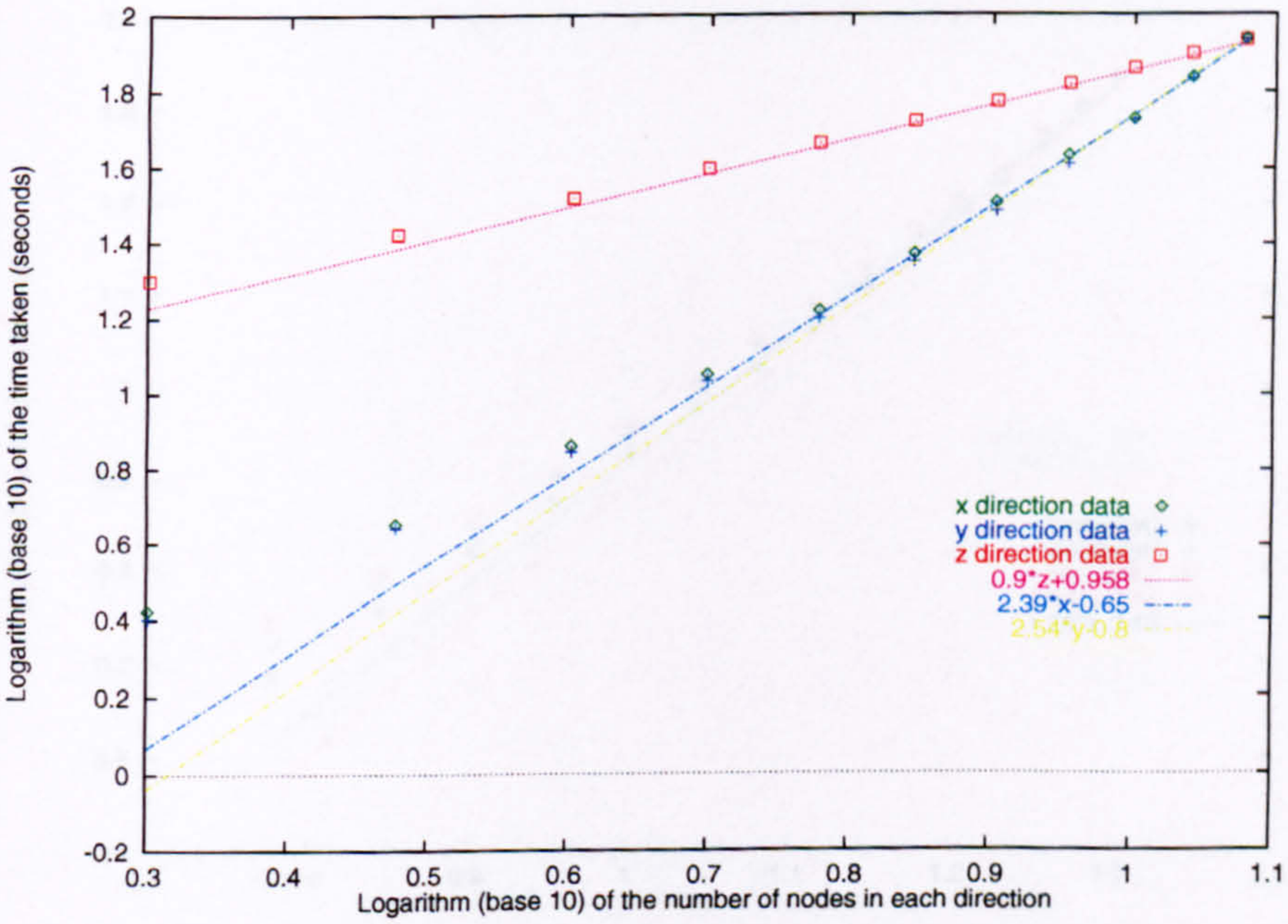

Figure B.2: Log-log plot of time taken against the number of nodes in a particular direction for Complete Inversion.

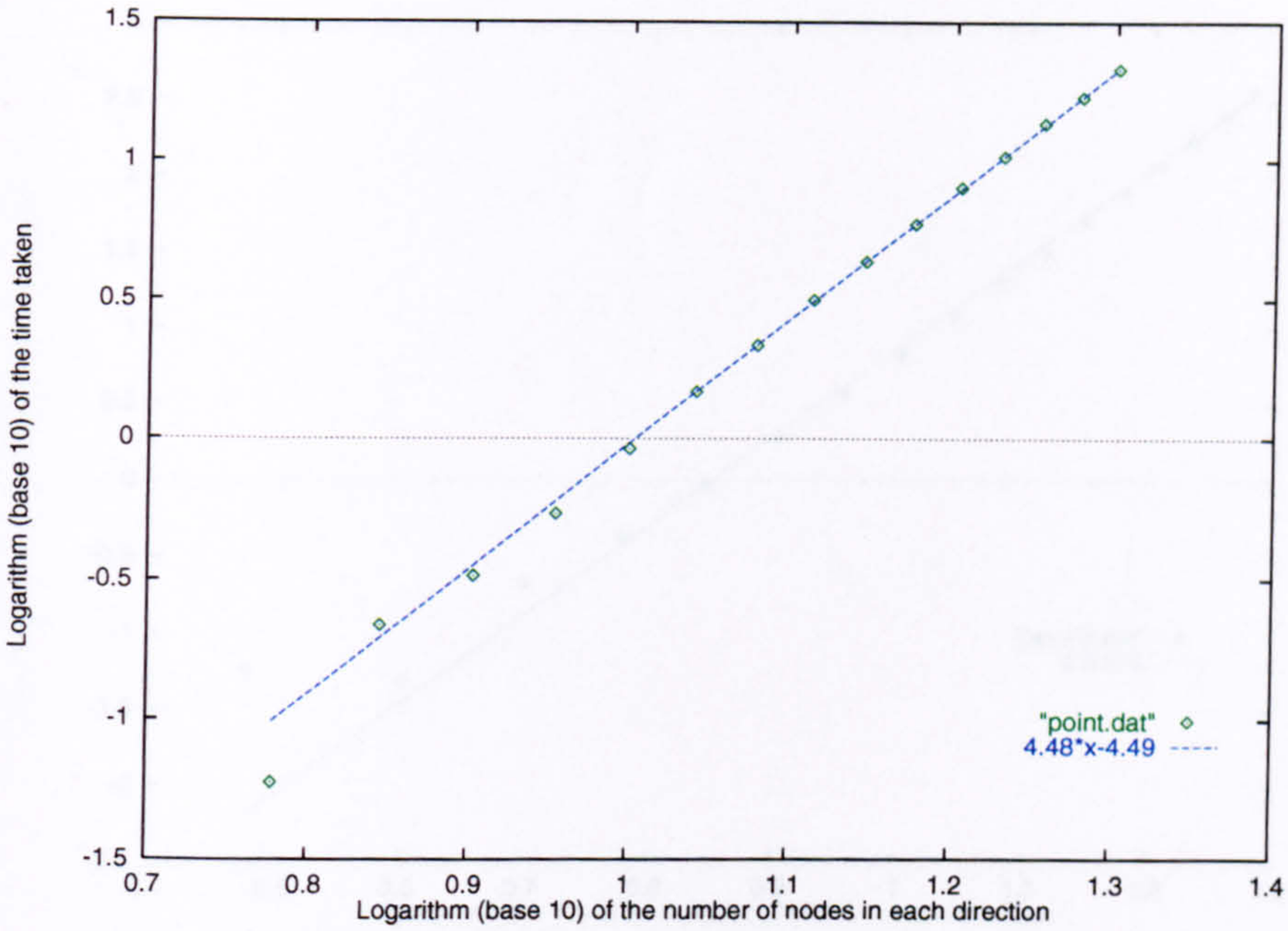

Figure B.3: Log-log plot for a cube of nodes for Point Iteration.

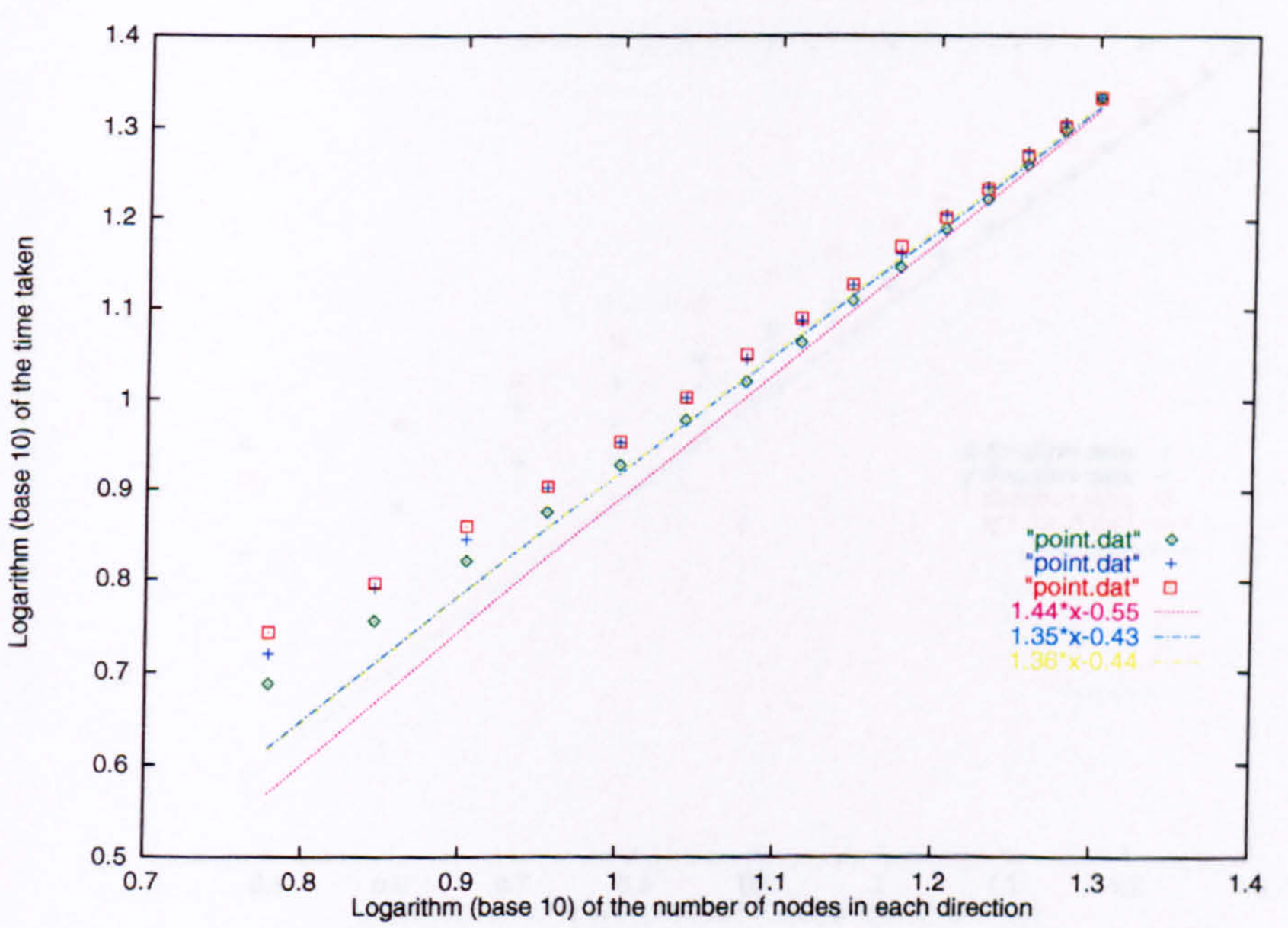

Figure B.4: Log-log plot of time taken against the number of nodes in a particular direction for Point Iteration.

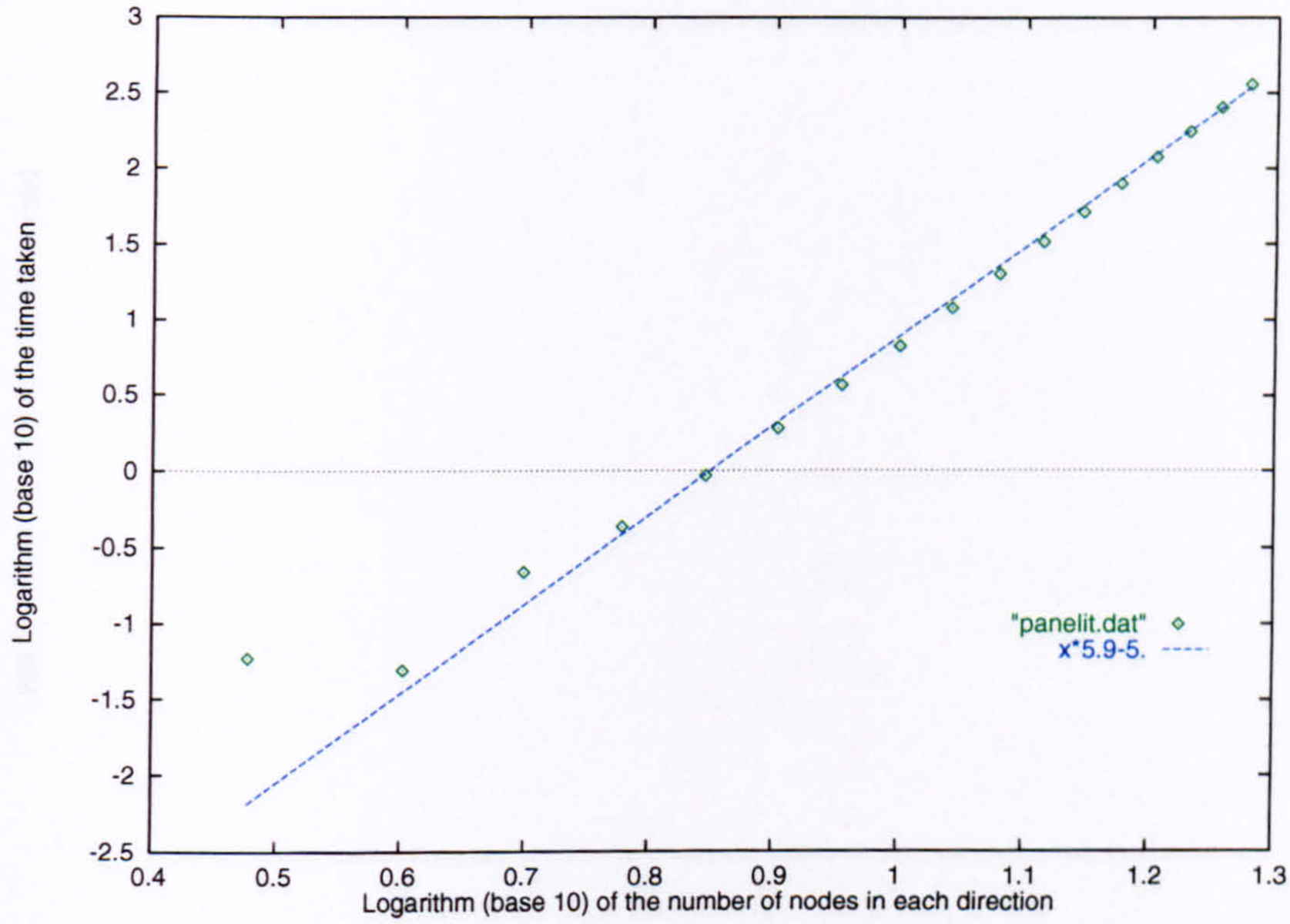

Figure B.5: Log-log plot for a cube of nodes for Line Iteration.

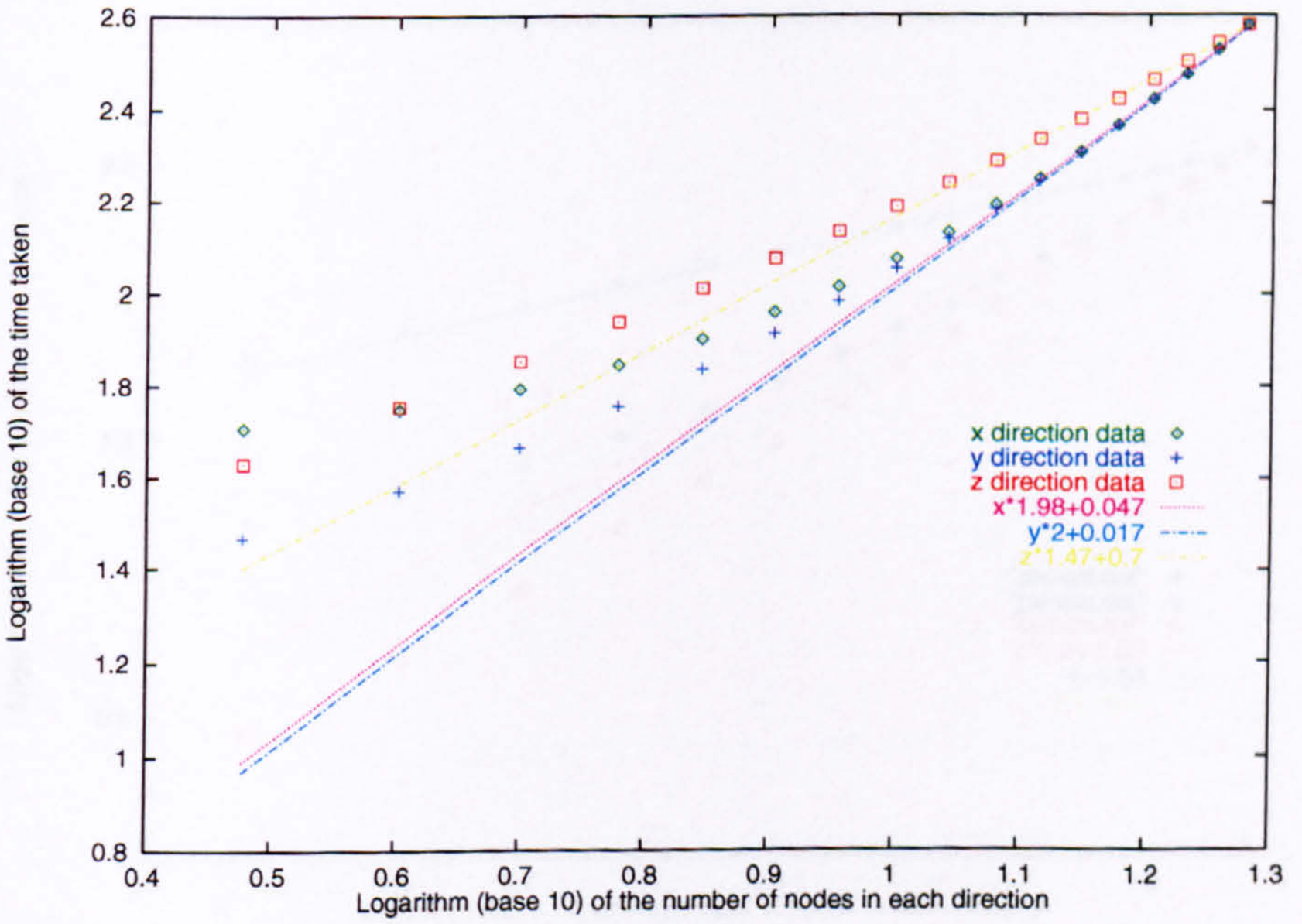

Figure B.6: Log-log plot of time taken against the number of nodes in a particular direction for Line Iteration.

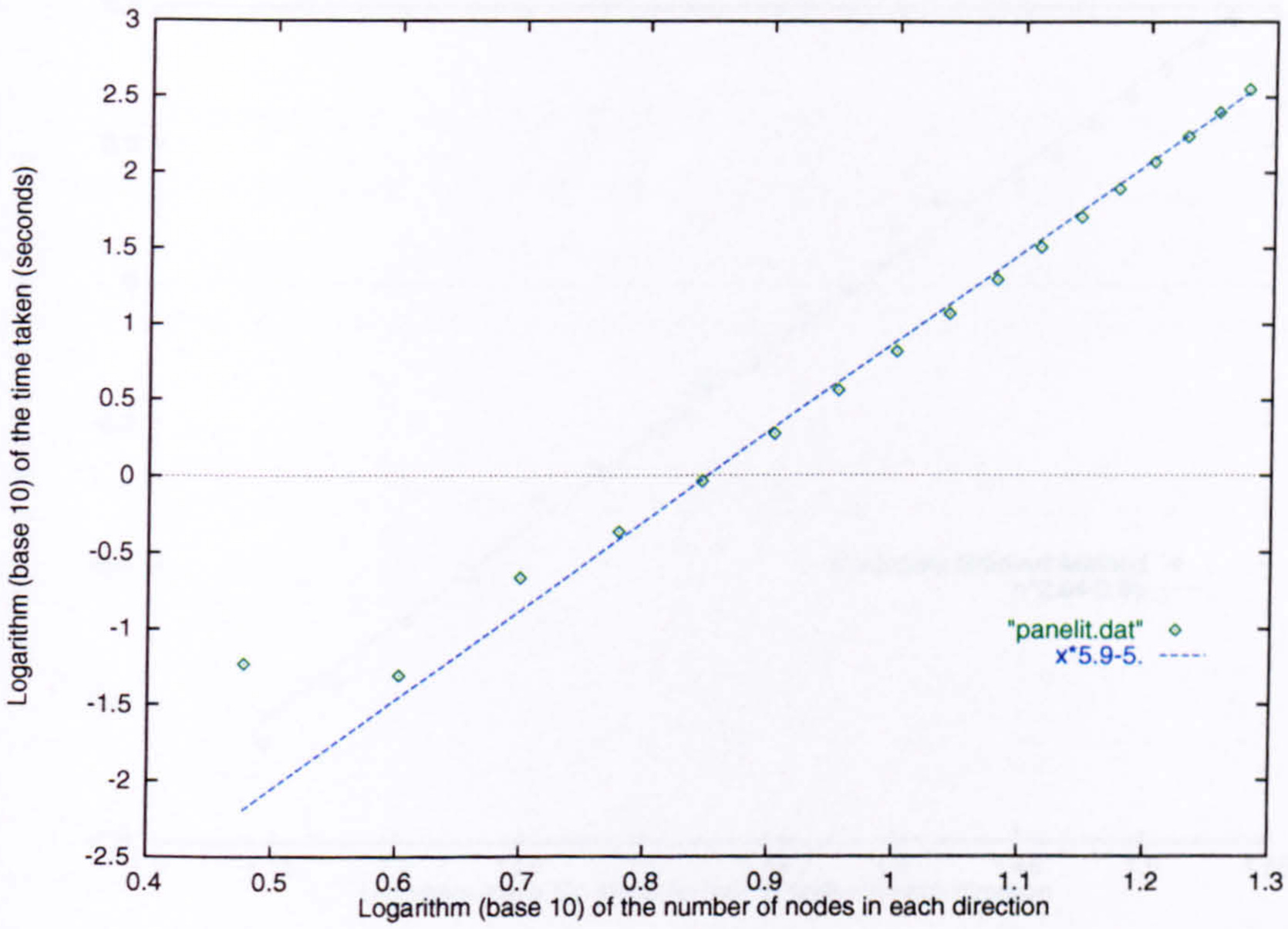

Figure B.7: Log-log plot for a cube of nodes for Panel Iteration.

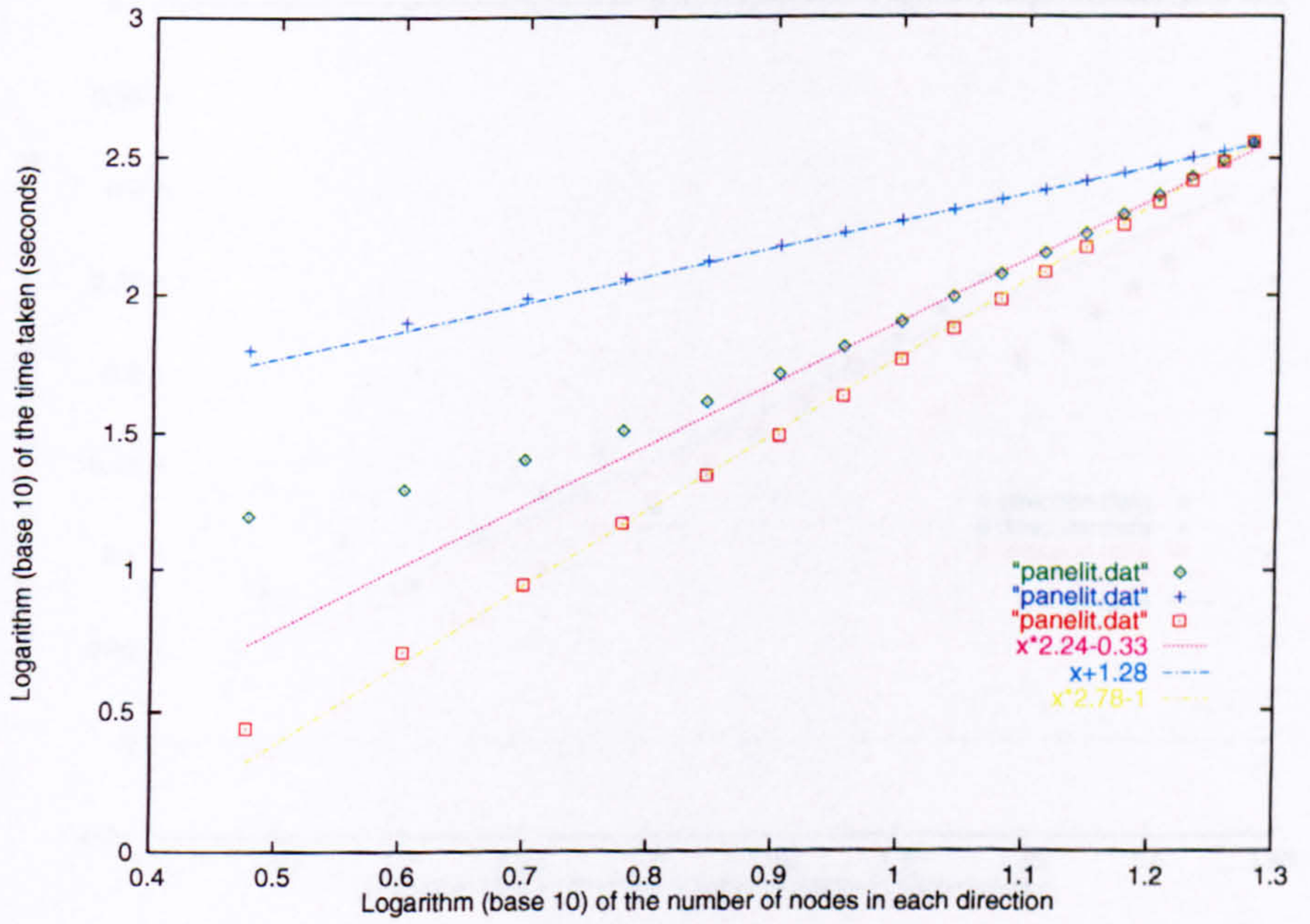

Figure B.8: Log-log plot of time taken against the number of nodes in a particular direction for Panel Iteration.

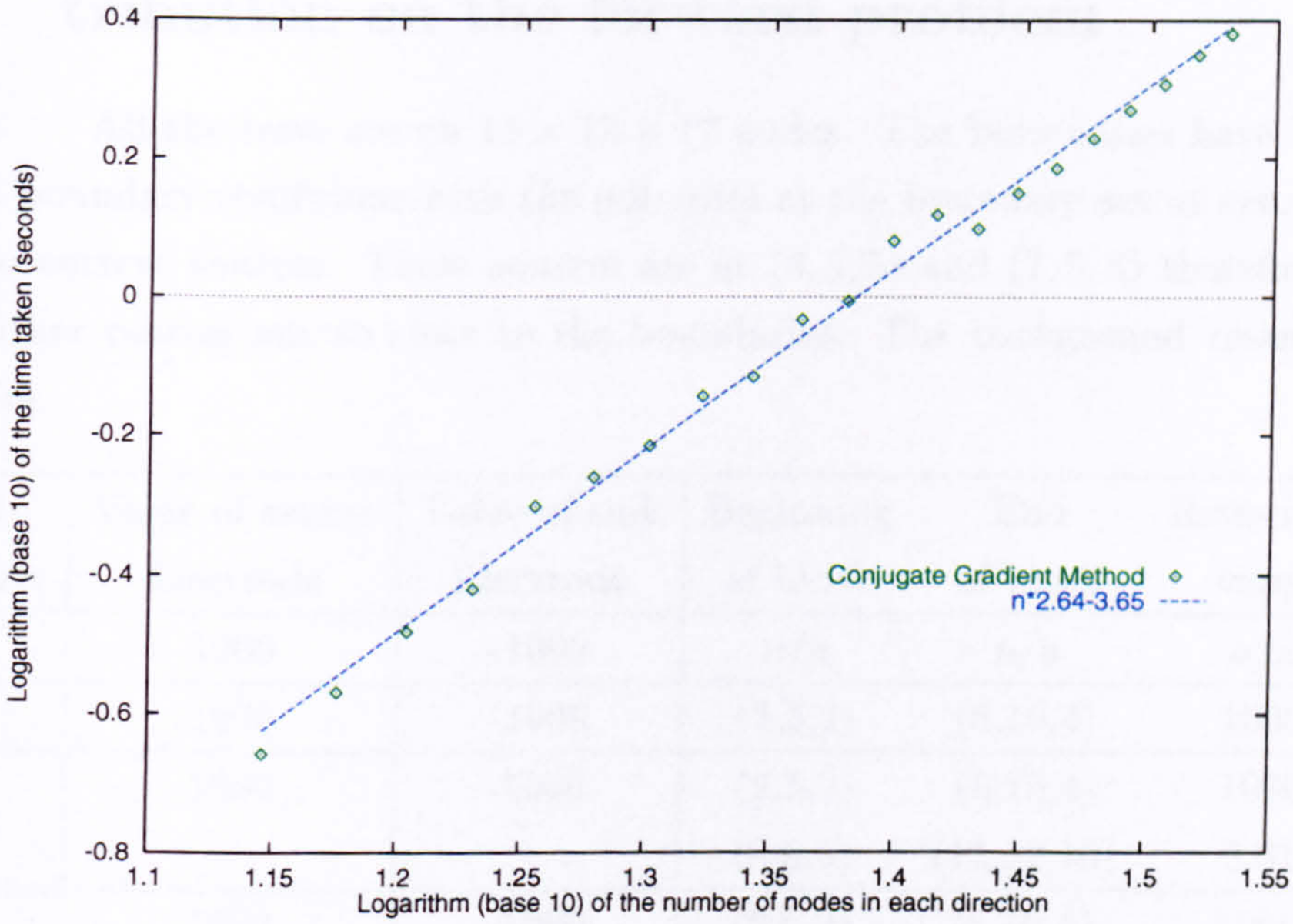

Figure B.9: Log-log plot for a cube of nodes for the Conjugate Gradient Method.

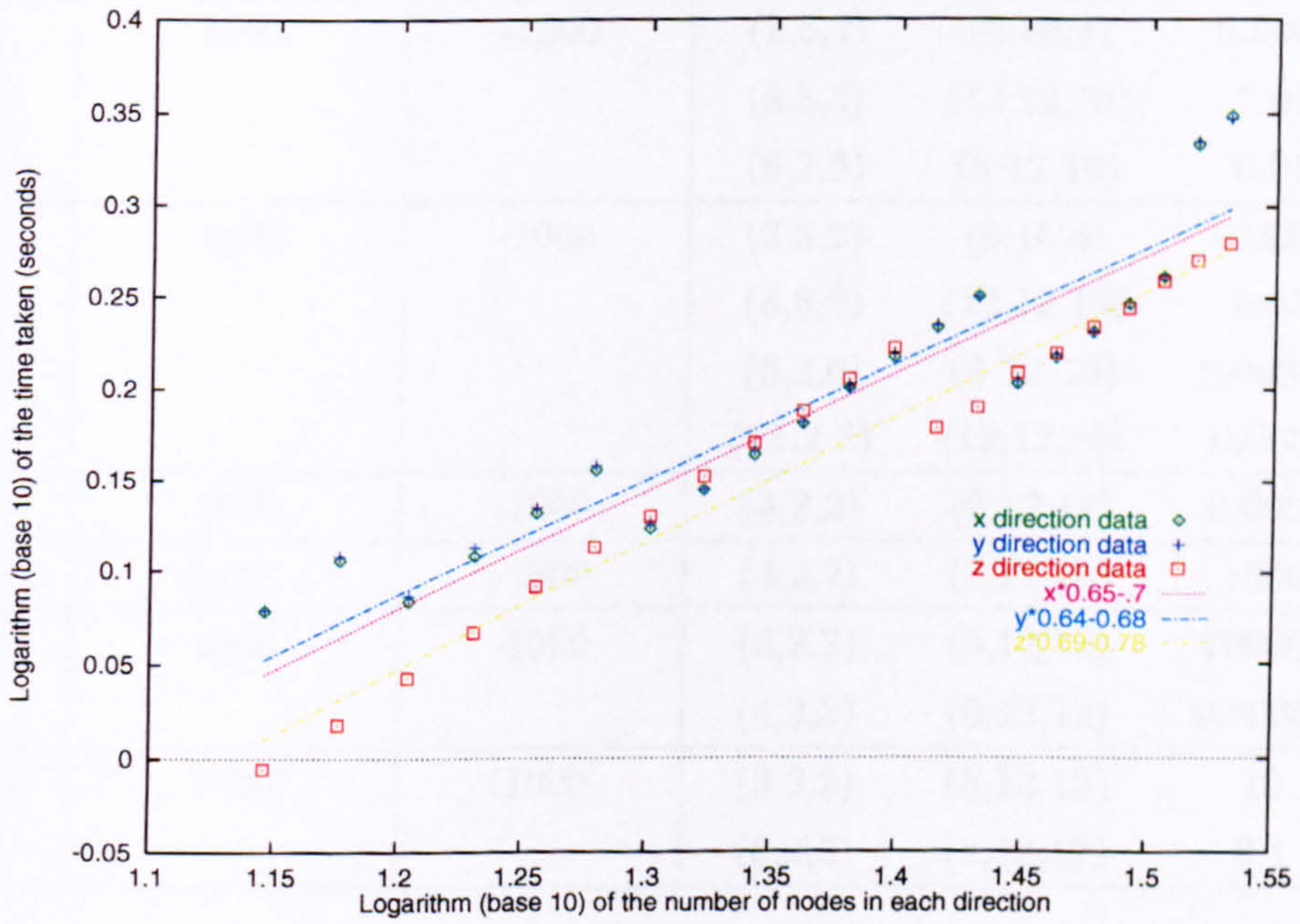

Figure B.10: Log-log plot of time taken against the number of nodes in a particular direction for the Conjugate Gradient Method.

B.2 The results of the effect of the resistivity distribution on the forward problem

All the tests are on $12 \times 12 \times 12$ nodes. The boundaries have Dirichet (fixed) boundary conditions with the potential at the boundary set at zero. There are two current sources. These sources are at $(3, 5, 5)$ and $(7, 5, 5)$ therefore these are neither central nor to close to the boundaries. The background resistivity is 1ohm/m.

test number	Value of source Electrode	Value of sink Electrode	Beginning of block	End of block	Resistivity value
1	1000	-1000	n/a	n/a	n/a
2	1000	-1000	(2,5,2)	(5,10,4)	1000
3	1000	-1000	(2,5,2)	(5,10,4)	1000
			(8,8,5)	(12,12,10)	0.01
4	1000	-1000	(2,5,2)	(5,10,4)	1000
			(8,8,5)	(12,12,10)	0.01
			(6,2,6)	(8 12 10)	2000
5	1000	-1000	(2,5,2)	(5,10,4)	0.0001
			(8,8,5)	(12,12,10)	0.01
			(6,2,6)	(8 12 10)	0.01
6	1000	-1000	(2,5,2)	(5,10,4)	0.0001
			(8,8,5)	(12,12,10)	0.01
			(6,2,6)	(8 12 10)	0.00001
			(11,2 2)	(12,12,10)	100000
7	1000	-1000	(4,2,2)	(6,12,12)	0.0001
8	0.001	-1000	(4,2,2)	(7,12,12)	1000
9	1000	-1000	(3,2,2)	(5,12,12)	100000
			(4,2,2)	(6,12,12)	0.00001
10	1000	-1000	(3,2,2)	(5,12,12)	10
			(6,2,2)	(8,12,12)	0.1

The first test is the homogeneous case. The rest have heterogeneous resistivity distributions. These heterogeneous blocks which can be described by two points (a beginning and an end). If the block is superimposed on another it deletes the previous values.

B.3 The results of the starting close to the solution

These are the same tests as described in appendix B.2 except that each has been perturbed by the following (using the same rules for defining the perturbed blocks as in appendix B.2).

test number	Beginning of block	End of block	Resistivity value
1	(6,2,4)	(8,4,6)	1.01
2	(2,2,2)	(4,4,4)	1010
3	(6,2,6)	(8,4,10)	0.0101
4	(6,2,6)	(8,4,10)	2020
5	(6,2,6)	(8,4,10)	0.0101
6	(6,2,6)	(8,4,10)	0.0000101
7	(4,2,6)	(6,4,10)	0.000101
8	(4,2,6)	(6,4,10)	1010
9	(6,2,6)	(8,4,10)	0.0000101
10	(6,2,6)	(8,4,10)	0.101

Appendix C

Derivation of Anisotropic Adjoint to the Forward Problem

This appendix runs in parallel to section 5.1.2 and mirrors the first half of Park & Van [1991] except this is the anisotropic version.

Park and Van start not with Poisson's equation but with a pair of coupled first order P.D.E.s. By taking equation (5.2)

$$\rho \mathbf{J} + \nabla \phi = \mathbf{0}$$

and substituting for $-\nabla\phi$ in Ohm's Law into Poisson's equation to produce equation (5.3)

$$\nabla . \mathbf{J} = I_s$$

where ρ = resistivity, $\mathbf{J}$ = current density, ϕ = electric potential and I_s current sources and is $-\sigma$. The two above equations can be rewritten as equation (5.4)

$$\begin{bmatrix} \rho \underline{\mathbf{I}} & \nabla \\ \nabla . & 0 \end{bmatrix} \begin{bmatrix} \mathbf{J} \\ \phi \end{bmatrix} = \begin{bmatrix} \mathbf{0} \\ I_s \end{bmatrix}$$

where $\underline{\mathbf{I}}$ is a 3×3 identity matrix. Let us replace the matrix $\rho\underline{\mathbf{I}}$ with a more general matrix $\underline{\mathbf{R}}$ which describes the resistivity in Cartesian co-ordinates. Equation (5.5) is

$$\begin{bmatrix} \underline{\mathbf{R}} & \nabla \\ \nabla . & 0 \end{bmatrix} \begin{bmatrix} \mathbf{J} \\ \phi \end{bmatrix} = \begin{bmatrix} \mathbf{0} \\ I_s \end{bmatrix}$$

Perturbation of material properties and field quantities in equation (5.4) produces equation (5.6),

$$\begin{bmatrix} \underline{\mathbf{R}} & \nabla \\ \nabla . & 0 \end{bmatrix} \begin{bmatrix} \delta \mathbf{J} \\ \delta \phi \end{bmatrix} = \begin{bmatrix} -\underline{\delta \mathbf{R}} \mathbf{J} \\ 0 \end{bmatrix}$$

where $\delta\mathbf{J}$ and $\delta\phi$ are first-order quantities. Higher order perturbations are neglected. The term neglected at this point is $\underline{\delta\mathbf{R}}\delta\mathbf{J}$. Park and Van next use reciprocity by applying the bilinear identity

$$\int_\tau \left[\mathbf{u}^{\mathbf{T}}\left(\underline{\mathbf{D}}\delta\mathbf{v}\right) - \delta\mathbf{v}^{\mathbf{T}}\left(\overline{\underline{\mathbf{D}}}\delta\mathbf{v}\right)^*\right] d\tau = \int_s (\text{Boundary Terms})\, ds \qquad \text{(C.1)}$$

to equation (5.6) and the adjoint to equation (5.5). For the above equation, $\mathbf{u}$ is the solution to the adjoint problem, $\underline{\mathbf{D}}$ is the normal operator, $\overline{\underline{\mathbf{D}}}$ is the adjoint operator, $\delta\mathbf{v}$ is the solution to the normal problem for secondary fields and s is the surface enclosing the volume τ. This identity is outlined in Lanczos (1961).

By substituting these

$$\underline{\mathbf{D}} = \begin{bmatrix} \underline{\mathbf{R}} & \nabla \\ \nabla. & 0 \end{bmatrix},\ \delta\mathbf{v} = \begin{bmatrix} \delta\mathbf{J} \\ \delta\phi \end{bmatrix},\ \overline{\underline{\mathbf{D}}} = \begin{bmatrix} \underline{\mathbf{R}} & -\nabla \\ -\nabla. & 0 \end{bmatrix},\ \text{and}\ \mathbf{u} = \begin{bmatrix} -\mathbf{J}' \\ \phi' \end{bmatrix}$$

into the left hand side of equation (C.1) we get

$$\int_\tau \left(\begin{bmatrix} -\mathbf{J}' & \phi' \end{bmatrix} \begin{bmatrix} \underline{\mathbf{R}} & \nabla \\ \nabla. & 0 \end{bmatrix} \begin{bmatrix} \delta\mathbf{J} \\ \delta\phi \end{bmatrix} - \begin{bmatrix} \delta\mathbf{J} & \delta\phi \end{bmatrix} \begin{bmatrix} \underline{\mathbf{R}} & -\nabla \\ -\nabla. & 0 \end{bmatrix} \begin{bmatrix} -\mathbf{J}' \\ \phi' \end{bmatrix} \right) d\tau \qquad \text{(C.2)}$$

By multiplying out equation (C.2) we obtain

$$\int_\tau \left(\phi'\nabla.\delta\mathbf{J} - \mathbf{J}'.\left(\underline{\mathbf{R}}\delta\mathbf{J}\right) - \mathbf{J}'.\nabla\delta\phi + \delta\mathbf{J}.\left(\underline{\mathbf{R}}\mathbf{J}'\right) + \delta\mathbf{J}.\nabla\phi' - \delta\phi\nabla.\mathbf{J}'\right) d\tau \qquad \text{(C.3)}$$

To simplify equation (C.3), R must satisfy equation (5.9)

$$\mathbf{J}'.\left(\underline{\mathbf{R}}\delta\mathbf{J}\right) = \delta\mathbf{J}.\left(\underline{\mathbf{R}}\mathbf{J}'\right)$$

(See section 5.1.2 for details.)

By applying the identity $\nabla.\left(\phi\mathbf{J}\right) = \mathbf{J}.\nabla\phi + \phi\nabla.\mathbf{J}$ and assuming equation (5.9) holds then (C.3) becomes

$$\int_\tau \nabla.\left(\phi'\delta\mathbf{J} - \delta\phi\mathbf{J}'\right) d\tau \qquad \text{(C.4)}$$

Using the divergence theorem on the equation (C.4) it becomes

$$\int_s \left(\phi'\delta\mathbf{J} - \delta\phi\mathbf{J}'\right).d\mathbf{s} \qquad \text{(C.5)}$$

Therefore (C.2) equals (C.5)

$$\int_\tau \left(\begin{bmatrix} -\mathbf{J}' & \phi' \end{bmatrix} \begin{bmatrix} \underline{\mathbf{R}} & \nabla \\ \nabla. & 0 \end{bmatrix} \begin{bmatrix} \delta\mathbf{J} \\ \delta\phi \end{bmatrix} - \begin{bmatrix} \delta\mathbf{J} & \delta\phi \end{bmatrix} \begin{bmatrix} \underline{\mathbf{R}} & -\nabla \\ -\nabla. & 0 \end{bmatrix} \begin{bmatrix} -\mathbf{J}' \\ \phi' \end{bmatrix} \right) d\tau$$

$$= \int_s (\phi' \delta \mathbf{J} - \delta\phi \mathbf{J}')\, ds \tag{C.6}$$

where **s** is the unit vector normal to the surface.

The adjoint problem for this system is

$$\begin{bmatrix} \underline{\mathbf{R}} & -\nabla \\ -\nabla. & 0 \end{bmatrix} \begin{bmatrix} -\mathbf{J}' \\ \phi' \end{bmatrix} = \beta \tag{C.7}$$

where β is a source term for the adjoint. If $\beta = [0 \quad I_s']^T$ and we expand equation (C.7), the coupled equations are:

$$\begin{bmatrix} \underline{\mathbf{R}} & \nabla \\ \nabla. & 0 \end{bmatrix} \begin{bmatrix} \mathbf{J}' \\ \phi' \end{bmatrix} = \begin{bmatrix} \mathbf{0} \\ I_s \end{bmatrix} \tag{C.8}$$

This is the adjoint to equation (5.5) which is the adjoint for the system for the more general form. For the original proof $\underline{\mathbf{R}}$ is substituted by $\rho\underline{\mathbf{I}}$ to obtain the adjoint of the original system.

$$\rho\mathbf{J}' + \nabla\phi' = \mathbf{0} \tag{C.9}$$

and

$$\nabla.\mathbf{J}' = \mathbf{I}_s' \tag{C.10}$$

From the above and equations (5.2) and (5.3) it is easy to see that the normal problem is identical to the adjoint problem. However equation (C.6) can be further simplified by substituting the right hand side of equation (5.6) for the first term and the right hand side of equation (C.7) for the second term, obtaining

$$\int_\tau \left([-\mathbf{J}' \quad \phi'] \begin{bmatrix} -\underline{\delta\mathbf{R}}\mathbf{J} \\ 0 \end{bmatrix} - [\delta\mathbf{J} \quad \delta\phi] \begin{bmatrix} 0 \\ I_s' \end{bmatrix} \right) d\tau = \int_s (\phi' \delta \mathbf{J} - \delta\phi \mathbf{J}')\, ds \tag{C.11}$$

(It should be noted that there is a typographical error in the equivalent equation in Park & Van [1991]. They have $-\delta\mathbf{J}$ where it should be $-\delta\rho\mathbf{J}$.) The boundaries of the problem, five of which are chosen to be far enough away for the secondary field to be zero and the other is the surface (surface of the earth) cause the secondary fields also to vanish because both $\mathbf{J}'$ and $\delta\mathbf{J}$ are both parallel to the surface, but **s** is the unit normal to it. Thus all the boundary terms in equation (C.11) are zero, and it can be written as equation (5.7)

$$\int_\tau (\underline{\delta\mathbf{R}}\mathbf{J}).\mathbf{J}' d\tau = \int_\tau \mathbf{I}_s' \delta\phi d\tau$$

If I_s' is a delta function on at the receiver location (x_{P1}, y_{P1}, z_{P1}) then $\mathbf{J}'$ is the current from a point at the receiver location (i.e. a Green's function). This choice reduces equation (C.6) to equation (5.8)

$$\delta\phi\,(x_{P1},\ y_{P1},\ z_{P1}) = \int_\tau (\underline{\delta\mathbf{R}}\mathbf{J})\,\mathbf{J}.\mathbf{J}' d\tau$$

Appendix D

Algorithm for Calculating the Adjoint Method Jacobian from Finite Difference Potential

This appendix gives the algorithm used for calculating the Adjoint Jacobian. Equation (5.47) is

$$\underline{\mathcal{J}}_{q,r} = \frac{1}{i_{C1}} \sum_{p=1}^{no.cells} \begin{pmatrix} J_{C1,x,q,p}.\left(J_{P1,x,q,p} - J_{P2,x,q,p}\right)\delta x_p.\delta y_p.\delta z_p \\ +J_{C1,y,q,p}.\left(J_{P1,y,q,p} - J_{P2,y,q,p}\right)\delta x_p.\delta y_p.\delta z_p \\ +J_{C1,z,q,p}.\left(J_{P1,z,q,p} - J_{P2,z,q,p}\right)\delta x_p.\delta y_p.\delta z_p \end{pmatrix}$$

By substituting equations (5.44), (5.45) and (5.46) into equation (5.47) the following is obtained

$$\begin{aligned} \underline{\mathcal{J}}_{q,r} = \frac{1}{i_{C1}} \sum_{in\ r}^{no.cells} \quad & \left(\left(\frac{\left(\phi_{C1,q,k-1,l,m} - \phi_{C1,q,k,l,m}\right) C_{w,k,l,m}}{2\delta y_{k,l,m}\delta z_{k,l,m}}\right.\right. \\ & \left.\left. + \frac{\left(\phi_{C1,q,k,l,m} - \phi_{C1,q,k+1,l,m}\right) C_{e,k,l,m}}{2\delta y_{k,l,m}\delta z_{k,l,m}}\right) \\ & .\left(\left(\frac{\left(\phi_{P1,q,k-1,l,m} - \phi_{P1,q,k,l,m}\right) C_{w,k,l,m}}{2\delta y_{k,l,m}\delta z_{k,l,m}}\right.\right. \\ & \left.\left. + \frac{\left(\phi_{P1,q,k,l,m} - \phi_{P1,q,k+1,l,m}\right) C_{e,k,l,m}}{2\delta y_{k,l,m}\delta z_{k,l,m}}\right)\right. \\ & \left. - \left(\frac{\left(\phi_{P2,q,k-1,l,m} - \phi_{P2,q,k,l,m}\right) C_{w,k,l,m}}{2\delta y_{k,l,m}\delta z_{k,l,m}}\right.\right. \\ & \left.\left. + \frac{\left(\phi_{P2,q,k,l,m} - \phi_{P2,q,k+1,l,m}\right) C_{e,k,l,m}}{2\delta y_{k,l,m}\delta z_{k,l,m}}\right)\right) \\ & .\delta x_{k,l,m}\delta y_{k,l,m}\delta z_{k,l,m} \\ & + \left(\frac{\left(\phi_{C1,q,k,l-1,m} - \phi_{C1,q,k,l,m}\right) C_{n,k,l,m}}{2\delta x_{k,l,m}\delta z_{k,l,m}}\right. \end{aligned}$$

$$
\begin{aligned}
&+\frac{(\phi_{C1,q,k,l,m}-\phi_{C1,q,k,l+1,m})\,C_{s,k,l,m}}{2\delta x_{k,l,m}\delta z_{k,l,m}}\Bigg)\\
&\cdot\Bigg(\Bigg(\frac{(\phi_{P1,q,k,l-1,m}-\phi_{P1,q,k,l,m})\,C_{n,k,l,m}}{2\delta x_{k,l,m}\delta z_{k,l,m}}\\
&+\frac{(\phi_{P1,q,k,l,m}-\phi_{P1,q,k,l+1,m})\,C_{s,k,l,m}}{2\delta x_{k,l,m}\delta z_{k,l,m}}\Bigg)\\
&-\Bigg(\frac{(\phi_{P2,q,k,l-1,m}-\phi_{P2,q,k,l,m})\,C_{n,k,l,m}}{2\delta x_{k,l,m}\delta z_{k,l,m}}\\
&+\frac{(\phi_{P2,q,k,l,m}-\phi_{P2,q,k,l+1,m})\,C_{s,k,l,m}}{2\delta x_{k,l,m}\delta z_{k,l,m}}\Bigg)\Bigg)\\
&.\delta y_{k,l,m}\delta x_{k,l,m}\delta z_{k,l,m}\\
&\Bigg(\frac{(\phi_{C1,q,k,l,m-1}-\phi_{C1,q,k,l,m})\,C_{t,k,l,m}}{\delta x_{k,l,m}\delta y_{k,l,m}}\\
&+\frac{(\phi_{C1,q,k,l,m}-\phi_{C1,q,k,l,m+1})\,C_{b,k,l,m}}{\delta x_{k,l,m}\delta y_{k,l,m}}\Bigg)\\
&\cdot\Bigg(\Bigg(\frac{(\phi_{P1,q,k,l,m-1}-\phi_{P1,q,k,l,m})\,C_{t,k,l,m}}{\delta x_{k,l,m}\delta y_{k,l,m}}\\
&+\frac{(\phi_{P1,q,k,l,m}-\phi_{P1,q,k,l,m+1})\,C_{b,k,l,m}}{\delta x_{k,l,m}\delta y_{k,l,m}}\Bigg)\\
&-\Bigg(\frac{(\phi_{P2,q,k,l,m-1}-\phi_{P2,q,k,l,m})\,C_{t,k,l,m}}{\delta x_{k,l,m}\delta y_{k,l,m}}\\
&+\frac{(\phi_{P2,q,k,l,m}-\phi_{P2,q,k,l,m+1})\,C_{b,k,l,m}}{\delta x_{k,l,m}\delta y_{k,l,m}}\Bigg)\Bigg)\\
&.\delta z_{k,l,m}\delta x_{k,l,m}\delta y_{k,l,m}) \qquad \text{(D.1)}
\end{aligned}
$$

This can be simplified to

$$
\begin{aligned}
\underline{\mathcal{J}}_{q,r}=\frac{1}{i_{C1}}\sum_{in\ r}^{no.cells}\quad
&(((\phi_{C1,q,k-1,l,m}-\phi_{C1,q,k,l,m})\,C_{w,k,l,m}\\
&+(\phi_{C1,q,k,l,m}-\phi_{C1,q,k+1,l,m})\,C_{e,k,l,m})\\
&\cdot(((\phi_{P1,q,k-1,l,m}-\phi_{P1,q,k,l,m})\,C_{w,k,l,m}\\
&+(\phi_{P1,q,k,l,m}-\phi_{P1,q,k+1,l,m})\,C_{e,k,l,m})\\
&-((\phi_{P2,q,k-1,l,m}-\phi_{P2,q,k,l,m})\,C_{w,k,l,m}\\
&+(\phi_{P2,q,k,l,m}-\phi_{P2,q,k+1,l,m})\,C_{e,k,l,m}))\\
&\cdot\frac{\delta x_{k,l,m}}{4\delta y_{k,l,m}\delta z_{k,l,m}}\\
&+((\phi_{C1,q,k,l-1,m}-\phi_{C1,q,k,l,m})\,C_{n,k,l,m}\\
&+(\phi_{C1,q,k,l,m}-\phi_{C1,q,k,l+1,m})\,C_{s,k,l,m})\\
&\cdot(((\phi_{P1,q,k,l-1,m}-\phi_{P1,q,k,l,m})\,C_{n,k,l,m}
\end{aligned}
$$

$$
\begin{aligned}
&+\left(\phi_{P1,q,k,l,m}-\phi_{P1,q,k,l+1,m}\right)C_{s,k,l,m}\Big) \\
&-\Big(\left(\phi_{P2,q,k,l-1,m}-\phi_{P2,q,k,l,m}\right)C_{n,k,l,m} \\
&+\left(\phi_{P2,q,k,l,m}-\phi_{P2,q,k,l+1,m}\right)C_{s,k,l,m}\Big) \\
&\cdot\frac{\delta y_{k,l,m}}{4\delta x_{k,l,m}\delta z_{k,l,m}} \\
&\Big(\left(\phi_{C1,q,k,l,m-1}-\phi_{C1,q,k,l,m}\right)C_{t,k,l,m} \\
&+\left(\phi_{C1,q,k,l,m}-\phi_{C1,q,k,l,m+1}\right)C_{b,k,l,m}\Big) \\
&\cdot\Big(\Big(\left(\phi_{P1,q,k,l,m-1}-\phi_{P1,q,k,l,m}\right)C_{t,k,l,m} \\
&+\left(\phi_{P1,q,k,l,m}-\phi_{P1,q,k,l,m+1}\right)C_{b,k,l,m}\Big) \\
&-\Big(\left(\phi_{P2,q,k,l,m-1}-\phi_{P2,q,k,l,m}\right)C_{t,k,l,m} \\
&+\left(\phi_{P2,q,k,l,m}-\phi_{P2,q,k,l,m+1}\right)C_{b,k,l,m}\Big)\Big) \\
&\cdot\frac{\delta z_{k,l,m}}{4\delta x_{k,l,m}\delta y_{k,l,m}}\Bigg)
\end{aligned}
\tag{D.2}
$$

Equation (D.2) was implemented and the results of this are displayed in chapter 6 and the Jacobians shown in chapter 7. However, some explanation of the subscripts is in order, k, l, m are the indices of the nodes in the finite difference grid. They are not related to the zones but to a grid covering all the zones. The summation is over all the nodes within a zone, therefore there is no limit on the shape or size of the zone. All this information is contained within r. $C1$, $P1$ and $P2$ are the electrodes and in conjunction with q define which electrode in the electrode array, is the current source for the potentials. n, s, e, w, t and b are the direction for the conductivities and correspond to north, south, east, west, top and bottom. The whole expression is normalised by i_{C1} as the current can change between measurements, but for the example used in Chapter 6 i_{C1} is a constant.

Appendix E

Derivation of Adjoint Jacobian for Pole–Pole Surveys

This appendix is an extension of the work done in Park & Van [1991], and it will follow the derivation in section 5.3.2 and 5.4.1 also the analytical homogeneous formula will be given at the end of this appendix.

Starting from equation (5.24)

$$\underline{\mathcal{J}}_{q,r} = \frac{\partial F_q\,[\mathbf{m}]}{\partial m_r} = \frac{\delta v_{q,r}}{\delta \rho_r}$$

$\delta v_{q,r}$ is just a potential at the $P1$. Therefore equation (5.25) becomes

$$\underline{\mathcal{J}}_{q,r} = \frac{\delta \phi_{P1,q,r}}{\delta \rho_r i_{C1}} \tag{E.1}$$

Now by substituting equations (5.7) and (5.27) into equation (E.1) produces

$$\underline{\mathcal{J}}_{q,r} = \frac{\int_{\tau_r} \left(\delta \rho_r \underline{\mathbf{S}}_r \mathbf{J_{C1,q}}\right) \cdot \left(\mathbf{J'_{P1,q}}\right) d\tau_r}{\delta \rho_r i_{C1}} \tag{E.2}$$

which can be simplified to

$$\underline{\mathcal{J}}_{q,r} = \frac{1}{i_{C1}} \int_{\tau_r} \left(\underline{\mathbf{S}}_r \mathbf{J_{C1,q}}\right) \cdot \left(\mathbf{J'_{P1,q}}\right) d\tau_r \tag{E.3}$$

For the isotropic case, equation (E.3) becomes

$$\underline{\mathcal{J}}_{q,r} = \frac{1}{\mathrm{i_{C1}}} \int_{\tau_r} \left(\mathbf{J_{C1,q}}\right) \cdot \left(\mathbf{J'_{P1,q}}\right) d\tau_r \tag{E.4}$$

This can be discretised to

$$\mathcal{J}_{q,r} = \frac{1}{i_{C1}} \sum_{\tau} \mathbf{J_{q,C1}} . \mathbf{J_{q,P1}} \delta \mathbf{x} \delta \mathbf{y} \delta \mathbf{z} \tag{E.5}$$

Expanding the scalar product,

$$\underline{\mathcal{J}}_{q,r} = \frac{1}{i_{C1}} \sum_{p=1}^{no.cells} \begin{pmatrix} J_{C1,x,q,p}.J_{P1,x,q,p}\delta x_p.\delta y_p.\delta z_p \\ +J_{C1,y,q,p}.J_{P1,y,q,p}\delta x_p.\delta y_p.\delta z_p \\ +J_{C1,z,q,p}.J_{P1,z,q,p}\delta x_p.\delta y_p.\delta z_p \end{pmatrix} \tag{E.6}$$

The actual algorithm can be produced by substituting equations (5.44), (5.45) and (5.46) into equation (E.6) to obtain the pole–pole version of equation (D.1). This can be simplified to give the pole–pole equivalent to equation (D.2).

The pole–pole equivalent to equation (5.54)

$$\underline{\mathcal{J}}_{q,r} = \frac{i_{C1,q}}{4\pi^2} \int_{z_{b,r}}^{z_{e,r}} \int_{y_{b,r}}^{y_{e,r}} \int_{x_{b,r}}^{x_{e,r}}$$

$$\left(\frac{\left((x-x_{C1,q})(x-x_{P1,q})+(y-y_{C1,q})(y-y_{P1,q})+(z-z_{C1,q})(z-z_{P1,q})\right)}{\left((x-x_{C1,q})^2+(y-y_{C1,q})^2+(z-z_{C1,q})^2\right)^{\frac{3}{2}}\left((x-x_{P1,q})^2+(y-y_{P1,q})^2+(z-z_{P1,q})^2\right)^{\frac{3}{2}}} \right)$$

$$.dx.dy.dz \tag{E.7}$$

This is the equation which has to be solved to produce the analytic homogeneous case.

Appendix F

Derivation of Adjoint Jacobian for Dipole–Pole Surveys

This appendix contains the derivation of the adjoint Jacobian for dipole–pole surveys and as such will mirror the derivation in chapter 5. This will follow the derivation in section 5.3.2 and 5.4.1. The analytical homogeneous formula will be given at the end of this appendix.

Starting from equation (5.24)

$$\underline{\mathcal{J}}_{q,r} = \frac{\partial F_q\left[\mathbf{m}\right]}{\partial m_r} = \frac{\delta v_{q,r}}{\delta \rho_r}$$

$\delta v_{q,r}$ is just a potential at the $P1$. Therefore equation (5.25) becomes

$$\underline{\mathcal{J}}_{q,r} = \frac{\delta \phi_{P1,q,r}}{\delta \rho_r i_{C1}} \tag{F.1}$$

Now by substituting equations (5.12) and (5.27) into equation (F.1) produces

$$\underline{\mathcal{J}}_{q,r} = \frac{\int_{\tau_r} \left(\delta \rho_r \underline{\mathbf{S}}_r \left(\mathbf{J_{C1,q}} - \mathbf{J_{C2,q}}\right)\right) . \left(\mathbf{J'_{P1,q}}\right) d\tau_r}{\delta \rho_r i_{C1}} \tag{F.2}$$

which can be simplified to

$$\underline{\mathcal{J}}_{q,r} = \frac{1}{i_{C1}} \int_{\tau_r} \left(\underline{\mathbf{S}}_r \left(\mathbf{J_{C1,q}} - \mathbf{J_{C2,q}}\right)\right) . \left(\mathbf{J'_{P1,q}}\right) d\tau_r \tag{F.3}$$

For the isotropic case equation (F.3) becomes

$$\underline{\mathcal{J}}_{q,r} = \frac{1}{i_{C1}} \int_{\tau_r} \left(\mathbf{J_{C1,q}} - \mathbf{J_{C2,q}}\right) . \left(\mathbf{J'_{P1,q}}\right) d\tau_r \tag{F.4}$$

This can be discretised to

$$\mathcal{J}_{q,r} = \frac{1}{i_{C1}} \sum_{\tau} \left(\mathbf{J_{q,C1}} - \mathbf{J_{q,C2}}\right) . \mathbf{J_{q,P1}} \delta \mathbf{x} \delta \mathbf{y} \delta \mathbf{z} \tag{F.5}$$

Expanding the scalar products,

$$\underline{\mathcal{J}}_{q,r} = \frac{1}{i_{C1}} \sum_{p=1}^{no.cells} \begin{pmatrix} \left(J_{C1,x,q,p} - J_{C2,x,q,p}\right) . J_{P1,x,q,p} \delta x_p . \delta y_p . \delta z_p \\ + \left(J_{C1,y,q,p} - J_{C2,y,q,p}\right) . J_{P1,y,q,p} \delta x_p . \delta y_p . \delta z_p \\ + \left(J_{C1,z,q,p} - J_{C2,z,q,p}\right) . J_{P1,z,q,p} \delta x_p . \delta y_p . \delta z_p \end{pmatrix} \qquad \text{(F.6)}$$

The actual algorithm can be produced by substituting equations (5.44), (5.45) and (5.46) into equation (F.6) to obtain the dipole–pole version of equation (D.1). This can be simplified to give the dipole–pole equivalent to equation (D.2).

The dipole–pole equivalent to equation (5.54)

$$\underline{\mathcal{J}}_{q,r} = \frac{i_{C1,q}}{4\pi^2} \int_{z_{b,r}}^{z_{e,r}} \int_{y_{b,r}}^{y_{e,r}} \int_{x_{b,r}}^{x_{e,r}}$$

$$\left(\frac{\left(\left(x-x_{C1,q}\right)\left(x-x_{P1,q}\right)+\left(y-y_{C1,q}\right)\left(y-y_{P1,q}\right)+\left(z-z_{C1,q}\right)\left(z-z_{P1,q}\right)\right)}{\left(\left(x-x_{C1,q}\right)^2+\left(y-y_{C1,q}\right)^2+\left(z-z_{C1,q}\right)^2\right)^{\frac{3}{2}} \left(\left(x-x_{P1,q}\right)^2+\left(y-y_{P1,q}\right)^2+\left(z-z_{P1,q}\right)^2\right)^{\frac{3}{2}}} \right.$$

$$\left. - \frac{\left(\left(x-x_{C2,q}\right)\left(x-x_{P1,q}\right)+\left(y-y_{C2,q}\right)\left(y-y_{P1,q}\right)+\left(z-z_{C2,q}\right)\left(z-z_{P1,q}\right)\right)}{\left(\left(x-x_{C2,q}\right)^2+\left(y-y_{C2,q}\right)^2+\left(z-z_{C2,q}\right)^2\right)^{\frac{3}{2}} \left(\left(x-x_{P1,q}\right)^2+\left(y-y_{P1,q}\right)^2+\left(z-z_{P1,q}\right)^2\right)^{\frac{3}{2}}} \right)$$

$$.dx.dy.dz \qquad \text{(F.7)}$$

This is the equation which has to be solved to produce the analytic homogeneous case.

Appendix G

Derivation of Adjoint Jacobian for Dipole–Dipole Surveys

This appendix contains the derivation of the Adjoint Jacobian for dipole – dipole surveys and as such will mirror the derivation in chapter 5. This will refer follow the derivation in section 5.3.2 and 5.4.1 also the analytical homogeneous formula will be given at the end of this appendix.

Starting from equation (5.24)

$$\underline{\mathcal{J}}_{q,r} = \frac{\partial F_q\left[\mathbf{m}\right]}{\partial m_r} = \frac{\delta v_{q,r}}{\delta \rho_r}$$

$\delta v_{q,r}$ is a potential difference between electrodes $P1$ and $P2$. Therefore equation (5.25) becomes

$$\underline{\mathcal{J}}_{q,r} = \frac{\delta \phi_{P1,q,r} - \delta \phi_{P1,q,r}}{\delta \rho_r i_{C1}} \tag{G.1}$$

Now by substituting equations (5.17) and (5.27) into equation (G.1) produces

$$\underline{\mathcal{J}}_{q,r} = \frac{\int_{\tau_r} \left(\delta \rho_r \underline{\mathbf{S}}_r \left(\mathbf{J_{C1,q}} - \mathbf{J_{C2,q}}\right)\right) \cdot \left(\mathbf{J'_{P1,q}} - \mathbf{J'_{P2,q}}\right) d\tau_r}{\delta \rho_r i_{C1}} \tag{G.2}$$

which can be simplified to

$$\underline{\mathcal{J}}_{q,r} = \frac{1}{i_{C1}} \int_{\tau_r} \left(\underline{\mathbf{S}}_r \left(\mathbf{J_{C1,q}} - \mathbf{J_{C2,q}}\right)\right) \cdot \left(\mathbf{J'_{P1,q}} - \mathbf{J'_{P2,q}}\right) d\tau_r \tag{G.3}$$

For the isotropic case equation (G.3) becomes

$$\underline{\mathcal{J}}_{q,r} = \frac{1}{i_{C1}} \int_{\tau_r} \left(\mathbf{J_{C1,q}} - \mathbf{J_{C2,q}}\right) \cdot \left(\mathbf{J'_{P1,q}} - \mathbf{J'_{P2,q}}\right) d\tau_r \tag{G.4}$$

This can be discretised to

$$\mathcal{J}_{q,r} = \frac{1}{i_{C1}} \sum_{\tau} \left(\mathbf{J_{q,C1}} - \mathbf{J_{q,C2}}\right) . \left(\mathbf{J_{q,P1}} - \mathbf{J_{P2,q}}\right) \delta x \delta y \delta z \qquad \text{(G.5)}$$

Expanding out the dot product produces

$$\underline{\mathcal{J}}_{q,r} = \frac{1}{i_{C1}} \sum_{p=1}^{no.cells} \begin{pmatrix} \left(J_{C1,x,q,p} - J_{C2,x,q,p}\right) . J_{P1,x,q,p} \delta x_p . \delta y_p . \delta z_p \\ + \left(J_{C1,y,q,p} - J_{C2,y,q,p}\right) . J_{P1,y,q,p} \delta x_p . \delta y_p . \delta z_p \\ + \left(J_{C1,z,q,p} - J_{C2,z,q,p}\right) . J_{P1,z,q,p} \delta x_p . \delta y_p . \delta z_p \end{pmatrix} \qquad \text{(G.6)}$$

The actual algorithm can be produced by substituting equations (5.44), (5.45) and (5.46) into equation (G.6) to obtain the dipole–pole version of equation (D.1). This can be simplified to give the dipole–dipole equivalent to equation (D.2).

The dipole–dipole equivalent to equation (5.54)

$$\underline{\mathcal{J}}_{q,r} = \frac{i_{C1,q}}{4\pi^2} \int_{z_{b,r}}^{z_{e,r}} \int_{y_{b,r}}^{y_{e,r}} \int_{x_{b,r}}^{x_{e,r}}$$

$$\left(\frac{\left((x-x_{C1,q})(x-x_{P1,q})+(y-y_{C1,q})(y-y_{P1,q})+(z-z_{C1,q})(z-z_{P1,q})\right)}{\left((x-x_{C1,q})^2+(y-y_{C1,q})^2+(z-z_{C1,q})^2\right)^{\frac{3}{2}} \left((x-x_{P1,q})^2+(y-y_{P1,q})^2+(z-z_{P1,q})^2\right)^{\frac{3}{2}}} \right.$$

$$- \frac{\left((x-x_{C2,q})(x-x_{P1,q})+(y-y_{C2,q})(y-y_{P1,q})+(z-z_{C2,q})(z-z_{P1,q})\right)}{\left((x-x_{C2,q})^2+(y-y_{C2,q})^2+(z-z_{C2,q})^2\right)^{\frac{3}{2}} \left((x-x_{P1,q})^2+(y-y_{P1,q})^2+(z-z_{P1,q})^2\right)^{\frac{3}{2}}}$$

$$- \frac{\left((x-x_{C1,q})(x-x_{P2,q})+(y-y_{C1,q})(y-y_{P2,q})+(z-z_{C1,q})(z-z_{P2,q})\right)}{\left((x-x_{C1,q})^2+(y-y_{C1,q})^2+(z-z_{C1,q})^2\right)^{\frac{3}{2}} \left((x-x_{P2,q})^2+(y-y_{P2,q})^2+(z-z_{P2,q})^2\right)^{\frac{3}{2}}}$$

$$\left. + \frac{\left((x-x_{C2,q})(x-x_{P2,q})+(y-y_{C2,q})(y-y_{P2,q})+(z-z_{C2,q})(z-z_{P2,q})\right)}{\left((x-x_{C2,q})^2+(y-y_{C2,q})^2+(z-z_{C2,q})^2\right)^{\frac{3}{2}} \left((x-x_{P2,q})^2+(y-y_{P2,q})^2+(z-z_{P2,q})^2\right)^{\frac{3}{2}}} \right)$$

$$.dx.dy.dz \qquad \text{(G.7)}$$

This is the equation which has to be solved to produce the analytic homogeneous case. Note, this is effectively four pole – pole surveys joined together.

Appendix H

Results of Inversions

H.1 Table of the first two measurements for the homogeneous Jacobian

Meas.	Zone	Brute Force	Adjoint	Adjoint mes	Adjoint pot
1	1	-.6137E-04	-.6309E-04	-.5818E-04	-.5382E-04
1	2	.8042E-03	-.4012E-04	-.3699E-04	-.3834E-04
1	3	.7872E-02	.1328E-01	.1225E-01	.1326E-01
1	4	.2126E-03	.1969E-03	.1815E-03	.1940E-03
1	5	.1296E-04	.1014E-04	.9354E-05	.1022E-04
1	6	.3217E-05	.2060E-05	.1900E-05	.2074E-05
1	7	.1104E-05	.6324E-06	.5831E-06	.6454E-06
1	8	.4595E-06	.2430E-06	.2241E-06	.2510E-06
1	9	.2178E-06	.1086E-06	.1002E-06	.1125E-06
1	10	.1126E-06	.5407E-07	.4986E-07	.5572E-07
1	11	.6183E-07	.2902E-07	.2676E-07	.2965E-07
1	12	.3546E-07	.1639E-07	.1511E-07	.1657E-07
1	13	.2102E-07	.9512E-08	.8771E-08	.9515E-08
1	14	.1280E-07	.5521E-08	.5091E-08	.5464E-08
1	15	.7984E-08	.3061E-08	.2823E-08	.3002E-08
1	16	.1139E-07	.1586E-08	.1463E-08	.1629E-08
1	17	-.3863E-04	-.7333E-04	-.6762E-04	-.6326E-04
1	18	-.3326E-03	-.5481E-03	-.5054E-03	-.5440E-03
1	19	.5993E-02	.5715E-02	.5270E-02	.5683E-02
1	20	.1841E-03	.2087E-03	.1925E-03	.2062E-03
1	21	.1469E-04	.1695E-04	.1563E-04	.1733E-04
1	22	.2943E-05	.3637E-05	.3354E-05	.3742E-05
1	23	.8061E-06	.1162E-05	.1072E-05	.1203E-05
1	24	.2769E-06	.4584E-06	.4227E-06	.4769E-06
1	25	.1133E-06	.2082E-06	.1919E-06	.2164E-06
1	26	.5276E-07	.1046E-06	.9646E-07	.1080E-06
1	27	.2695E-07	.5651E-07	.5211E-07	.5781E-07
1	28	.1472E-07	.3205E-07	.2955E-07	.3243E-07
1	29	.8458E-08	.1866E-07	.1721E-07	.1868E-07
1	30	.5054E-08	.1085E-07	.1001E-07	.1075E-07
1	31	.3120E-08	.6023E-08	.5554E-08	.5911E-08
1	32	.1208E-08	.3094E-08	.2853E-08	.3180E-08

Meas.	Zone	Brute Force	Adjoint	Adjoint mes	Adjoint pot
1	33	-.2216E-04	-.4901E-04	-.4519E-04	-.4211E-04
1	34	-.1614E-03	-.1729E-03	-.1594E-03	-.1680E-03
1	35	.9888E-03	.9906E-03	.9134E-03	.9676E-03
1	36	.8694E-04	.1059E-03	.9766E-04	.1048E-03
1	37	.8283E-05	.1340E-04	.1235E-04	.1386E-04
1	38	.1851E-05	.3219E-05	.2968E-05	.3368E-05
1	39	.5947E-06	.1081E-05	.9969E-06	.1131E-05
1	40	.2272E-06	.4376E-06	.4035E-06	.4578E-06
1	41	.9903E-07	.2016E-06	.1859E-06	.2102E-06
1	42	.4783E-07	.1022E-06	.9423E-07	.1057E-06
1	43	.2499E-07	.5550E-07	.5118E-07	.5683E-07
1	44	.1386E-07	.3159E-07	.2913E-07	.3199E-07
1	45	.8045E-08	.1843E-07	.1700E-07	.1846E-07
1	46	.4841E-08	.1073E-07	.9899E-08	.1063E-07
1	47	.3004E-08	.5956E-08	.5493E-08	.5847E-08
1	48	.1167E-08	.3013E-08	.2778E-08	.3100E-08
1	49	-.4401E-04	-.2467E-04	-.2275E-04	-.2155E-04
1	50	-.5147E-04	-.4831E-04	-.4455E-04	-.4540E-04
1	51	.2304E-03	.2097E-03	.1934E-03	.2009E-03
1	52	.5662E-04	.5010E-04	.4620E-04	.5185E-04
1	53	.1342E-04	.9773E-05	.9012E-05	.1055E-04
1	54	.4526E-05	.2795E-05	.2577E-05	.3012E-05
1	55	.1805E-05	.1008E-05	.9299E-06	.1071E-05
1	56	.8114E-06	.4218E-06	.3890E-06	.4443E-06
1	57	.4004E-06	.1976E-06	.1822E-06	.2065E-06
1	58	.2118E-06	.1010E-06	.9316E-07	.1046E-06
1	59	.1179E-06	.5515E-07	.5086E-07	.5648E-07
1	60	.6823E-07	.3150E-07	.2905E-07	.3189E-07
1	61	.4069E-07	.1843E-07	.1699E-07	.1845E-07
1	62	.2489E-07	.1075E-07	.9916E-08	.1065E-07
1	63	.1557E-07	.5977E-08	.5511E-08	.5865E-08
1	64	.2228E-07	.3033E-08	.2797E-08	.3121E-08

Meas.	Zone	Brute Force	Adjoint	Adjoint mes	Adjoint pot
1	65	-.5582E-05	-.1440E-04	-.1328E-04	-.1442E-04
1	66	-.3680E-05	-.1489E-04	-.1373E-04	-.1425E-04
1	67	.5331E-04	.6162E-04	.5682E-04	.5857E-04
1	68	.1775E-04	.2512E-04	.2316E-04	.2702E-04
1	69	.5896E-05	.6954E-05	.6412E-05	.7578E-05
1	70	.1902E-05	.2273E-05	.2096E-05	.2452E-05
1	71	.6434E-06	.8723E-06	.8044E-06	.9297E-06
1	72	.2445E-06	.3792E-06	.3496E-06	.4009E-06
1	73	.1051E-06	.1823E-06	.1681E-06	.1911E-06
1	74	.5020E-07	.9496E-07	.8756E-07	.9852E-07
1	75	.2600E-07	.5254E-07	.4845E-07	.5388E-07
1	76	.1432E-07	.3032E-07	.2796E-07	.3072E-07
1	77	.8270E-08	.1788E-07	.1649E-07	.1792E-07
1	78	.4957E-08	.1051E-07	.9690E-08	.1042E-07
1	79	.3066E-08	.5881E-08	.5423E-08	.5778E-08
1	80	.1201E-08	.3033E-08	.2797E-08	.3138E-08
1	81	-.5035E-05	-.1117E-04	-.1030E-04	-.1146E-04
1	82	-.8229E-05	-.6651E-05	-.6133E-05	-.6060E-05
1	83	.2182E-04	.2699E-04	.2489E-04	.2468E-04
1	84	.1138E-04	.1448E-04	.1335E-04	.1594E-04
1	85	.2974E-05	.5033E-05	.4641E-05	.5453E-05
1	86	.9287E-06	.1836E-05	.1693E-05	.1976E-05
1	87	.3580E-06	.7496E-06	.6912E-06	.8020E-06
1	88	.1571E-06	.3395E-06	.3131E-06	.3606E-06
1	89	.7548E-07	.1679E-06	.1548E-06	.1767E-06
1	90	.3896E-07	.8912E-07	.8218E-07	.9272E-07
1	91	.2128E-07	.4997E-07	.4608E-07	.5134E-07
1	92	.1217E-07	.2910E-07	.2683E-07	.2953E-07
1	93	.7212E-08	.1727E-07	.1592E-07	.1732E-07
1	94	.4404E-08	.1018E-07	.9389E-08	.1010E-07
1	95	.2761E-08	.5695E-08	.5252E-08	.5599E-08
1	96	.1090E-08	.2801E-08	.2583E-08	.2907E-08

Meas.	Zone	Brute Force	Adjoint	Adjoint mes	Adjoint pot
1	97	-.2374E-04	-.2151E-04	-.1983E-04	-.2235E-04
1	98	-.8022E-05	-.9307E-05	-.8582E-05	-.7502E-05
1	99	.2572E-04	.2365E-04	.2181E-04	.1989E-04
1	100	.2221E-04	.2061E-04	.1901E-04	.2187E-04
1	101	.1198E-04	.1123E-04	.1036E-04	.1218E-04
1	102	.6187E-05	.5689E-05	.5246E-05	.6216E-05
1	103	.3243E-05	.2934E-05	.2706E-05	.3204E-05
1	104	.1754E-05	.1574E-05	.1451E-05	.1705E-05
1	105	.9824E-06	.8815E-06	.8129E-06	.9427E-06
1	106	.5672E-06	.5137E-06	.4737E-06	.5409E-06
1	107	.3361E-06	.3093E-06	.2852E-06	.3206E-06
1	108	.2035E-06	.1907E-06	.1759E-06	.1946E-06
1	109	.1255E-06	.1188E-06	.1096E-06	.1196E-06
1	110	.7866E-07	.7323E-07	.6752E-07	.7279E-07
1	111	.5011E-07	.4272E-07	.3940E-07	.4209E-07
1	112	.6041E-07	.2246E-07	.2071E-07	.2383E-07
2	1	-.1139E-04	-.8491E-05	-.7829E-05	-.7650E-05
2	2	-.3923E-04	-.3818E-04	-.3520E-04	-.3617E-04
2	3	.8047E-03	-.4220E-04	-.3891E-04	-.4041E-04
2	4	.7871E-02	.1328E-01	.1225E-01	.1326E-01
2	5	.2126E-03	.1966E-03	.1813E-03	.1937E-03
2	6	.1294E-04	.1013E-04	.9344E-05	.1021E-04
2	7	.3206E-05	.2058E-05	.1898E-05	.2071E-05
2	8	.1099E-05	.6312E-06	.5820E-06	.6438E-06
2	9	.4572E-06	.2419E-06	.2230E-06	.2496E-06
2	10	.2166E-06	.1076E-06	.9920E-07	.1113E-06
2	11	.1120E-06	.5304E-07	.4890E-07	.5461E-07
2	12	.6154E-07	.2800E-07	.2582E-07	.2857E-07
2	13	.3532E-07	.1535E-07	.1415E-07	.1549E-07
2	14	.2098E-07	.8434E-08	.7776E-08	.8418E-08
2	15	.1283E-07	.4382E-08	.4041E-08	.4333E-08

Meas.	Zone	Brute Force	Adjoint	Adjoint mes	Adjoint pot
2	16	.1787E-07	.1466E-08	.1352E-08	.1608E-08
2	17	-.5372E-05	-.1235E-04	-.1139E-04	-.1191E-04
2	18	-.4449E-04	-.5613E-04	-.5175E-04	-.5375E-04
2	19	-.3338E-03	-.5358E-03	-.4941E-03	-.5318E-03
2	20	.5993E-02	.5714E-02	.5268E-02	.5682E-02
2	21	.1849E-03	.2083E-03	.1921E-03	.2058E-03
2	22	.1470E-04	.1694E-04	.1562E-04	.1731E-04
2	23	.2937E-05	.3634E-05	.3351E-05	.3737E-05
2	24	.8034E-06	.1160E-05	.1070E-05	.1200E-05
2	25	.2757E-06	.4563E-06	.4207E-06	.4743E-06
2	26	.1128E-06	.2061E-06	.1900E-06	.2140E-06
2	27	.5252E-07	.1026E-06	.9459E-07	.1058E-06
2	28	.2683E-07	.5450E-07	.5025E-07	.5567E-07
2	29	.1468E-07	.3000E-07	.2766E-07	.3031E-07
2	30	.8458E-08	.1653E-07	.1524E-07	.1651E-07
2	31	.5080E-08	.8596E-08	.7925E-08	.8505E-08
2	32	.1940E-08	.2813E-08	.2594E-08	.3096E-08
2	33	-.3260E-05	-.1002E-04	-.9240E-05	-.1012E-04
2	34	-.2554E-04	-.3497E-04	-.3224E-04	-.3345E-04
2	35	-.1598E-03	-.1724E-03	-.1589E-03	-.1675E-03
2	36	.9882E-03	.9896E-03	.9124E-03	.9667E-03
2	37	.8671E-04	.1057E-03	.9745E-04	.1046E-03
2	38	.8265E-05	.1338E-04	.1234E-04	.1384E-04
2	39	.1845E-05	.3217E-05	.2966E-05	.3364E-05
2	40	.5923E-06	.1079E-05	.9949E-06	.1128E-05
2	41	.2262E-06	.4356E-06	.4016E-06	.4553E-06
2	42	.9856E-07	.1996E-06	.1841E-06	.2079E-06
2	43	.4761E-07	.1002E-06	.9240E-07	.1036E-06
2	44	.2489E-07	.5351E-07	.4934E-07	.5472E-07
2	45	.1382E-07	.2955E-07	.2725E-07	.2988E-07
2	46	.8044E-08	.1631E-07	.1504E-07	.1630E-07
2	47	.4866E-08	.8482E-08	.7821E-08	.8395E-08
2	48	.1866E-08	.2688E-08	.2478E-08	.2971E-08

Meas.	Zone	Brute Force	Adjoint	Adjoint mes	Adjoint pot
2	49	-.1469E-04	-.7642E-05	-.7046E-05	-.8352E-05
2	50	-.2233E-04	-.1982E-04	-.1827E-04	-.1984E-04
2	51	-.5271E-04	-.4738E-04	-.4368E-04	-.4446E-04
2	52	.2298E-03	.2091E-03	.1928E-03	.2003E-03
2	53	.5648E-04	.4999E-04	.4609E-04	.5173E-04
2	54	.1337E-04	.9764E-05	.9003E-05	.1054E-04
2	55	.4506E-05	.2793E-05	.2576E-05	.3009E-05
2	56	.1797E-05	.1007E-05	.9282E-06	.1068E-05
2	57	.8073E-06	.4200E-06	.3873E-06	.4420E-06
2	58	.3983E-06	.1957E-06	.1805E-06	.2044E-06
2	59	.2107E-06	.9914E-07	.9141E-07	.1025E-06
2	60	.1173E-06	.5324E-07	.4909E-07	.5445E-07
2	61	.6796E-07	.2951E-07	.2721E-07	.2983E-07
2	62	.4061E-07	.1634E-07	.1507E-07	.1632E-07
2	63	.2493E-07	.8524E-08	.7859E-08	.8434E-08
2	64	.3487E-07	.2757E-08	.2542E-08	.3041E-08
2	65	-.2579E-05	-.5552E-05	-.5119E-05	-.6169E-05
2	66	-.7687E-05	-.1178E-04	-.1086E-04	-.1219E-04
2	67	-.5026E-05	-.1594E-04	-.1470E-04	-.1531E-04
2	68	.5341E-04	.6123E-04	.5646E-04	.5818E-04
2	69	.1784E-04	.2506E-04	.2311E-04	.2696E-04
2	70	.5892E-05	.6950E-05	.6408E-05	.7571E-05
2	71	.1897E-05	.2272E-05	.2095E-05	.2450E-05
2	72	.6409E-06	.8711E-06	.8032E-06	.9277E-06
2	73	.2434E-06	.3777E-06	.3482E-06	.3990E-06
2	74	.1046E-06	.1807E-06	.1666E-06	.1893E-06
2	75	.4996E-07	.9328E-07	.8600E-07	.9667E-07
2	76	.2589E-07	.5079E-07	.4683E-07	.5201E-07
2	77	.1428E-07	.2846E-07	.2624E-07	.2880E-07
2	78	.8267E-08	.1590E-07	.1466E-07	.1590E-07
2	79	.4980E-08	.8373E-08	.7721E-08	.8296E-08
2	80	.1927E-08	.2812E-08	.2592E-08	.3118E-08

Meas.	Zone	Brute Force	Adjoint	Adjoint mes	Adjoint pot
2	81	-.1368E-05	-.4452E-05	-.4105E-05	-.4864E-05
2	82	-.5167E-05	-.6925E-05	-.6385E-05	-.7278E-05
2	83	-.8286E-05	-.8556E-05	-.7889E-05	-.7962E-05
2	84	.2181E-04	.2680E-04	.2471E-04	.2449E-04
2	85	.1134E-04	.1446E-04	.1333E-04	.1591E-04
2	86	.2961E-05	.5031E-05	.4639E-05	.5450E-05
2	87	.9244E-06	.1835E-05	.1692E-05	.1975E-05
2	88	.3562E-06	.7487E-06	.6903E-06	.8003E-06
2	89	.1563E-06	.3382E-06	.3118E-06	.3589E-06
2	90	.7509E-07	.1664E-06	.1534E-06	.1749E-06
2	91	.3876E-07	.8753E-07	.8070E-07	.9095E-07
2	92	.2119E-07	.4827E-07	.4451E-07	.4953E-07
2	93	.1213E-07	.2729E-07	.2516E-07	.2764E-07
2	94	.7209E-08	.1532E-07	.1412E-07	.1533E-07
2	95	.4424E-08	.8061E-08	.7432E-08	.7992E-08
2	96	.1730E-08	.2452E-08	.2261E-08	.2758E-08
2	97	-.1340E-04	-.1203E-04	-.1109E-04	-.1297E-04
2	98	-.1180E-04	-.1194E-04	-.1101E-04	-.1233E-04
2	99	-.8552E-05	-.9426E-05	-.8691E-05	-.7626E-05
2	100	.2548E-04	.2361E-04	.2177E-04	.1983E-04
2	101	.2206E-04	.2062E-04	.1901E-04	.2187E-04
2	102	.1190E-04	.1124E-04	.1037E-04	.1218E-04
2	103	.6147E-05	.5697E-05	.5253E-05	.6220E-05
2	104	.3222E-05	.2937E-05	.2708E-05	.3204E-05
2	105	.1743E-05	.1573E-05	.1451E-05	.1702E-05
2	106	.9763E-06	.8783E-06	.8098E-06	.9379E-06
2	107	.5638E-06	.5085E-06	.4688E-06	.5347E-06
2	108	.3342E-06	.3024E-06	.2788E-06	.3129E-06
2	109	.2025E-06	.1821E-06	.1679E-06	.1855E-06
2	110	.1251E-06	.1083E-06	.9981E-07	.1087E-06
2	111	.7868E-07	.6033E-07	.5562E-07	.6003E-07
2	112	.9336E-07	.2236E-07	.2062E-07	.2549E-07

H.2 Test model

Table H.1: These are the resistivities of the test model.

89.22	446.10	446.10	446.10	446.10	446.10	446.10	446.10	446.10	446.10	446.10	446.10	446.10	446.10	446.10	446.10
446.10	892.20	892.20	892.20	892.20	892.20	892.20	892.20	892.20	44.61	44.61	44.61	44.61	44.61	44.61	44.61
89.22	44.61	44.61	44.61	44.61	44.61	44.61	44.61	44.61	44.61	44.61	44.61	44.61	44.61	44.61	89.22
89.22	892.20	892.20	892.20	892.20	892.20	892.20	892.20	892.20	8.92	8.92	8.92	8.92	8.92	8.92	89.22
89.22	892.20	892.20	892.20	892.20	892.20	892.20	892.20	892.20	.89	.89	.89	.89	.89	.89	89.22
89.22	892.20	892.20	892.20	892.20	892.20	892.20	892.20	892.20	.89	.89	.89	.89	.89	.89	89.22
89.22	892.20	892.20	892.20	892.20	892.20	892.20	892.20	892.20	892.20	892.20	892.20	892.20	892.20	892.20	89.22

Table H.2: These are the resistivities of the homogeneous starting point used.

89.22	89.22	89.22	89.22	89.22	89.22	89.22	89.22	89.22	89.22	89.22	89.22	89.22	89.22	89.22	89.22
89.22	89.22	89.22	89.22	89.22	89.22	89.22	89.22	89.22	89.22	89.22	89.22	89.22	89.22	89.22	89.22
89.22	89.22	89.22	89.22	89.22	89.22	89.22	89.22	89.22	89.22	89.22	89.22	89.22	89.22	89.22	89.22
89.22	89.22	89.22	89.22	89.22	89.22	89.22	89.22	89.22	89.22	89.22	89.22	89.22	89.22	89.22	89.22
89.22	89.22	89.22	89.22	89.22	89.22	89.22	89.22	89.22	89.22	89.22	89.22	89.22	89.22	89.22	89.22
89.22	89.22	89.22	89.22	89.22	89.22	89.22	89.22	89.22	89.22	89.22	89.22	89.22	89.22	89.22	89.22
89.22	89.22	89.22	89.22	89.22	89.22	89.22	89.22	89.22	89.22	89.22	89.22	89.22	89.22	89.22	89.22

H.3 Results of perturbation method

Table H.3: These are the resistivities after the first iteration using the perturbation method Jacobian.

1784.4	1784.4	1784.4	1784.4	1784.4	1784.4	1784.4	1784.4	1784.4	942.76	608.53	639.49	680.08	642.36	516.01	269.26
1784.4	1784.4	1784.4	1784.4	1784.4	1784.4	1784.4	1784.4	949.62	112.69	64.25	64.46	68.20	77.70	96.65	92.30
1202.9	1614.1	1784.4	1784.4	1784.4	1784.4	1784.4	810.26	111.00	19.53	16.19	16.39	13.12	13.26	18.25	26.12
284.74	337.26	544.34	885.90	1081.73	805.11	358.81	98.95	20.89	9.36	14.19	18.18	13.63	10.88	11.69	15.52
88.17	97.07	147.58	228.62	255.33	167.63	68.01	21.93	8.90	8.76	18.80	31.14	28.75	21.77	18.55	19.52
40.26	42.11	60.10	86.20	87.76	53.49	21.83	8.56	5.44	9.00	29.11	66.27	72.28	53.41	38.78	33.21
30.64	31.42	41.92	55.23	52.61	31.54	13.64	6.25	5.04	10.19	36.58	93.54	114.71	88.33	61.40	47.74

Table H.4: These are the resistivities after the 2nd iteration using the perturbation method Jacobian.

846.52	922.52	912.54	896.19	891.79	885.38	901.07	916.42	844.03	408.72	326.27	364.48	373.25	349.77	283.47	214.53
759.38	867.27	909.37	897.17	892.23	897.23	933.39	902.17	629.82	179.92	111.48	109.27	111.63	122.75	133.84	127.15
571.20	602.31	662.59	741.64	797.92	799.22	727.91	515.58	231.48	65.23	33.41	28.86	29.98	36.68	47.30	53.54
423.47	432.26	477.90	550.09	590.84	544.39	405.29	220.34	82.65	25.77	13.09	11.19	11.83	14.59	19.33	23.32
334.32	337.15	363.38	396.39	395.94	329.26	212.89	102.55	38.42	14.04	7.60	6.33	6.63	8.03	10.31	12.40
286.19	284.79	296.28	304.07	281.53	215.74	129.58	60.86	24.38	10.27	5.95	4.90	5.03	5.90	7.24	8.48
270.00	266.51	269.48	264.41	233.01	171.46	101.14	48.63	21.02	9.79	5.94	4.83	4.83	5.46	6.44	7.32

Table H.5: These are the resistivities after the 3rd iteration using the perturbation method Jacobian.

552.91	633.25	627.54	616.69	627.37	621.01	611.09	616.90	636.36	359.88	335.91	351.35	345.76	334.92	285.35	201.88
477.78	576.01	610.55	595.79	578.15	575.04	604.22	635.42	519.24	107.28	79.66	87.83	87.30	93.99	107.83	103.90
336.91	381.66	440.02	475.27	490.84	508.42	523.97	448.45	214.89	40.79	22.38	22.98	23.61	26.04	32.46	37.98
227.37	247.68	303.15	368.05	416.84	437.37	402.95	270.55	103.96	25.24	12.32	10.93	10.85	11.50	13.57	16.11
170.98	184.50	231.72	298.79	357.33	369.95	306.44	179.51	68.90	21.52	10.37	7.99	7.36	7.37	8.04	9.12
144.93	156.34	199.80	266.25	323.57	325.81	251.81	140.12	57.21	21.36	10.67	7.59	6.50	6.13	6.26	6.75
140.41	151.66	192.08	253.19	302.67	296.30	222.06	123.80	54.31	22.78	11.84	8.11	6.65	6.04	5.93	6.16

Table H.6: These are the resistivities after the 4th iteration using the perturbation method Jacobian.

462.68	569.92	557.50	557.48	589.68	589.27	550.81	528.38	554.38	358.63	379.33	391.18	389.70	382.82	337.04	220.18
391.51	539.14	574.23	545.87	510.20	494.47	523.28	600.68	610.11	90.67	71.44	75.23	73.45	76.79	92.56	96.59
253.74	310.46	374.07	393.77	390.33	409.91	470.14	475.24	244.33	31.34	18.65	20.63	20.71	21.36	26.63	34.04
161.94	186.65	250.82	314.05	356.94	394.89	412.58	310.39	109.83	18.98	10.54	11.58	12.10	12.17	13.80	16.87
126.89	146.80	210.15	294.83	371.23	410.07	367.92	220.28	73.13	17.87	9.64	9.60	10.21	10.36	10.93	12.18
116.42	137.91	210.70	325.93	430.76	453.94	354.05	182.78	61.49	19.12	10.75	10.06	10.53	10.65	10.75	11.16
120.67	144.98	223.48	350.95	461.45	464.03	335.34	165.59	59.53	21.62	12.51	11.11	11.29	11.33	11.23	11.23

Table H.7: These are the resistivities after the 5th iteration using the perturbation method Jacobian.

346.23	526.11	514.48	520.26	557.10	611.71	583.98	514.16	480.86	397.06	418.00	427.23	415.90	409.84	386.84	225.98
301.22	622.01	644.55	627.23	583.94	493.16	498.90	585.20	734.31	72.33	61.46	60.38	65.23	67.06	77.29	82.84
176.41	272.44	314.61	293.57	288.26	290.99	371.00	473.32	283.51	28.76	21.39	21.56	19.42	18.69	20.95	27.85
107.45	143.53	200.97	217.78	235.91	272.07	351.40	355.88	131.79	18.66	13.93	14.55	12.75	12.22	12.82	15.93
102.97	138.69	223.87	286.02	340.01	390.68	409.71	293.67	90.67	17.11	10.43	10.50	11.00	12.10	13.04	14.69
122.72	179.62	361.13	602.57	755.85	749.36	564.01	258.35	61.36	13.65	8.59	9.55	11.52	13.98	15.89	16.93
152.57	235.29	518.05	969.21	1224.6	1073.1	644.78	234.06	51.74	12.85	8.21	9.40	12.14	15.61	18.34	18.94

Table H.8: These are the resistivities after the 6th iteration using the perturbation method Jacobian.

278.66	522.25	508.78	497.91	521.88	587.03	586.61	503.95	461.24	400.61	428.55	441.15	424.65	416.26	398.27	212.95
239.72	635.82	665.79	688.24	653.32	533.82	523.57	607.76	777.47	68.20	55.35	52.55	60.07	63.07	70.87	72.96
143.17	255.50	270.63	234.93	246.68	253.90	300.22	411.64	263.27	28.96	23.60	24.26	20.92	20.18	20.14	25.39
96.50	150.75	197.82	177.77	190.20	219.30	277.49	335.52	129.49	18.68	16.38	16.91	14.49	14.07	13.27	15.74
112.57	172.31	262.74	269.96	310.04	375.20	425.40	362.09	102.88	15.73	9.91	9.45	10.08	12.29	13.66	15.48
153.69	255.90	543.18	807.78	984.91	1057.1	901.44	437.60	77.00	11.58	6.78	7.13	8.82	12.40	16.31	18.56
203.88	359.23	897.89	1642.8	1784.4	1784.4	1306.5	461.37	69.33	10.74	5.98	6.46	8.59	13.05	18.63	21.00

Table H.9: These are the resistivities after the 7th iteration using the perturbation method Jacobian.

165.80	482.45	472.89	468.66	475.82	499.75	512.85	474.95	452.08	431.33	448.52	455.46	436.69	424.40	409.80	159.96
147.05	739.10	775.40	788.84	767.62	698.66	706.40	736.44	806.91	52.52	45.67	44.08	53.02	59.22	69.09	47.52
84.73	211.70	172.16	158.19	179.10	200.74	186.61	220.57	230.16	40.21	31.25	34.55	26.78	22.91	15.83	15.83
66.33	140.12	156.82	140.06	140.15	139.06	129.43	213.31	159.60	23.15	22.39	18.95	15.27	13.69	10.03	11.73
122.49	234.97	325.12	301.41	324.44	349.14	370.23	521.95	187.54	11.65	5.65	4.34	5.69	10.31	14.90	19.83
253.12	546.46	1318.3	1784.4	1784.4	1784.4	1784.4	1561.7	131.59	5.01	2.78	3.59	5.97	13.81	32.35	47.68
421.96	999.48	1784.4	1784.4	1784.4	1784.4	1784.4	1784.4	131.29	4.61	2.71	4.46	8.40	21.30	58.23	81.40

Table H.10: These are the resistivities after the 8th iteration using the perturbation method Jacobian.

155.40	479.32	469.11	463.25	466.35	474.94	469.55	452.49	440.05	433.27	456.81	456.46	451.87	441.08	423.38	127.61
144.15	746.71	794.11	816.78	810.66	786.01	813.66	855.35	846.12	47.66	39.18	40.90	42.91	49.35	62.21	37.17
83.10	203.17	134.06	117.39	122.72	131.02	122.67	113.75	199.25	58.29	48.94	48.68	45.28	35.22	17.60	17.41
67.65	154.71	152.76	145.23	133.75	121.00	103.27	110.68	112.41	9.47	12.90	11.61	13.09	13.92	12.10	19.41
140.79	280.25	396.31	476.92	578.93	680.57	747.38	695.26	199.08	4.27	1.52	.92	1.43	4.20	16.69	42.77
325.15	718.22	1784.4	1784.4	1784.4	1784.4	1784.4	1784.4	575.15	9.67	2.79	2.04	2.82	8.14	53.12	160.41
575.71	1399.3	1784.4	1784.4	1784.4	1784.4	1784.4	1784.4	1627.0	32.02	10.29	8.79	10.54	24.91	146.65	364.92

Table H.11: These are the resistivities after the 9th iteration using the perturbation method Jacobian.

138.64	458.54	454.85	453.10	450.76	444.42	449.36	461.60	441.65	442.44	451.56	448.29	445.97	444.05	436.20	191.75
132.91	820.98	848.97	859.34	873.63	895.42	863.86	837.41	908.80	47.94	41.70	42.87	43.44	44.67	53.05	63.75
65.64	149.84	93.66	84.91	72.62	64.91	84.65	88.38	61.80	37.54	50.61	55.00	56.43	56.40	29.42	56.18
59.76	139.62	141.32	143.15	155.57	149.73	143.41	155.56	360.05	16.94	5.31	3.92	3.56	3.89	10.79	76.27
72.94	373.42	625.46	874.66	1122.4	1088.7	863.55	697.80	464.93	5.06	.34	.27	.35	.69	9.23	116.27
43.82	1348.3	1784.4	1784.4	1784.4	1784.4	1784.4	1784.4	848.46	31.73	6.69	5.63	7.38	17.73	164.26	915.71
1120.4	1784.4	1784.4	1784.4	1784.4	1784.4	1784.4	1784.4	1784.4	323.08	241.93	250.50	273.68	511.59	1784.4	1784.4

Table H.12: These are the resistivities after the 10th iteration using the perturbation method Jacobian.

138.27	460.90	455.98	452.93	453.61	456.52	455.53	457.77	439.30	437.43	446.37	445.01	443.54	440.98	430.83	333.22
133.84	812.45	845.69	858.91	857.68	847.70	849.09	850.24	879.02	50.81	44.47	44.90	45.48	47.45	56.12	113.63
68.02	148.34	87.07	78.70	79.59	83.34	84.27	77.47	98.44	37.27	45.35	47.25	46.90	42.68	23.89	68.20
64.46	140.25	162.55	175.08	164.47	166.40	162.06	174.94	173.04	6.60	5.47	5.66	5.33	5.79	10.48	78.92
196.64	388.57	705.69	1048.3	1217.6	1242.1	1120.3	921.21	413.48	9.39	2.35	1.65	1.66	2.55	8.58	58.88
678.06	1466.1	1784.4	1784.4	1784.4	1784.4	1784.4	1784.4	1784.4	144.82	36.07	20.59	18.96	26.89	64.45	165.44
1447.5	1784.4	1784.4	1784.4	1784.4	1784.4	1784.4	1784.4	1784.4	1021.1	414.04	251.07	208.87	229.30	330.68	400.97

Table H.13: These are the resistivities after the 11th iteration using the perturbation method Jacobian.

128.89	456.41	454.77	452.17	451.55	451.40	451.19	453.20	441.93	442.75	447.20	446.80	444.11	440.07	434.19	249.75
127.69	832.57	850.98	861.79	865.54	865.88	865.23	865.56	887.71	48.10	43.80	43.95	45.22	48.04	54.09	77.38
61.48	129.56	83.47	77.68	74.70	73.38	74.33	64.45	66.88	37.60	48.91	48.36	47.97	42.66	25.69	49.03
62.74	146.64	166.45	174.05	167.91	163.43	178.71	252.72	342.01	7.56	3.47	4.05	3.45	3.50	8.75	49.28
209.86	430.56	755.08	1065.0	1199.2	1156.4	1038.3	875.70	398.30	6.59	1.30	1.22	1.33	2.54	14.85	84.14
742.05	1608.2	1784.4	1784.4	1784.4	1784.4	1784.4	1784.4	867.69	70.81	20.90	17.87	19.57	40.52	183.02	494.26
1562.3	1784.4	1784.4	1784.4	1784.4	1784.4	1784.4	1784.4	1706.6	460.84	280.31	267.47	249.20	395.62	1114.1	1604.3

Table H.14: These are the resistivities after the 12th iteration using the perturbation method Jacobian.

117.94	450.32	452.03	449.95	449.90	449.51	448.00	449.53	444.27	443.74	446.74	447.10	446.41	444.53	443.72	296.65
124.09	866.48	864.13	871.04	872.85	873.70	876.86	878.19	892.04	46.65	43.99	43.73	44.04	45.32	47.05	72.89
51.22	90.35	72.63	70.59	68.15	68.52	69.06	55.71	53.02	41.91	48.84	49.09	49.24	47.20	39.60	76.25
60.38	196.93	188.09	187.84	191.53	188.20	174.78	328.86	487.89	6.27	3.11	3.44	3.29	2.91	7.63	74.21
234.80	599.52	916.51	1141.1	1243.0	1256.8	1240.0	1524.3	680.51	3.72	1.15	1.09	1.10	1.55	8.41	61.44
746.43	1753.9	1784.4	1784.4	1784.4	1784.4	1784.4	1784.4	1742.6	66.48	26.14	23.22	20.48	25.28	75.87	198.55
1365.1	1784.4	1784.4	1784.4	1784.4	1784.4	1784.4	1784.4	1784.4	523.12	537.29	590.42	385.07	276.74	407.86	505.86

Table H.15: These are the resistivities after the 13th iteration using the perturbation method Jacobian.

110.91	450.20	451.49	449.52	449.53	448.83	447.44	449.07	444.53	444.09	446.96	447.25	446.52	444.84	444.01	276.17
132.31	866.52	866.75	872.94	874.51	876.53	879.70	879.80	891.78	46.48	43.91	43.72	44.03	45.10	46.59	58.44
59.26	86.96	69.07	68.43	66.38	66.36	65.78	54.15	52.38	41.29	48.47	48.28	48.67	47.21	38.94	59.40
61.00	219.55	208.95	201.35	204.50	201.90	184.52	373.25	503.27	7.71	4.21	4.91	4.52	3.15	7.04	51.46
225.08	632.81	986.44	1176.7	1266.5	1402.9	1598.6	1784.4	722.86	2.43	.83	.85	.83	1.24	8.08	58.24
640.68	1605.2	1784.4	1784.4	1784.4	1784.4	1784.4	1784.4	1784.4	65.85	18.77	13.22	13.72	25.94	116.08	322.96
1075.0	1784.4	1784.4	1784.4	1784.4	1784.4	1784.4	1784.4	1784.4	625.96	528.37	473.06	388.68	437.65	916.05	1147.0

Table H.16: These are the resistivities after the 14th iteration using the perturbation method Jacobian.

97.41	448.20	449.30	448.12	448.20	447.82	446.55	448.13	445.75	444.56	446.22	446.58	446.53	446.35	446.17	249.57
183.28	880.41	876.83	879.76	880.01	881.63	884.12	883.30	891.65	46.08	44.44	44.24	44.27	44.27	45.06	58.33
117.20	66.56	60.87	62.05	61.78	61.42	61.76	52.12	48.40	41.39	46.00	45.84	45.87	47.33	42.37	77.85
56.80	309.14	253.40	235.63	230.87	228.96	199.90	379.37	615.90	9.83	8.48	8.38	10.77	6.15	8.15	105.77
187.08	885.43	1232.8	1285.3	1291.2	1784.4	1784.4	1784.4	859.86	1.23	.60	.74	.53	.57	2.58	58.53
346.59	1194.3	1784.4	1784.4	1784.4	1784.4	1784.4	1784.4	1784.4	54.37	9.64	3.94	3.10	5.84	28.03	146.90
423.13	1226.6	1784.4	1784.4	1784.4	1784.4	1784.4	1784.4	1784.4	445.38	738.00	429.53	194.36	171.06	302.72	412.71

Table H.17: These are the resistivities after the 15th iteration using the perturbation method Jacobian.

88.86	448.24	448.82	448.04	448.10	447.89	446.73	447.99	445.47	444.30	445.21	446.01	445.41	445.72	445.80	293.28
246.76	880.33	878.64	880.29	880.35	881.61	884.07	883.81	892.50	46.11	45.23	44.72	45.18	44.87	45.48	49.49
172.14	63.75	59.71	61.19	60.96	60.05	60.58	51.72	48.36	42.03	42.90	43.70	42.50	44.11	38.99	91.87
69.96	304.81	261.57	247.83	251.48	258.37	218.59	402.02	621.52	8.38	10.91	9.63	11.94	9.37	17.20	114.61
148.62	825.51	1718.9	1211.3	1186.3	1721.3	1784.4	1784.4	611.15	1.49	.59	.86	.59	.68	1.65	46.24
172.25	1000.8	1784.4	1784.4	1784.4	1784.4	1784.4	1784.4	1784.4	55.81	4.02	2.46	4.11	5.16	12.38	67.95
177.67	989.21	1784.4	1784.4	1784.4	1784.4	1784.4	1784.4	1784.4	446.67	737.52	791.13	452.88	186.14	169.43	173.87

Table H.18: These are the resistivities after the 16th iteration using the perturbation method Jacobian.

83.05	448.18	448.49	448.09	447.71	446.65	445.95	446.98	446.31	445.07	445.26	445.77	445.26	445.37	445.68	447.32
301.14	881.17	879.72	880.38	882.02	886.96	889.56	888.27	890.88	45.48	45.33	44.96	45.32	45.24	45.36	42.84
304.94	62.09	60.14	60.03	58.66	55.57	52.69	48.68	46.61	42.75	41.59	42.70	41.80	42.17	39.65	86.71
52.10	275.91	234.32	292.38	316.49	330.79	323.17	505.65	783.61	9.81	12.56	10.94	12.24	11.50	14.08	96.93
62.92	741.95	1784.4	699.27	593.43	1006.3	1784.4	1581.9	490.44	.76	.73	.78	.63	.63	1.09	69.87
122.61	961.68	1784.4	1784.4	1784.4	1708.1	1784.4	1784.4	1784.4	21.29	1.04	1.81	3.54	3.31	8.58	57.18
297.56	1784.4	1784.4	1784.4	1784.4	1784.4	1784.4	1218.8	1784.4	242.46	1784.4	1387.7	519.88	255.72	264.85	118.81

Table H.19: These are the resistivities after the 17th iteration using the perturbation method Jacobian.

94.07	446.89	447.35	446.93	446.54	445.68	445.13	446.22	446.12	445.22	445.48	445.89	445.47	445.41	445.89	356.88
258.63	886.54	887.15	887.75	889.03	893.71	895.01	891.94	891.70	45.23	45.10	44.81	45.10	45.22	45.27	46.65
141.90	57.22	48.30	47.93	47.11	45.34	45.65	45.48	45.54	43.97	42.83	43.61	42.84	42.19	40.05	99.41
87.41	399.30	631.80	975.50	994.32	876.68	641.16	710.14	867.55	8.11	10.91	9.78	10.98	11.36	13.51	172.76
95.72	333.88	216.12	119.64	276.88	354.68	1004.3	1165.6	378.74	1.06	.81	.82	.72	.68	1.04	75.79
81.06	293.44	307.54	112.74	202.67	247.12	1009.7	1784.4	1784.4	4.27	1.59	1.76	1.57	1.49	3.10	27.11
143.04	1125.2	1784.4	406.33	371.51	543.16	949.74	586.31	998.08	384.21	1473.6	1784.4	907.72	449.86	240.82	67.57

Table H.20: These are the resistivities after the 18th iteration using the perturbation method Jacobian.

76.58	446.48	446.49	446.39	446.53	446.54	446.15	446.02	446.08	445.98	446.03	446.03	446.04	446.03	446.19	323.24
774.09	891.22	890.59	890.36	890.05	890.69	892.16	892.64	892.29	44.70	44.65	44.65	44.66	44.67	44.62	46.80
69.46	44.60	46.05	46.58	46.23	45.46	44.52	44.35	44.62	44.50	44.67	44.53	44.40	44.44	45.78	129.01
47.35	760.72	759.78	845.58	883.11	867.59	897.37	877.70	900.80	8.75	8.91	8.95	9.32	9.28	8.04	171.04
123.60	1784.4	804.85	515.67	487.94	865.97	1128.8	831.29	578.51	.95	.87	.87	.85	.89	1.10	68.68
155.35	250.32	166.22	548.96	572.52	626.52	975.90	1784.4	1784.4	1.12	1.18	1.15	1.00	.91	4.51	36.34
268.03	437.30	1324.9	1367.3	1047.3	913.66	555.04	689.82	960.48	626.85	743.50	582.36	872.06	897.20	457.43	70.69

Table H.21: These are the resistivities after the 19th iteration using the perturbation method Jacobian.

76.55	446.18	446.06	445.96	446.14	446.29	446.10	446.12	446.04	446.03	446.01	446.03	445.97	445.89	446.06	289.98
561.47	891.42	892.55	892.65	891.97	891.68	892.16	892.18	892.35	44.65	44.67	44.66	44.70	44.79	44.86	51.26
54.07	46.54	44.16	44.50	44.67	44.75	44.76	44.55	44.62	44.59	44.47	44.41	44.32	43.93	44.40	108.59
1250.5	856.41	879.98	908.85	919.99	903.14	888.26	889.20	892.79	8.76	9.03	9.08	9.18	9.58	7.47	229.52
55.62	146.53	1142.6	642.52	821.92	783.32	830.67	943.24	763.21	.92	.86	.90	.86	.89	1.30	81.02
22.41	646.90	1784.4	489.73	757.91	873.28	888.05	1227.0	1216.7	1.18	1.04	.98	1.05	.85	3.45	45.25
3.91	53.61	1784.4	1250.3	910.33	878.80	1024.7	745.46	893.96	691.43	878.60	914.65	843.49	670.23	372.65	66.62

Table H.22: These are the resistivities after the 20th iteration using the perturbation method Jacobian.

61.68	446.40	446.07	446.04	446.15	446.18	446.16	446.14	446.04	446.03	446.03	446.05	445.99	445.91	446.06	284.84
604.46	892.39	892.55	892.44	892.01	891.81	891.86	892.03	892.35	44.66	44.66	44.65	44.69	44.76	44.86	51.03
59.50	46.32	44.30	44.43	44.64	44.99	44.96	44.72	44.65	44.58	44.53	44.48	44.36	44.12	44.33	125.75
1433.9	720.71	845.30	891.41	902.97	891.62	887.99	883.23	884.06	8.76	8.93	9.01	9.15	9.33	7.64	209.24
1639.0	549.98	1784.4	1073.0	860.39	685.84	710.31	868.74	849.75	.93	.86	.89	.86	.88	1.26	77.61
290.57	108.21	274.99	534.90	809.49	1030.6	1071.2	1349.0	997.89	1.15	1.07	1.01	1.04	.91	3.39	40.50
175.20	219.08	1180.4	1080.8	853.83	980.18	941.97	714.23	959.21	713.86	906.26	855.82	949.15	775.46	377.09	70.07

Table H.23: These are the resistivities after the 21st iteration using the perturbation method Jacobian.

61.41	446.41	446.04	446.02	446.06	446.17	446.08	446.11	446.05	446.02	446.01	446.03	445.95	445.88	446.06	278.84
902.79	891.63	892.76	892.48	892.16	892.07	892.22	892.14	892.32	44.67	44.67	44.66	44.73	44.80	44.89	52.12
89.42	46.50	43.97	44.25	44.52	44.59	44.83	44.78	44.69	44.55	44.51	44.45	44.20	43.91	44.07	107.70
378.25	722.12	883.29	943.61	917.91	898.44	879.48	863.70	866.20	8.76	8.95	9.02	9.33	9.61	8.06	244.14
164.56	696.53	1427.6	868.48	919.80	904.81	824.82	1031.9	1048.3	.94	.86	.88	.85	.85	1.17	86.47
35.13	136.71	560.51	428.65	599.64	745.63	775.65	994.57	862.44	1.17	1.10	1.04	1.06	.93	3.41	47.21
23.13	183.18	1784.4	1003.1	919.56	945.55	1000.5	802.82	876.28	751.95	878.28	863.81	1117.6	795.89	291.09	64.14

Table H.24: These are the resistivities after the 22nd iteration using the perturbation method Jacobian.

239.36	478.67	460.73	454.97	458.90	478.76	488.71	481.41	440.22	423.90	433.72	436.11	434.10	435.06	422.02	345.95
272.59	753.99	831.57	853.25	839.02	780.41	771.27	781.08	854.75	61.16	51.74	50.15	51.24	51.83	60.08	119.31
172.13	226.24	103.35	95.31	106.83	111.77	124.83	131.38	181.36	27.42	33.46	38.96	38.46	32.36	27.22	54.71
120.22	111.82	95.61	99.59	105.04	110.50	121.44	148.05	132.98	24.34	12.86	8.76	8.64	12.34	23.12	49.38
182.10	197.54	238.60	299.01	324.93	315.03	288.85	246.92	136.71	25.60	5.59	1.91	1.80	4.53	18.46	48.62
368.19	499.54	789.68	1156.8	1302.4	1125.9	786.70	433.24	149.12	24.22	4.46	1.57	1.82	6.40	32.84	82.78
581.83	872.82	1535.4	1784.4	1784.4	1784.4	1287.5	546.10	151.74	26.27	5.40	2.33	3.07	10.83	52.12	112.76

H.4 Result of adjoint method

Table H.25: These are the resistivities after the first iteration using the Adjoint Method Jacobian.

1784.4	1784.4	1784.4	1784.4	1784.4	1784.4	1784.4	1784.4	1295.9	495.35	359.29	344.05	403.46	408.00	317.62	214.44
1784.4	1784.4	1784.4	1784.4	1784.4	1784.4	1784.4	1784.4	719.88	146.22	97.41	99.82	102.68	105.64	109.79	106.72
1390.6	1784.4	1784.4	1784.4	1784.4	1784.4	1784.4	738.70	158.39	40.79	27.55	27.24	22.65	23.00	31.77	43.36
635.19	869.45	1489.0	1784.4	1784.4	1187.2	491.26	149.76	40.27	17.96	16.31	17.66	14.86	14.76	20.76	30.39
295.20	349.42	514.04	666.56	598.78	332.92	126.60	41.33	16.70	13.28	18.44	25.47	25.18	25.28	32.32	42.48
166.69	177.17	228.39	269.01	226.40	122.07	47.78	18.60	11.07	14.05	28.82	52.20	61.86	64.24	75.05	84.57
134.67	135.69	158.94	172.09	138.49	75.74	32.18	14.76	11.04	17.09	40.36	82.07	108.95	117.43	129.84	131.68

Table H.26: These are the resistivities after the 2nd iteration using the Adjoint Method Jacobian.

1050.2	1148.2	1129.8	1108.4	1102.4	1091.8	1114.1	1154.3	907.27	413.72	327.03	322.96	350.94	346.86	276.65	193.98
902.49	810.63	890.47	889.68	897.46	920.35	950.01	880.14	466.24	119.78	85.39	92.49	94.07	96.07	104.82	101.58
799.00	593.10	611.40	678.23	714.23	705.63	631.34	423.70	158.03	37.77	21.86	22.65	23.19	25.18	33.01	40.56
740.94	536.54	494.27	545.33	566.73	514.59	386.50	210.11	74.90	22.41	12.07	10.86	10.99	12.41	16.43	21.06
569.42	460.96	424.11	447.74	448.81	381.64	259.69	133.67	53.05	20.36	11.34	9.26	9.11	10.27	12.96	15.83
435.57	385.24	369.26	382.43	372.35	305.44	201.75	106.86	48.50	22.47	13.34	10.52	10.07	11.11	13.35	15.33
383.51	355.13	346.94	350.99	331.79	267.33	177.17	98.33	49.34	25.63	15.95	12.42	11.62	12.49	14.39	15.78

Table H.27: These are the resistivities after the 3rd first iteration using the Adjoint Methods Jacobian.

722.68	850.16	840.96	801.02	789.65	775.01	787.69	817.34	727.70	385.03	332.16	336.46	351.87	345.34	290.66	199.79
579.13	501.57	568.45	591.08	599.74	622.12	648.76	643.92	425.89	108.09	79.67	89.50	89.93	91.46	101.08	99.02
583.28	373.44	352.19	399.48	450.82	481.69	465.45	357.92	158.97	35.94	20.50	22.17	22.67	23.82	30.10	37.43
722.68	400.53	298.61	321.19	372.49	389.52	334.08	207.69	80.29	22.13	11.32	10.40	10.58	11.58	14.77	19.00
588.34	372.37	277.48	289.47	331.89	334.63	263.47	149.36	59.66	20.63	10.58	8.56	8.43	9.33	11.54	14.15
403.95	303.36	254.97	273.00	310.26	304.38	230.42	129.28	56.29	23.19	12.51	9.57	9.10	9.92	11.81	13.64
323.31	270.01	247.86	267.76	296.25	282.67	211.14	121.27	57.40	26.63	15.12	11.33	10.47	11.10	12.72	14.00

Table H.28: These are the resistivities after the 4th first iteration using the Adjoint Methods Jacobian.

433.76	720.67	676.44	659.94	670.21	677.61	666.91	665.19	621.97	394.86	363.77	371.71	381.53	375.08	332.46	211.46
334.13	452.58	568.94	541.72	510.54	477.03	498.98	555.66	587.58	82.13	74.04	78.31	76.92	80.66	94.07	90.94
417.20	279.79	290.08	315.84	346.38	359.58	404.41	402.39	225.54	33.12	22.26	24.58	22.91	22.35	24.87	30.25
787.20	315.66	222.90	261.75	336.76	382.11	387.57	283.03	106.83	21.14	11.81	12.25	12.50	12.41	12.96	15.46
575.93	275.55	212.05	287.96	422.50	487.70	411.18	223.14	71.63	18.18	9.32	9.22	10.55	11.26	11.49	12.62
279.22	189.51	203.10	339.60	549.81	618.69	441.49	194.78	58.71	17.88	9.82	9.88	11.91	13.15	13.21	13.47
190.01	160.15	208.06	373.25	602.85	647.60	424.21	175.35	55.11	19.57	11.70	11.73	13.94	15.29	15.18	14.83

Table H.29: These are the resistivities after the 5th first iteration using the Adjoint Methods Jacobian.

344.60	660.87	599.00	586.11	613.92	635.11	613.99	581.81	553.95	399.58	385.01	392.32	397.93	391.82	356.41	219.31
263.40	455.00	587.30	572.73	520.71	473.77	488.14	576.53	648.73	77.66	67.80	70.24	70.22	73.97	86.66	87.35
358.96	277.82	285.49	302.20	332.10	349.90	396.53	426.98	247.75	29.28	23.26	25.64	22.52	21.35	23.03	28.52
797.96	320.58	218.47	242.21	308.33	365.05	388.67	307.33	115.95	19.60	12.73	13.54	13.08	12.60	12.73	15.09
579.01	274.09	216.19	285.14	404.25	481.32	431.43	249.34	78.16	17.79	9.74	9.77	10.97	11.67	11.79	12.84
247.35	175.41	211.30	361.66	562.98	640.46	480.86	220.49	63.64	17.55	9.76	9.87	11.92	13.44	13.73	14.01
160.72	143.86	216.17	409.19	642.43	690.35	467.76	196.15	58.23	18.86	11.19	11.29	13.54	15.32	15.68	15.46

Table H.30: These are the resistivities after the 6th first iteration using the Adjoint Methods Jacobian.

307.77	632.30	562.40	546.18	585.18	616.15	588.76	537.98	518.82	403.88	398.42	404.39	407.23	401.30	370.27	223.80
237.75	463.49	604.70	602.81	536.90	480.26	496.88	600.97	674.15	75.56	63.90	65.40	66.62	70.42	82.32	85.25
340.24	285.78	288.51	302.48	333.55	354.39	406.41	446.62	254.94	28.10	23.69	26.02	22.24	20.62	21.72	27.45
796.33	329.24	216.52	232.71	300.38	364.74	394.08	313.38	115.28	18.53	13.00	14.13	13.25	12.43	12.37	14.83
586.70	279.51	215.70	277.28	397.09	484.12	440.01	253.88	77.36	16.92	9.66	9.87	10.95	11.60	11.80	12.99
244.50	176.18	213.34	361.16	567.07	657.68	500.43	228.96	64.27	16.97	9.47	9.61	11.63	13.32	13.95	14.45
158.36	144.16	219.99	415.76	658.63	719.30	493.63	206.90	59.97	18.60	10.81	10.82	13.05	15.11	15.96	16.00

Table H.31: These are the resistivities after the 7th first iteration using the Adjoint Methods Jacobian.

242.27	605.35	535.50	518.74	561.26	609.93	585.17	519.65	494.21	409.87	410.23	414.75	414.48	408.92	380.92	225.46
188.37	508.50	642.32	650.56	579.65	491.56	498.55	601.36	718.77	70.33	59.16	60.55	63.62	67.34	79.25	82.08
292.53	281.11	272.28	268.03	290.70	306.98	365.14	438.64	268.85	28.55	26.16	27.28	22.27	20.39	19.94	25.17
797.64	317.93	198.97	201.19	252.46	313.67	363.67	321.11	120.25	17.52	13.04	14.08	13.13	12.39	11.51	13.64
598.64	276.08	222.74	291.39	411.03	505.75	477.84	286.10	81.50	15.10	8.25	8.69	10.52	11.84	11.68	12.62
230.99	174.82	252.52	481.64	768.88	877.98	654.20	283.41	68.34	14.79	7.79	8.51	11.65	14.39	14.87	15.03
146.80	145.68	278.87	623.83	1029.0	1092.9	705.82	265.35	64.13	16.58	9.32	10.23	13.87	17.07	17.80	17.33

Table H.32: These are the resistivities after the 8th first iteration using the Adjoint Methods Jacobian.

214.85	592.36	524.64	502.89	546.82	607.28	585.12	510.00	481.96	413.54	417.87	421.24	418.66	413.32	387.14	224.68
164.70	512.63	649.09	673.87	594.96	491.40	497.62	609.11	726.29	69.21	56.43	57.78	62.00	65.88	76.99	79.37
268.06	283.53	265.84	257.21	287.28	309.42	364.46	437.78	269.97	28.04	27.30	28.01	22.40	20.13	19.06	23.96
792.06	334.83	200.53	188.41	242.54	317.34	371.22	328.91	123.91	17.69	13.47	14.22	13.04	12.28	11.23	13.26
616.63	298.03	235.58	285.22	401.54	515.21	497.81	300.68	84.98	15.14	8.16	8.39	10.17	11.77	11.81	12.79
248.47	193.66	275.50	488.38	761.79	891.12	680.72	297.44	70.27	14.41	7.39	7.97	11.13	14.46	15.56	15.87
160.64	162.36	306.04	641.99	1026.9	1103.2	727.02	274.31	64.38	15.74	8.66	9.54	13.31	17.31	18.94	18.66

Table H.33: These are the resistivities after the 9th first iteration using the Adjoint Methods Jacobian.

177.26	569.39	508.97	486.84	523.98	592.11	582.62	506.59	471.70	419.13	426.24	428.33	423.03	418.11	392.63	228.15
134.15	569.02	689.36	726.78	664.38	540.66	529.74	616.53	754.45	63.51	51.82	53.77	59.57	63.25	76.06	78.90
226.23	267.62	234.44	211.43	229.42	247.51	290.59	386.04	277.93	31.27	32.37	31.34	23.74	20.88	17.62	22.42
787.68	313.88	176.60	153.85	182.81	236.52	292.52	312.95	130.08	15.84	12.16	12.91	12.24	12.07	10.17	12.13
636.55	301.13	262.86	325.69	423.60	519.02	522.55	356.78	96.28	12.38	5.66	5.96	8.45	11.37	11.35	12.37
234.01	202.53	389.13	813.04	1229.7	1341.4	1005.2	437.62	85.96	12.19	5.40	6.33	10.45	15.36	16.52	16.66
147.23	174.21	477.85	1272.6	1784.4	1784.4	1270.7	436.50	80.91	14.52	7.51	9.38	14.86	20.35	21.58	20.64

Table H.34: These are the resistivities after the 10th first iteration using the Adjoint Methods Jacobian.

159.34	557.89	503.35	478.25	511.61	589.17	584.57	504.97	466.82	422.38	432.05	433.15	426.02	421.12	396.37	225.03
117.85	575.56	693.89	742.32	673.79	528.84	524.62	623.45	756.84	62.60	49.32	51.44	57.81	62.12	74.48	75.75
200.99	261.63	224.23	201.75	228.40	253.47	285.26	359.36	267.64	30.78	34.66	33.52	24.96	21.10	16.95	21.19
781.60	331.23	181.88	147.83	185.51	258.12	311.48	321.39	142.00	17.30	12.18	12.32	12.05	12.17	10.08	11.85
654.38	326.79	286.59	330.38	447.10	586.88	594.45	401.60	111.11	13.39	5.39	5.34	7.87	11.41	11.75	12.74
252.88	224.74	420.96	808.89	1257.0	1462.5	1124.1	488.90	94.98	12.34	5.00	5.69	9.85	15.76	17.89	18.11
162.98	195.48	507.85	1233.7	1784.4	1784.4	1366.1	467.76	83.43	13.69	6.88	8.70	14.45	21.32	23.91	23.01

Table H.35: These are the resistivities after the 11th first iteration using the Adjoint Methods Jacobian.

146.83	541.47	493.70	469.82	497.14	568.76	569.88	500.22	462.67	426.69	437.49	437.92	429.44	424.54	399.74	229.48
105.07	619.49	725.82	775.13	722.45	588.77	586.58	658.76	769.26	58.07	46.17	48.53	55.19	59.78	73.77	76.94
172.86	238.69	197.10	173.62	192.71	210.02	222.06	284.51	265.74	35.55	39.97	38.23	28.03	22.59	16.27	20.98
776.23	308.24	163.22	132.62	156.66	202.30	235.96	277.25	146.03	14.79	9.75	10.08	10.70	11.79	9.48	11.59
672.42	332.63	328.08	406.79	516.91	617.13	615.37	465.65	130.84	11.08	3.64	3.55	5.90	10.35	11.36	12.81
238.33	238.66	599.11	1367.9	1784.4	1784.4	1634.9	726.44	125.06	11.31	4.01	4.78	8.99	15.91	18.46	18.83
151.84	215.10	792.81	1784.4	1784.4	1784.4	1784.4	742.33	109.71	13.42	6.72	9.67	16.78	24.40	25.97	24.35

Table H.36: These are the resistivities after the 12th first iteration using the Adjoint Methods Jacobian.

137.94	532.81	490.57	466.29	490.17	562.47	563.04	496.38	460.77	429.44	441.56	441.26	432.15	426.84	402.45	229.89
96.42	627.28	727.48	781.11	726.92	582.27	589.61	674.12	773.96	57.19	44.46	46.95	53.29	58.73	72.41	76.13
153.57	232.38	190.96	168.19	188.83	210.35	213.27	252.83	243.84	35.26	42.05	40.55	30.16	23.24	15.99	20.78
771.82	324.45	170.37	132.64	162.48	220.04	250.31	281.12	161.77	16.75	9.35	9.21	10.41	11.95	9.61	11.80
687.28	349.87	347.88	426.03	586.85	743.59	730.25	530.93	153.63	12.16	3.37	3.15	5.52	10.39	11.84	13.42
240.14	241.42	594.48	1384.4	1784.4	1784.4	1784.4	826.86	137.82	11.53	3.83	4.53	8.83	16.43	19.72	20.16
152.60	214.58	754.75	1784.4	1784.4	1784.4	1784.4	821.06	112.95	12.70	6.54	9.66	17.18	25.70	28.00	26.26

Table H.37: These are the resistivities after the 13th first iteration using the Adjoint Methods Jacobian.

133.07	519.25	482.75	461.70	481.09	539.03	536.16	486.42	456.72	432.62	445.15	444.39	435.18	429.78	405.68	237.74
90.25	669.62	758.82	805.13	765.42	655.79	681.00	737.42	794.94	53.72	42.39	45.08	50.83	56.33	70.91	79.72
134.26	207.09	164.35	145.90	159.36	168.88	158.36	174.74	218.22	39.70	46.22	45.10	34.60	25.52	16.06	22.24
768.45	302.26	156.89	127.12	145.95	175.17	190.82	232.18	165.13	13.95	6.97	6.72	8.32	11.27	9.52	12.54
702.43	365.88	431.27	583.14	758.86	863.81	841.46	681.49	208.94	11.54	2.40	2.01	3.72	8.94	11.61	13.86
208.81	254.74	908.81	1784.4	1784.4	1784.4	1784.4	1384.0	206.97	12.19	3.60	4.32	8.46	16.80	19.99	19.86
131.00	230.80	1233.8	1784.4	1784.4	1784.4	1784.4	1384.8	149.43	12.14	7.11	12.82	22.98	31.38	29.44	25.09

Table H.38: These are the resistivities after the 14th first iteration using the Adjoint Methods Jacobian.

127.89	511.20	479.47	460.09	476.63	527.60	520.99	480.05	455.19	435.01	447.83	446.56	437.53	431.77	408.66	243.63
86.30	679.98	763.63	809.28	771.62	665.62	696.61	755.91	799.52	52.78	41.47	44.14	49.34	55.29	69.15	81.98
121.47	201.72	156.03	138.90	149.67	159.45	145.45	149.54	199.06	39.57	47.63	46.45	36.56	26.40	16.19	23.69
767.26	315.01	161.11	129.13	150.62	183.88	198.69	232.58	183.92	15.58	6.37	6.16	8.04	11.58	10.25	13.91
714.05	373.25	448.51	652.46	940.90	1119.7	1040.7	751.99	227.16	11.75	2.15	1.86	3.57	9.10	12.62	15.19
192.14	240.44	899.25	1784.4	1784.4	1784.4	1784.4	1560.9	213.11	12.08	3.80	4.66	8.90	17.40	20.83	20.40
119.24	216.25	1214.4	1784.4	1784.4	1784.4	1784.4	1595.1	151.49	11.40	7.96	14.50	24.57	32.01	29.17	24.37

Table H.39: These are the resistivities after the 15th first iteration using the Adjoint Methods Jacobian.

123.00	498.02	471.53	456.74	469.06	500.96	491.38	467.97	450.70	437.38	450.16	448.21	439.74	434.34	414.14	264.21
84.61	725.74	798.81	831.57	809.38	757.65	795.51	827.51	837.44	50.22	40.20	43.28	47.58	52.97	65.07	93.74
112.70	174.95	128.45	118.17	122.68	120.57	104.95	96.03	147.39	42.78	50.41	49.80	41.56	29.60	17.17	31.10
774.19	295.00	152.71	130.78	142.19	151.91	173.41	226.80	199.95	12.03	4.36	3.93	5.34	10.03	11.80	19.26
721.47	411.83	628.03	1050.4	1441.3	1546.4	1510.8	1283.2	429.08	14.75	1.70	1.12	1.99	7.05	14.16	18.34
144.54	257.84	1578.3	1784.4	1784.4	1784.4	1784.4	1784.4	372.48	16.61	5.47	6.09	10.09	20.07	22.79	18.36
91.79	238.99	1784.4	1784.4	1784.4	1784.4	1784.4	1784.4	165.07	9.68	12.20	29.45	47.10	50.37	31.09	17.71

Table H.40: These are the resistivities after the 16th first iteration using the Adjoint Methods Jacobian.

112.53	489.77	467.44	455.34	464.88	486.93	475.25	460.20	448.49	439.50	451.45	448.87	440.91	435.51	419.94	281.51
86.16	738.75	808.12	837.43	820.01	778.81	817.28	847.61	837.98	49.42	40.30	43.29	47.15	52.83	61.41	103.46
110.27	169.71	116.74	108.58	108.94	106.64	92.32	80.62	141.63	41.29	50.02	48.77	41.57	29.42	16.93	40.00
805.50	307.61	159.01	139.30	152.23	164.76	182.65	220.66	207.65	15.96	4.41	4.68	5.93	10.62	16.63	32.22
701.58	401.52	649.56	1297.0	1784.4	1784.4	1784.4	1234.3	301.77	11.31	1.51	1.25	2.07	7.46	22.38	30.00
121.71	229.56	1573.2	1784.4	1784.4	1784.4	1784.4	1784.4	277.93	13.72	8.14	8.73	11.89	22.37	28.97	20.47
76.68	215.48	1784.4	1784.4	1784.4	1784.4	1784.4	1784.4	152.82	9.19	21.21	41.28	50.94	49.44	28.20	13.24

Table H.41: These are the resistivities after the 17th first iteration using the Adjoint Methods Jacobian.

96.72	480.88	462.41	453.00	459.80	472.30	460.86	454.25	446.15	441.23	452.14	448.17	440.74	436.15	426.51	337.39
90.90	768.35	829.76	852.62	841.75	825.81	858.85	873.26	862.30	47.75	40.32	44.28	47.61	51.94	56.51	144.89
115.83	152.80	100.13	95.17	94.15	89.22	77.03	65.08	113.88	45.18	48.54	47.65	42.20	33.32	19.41	70.51
856.29	297.08	166.93	150.17	157.58	162.38	197.34	266.92	207.56	8.49	4.38	4.18	4.65	6.33	15.38	47.84
694.43	428.99	845.33	1784.4	1784.4	1784.4	1784.4	1784.4	707.73	23.66	2.15	1.16	1.68	4.98	25.76	39.13
108.65	241.86	1784.4	1784.4	1784.4	1784.4	1784.4	1784.4	463.95	29.10	20.75	15.91	19.38	35.59	49.47	20.82
63.97	214.36	1784.4	1784.4	1784.4	1784.4	1784.4	1784.4	107.79	7.18	40.26	91.31	123.73	123.50	49.96	9.47

Table H.42: These are the resistivities after the 18th first iteration using the Adjoint Methods Jacobian.

108.28	474.34	460.26	452.01	457.33	465.26	452.28	451.29	445.83	443.41	452.01	446.68	439.35	435.80	428.27	323.05
76.11	786.60	835.20	856.10	847.26	837.70	872.35	876.39	854.93	46.79	41.03	45.50	49.26	52.76	57.78	135.01
117.81	136.53	92.53	89.64	86.83	81.95	71.21	60.48	120.65	41.98	46.34	44.42	39.75	31.19	15.77	68.43
984.57	320.56	173.88	155.11	163.58	166.66	192.73	251.37	276.37	17.75	5.49	5.83	6.11	7.93	23.74	86.66
643.51	477.15	883.10	1784.4	1784.4	1784.4	1784.4	1115.1	197.16	7.82	1.99	1.59	2.10	6.42	50.99	93.83
114.97	267.53	1784.4	1784.4	1784.4	1784.4	1784.4	1784.4	132.78	11.64	20.00	16.49	14.31	23.77	54.37	34.91
61.99	198.13	1784.4	1784.4	1784.4	1784.4	1784.4	1784.4	68.90	9.62	62.47	83.37	57.80	43.41	26.44	8.54

Table H.43: These are the resistivities after the 19th first iteration using the Adjoint Methods Jacobian.

105.95	471.93	459.62	451.62	456.18	463.32	449.74	450.57	443.78	444.29	451.23	445.31	438.86	436.34	430.78	438.77
74.29	785.21	835.12	857.61	849.62	837.61	871.80	877.61	867.51	46.70	41.92	46.49	49.08	51.67	55.63	211.19
117.09	138.80	90.85	86.32	83.16	78.96	68.94	56.98	117.92	42.16	43.13	43.36	38.51	32.67	20.28	101.50
1044.5	313.06	166.83	160.22	169.61	175.33	212.57	272.09	183.76	10.94	7.61	6.76	6.92	7.36	11.26	48.53
675.86	431.98	810.81	1784.4	1784.4	1784.4	1784.4	1784.4	599.00	26.00	2.24	1.17	2.22	6.00	20.31	37.45
104.74	229.38	1784.4	1784.4	1784.4	1784.4	1784.4	1784.4	256.65	29.79	15.18	10.86	15.97	31.43	40.96	21.58
56.11	177.36	1784.4	1784.4	1784.4	1784.4	1784.4	980.66	37.96	9.06	31.23	51.60	67.58	72.04	36.43	8.86

Table H.44: These are the resistivities after the 20th first iteration using the Adjoint Methods Jacobian.

104.19	467.36	456.91	450.51	453.85	456.31	443.47	448.63	444.03	444.86	450.97	444.53	438.90	436.98	428.89	301.99
71.15	807.32	850.85	865.01	860.56	869.66	899.22	892.84	873.03	46.98	41.59	46.33	48.74	50.94	59.93	129.93
123.95	121.38	81.16	80.88	77.18	69.69	60.41	49.88	93.73	37.48	44.78	45.68	42.30	34.26	15.37	69.14
1238.9	342.11	192.07	167.37	175.00	181.69	248.83	396.97	523.37	23.65	5.82	4.18	3.84	5.59	20.72	100.85
506.66	477.10	1081.0	1784.4	1784.4	1784.4	1784.4	1784.4	283.47	7.31	1.26	1.18	1.73	6.34	57.20	128.89
87.04	269.28	1784.4	1784.4	1784.4	1784.4	1784.4	1784.4	126.84	18.22	34.69	26.84	23.07	39.73	74.68	41.94
50.22	199.57	1784.4	1784.4	1784.4	1784.4	1784.4	1343.2	35.27	16.97	149.68	197.01	138.94	96.54	34.85	6.71

Table H.45: These are the resistivities after the 21st first iteration using the Adjoint Methods Jacobian.

105.94	463.90	455.45	449.97	452.91	455.09	444.33	449.57	443.51	446.02	449.87	442.66	438.51	437.18	431.85	306.89
67.84	816.37	854.23	868.08	863.24	861.27	881.81	880.24	876.49	45.46	43.19	48.10	48.91	50.68	56.01	140.48
130.73	115.40	77.28	76.60	74.07	71.51	63.05	50.79	95.05	40.25	41.17	42.83	41.30	35.93	17.77	88.59
1345.52	350.96	189.86	183.25	176.63	165.33	198.78	289.83	263.94	12.52	8.99	7.17	4.31	3.73	12.81	80.26
376.04	418.93	1032.2	1784.4	1784.4	1784.4	1784.4	1386.1	468.93	16.74	1.50	1.05	2.47	10.36	69.88	105.24
72.42	247.97	1784.4	1784.4	1784.4	1784.4	1784.4	1314.0	197.43	43.33	9.26	5.76	12.91	58.06	137.51	42.06
44.10	187.45	1784.4	1784.4	1784.4	1784.4	1784.4	457.71	26.66	32.51	25.75	21.61	37.28	86.25	54.36	6.50

Table H.46: These are the resistivities after the 22nd first iteration using the Adjoint Methods Jacobian.

91.36	463.73	454.64	449.81	452.77	453.21	442.33	448.06	442.36	444.52	450.76	443.82	439.92	437.64	433.39	373.07
71.93	807.10	855.55	867.41	863.16	874.16	897.78	893.46	879.02	48.97	41.16	45.80	47.16	49.90	55.14	229.16
142.41	124.12	75.80	76.11	71.77	64.20	57.11	46.64	88.12	33.60	46.54	48.74	45.91	38.49	18.83	193.56
1582.0	355.92	185.35	172.23	185.07	203.87	291.18	428.56	433.86	19.18	5.62	3.63	2.33	2.98	12.26	170.90
397.54	349.82	834.57	1784.4	1784.4	1784.4	1784.4	1784.4	419.31	11.86	1.18	.86	1.46	7.18	57.97	142.03
67.95	187.90	1784.4	1784.4	1784.4	1784.4	1784.4	1784.4	126.97	31.03	19.04	14.79	20.76	86.05	147.11	36.84
43.19	156.79	1784.4	1784.4	1784.4	1784.4	1784.4	763.48	22.49	46.66	112.62	114.36	135.07	345.31	126.02	5.05

Table H.47: These are the resistivities after the 23rd first iteration using the Adjoint Methods Jacobian.

95.29	459.32	453.50	448.72	450.85	452.80	444.52	448.94	442.85	445.01	450.17	443.80	439.74	439.29	424.47	124.92
68.20	847.80	863.69	876.30	871.79	868.79	883.82	881.80	888.00	47.03	42.45	46.26	48.46	47.97	68.99	88.38
138.60	92.72	68.91	69.97	68.74	64.62	57.51	48.26	75.81	35.55	43.88	45.49	43.99	38.71	13.07	99.32
878.63	404.75	247.49	207.48	199.33	183.23	277.46	451.80	481.94	12.62	7.97	7.51	3.57	4.80	5.16	120.81
230.40	618.68	1298.4	1784.4	1784.4	1784.4	1784.4	1563.8	471.12	11.31	.99	1.26	2.05	22.84	194.18	370.45
53.92	326.92	1784.4	1784.4	1784.4	1784.4	1784.4	1108.4	174.99	138.07	11.33	4.52	7.80	88.27	275.60	104.56
44.17	185.86	1784.4	1784.4	1784.4	1784.4	1784.4	399.40	29.23	139.16	40.65	14.82	23.66	126.61	76.14	4.76

Table H.48: These are the resistivities after the 24th first iteration using the Adjoint Methods Jacobian.

99.58	457.73	453.00	449.08	450.98	450.42	442.42	446.64	441.43	444.08	450.40	443.95	440.36	439.41	424.53	184.67
63.86	836.64	861.21	871.32	870.84	881.76	898.60	899.08	886.85	48.60	41.61	46.03	47.22	48.79	63.36	126.98
141.06	100.28	71.78	71.08	67.80	61.35	53.97	44.89	75.02	34.73	46.67	46.73	46.42	39.27	19.01	150.97
880.98	274.93	164.76	176.74	185.12	198.30	333.63	604.62	492.72	9.56	4.86	5.71	2.02	2.89	2.19	98.09
308.52	407.66	908.78	1784.4	1784.4	1784.4	1784.4	1784.4	393.74	18.03	1.67	.81	1.22	29.19	97.95	179.53
72.27	256.28	1784.4	1784.4	1784.4	1784.4	1784.4	1300.7	91.00	53.49	7.92	10.88	25.80	526.48	615.44	55.95
39.45	149.87	1784.4	1784.4	1784.4	1784.4	1784.4	511.09	35.44	120.52	31.52	71.39	171.44	1601.8	365.85	4.20

Table H.49: These are the resistivities after the 25th first iteration using the Adjoint Methods Jacobian.

102.82	456.68	453.19	448.85	450.71	452.35	445.49	448.41	441.98	444.04	449.63	444.70	440.18	440.04	422.15	139.97
60.20	848.09	864.00	875.34	868.01	864.03	880.90	883.65	893.65	47.82	42.54	44.88	48.03	48.24	65.64	97.82
131.68	89.08	66.39	68.33	69.24	66.73	56.97	47.06	66.12	35.83	47.81	48.64	45.45	37.83	17.96	247.28
779.02	379.00	257.15	194.82	182.75	147.92	211.68	369.77	459.98	7.97	2.91	3.58	2.25	6.68	2.23	489.96
188.55	656.67	1712.4	1784.4	1784.4	1784.4	1731.2	1494.8	633.65	20.73	1.44	1.55	1.58	55.67	233.97	1089.3
89.27	446.90	1784.4	1784.4	1784.4	1784.4	1784.4	1252.3	241.25	103.24	17.14	8.65	9.81	75.45	167.68	114.74
41.21	151.14	1784.4	1784.4	1784.4	1784.4	1784.4	505.23	47.48	160.87	124.82	56.28	36.19	48.82	20.09	3.72

Table H.50: These are the resistivities after the 26th first iteration using the Adjoint Methods Jacobian.

104.38	455.84	452.15	449.07	451.01	448.26	442.01	446.32	443.03	443.42	450.33	445.93	442.12	441.53	420.94	116.30
57.30	840.06	865.80	873.85	874.18	892.89	906.15	903.31	885.83	48.58	41.15	44.19	45.82	46.67	65.82	192.13
138.39	97.37	68.15	67.28	64.76	59.27	50.67	41.91	62.20	36.76	51.35	48.95	48.61	42.23	20.05	180.72
892.64	301.85	183.84	209.85	209.19	204.17	379.22	1096.6	912.04	6.96	1.30	5.39	1.72	2.22	2.39	65.89
391.75	451.55	1007.0	1784.4	1784.4	1784.4	1784.4	1784.4	423.58	27.69	2.24	.57	1.09	146.68	393.41	230.97
92.39	230.92	1784.4	1784.4	1784.4	1784.4	1784.4	1265.5	84.96	205.72	65.08	17.29	55.16	1784.4	956.55	81.35
41.82	107.18	1737.6	1784.4	1784.4	1784.4	1784.4	508.29	42.79	691.01	424.79	59.19	83.13	1057.7	15.27	3.52

Table H.51: These are the resistivities after the 27th first iteration using the Adjoint Methods Jacobian.

61.23	459.08	451.15	447.85	450.07	448.52	443.27	448.35	443.23	443.24	449.53	447.14	443.98	443.03	420.97	48.81
83.01	827.96	871.35	883.47	873.69	879.56	890.04	882.69	887.49	47.82	42.67	43.25	44.88	45.76	65.22	47.15
139.91	110.86	62.09	62.47	64.22	62.62	53.84	43.81	61.16	37.44	50.79	49.95	49.96	43.47	20.41	314.43
482.61	357.19	300.56	246.53	216.59	148.08	205.85	536.61	435.00	5.63	.90	3.58	1.73	2.96	3.27	1784.4
110.96	441.91	1534.6	1784.4	1784.4	1784.4	1349.7	1416.1	686.93	89.14	2.62	1.57	1.15	9.30	77.27	1784.4
127.10	282.09	1784.4	1784.4	1784.4	1784.4	1784.4	615.09	129.67	260.34	50.77	22.39	13.71	26.62	56.63	121.98
58.01	62.47	1521.4	1784.4	1784.4	1784.4	1784.4	279.34	31.92	186.31	187.61	114.48	50.17	20.84	5.14	3.13

Table H.52: These are the resistivities after the 28th first iteration using the Adjoint Methods Jacobian.

38.42	459.60	451.92	448.20	450.50	447.39	442.57	447.26	443.12	443.05	450.08	448.04	445.66	444.27	419.20	94.50
136.67	826.13	861.70	876.90	873.63	892.49	903.57	899.97	893.64	47.88	41.34	43.08	43.88	45.01	66.24	83.02
172.03	120.89	67.16	64.12	63.22	56.28	49.00	41.34	55.41	39.16	52.23	51.70	50.75	44.45	21.35	122.41
358.31	272.81	174.97	194.84	215.47	231.03	371.53	879.25	983.11	5.28	1.16	2.41	1.24	1.45	4.27	58.60
452.04	450.18	762.31	1784.4	1784.4	1784.4	1784.4	1784.4	397.37	34.04	1.83	.83	2.37	200.42	212.61	187.13
447.16	210.46	1053.6	1784.4	1784.4	1784.4	1784.4	1258.3	100.47	634.97	242.66	67.77	188.86	1784.4	260.76	92.08
213.89	42.42	560.35	1784.4	1784.4	1784.4	1784.4	308.28	33.70	1784.4	1784.4	466.99	135.97	89.33	.91	3.13

Table H.53: These are the resistivities after the 29th first iteration using the Adjoint Methods Jacobian.

35.91	453.82	451.24	446.89	449.03	450.51	446.51	447.12	442.23	443.50	449.56	449.13	447.30	445.30	424.13	87.49
153.93	890.22	878.03	891.77	880.34	866.35	880.63	892.93	901.11	46.67	42.40	42.06	43.06	45.12	58.09	46.48
182.92	72.45	53.40	54.97	60.07	64.12	53.20	41.77	51.09	40.63	51.90	52.91	52.78	44.58	30.55	263.08
267.48	335.28	567.14	374.60	277.97	118.49	188.73	876.35	432.19	3.74	.84	1.63	.59	2.01	4.63	457.78
542.91	1784.4	1784.4	1784.4	1784.4	1784.4	1599.2	1784.4	1784.4	392.43	4.17	1.28	18.25	46.28	177.47	708.03
1677.1	859.08	1784.4	1784.4	1784.4	1784.4	1784.4	1093.0	111.46	235.65	37.19	18.68	77.77	68.27	59.88	87.76
861.49	31.11	197.58	1784.4	1784.4	1784.4	1784.4	551.36	35.97	111.01	86.92	56.39	46.11	8.05	.77	3.13

Table H.54: These are the resistivities after the 30th first iteration using the Adjoint Methods Jacobian.

38.80	452.64	452.16	448.10	450.68	448.01	444.14	446.81	444.19	443.97	451.18	450.32	448.40	446.73	423.81	128.85
104.12	871.40	864.94	878.33	877.06	884.31	898.97	903.16	892.04	46.57	39.98	41.78	42.92	43.63	63.50	71.08
208.82	73.94	58.25	56.18	59.70	66.72	51.66	40.20	49.24	43.21	54.50	54.02	52.39	43.91	21.92	316.35
1126.5	436.72	271.79	359.07	202.00	110.89	205.90	552.43	1657.2	3.93	1.64	.77	1.11	5.80	4.78	206.65
1205.1	378.57	776.32	1784.4	1784.4	1784.4	1784.4	1784.4	76.06	2.32	.45	5.49	798.76	1784.4	1292.7	536.69
1784.40	221.00	437.22	1784.4	1784.4	1784.4	1784.4	1784.4	76.28	239.46	150.11	559.87	1784.4	1784.4	636.55	116.31
1784.4	77.20	113.26	1685.8	1784.4	1784.4	1784.4	1784.4	17.89	1784.4	1784.4	478.65	81.38	4.84	.57	3.15

Table H.55: These are the resistivities after the 31st first iteration using the Adjoint Methods Jacobian.

32.68	453.89	452.90	449.18	451.00	446.67	446.68	448.63	443.44	443.70	451.34	451.14	448.73	447.53	424.80	51.88
161.63	869.32	863.06	874.70	874.53	886.20	882.73	891.90	901.40	46.27	40.50	41.22	42.60	43.28	60.31	63.16
195.31	72.96	60.46	57.81	62.11	65.34	55.71	40.48	40.66	47.13	53.27	54.71	52.58	48.73	27.23	475.77
681.42	362.17	351.13	240.78	153.83	162.32	178.66	906.69	1524.9	4.28	2.01	.61	.77	2.02	4.20	1238.1
951.20	461.66	1438.5	1784.4	1784.4	1784.4	1784.4	1784.4	1784.4	2.23	.69	14.37	14.53	15.82	47.52	1480.4
1232.8	227.85	581.51	1784.4	1784.4	1784.4	1784.4	1784.4	115.55	10.76	9.14	93.90	100.81	22.15	18.22	226.91
1300.2	97.35	144.47	1784.4	1784.4	1784.4	1784.4	633.31	14.11	11.56	31.75	168.95	97.74	3.75	.49	3.10

H.5 Result of measurement-corrected adjoint method

Table H.56: These are the resistivities after the 1st iteration using the measurement-corrected adjoint method Jacobian.

1784.4	1784.4	1784.4	1784.4	1784.4	1784.4	1784.4	1784.4	1693.8	575.70	407.08	387.62	454.95	459.94	353.91	235.50
1784.4	1784.4	1784.4	1784.4	1784.4	1784.4	1784.4	1784.4	835.77	152.10	94.33	95.46	98.25	103.34	112.44	112.25
1468.3	1784.4	1784.4	1784.4	1784.4	1784.4	1784.4	807.91	160.20	38.91	25.62	25.70	21.38	21.61	30.96	43.68
523.03	734.64	1332.0	1784.4	1784.4	1212.37	493.39	145.10	37.95	17.14	16.20	18.26	15.27	14.64	20.46	30.21
191.97	228.06	352.34	493.97	482.02	283.69	111.06	36.84	15.38	13.15	19.90	28.98	28.24	26.75	32.69	42.23
91.71	96.76	130.69	167.81	156.17	91.72	38.30	15.80	10.16	14.37	32.85	62.85	72.92	70.48	76.86	83.76
69.72	69.70	85.38	100.71	89.86	54.07	24.91	12.34	10.15	17.67	46.44	99.38	129.03	129.63	133.29	130.31

Table H.57: These are the resistivities after the 2nd iteration using the measurement-corrected adjoint method Jacobian.

1018.0	1113.9	1095.8	1090.6	1065.9	1046.7	1058.6	1118.7	1070.1	450.24	348.11	342.81	373.80	370.66	289.37	199.97
845.91	735.07	791.90	767.50	794.03	852.62	883.79	823.21	486.25	113.24	80.04	87.40	88.31	91.12	102.58	101.68
749.64	565.62	591.66	629.94	664.90	678.80	611.16	408.28	153.49	34.22	20.16	21.45	21.61	23.34	31.70	40.15
714.81	550.36	529.31	570.04	582.35	530.05	394.63	210.67	73.70	21.47	11.87	10.96	10.94	12.21	16.41	21.38
597.72	513.43	492.70	513.31	501.46	418.61	278.92	140.25	54.70	20.95	11.97	9.96	9.73	10.85	13.69	16.77
500.20	461.73	455.13	465.42	439.53	350.18	224.96	116.22	52.01	24.25	14.72	11.78	11.26	12.34	14.74	16.83
461.00	439.78	436.26	435.24	399.06	311.49	200.54	108.67	53.86	28.14	17.82	14.06	13.20	14.13	16.19	17.59

Table H.58: These are the resistivities after the 3rd iteration using the measurement-corrected adjoint method Jacobian.

673.26	816.57	808.36	783.87	756.61	736.48	740.38	783.66	791.57	401.29	345.52	349.15	365.72	360.05	298.77	202.38
522.65	458.38	513.42	519.24	537.72	575.15	601.54	603.82	429.59	102.05	76.24	86.32	86.05	87.68	98.85	97.77
534.95	347.87	333.14	366.80	418.59	458.92	447.48	345.07	153.35	32.44	18.94	21.13	21.34	22.21	28.69	36.39
710.49	401.04	307.63	328.15	381.58	402.81	345.55	212.27	79.66	20.84	10.81	10.22	10.35	11.22	14.45	18.84
627.22	403.95	310.44	327.16	376.59	379.49	295.78	163.92	63.15	21.03	10.80	8.89	8.77	9.64	11.93	14.68
454.26	347.73	301.88	330.27	378.66	370.17	275.82	150.55	63.28	25.32	13.61	10.50	10.02	10.87	12.90	14.84
371.22	315.91	299.24	331.66	371.36	353.17	259.32	144.88	66.43	30.10	17.00	12.80	11.85	12.53	14.29	15.61

Table H.59: These are the resistivities after the 4th iteration using the measurement-corrected adjoint method Jacobian.

385.80	702.94	653.46	648.94	651.88	655.81	639.92	638.06	641.52	403.29	373.63	380.33	390.40	385.20	339.97	212.55
283.96	439.24	562.63	525.78	496.05	463.29	480.55	545.80	606.39	77.77	71.38	75.86	74.11	77.43	91.94	88.73
364.86	268.54	287.47	299.89	329.08	342.41	388.25	400.86	227.30	30.96	21.40	23.77	21.67	21.03	23.46	28.70
772.30	317.31	225.62	255.98	326.49	370.99	383.14	289.36	108.20	19.77	11.02	11.54	11.92	12.00	12.46	14.87
621.02	293.03	224.33	300.13	436.04	501.98	428.44	236.27	74.31	17.67	8.81	8.89	10.65	11.72	11.86	12.87
308.79	206.74	222.90	375.25	605.66	677.65	483.57	212.43	62.23	18.18	9.94	10.40	13.26	15.05	14.88	14.78
208.55	174.89	231.41	423.73	687.04	733.26	475.98	193.53	59.12	20.61	12.56	13.27	16.62	18.58	18.04	17.03

Table H.60: These are the resistivities after the 5th iteration using the measurement-corrected adjoint method Jacobian.

307.96	649.19	582.59	574.54	602.45	626.09	602.11	563.94	555.55	404.13	392.58	398.08	403.51	398.63	362.37	218.16
226.95	460.17	596.01	585.68	528.42	474.59	485.54	577.98	659.50	75.87	65.95	68.38	68.66	71.90	84.74	84.25
316.01	272.90	283.69	289.72	321.86	340.92	388.96	428.89	248.42	27.62	22.90	25.16	21.53	20.22	21.67	26.71
778.60	321.82	215.17	228.94	294.39	355.30	386.02	313.43	116.91	18.42	12.03	12.72	12.37	12.13	12.20	14.41
627.30	288.84	220.38	283.07	403.02	487.88	445.87	262.22	80.92	17.38	9.28	9.27	10.82	12.00	12.16	13.11
271.43	187.56	223.04	380.77	595.70	683.85	518.36	238.49	67.51	17.93	9.85	10.11	12.81	15.10	15.52	15.55
172.94	152.84	231.65	444.76	703.71	759.02	514.53	214.20	62.31	19.80	11.87	12.35	15.50	18.21	18.72	18.04

Table H.61: These are the resistivities after the 6th iteration using the measurement-corrected adjoint method Jacobian.

277.05	624.68	551.91	535.01	576.32	612.42	584.44	527.12	516.18	406.60	404.07	408.24	410.65	405.79	374.64	222.65
206.90	469.54	613.85	619.54	547.40	482.63	496.11	603.32	680.42	74.63	62.58	64.00	65.86	69.28	80.93	82.80
301.79	280.64	284.15	290.10	322.62	345.73	399.03	447.44	255.51	27.05	23.68	25.85	21.49	19.66	20.56	26.02
776.38	331.13	212.04	218.93	285.33	355.09	391.30	317.98	115.81	17.55	12.39	13.36	12.54	11.95	11.93	14.36
637.21	296.97	220.25	274.50	394.84	491.57	455.20	265.89	79.54	16.46	9.17	9.33	10.70	11.83	12.21	13.44
271.00	191.23	226.99	380.66	600.62	705.30	541.81	247.83	67.93	17.21	9.46	9.72	12.28	14.75	15.73	16.17
173.23	156.00	238.20	453.34	723.47	795.25	546.63	227.13	64.27	19.43	11.33	11.63	14.63	17.64	18.92	18.71

Table H.62: These are the resistivities after the 7th iteration using the measurement-corrected adjoint method Jacobian.

220.26	599.05	528.29	508.80	552.86	607.35	585.20	513.54	490.57	411.82	414.75	417.56	416.57	411.94	384.29	224.42
165.50	518.41	652.58	669.58	594.41	496.58	498.17	603.38	725.63	69.52	57.81	59.33	63.12	66.60	78.22	80.07
259.91	275.78	265.32	255.37	278.60	296.84	352.03	432.38	269.75	27.98	26.72	27.70	21.96	19.70	18.93	23.95
775.97	319.48	193.16	187.77	236.44	300.64	353.60	321.83	121.63	16.72	12.34	13.11	12.31	11.87	11.06	13.23
651.54	294.70	228.31	290.02	408.15	510.44	490.04	299.79	84.85	14.70	7.62	7.87	9.93	11.88	12.04	13.11
258.07	191.89	273.06	518.11	826.82	949.66	712.37	310.22	73.37	15.04	7.63	8.32	11.95	15.73	16.79	16.98
161.85	159.56	308.36	698.97	1157.4	1229.1	792.29	295.83	69.82	17.45	9.73	10.86	15.35	19.84	21.23	20.52

Table H.63: These are the resistivities after the 8th iteration using the measurement-corrected adjoint method Jacobian.

196.98	587.63	520.56	494.83	538.94	605.15	587.27	507.21	479.76	414.85	421.43	423.38	419.87	415.29	389.70	223.45
145.47	518.61	654.46	689.90	609.15	495.88	497.06	609.50	727.54	68.86	55.38	56.75	61.74	65.56	76.22	77.59
238.63	277.66	259.94	245.78	276.08	300.62	352.06	429.92	270.56	27.73	28.11	28.79	22.32	19.58	18.14	22.90
771.07	338.44	197.05	177.06	228.30	306.73	363.68	331.28	126.52	17.09	12.76	13.28	12.30	11.83	10.86	12.98
669.36	319.80	243.74	284.66	399.13	522.32	514.02	317.60	89.44	14.86	7.52	7.58	9.59	11.84	12.26	13.44
278.23	213.61	298.21	520.42	809.85	957.38	740.40	326.67	75.92	14.70	7.21	7.74	11.35	15.74	17.63	18.10
177.98	178.64	336.94	707.12	1132.4	1222.6	809.75	305.15	70.14	16.53	8.99	10.04	14.59	19.96	22.56	22.23

Table H.64: These are the resistivities after the 9th iteration using the measurement-corrected adjoint method Jacobian.

166.49	564.50	505.50	480.53	516.71	588.52	584.37	505.60	470.13	420.39	429.27	430.15	423.94	419.59	394.84	227.51
121.18	580.56	698.60	741.01	679.92	548.90	533.95	619.19	756.07	62.74	50.63	52.70	59.00	62.82	75.40	77.59
201.81	258.33	225.86	202.85	220.59	239.51	275.87	369.55	278.80	31.55	33.86	33.02	24.39	20.71	16.87	21.60
766.68	313.13	171.49	146.54	173.50	226.85	279.53	308.24	133.69	15.24	11.11	11.54	11.28	11.55	9.80	11.91
689.06	320.72	272.37	332.76	429.49	527.35	533.37	375.33	102.97	12.10	4.99	5.03	7.51	11.11	11.67	12.99
259.75	222.06	425.12	890.95	1343.2	1459.5	1095.6	484.51	94.88	12.58	5.23	6.00	10.34	16.46	18.64	19.03
160.99	190.40	532.15	1441.2	1784.4	1784.4	1426.1	490.40	89.81	15.58	8.01	10.12	16.46	23.59	25.82	24.69

Table H.65: These are the resistivities after the 10th iteration using the measurement-corrected adjoint method Jacobian.

152.15	554.00	501.58	473.64	505.01	584.44	585.34	504.71	466.71	423.40	434.62	434.69	426.75	422.16	398.31	224.87
107.90	582.05	696.92	752.51	686.60	536.50	529.14	627.01	753.96	62.17	48.36	50.55	57.20	61.91	73.81	74.84
179.43	252.57	218.89	194.85	220.24	246.24	271.08	341.37	266.53	31.16	36.21	35.41	25.95	21.07	16.28	20.62
761.94	332.94	180.27	142.77	178.21	250.36	300.20	317.40	147.58	16.94	11.08	10.95	11.16	11.76	9.84	11.82
705.74	347.64	299.05	339.75	459.89	605.94	614.53	425.86	120.39	13.28	4.76	4.51	7.03	11.22	12.21	13.58
275.78	241.99	452.27	874.80	1381.1	1612.7	1235.9	542.65	105.25	12.86	4.90	5.46	9.82	16.91	20.22	20.80
174.31	208.40	549.04	1360.8	1784.4	1784.4	1539.83	524.00	92.06	14.67	7.40	9.47	16.07	24.58	28.41	27.46

Table H.66: These are the resistivities after the 11th iteration using the measurement-corrected adjoint method Jacobian.

141.86	537.53	492.11	466.57	491.91	563.34	567.75	499.64	462.62	427.64	439.69	439.18	430.23	425.49	401.77	229.72
97.33	630.13	731.65	783.43	734.09	599.47	598.72	667.74	768.89	57.41	45.25	47.77	54.35	59.35	72.88	76.33
154.29	227.95	190.57	167.67	185.67	202.82	208.70	262.47	262.38	36.25	41.53	40.36	29.69	22.93	15.84	20.71
757.87	307.72	161.49	130.27	152.65	196.13	225.06	268.05	151.30	14.37	8.66	8.62	9.62	11.29	9.32	11.69
722.40	352.69	346.19	430.92	546.89	647.09	640.50	495.27	143.94	11.16	3.21	2.93	5.06	9.94	11.75	13.62
252.46	253.54	652.24	1528.3	1784.4	1784.4	1784.4	813.44	140.61	12.08	4.05	4.69	8.99	17.04	20.79	21.34
157.26	225.52	866.53	1784.4	1784.4	1784.4	1784.4	832.14	120.74	14.49	7.48	11.03	19.36	28.76	30.96	28.61

Table H.67: These are the resistivities after the 12th iteration using the measurement-corrected adjoint method Jacobian.

134.72	529.40	489.67	463.96	485.54	555.46	558.05	494.95	461.37	430.27	443.48	442.33	432.93	427.57	404.47	231.34
90.22	634.97	730.32	787.70	737.77	595.55	604.02	684.75	771.51	56.73	43.76	46.35	52.52	58.43	71.47	76.23
137.21	222.41	185.39	162.24	180.96	201.47	199.10	231.59	239.47	35.96	43.38	42.35	31.86	23.68	15.68	20.88
755.19	325.60	169.98	130.88	158.33	211.90	237.99	272.18	169.25	16.41	8.33	7.98	9.43	11.54	9.59	12.16
735.99	370.27	368.93	456.08	629.07	787.67	766.15	565.74	168.86	12.18	2.98	2.66	4.81	10.06	12.37	14.45
247.97	252.07	645.90	1572.6	1784.4	1784.4	1784.4	925.57	153.38	12.24	3.95	4.60	9.01	17.62	22.07	22.74
153.54	220.31	821.49	1784.4	1784.4	1784.4	1784.4	921.61	122.88	13.59	7.47	11.30	20.01	29.98	32.71	30.29

Table H.68: These are the resistivities after the 13th iteration using the measurement-corrected adjoint method Jacobian.

130.12	515.68	481.60	460.05	477.33	531.43	528.48	483.96	456.61	433.37	446.80	445.18	435.91	430.47	408.07	240.20
85.21	679.93	764.46	810.89	775.46	673.31	702.00	752.34	798.01	53.22	41.78	44.66	50.16	55.87	69.54	80.39
121.16	197.57	157.84	140.43	152.38	160.13	147.28	157.60	209.03	40.16	47.11	46.46	36.38	26.23	16.02	22.88
753.69	303.36	156.76	127.36	144.31	169.41	183.60	225.20	170.96	13.61	6.21	5.74	7.33	10.77	9.68	13.21
749.58	389.05	465.54	642.37	838.49	939.64	908.04	740.19	234.95	12.13	2.20	1.71	3.19	8.53	12.20	14.92
208.21	263.47	1003.3	1784.4	1784.4	1784.4	1784.4	1553.4	231.37	13.50	3.99	4.64	8.95	18.38	22.44	21.82
127.36	233.76	1356.3	1784.4	1784.4	1784.4	1784.4	1521.5	156.58	12.81	8.57	16.07	28.48	38.28	34.65	27.91

Table H.69: These are the resistivities after the 14th iteration using the measurement-corrected adjoint method Jacobian.

125.32	507.87	478.60	458.85	472.94	518.42	511.68	477.10	455.22	435.67	449.14	447.04	438.10	432.26	411.35	247.64
82.24	688.11	767.23	814.19	782.36	686.76	717.65	769.30	799.62	52.51	41.16	43.95	48.89	55.05	67.57	83.57
110.71	193.51	149.98	133.36	142.02	149.62	134.93	135.17	192.11	39.64	48.04	47.24	37.92	26.99	16.22	25.03
756.24	316.74	161.16	129.62	148.36	176.56	191.17	227.26	192.98	15.51	5.80	5.50	7.24	11.20	10.81	15.37
757.80	393.09	480.09	723.11	1049.2	1226.0	1120.0	802.03	246.78	12.17	2.00	1.65	3.13	8.76	13.74	16.96
186.50	244.32	987.30	1784.4	1784.4	1784.4	1784.4	1705.0	227.19	13.16	4.47	5.29	9.60	18.96	23.35	22.25
113.47	217.00	1345.1	1784.4	1784.4	1784.4	1784.4	1714.9	152.77	11.85	10.22	18.91	30.41	38.10	33.13	25.93

Table H.70: These are the resistivities after the 15th iteration using the measurement-corrected adjoint method Jacobian.

118.85	494.61	470.48	455.79	465.67	492.36	482.74	465.19	450.35	438.06	451.12	448.27	439.94	434.59	417.49	268.77
81.30	735.76	804.03	836.12	819.52	778.90	814.55	838.35	841.26	49.85	40.07	43.37	47.48	52.88	62.95	96.36
104.82	167.43	123.00	113.46	116.70	113.56	98.81	88.76	141.17	42.72	50.15	49.71	42.17	30.15	17.34	34.40
769.10	296.40	154.35	133.18	142.36	149.55	173.67	231.16	206.09	11.50	4.07	3.67	4.88	9.36	13.00	23.08
761.16	432.78	676.13	1181.2	1643.8	1742.2	1675.5	1412.3	479.33	16.32	1.70	1.06	1.81	6.69	16.38	21.75
138.43	260.93	1728.5	1784.4	1784.4	1784.4	1784.4	1784.4	391.61	19.47	7.56	7.74	11.85	23.30	27.23	19.84
86.68	239.73	1784.4	1784.4	1784.4	1784.4	1784.4	1784.4	152.26	9.96	17.99	42.54	64.05	66.16	37.13	17.61

Table H.71: These are the resistivities after the 16th iteration using the measurement-corrected adjoint method Jacobian.

107.13	486.87	466.76	454.41	461.53	479.11	467.68	457.88	448.10	440.18	451.95	448.35	440.37	435.10	423.48	282.02
83.27	745.97	810.77	841.70	829.42	797.24	831.93	853.88	837.71	49.27	40.54	43.80	47.72	53.42	59.35	104.47
104.63	163.02	112.33	104.24	103.73	100.49	87.59	76.15	140.23	40.18	48.74	47.63	41.21	29.38	16.88	44.30
816.76	309.87	161.39	141.79	153.02	163.25	182.27	222.36	219.19	17.81	4.87	5.18	5.89	9.84	18.74	40.77
726.19	415.30	693.90	1446.9	1784.4	1784.4	1784.4	1211.2	270.39	10.43	1.60	1.32	1.99	7.15	28.18	39.03
119.40	232.64	1712.5	1784.4	1784.4	1784.4	1784.4	1784.4	236.52	12.95	10.81	10.86	13.41	25.69	37.65	23.71
73.35	215.03	1784.4	1784.4	1784.4	1784.4	1784.4	1784.4	136.47	9.66	30.97	54.69	62.44	61.68	34.81	13.19

Table H.72: These are the resistivities after the 17th iteration using the measurement-corrected adjoint method Jacobian.

98.92	478.32	462.21	452.25	456.84	466.21	455.37	454.46	446.24	442.54	452.07	447.61	439.88	435.68	428.15	306.23
83.39	777.25	831.05	855.81	849.64	840.32	868.07	867.59	859.35	46.69	40.75	44.57	48.33	52.41	56.70	126.08
106.93	144.24	97.32	92.08	90.69	85.48	74.86	64.55	121.98	45.74	46.98	47.14	40.98	32.40	18.11	64.34
868.81	301.07	171.19	153.55	157.95	160.06	197.77	271.15	207.19	8.32	4.68	4.45	5.07	6.55	15.83	54.61
722.98	458.94	906.99	1784.4	1784.4	1784.4	1784.4	1784.4	644.83	24.42	2.06	1.17	2.05	6.07	32.28	53.32
113.46	255.82	1784.4	1784.4	1784.4	1784.4	1784.4	1784.4	382.43	34.71	21.40	15.02	19.47	37.87	58.88	28.31
63.50	212.64	1784.4	1784.4	1784.4	1784.4	1784.4	1784.4	79.11	8.56	45.21	84.31	105.69	109.12	49.76	10.79

Table H.73: These are the resistivities after the 18th iteration using the measurement-corrected adjoint method Jacobian.

101.47	472.62	460.16	451.34	454.66	459.96	448.19	453.01	446.13	444.20	451.82	446.29	438.70	435.32	429.85	306.61
76.14	790.17	836.08	858.78	853.99	850.71	878.14	869.23	850.14	46.81	41.21	45.56	49.49	53.18	57.80	129.85
111.14	132.72	90.57	87.06	84.23	79.24	69.99	59.92	128.47	40.90	45.69	44.80	39.75	30.32	14.46	68.62
1015.1	321.56	175.38	156.71	162.49	164.19	193.38	269.51	316.60	17.42	5.44	5.37	5.54	8.04	23.49	94.96
670.38	475.91	912.39	1784.4	1784.4	1784.4	1784.4	1079.0	203.56	9.01	1.88	1.46	2.29	8.89	64.34	116.21
109.45	261.66	1784.4	1784.4	1784.4	1784.4	1784.4	1784.4	117.97	15.39	19.88	15.97	16.57	33.74	71.72	44.40
59.14	200.60	1784.4	1784.4	1784.4	1784.4	1784.4	1484.03	51.30	13.04	65.27	83.07	65.19	55.05	30.73	9.94

Table H.74: These are the resistivities after the 19th iteration using the measurement-corrected adjoint method Jacobian.

94.74	470.65	459.71	451.00	453.70	458.77	447.50	452.41	443.88	445.19	451.02	445.16	438.50	435.80	432.84	398.35
77.14	790.06	836.01	860.56	856.09	848.48	873.05	872.49	865.48	46.48	42.05	46.22	49.00	51.92	55.21	193.37
111.64	133.81	88.31	83.69	81.02	77.43	69.05	57.37	122.16	40.22	43.72	44.36	39.56	32.98	18.48	101.26
1085.5	320.19	174.49	164.62	169.12	171.14	207.16	268.47	191.08	10.87	6.38	6.12	5.67	5.97	10.87	56.69
709.16	446.07	871.70	1784.4	1784.4	1784.4	1784.4	1704.2	615.05	30.51	1.82	1.09	2.33	7.67	29.84	54.22
101.55	226.48	1784.4	1784.4	1784.4	1784.4	1784.4	1784.4	244.88	45.12	17.00	11.93	20.50	50.90	65.55	30.51
53.29	174.09	1784.4	1784.4	1784.4	1784.4	1784.4	696.08	30.81	15.09	41.64	61.43	87.10	105.92	44.53	9.81

Table H.75: These are the resistivities after the 20th iteration using the measurement-corrected adjoint method Jacobian.

89.73	466.07	456.92	449.87	451.69	453.19	442.22	449.66	443.19	445.08	450.48	444.85	439.13	436.70	430.04	262.35
75.57	813.69	852.09	867.77	866.40	877.52	900.25	888.20	872.45	47.52	41.88	45.71	48.26	50.75	60.94	112.68
120.68	116.83	79.19	78.81	75.41	67.53	60.30	51.63	98.30	35.35	45.65	46.83	43.65	35.40	14.25	62.57
1237.2	353.61	202.11	170.81	176.84	186.77	255.72	367.22	521.76	19.91	4.69	3.79	3.06	4.24	16.34	99.58
486.31	489.52	1091.0	1784.4	1784.4	1784.4	1784.4	1784.4	279.69	8.69	1.33	1.14	1.98	8.82	83.71	169.34
88.42	269.03	1784.4	1784.4	1784.4	1784.4	1784.4	1784.4	111.73	31.87	34.04	22.49	25.37	63.63	135.68	56.52
50.89	191.61	1784.4	1784.4	1784.4	1784.4	1784.4	1007.1	29.37	50.25	176.73	157.75	137.33	142.34	58.62	7.63

Table H.76: These are the resistivities after the 21st iteration using the measurement-corrected adjoint method Jacobian.

90.71	463.25	456.05	449.46	451.14	453.36	445.44	452.24	443.18	445.35	449.48	443.92	439.32	437.00	431.16	245.88
70.96	818.89	851.32	869.30	866.82	863.31	874.13	863.51	870.78	46.96	42.98	46.52	48.22	50.45	58.40	113.87
127.46	113.18	77.50	75.97	73.56	69.26	63.73	55.48	99.94	35.29	44.26	45.50	43.87	36.66	14.88	79.23
1269.6	342.58	187.51	176.66	174.73	162.95	200.05	308.02	361.91	12.83	5.43	4.72	2.87	3.32	12.25	87.12
452.26	439.27	983.42	1784.4	1784.4	1784.4	1483.9	882.96	375.36	15.56	1.30	1.34	2.74	14.55	95.54	141.73
85.60	241.73	1784.4	1784.4	1784.4	1784.4	1784.4	713.22	122.79	78.03	14.43	8.80	17.14	80.03	178.40	54.07
49.44	167.57	1784.4	1784.4	1784.4	1784.4	1784.4	359.83	27.47	110.82	66.70	39.74	56.11	126.75	72.76	7.39

Table H.77: These are the resistivities after the 22nd iteration using the measurement-corrected adjoint method Jacobian.

97.45	462.27	456.19	449.58	450.92	453.07	445.63	450.69	441.63	444.61	449.33	444.73	440.40	437.28	431.11	245.00
62.74	819.00	849.68	867.70	868.09	869.23	883.89	880.01	881.01	48.45	42.35	45.07	47.07	50.16	59.11	137.62
130.82	112.07	78.24	75.64	71.64	64.81	59.83	53.09	91.79	33.79	47.48	48.32	46.21	38.21	13.75	120.25
1341.3	328.94	179.40	171.36	186.18	202.40	283.82	399.59	330.78	10.20	3.18	3.21	2.06	2.77	14.47	173.60
583.00	450.90	872.19	1784.4	1784.4	1784.4	1784.4	1784.4	480.54	24.31	1.56	1.15	2.36	13.68	120.92	247.57
88.36	238.34	1784.4	1784.4	1784.4	1784.4	1784.4	1344.4	172.74	102.63	24.72	16.66	29.11	123.86	232.13	63.77
49.49	175.89	1784.4	1784.4	1784.4	1784.4	1784.4	461.08	38.39	144.22	134.60	111.87	147.54	293.20	102.90	6.06

Table H.78: These are the resistivities after the 23rd iteration using the measurement-corrected adjoint method Jacobian.

105.25	459.18	454.26	448.76	449.70	451.65	446.36	449.45	442.35	444.49	448.77	444.91	440.53	437.97	427.80	139.40
58.17	842.58	861.56	874.42	873.74	872.72	882.58	881.94	886.10	48.10	42.97	45.09	47.66	49.19	63.90	94.11
128.01	94.11	72.74	72.02	69.27	64.48	58.29	52.60	76.11	33.25	48.44	47.24	45.50	38.99	11.54	117.65
1141.7	347.41	206.66	184.60	190.01	185.32	283.97	454.50	469.18	9.86	2.04	3.78	2.96	3.08	9.68	159.05
371.68	595.19	1364.1	1784.4	1784.4	1784.4	1784.4	1784.4	612.08	22.82	1.94	1.67	1.94	20.70	193.32	283.19
70.05	349.39	1784.4	1784.4	1784.4	1784.4	1784.4	1317.4	228.62	210.31	42.91	14.75	19.60	196.39	535.13	79.67
43.19	216.18	1784.4	1784.4	1784.4	1784.4	1784.4	457.13	50.84	284.32	187.38	71.91	99.12	506.20	264.90	5.69

Table H.79: These are the resistivities after the 24th iteration using the measurement-corrected adjoint method Jacobian.

106.05	457.59	453.37	448.66	449.65	450.70	447.36	448.99	442.54	444.08	447.81	445.17	440.79	437.40	426.32	110.16
55.53	836.86	861.54	873.15	873.20	873.76	878.27	880.71	886.57	48.51	43.87	44.66	47.32	50.64	64.17	78.87
139.56	97.23	72.44	71.40	68.42	64.71	58.70	52.78	73.15	32.66	48.86	46.64	45.89	36.90	10.22	171.21
1142.5	307.61	181.94	177.30	183.89	181.77	266.05	428.65	311.60	7.78	1.26	3.69	2.90	3.43	11.67	411.40
299.68	420.66	1106.7	1784.4	1784.4	1784.4	1784.4	1784.4	758.80	52.05	3.25	2.37	2.27	23.51	232.65	562.53
60.35	290.19	1784.4	1784.4	1784.4	1784.4	1784.4	1376.0	302.98	294.02	52.99	17.59	14.43	131.39	390.43	94.00
40.40	231.76	1784.4	1784.4	1784.4	1784.4	1784.4	464.07	68.37	302.82	181.74	66.00	54.00	268.54	159.51	5.37

Table H.80: These are the resistivities after the 25th iteration using the measurement-corrected adjoint method Jacobian.

110.20	456.49	453.64	448.97	449.76	450.73	446.88	447.90	443.13	443.30	447.33	445.88	440.91	437.72	424.75	116.47
53.72	845.49	858.95	871.32	871.56	872.63	884.26	887.78	889.79	49.30	43.63	44.09	47.57	49.80	66.10	79.54
139.43	94.08	73.43	72.23	69.24	64.94	57.04	51.30	66.05	32.52	49.61	48.01	45.84	37.17	9.88	84.48
581.04	268.76	178.71	168.83	176.41	181.15	288.20	468.09	427.52	7.55	.98	2.44	2.25	3.79	7.02	98.54
237.91	518.76	1101.8	1784.4	1784.4	1784.4	1784.4	1784.4	834.13	68.95	5.71	3.50	3.10	25.86	196.31	256.89
56.50	424.88	1784.4	1784.4	1784.4	1784.4	1784.4	1784.4	407.28	233.05	52.68	24.80	33.01	376.08	984.22	98.73
35.93	342.81	1784.4	1784.4	1784.4	1784.4	1784.4	834.62	117.31	231.62	128.83	70.98	122.01	1169.0	558.48	5.21

Table H.81: These are the resistivities after the 26th iteration using the measurement-corrected adjoint method Jacobian.

109.66	454.88	452.76	448.91	449.84	450.15	446.85	447.09	443.94	442.59	446.93	446.51	441.58	437.89	422.09	96.68
54.16	856.51	864.77	873.56	871.16	872.92	882.73	890.51	889.86	49.45	43.79	43.64	46.96	50.37	67.60	35.96
135.22	87.24	70.96	71.05	70.57	68.33	57.40	49.68	61.51	32.77	50.60	47.75	47.04	36.33	9.20	90.32
495.76	301.02	195.19	177.42	162.57	145.20	259.97	551.30	467.93	7.00	.83	2.48	1.96	3.33	9.03	526.50
111.91	553.88	1337.3	1784.4	1784.4	1784.4	1784.4	1784.4	752.15	77.19	7.45	5.51	3.85	44.09	304.60	1138.7
75.98	701.52	1784.4	1784.4	1784.4	1784.4	1784.4	1784.4	413.39	505.08	135.04	37.67	20.52	112.61	277.58	157.50
31.32	424.91	1784.4	1784.4	1784.4	1784.4	1784.4	944.15	168.50	828.65	444.52	93.82	45.07	105.63	52.17	4.85

Table H.82: These are the resistivities after the 27th iteration using the measurement-corrected adjoint method Jacobian.

119.85	454.52	453.42	449.29	450.21	449.92	446.95	447.03	445.01	442.92	447.27	447.18	441.91	438.65	421.58	109.42
50.36	848.06	857.67	871.42	872.07	873.38	882.48	888.57	889.21	48.73	43.10	43.44	47.03	48.94	67.74	41.66
129.07	93.38	75.09	70.94	70.00	70.12	56.89	48.77	59.50	33.66	51.91	48.09	47.65	38.00	9.92	67.55
393.84	238.88	153.48	180.28	172.34	147.05	287.28	594.27	392.46	6.78	.76	2.27	1.34	3.38	6.45	74.72
196.01	474.17	945.48	1784.4	1784.4	1784.4	1784.4	1760.5	558.76	136.78	4.48	5.50	6.93	45.98	351.19	407.82
106.89	545.89	1784.4	1784.4	1784.4	1784.4	1784.4	1721.8	370.99	1035.5	218.76	79.35	68.89	419.34	1265.9	199.58
30.31	337.11	1784.4	1784.4	1784.4	1784.4	1784.4	1207.3	251.95	1784.4	1437.0	261.49	113.26	344.25	179.58	4.45

Table H.83: These are the resistivities after the 28th iteration using the measurement-corrected adjoint method Jacobian.

122.01	454.18	452.33	449.49	450.27	447.85	446.58	448.52	445.08	443.13	446.81	447.48	442.67	439.67	419.78	183.95
50.59	856.68	867.01	872.11	869.79	880.25	880.71	879.78	889.73	48.56	43.87	43.27	46.36	48.58	67.98	36.89
117.85	86.69	70.85	70.19	71.56	71.99	59.40	50.35	57.90	34.04	51.42	47.93	48.24	39.16	11.24	55.27
330.30	284.85	196.14	182.43	150.77	133.44	214.95	435.69	329.38	6.50	.69	3.06	1.46	2.62	6.43	184.06
253.50	860.68	1612.3	1784.4	1784.4	1784.4	1784.4	1587.1	1496.3	414.48	5.81	3.58	6.71	38.37	194.92	834.68
155.66	870.66	1784.4	1784.4	1784.4	1784.4	1784.4	1210.1	725.86	1577.9	160.22	47.05	65.94	243.32	354.00	170.68
26.92	301.90	1784.4	1784.4	1784.4	1784.4	1784.4	591.22	241.09	1212.1	614.47	194.20	179.26	303.72	71.26	4.34

Table H.84: These are the resistivities after the 29th iteration using the measurement-corrected adjoint method Jacobian.

124.22	452.92	451.65	449.11	449.65	446.87	446.29	448.23	445.33	443.20	446.48	447.80	443.13	440.23	419.31	174.78
49.42	859.17	867.12	874.17	874.83	884.90	887.30	884.66	890.92	48.42	43.93	43.04	46.12	48.09	67.78	30.00
119.10	86.39	70.45	68.99	70.77	68.62	55.53	49.07	55.32	34.41	51.83	48.29	48.85	39.95	11.91	112.08
299.17	233.21	181.88	185.20	147.94	153.87	340.32	825.82	473.82	6.48	.61	2.18	1.41	2.79	6.33	168.25
216.68	719.78	1405.0	1784.4	1784.4	1784.4	1784.4	1623.0	461.78	128.06	6.37	7.67	4.23	38.37	420.95	813.72
235.18	1135.2	1784.4	1784.4	1784.4	1784.4	1784.4	1675.8	928.27	1784.4	593.98	124.94	73.02	406.31	1139.7	267.50
24.57	392.32	1784.4	1784.4	1784.4	1784.4	1784.4	943.48	1052.1	1784.4	1784.4	495.51	216.60	431.94	99.86	3.97

Table H.85: These are the resistivities after the 30th iteration using the measurement-corrected adjoint method Jacobian.

124.53	452.33	450.93	448.96	449.52	448.44	448.88	449.01	445.32	443.54	446.19	447.90	443.46	440.45	419.69	198.11
50.12	863.04	870.24	875.33	872.31	867.44	868.21	878.03	896.09	47.74	44.24	43.08	45.93	48.26	66.69	31.86
115.80	84.37	68.68	68.07	72.95	79.64	61.97	50.97	52.44	34.99	52.04	47.70	48.45	40.00	13.33	94.53
206.42	233.40	190.90	180.18	132.29	93.91	157.30	344.90	226.30	5.97	.56	3.62	1.71	2.68	5.75	276.37
514.93	1155.8	1784.4	1784.4	1784.4	1784.4	1189.9	1784.4	1784.4	617.17	9.33	2.43	4.48	42.21	309.50	1465.4
258.95	1039.6	1784.4	1784.4	1784.4	1784.4	1784.4	1589.0	1784.4	1784.4	221.58	46.09	61.42	331.14	691.93	293.53
22.23	245.1	1784.4	1784.4	1784.4	1784.4	1784.4	1024.4	1292.0	1784.4	943.87	273.72	221.74	412.14	95.15	3.87

Table H.86: These are the resistivities after the 31st iteration using the measurement-corrected adjoint method Jacobian.

126.70	451.77	449.66	448.38	449.04	445.83	448.32	449.83	446.53	443.29	446.08	448.25	443.40	440.43	420.32	156.89
50.27	863.23	876.63	879.90	879.00	887.52	883.79	876.96	887.57	48.65	43.93	42.70	46.15	48.23	65.98	32.75
118.71	84.55	63.93	64.27	69.76	77.46	56.42	48.31	48.09	35.35	52.42	48.60	48.55	40.35	14.47	126.76
100.62	221.20	249.87	213.83	141.36	101.51	346.58	1558.1	777.23	5.85	.51	2.44	1.35	2.55	5.30	255.60
861.27	1784.4	1784.4	1784.4	1784.4	1784.4	1784.4	1784.4	1147.0	175.32	11.53	4.55	5.07	41.45	447.48	1507.7
503.90	1284.3	1784.4	1784.4	1784.4	1784.4	1784.4	1784.4	1336.7	1522.8	548.05	149.63	121.78	595.05	1556.0	409.86
21.38	126.21	1784.4	1784.4	1784.4	1784.4	1784.4	1194.4	779.32	1784.4	1784.4	941.72	467.78	798.30	143.31	3.64

H.6 Result of potential-corrected adjoint method Jacobian

Table H.87: These are the resistivities after the 1st iteration using the potential-corrected adjoint method Jacobian.

1784.4	1784.4	1784.4	1784.4	1784.4	1784.4	1784.4	1784.4	1321.56	499.12	363.49	346.95	401.05	404.53	322.68	217.78
1784.4	1784.4	1784.4	1784.4	1784.4	1784.4	1784.4	1784.4	745.06	143.12	96.05	98.80	101.65	105.51	110.90	107.92
1589.2	1784.4	1784.4	1784.4	1784.4	1784.4	1784.4	793.75	166.48	40.40	27.40	27.19	22.79	23.42	32.12	43.64
728.36	969.71	1606.6	1784.4	1784.4	1280.2	533.67	162.09	42.62	18.38	17.02	18.49	15.34	15.08	20.81	30.24
334.23	387.79	558.05	721.09	651.81	365.43	139.07	44.90	17.81	14.07	20.34	28.20	26.72	25.75	31.93	41.55
185.72	194.84	248.36	293.49	249.19	135.25	52.79	20.31	11.96	15.32	33.00	59.90	67.05	65.36	73.15	81.36
148.55	148.48	173.12	188.51	152.97	84.06	35.58	16.16	12.04	18.93	46.63	94.88	119.08	119.82	126.17	126.02

Table H.88: These are the resistivities after the 2nd iteration using the potential-corrected adjoint method Jacobian.

1062.8	1152.4	1131.1	1108.1	1102.6	1092.0	1112.8	1153.1	921.66	416.31	329.48	324.70	349.67	344.87	278.74	194.34
923.33	794.24	883.98	885.62	893.09	917.37	947.81	882.77	472.89	119.27	84.45	91.66	93.71	95.92	104.43	100.90
862.77	595.78	608.69	678.49	712.30	702.58	629.04	423.93	157.99	37.24	21.41	22.34	23.39	25.61	33.09	40.37
825.36	553.03	494.27	546.51	566.80	513.43	385.34	209.40	74.33	22.11	11.98	10.97	11.38	12.95	16.87	21.40
604.33	466.08	418.96	444.62	447.79	381.17	259.28	133.36	52.91	20.44	11.60	9.72	9.79	11.11	13.82	16.69
435.52	374.84	356.61	374.37	369.12	304.69	201.72	107.04	48.86	23.02	14.04	11.40	11.19	12.44	14.80	16.80
372.53	339.49	331.78	340.88	327.20	266.10	177.21	98.81	50.10	26.59	17.04	13.66	13.11	14.22	16.30	17.66

Table H.89: These are the resistivities after the 3rd iteration using the potential-corrected adjoint method Jacobian.

744.01	853.27	842.52	800.74	790.11	775.57	787.32	817.84	735.25	386.89	334.07	337.66	351.42	344.64	293.00	200.87
600.52	494.00	562.71	588.40	596.73	619.11	645.61	642.16	427.07	107.50	79.11	89.10	90.02	91.13	100.31	98.73
624.58	376.34	349.06	398.49	448.89	478.70	462.30	355.54	157.68	35.46	20.06	21.74	22.60	23.78	29.86	37.32
787.03	409.90	296.48	320.38	372.31	389.33	334.02	207.59	80.02	21.96	11.20	10.35	10.68	11.71	14.88	19.20
606.84	369.94	271.37	286.61	332.26	337.18	266.63	151.58	60.60	20.99	10.80	8.81	8.77	9.71	11.97	14.69
392.29	289.56	244.31	267.67	310.43	308.74	235.99	133.42	58.49	24.30	13.24	10.22	9.78	10.67	12.66	14.58
306.07	253.72	235.76	261.34	296.03	287.43	217.48	126.28	60.43	28.41	16.33	12.34	11.46	12.16	13.89	15.21

Table H.90: These are the resistivities after the 4th iteration using the potential-corrected adjoint method Jacobian.

459.15	725.03	677.07	660.51	671.37	678.78	667.60	666.23	624.92	395.79	364.60	371.60	380.38	374.46	335.63	215.44
356.96	445.30	567.59	538.96	509.25	475.87	497.66	553.47	590.22	81.70	74.40	78.92	77.61	81.04	92.44	91.99
451.91	279.37	288.93	316.31	342.45	353.40	399.02	401.99	228.99	32.33	21.56	23.62	22.49	21.71	24.17	30.56
848.75	315.97	221.96	264.83	334.94	375.00	381.32	282.41	107.38	20.53	11.61	12.10	12.37	12.05	12.74	15.78
578.63	265.98	208.62	292.83	425.80	483.84	406.79	222.52	71.63	18.00	9.61	9.67	10.88	11.31	11.69	13.21
254.37	173.07	195.74	344.82	560.21	621.88	440.38	194.48	58.78	18.13	10.64	10.99	12.89	13.78	13.94	14.47
168.50	144.36	199.14	377.18	616.23	655.88	425.63	175.38	55.33	20.14	12.97	13.42	15.49	16.43	16.34	16.10

Table H.91: These are the resistivities after the 5th iteration using the potential-corrected adjoint method Jacobian.

376.03	664.93	598.42	586.68	615.50	637.03	615.30	582.60	554.64	400.06	384.99	391.45	396.53	391.24	359.62	220.99
292.71	449.74	587.91	571.38	519.22	471.96	486.69	574.85	650.85	77.32	68.61	71.13	71.15	74.39	85.44	86.98
399.72	279.30	285.20	302.98	328.97	344.96	392.99	428.26	250.92	28.66	22.47	24.45	21.82	20.68	22.36	28.19
863.38	318.91	218.33	246.04	308.90	361.74	385.89	308.42	116.38	19.04	12.46	13.27	12.77	12.17	12.45	15.06
563.11	258.00	213.16	292.52	412.23	483.81	431.14	249.54	77.79	17.49	9.99	10.22	11.25	11.76	11.98	13.21
215.55	155.42	204.24	371.35	580.99	651.74	483.01	219.60	62.86	17.49	10.49	11.03	12.99	14.27	14.60	14.95
137.09	126.58	207.73	418.04	664.12	705.85	470.76	194.66	57.31	18.96	12.29	13.01	15.26	16.79	17.15	16.84

Table H.92: These are the resistivities after the 6th iteration using the potential-corrected adjoint method Jacobian.

344.54	635.86	560.88	546.56	586.98	618.36	590.15	538.41	518.56	404.07	397.95	403.14	405.73	400.65	373.18	224.49
273.61	458.88	606.16	601.90	535.36	478.53	495.80	599.92	675.79	75.38	64.77	66.41	67.65	70.91	81.43	84.48
389.11	288.63	288.42	303.33	330.11	349.38	403.36	448.67	258.13	27.70	22.91	24.73	21.40	19.94	21.15	26.96
866.23	326.42	216.59	237.03	301.35	361.79	391.71	314.46	115.45	18.04	12.71	13.79	12.83	11.99	12.09	14.68
555.23	258.28	212.25	285.55	406.34	487.45	439.57	253.14	76.45	16.55	9.87	10.30	11.23	11.72	11.98	13.26
206.43	152.77	205.46	372.05	587.25	669.94	501.38	226.37	62.76	16.75	10.14	10.80	12.78	14.26	14.88	15.35
131.42	124.52	210.50	425.51	682.37	735.26	494.72	203.47	58.24	18.47	11.85	12.59	14.91	16.77	17.56	17.41

Table H.93: These are the resistivities after the 7th iteration using the potential-corrected adjoint method Jacobian.

272.55	608.77	533.14	519.18	563.09	611.71	586.16	520.30	493.63	409.74	409.37	413.07	412.70	407.95	383.50	226.74
219.28	503.22	645.61	649.41	578.77	490.95	498.33	598.64	719.02	70.37	60.25	61.86	64.86	68.14	78.30	81.79
338.12	282.24	270.62	267.11	286.62	301.92	363.16	443.96	276.25	28.15	25.18	25.56	21.34	19.73	19.50	25.00
873.45	312.85	200.13	205.74	252.57	308.80	360.48	324.38	121.79	17.01	12.91	13.79	12.60	11.76	11.21	13.61
554.43	251.63	222.77	305.02	421.09	503.58	471.76	283.43	80.07	14.64	8.67	9.33	10.78	11.75	11.74	12.90
185.92	147.97	247.07	505.61	797.18	880.60	640.67	273.09	64.71	14.24	8.67	10.10	13.02	15.20	15.64	15.87
116.46	122.95	269.56	647.29	1064.5	1097.3	687.17	251.21	59.38	15.86	10.60	12.72	16.32	18.80	19.32	18.68

Table H.94: These are the resistivities after the 8th iteration using the potential-corrected adjoint method Jacobian.

244.09	596.08	521.91	503.26	548.76	609.26	586.08	510.55	481.12	413.24	416.76	419.28	416.62	412.08	389.32	224.70
194.72	505.94	652.24	673.24	593.66	490.26	497.06	606.54	726.95	69.29	57.62	59.24	63.47	66.81	76.43	78.54
315.72	287.67	264.83	255.50	282.62	303.72	362.38	444.05	277.46	27.73	26.18	26.05	21.28	19.46	18.66	23.49
873.24	330.83	202.02	192.76	244.07	314.33	369.66	333.15	125.25	17.24	13.40	13.91	12.44	11.64	10.88	13.00
559.59	267.94	235.11	299.98	417.16	520.84	496.27	298.16	82.86	14.64	8.63	9.04	10.45	11.74	11.82	12.87
192.23	159.68	267.65	514.99	802.77	910.61	673.76	285.53	65.41	13.68	8.27	9.57	12.64	15.50	16.44	16.66
122.57	133.51	293.38	668.42	1077.8	1126.5	713.68	257.62	58.23	14.72	9.87	12.04	16.02	19.48	20.81	20.17

Table H.95: These are the resistivities after the 9th iteration using the potential-corrected adjoint method Jacobian.

193.38	572.57	506.23	487.29	525.71	592.98	583.28	508.27	471.03	418.43	424.84	425.90	420.58	416.48	394.72	229.29
153.72	562.43	693.50	726.47	663.23	541.58	529.22	609.18	751.88	64.01	53.26	55.62	61.33	64.43	75.09	78.76
265.18	273.95	229.85	207.35	225.58	243.27	290.25	396.89	292.56	30.74	30.49	28.48	22.45	20.33	17.46	22.49
875.76	315.15	180.44	158.22	184.16	232.90	292.27	324.21	134.88	15.44	12.55	12.88	11.54	11.19	9.85	12.16
567.72	274.85	273.32	349.94	438.79	515.56	515.71	355.44	93.84	11.90	6.44	6.83	8.65	10.97	11.20	12.54
173.24	167.72	393.93	871.78	1274.0	1323.0	961.16	406.03	75.78	10.98	6.61	8.50	12.18	15.93	16.96	17.27
108.99	144.10	471.66	1330.2	1784.4	1784.4	1184.3	384.66	66.46	12.34	9.24	13.52	18.78	22.33	22.93	21.77

Table H.96: These are the resistivities after the 10th iteration using the potential-corrected adjoint method Jacobian.

171.16	561.08	500.72	478.49	512.82	588.99	584.75	506.70	465.89	421.41	430.39	430.35	423.10	419.15	397.99	225.36
133.55	567.08	697.98	743.73	674.82	532.29	525.87	617.24	755.61	63.21	50.97	53.48	59.95	63.44	74.04	75.29
239.15	273.30	219.57	195.99	221.61	245.79	281.67	368.56	281.69	30.11	32.27	30.17	23.40	20.54	16.80	20.95
873.93	335.66	184.34	151.43	186.90	252.96	308.84	332.34	146.87	16.95	12.86	12.32	11.24	11.27	9.67	11.55
576.53	295.81	295.02	357.33	474.10	595.84	593.58	401.13	107.29	12.89	6.33	6.13	8.03	11.06	11.49	12.59
182.57	183.36	422.60	881.81	1358.2	1506.2	1103.6	453.97	81.50	10.84	6.33	7.80	11.72	16.73	18.47	18.56
118.19	160.15	500.76	1321.1	1784.4	1784.4	1310.6	409.88	65.51	11.01	8.61	12.84	18.89	24.27	25.90	24.37

Table H.97: These are the resistivities after the 11th iteration using the potential-corrected adjoint method Jacobian.

153.58	544.21	491.27	470.03	497.97	567.39	569.81	502.75	462.02	425.43	435.64	434.87	426.05	422.31	401.46	229.64
117.90	610.22	730.95	776.31	722.68	593.17	587.42	649.11	764.91	59.02	47.97	50.68	57.61	61.18	72.89	76.35
209.55	253.12	189.31	167.96	187.61	204.57	219.15	293.77	285.05	34.41	36.62	34.27	26.24	22.17	16.32	20.96
873.05	316.88	166.67	137.42	159.15	199.05	235.25	293.26	155.10	14.65	10.86	10.32	9.77	10.75	9.17	11.48
584.26	306.00	346.22	444.66	546.39	621.48	613.86	471.63	127.24	10.81	4.71	4.29	5.89	9.80	11.08	12.68
169.56	198.61	615.09	1481.0	1784.4	1784.4	1561.9	657.41	101.85	9.44	5.74	7.38	10.95	16.54	18.70	18.95
111.10	181.46	793.87	1784.4	1784.4	1784.4	1784.4	612.12	77.59	9.54	9.28	16.45	23.16	27.41	27.42	25.01

Table H.98: These are the resistivities after the 12th iteration using the potential-corrected adjoint method Jacobian.

142.08	535.44	488.20	466.24	490.40	559.41	561.80	498.40	459.84	427.83	439.46	437.87	428.26	424.39	403.97	230.33
107.58	616.78	733.21	784.15	730.11	591.32	594.71	668.15	771.69	58.51	46.46	49.30	55.98	60.20	71.76	75.71
191.07	250.73	182.69	161.33	181.13	201.67	206.89	257.43	260.01	33.24	37.98	36.23	28.24	22.83	16.14	20.72
872.11	333.68	171.67	137.04	164.52	214.43	246.41	295.65	173.04	17.03	10.86	9.28	9.33	10.83	9.25	11.48
590.61	317.56	360.60	467.72	629.11	756.74	731.60	539.69	150.58	12.41	4.74	3.80	5.42	9.82	11.43	12.96
170.92	200.19	606.48	1532.1	1784.4	1784.4	1784.4	740.21	109.17	9.61	6.06	7.28	11.05	17.53	20.01	19.90
112.48	182.19	762.68	1784.4	1784.4	1784.4	1784.4	655.80	74.35	8.38	9.60	17.05	24.70	30.14	30.00	26.75

Table H.99: These are the resistivities after the 13th iteration using the potential-corrected adjoint method Jacobian.

133.64	521.33	480.63	461.57	480.98	535.29	534.42	488.58	456.21	430.91	442.90	440.87	430.96	427.24	407.65	238.73
100.61	659.65	764.61	807.55	767.57	664.05	685.80	730.50	788.18	55.13	44.41	47.39	53.58	57.78	69.67	79.34
172.26	224.70	155.17	140.05	153.55	163.15	153.07	176.78	241.71	37.28	41.60	40.83	32.63	25.15	16.37	22.59
873.12	311.98	159.89	132.90	149.32	173.28	189.18	244.18	177.22	13.99	8.43	6.69	7.21	10.23	9.53	12.67
594.80	334.46	450.39	635.31	805.04	879.19	847.66	693.29	200.32	11.86	3.84	2.49	3.56	8.53	11.64	13.66
150.89	216.20	922.65	1784.4	1784.4	1784.4	1784.4	1211.2	154.39	9.82	7.22	8.17	11.10	18.07	20.22	19.03
100.40	202.22	1229.8	1784.4	1784.4	1784.4	1784.4	1052.7	89.07	7.12	12.88	27.52	35.44	36.57	30.37	23.94

Table H.100: These are the resistivities after the 14th iteration using the potential-corrected adjoint method Jacobian.

126.30	512.87	477.37	459.74	476.00	522.45	517.93	481.26	454.66	433.12	445.39	442.56	432.71	429.13	410.90	246.64
96.12	670.26	770.25	813.11	776.75	679.60	706.39	753.37	795.53	54.63	43.69	46.83	52.46	56.77	67.70	82.57
161.03	220.85	146.51	132.45	141.99	150.91	138.06	149.03	217.35	35.41	42.05	41.58	34.32	26.02	16.79	24.53
877.09	323.58	162.53	135.40	154.13	181.07	196.28	244.51	201.84	17.01	8.37	6.11	6.90	10.28	10.22	14.05
594.65	335.52	458.03	710.73	1007.1	1152.3	1055.7	761.88	219.44	13.21	3.95	2.34	3.44	8.61	12.46	14.65
142.55	205.50	905.05	1784.4	1784.4	1784.4	1784.4	1333.8	153.05	9.87	9.08	9.47	12.43	19.48	21.09	19.08
94.18	191.84	1217.2	1784.4	1784.4	1784.4	1784.4	1178.0	85.33	6.28	16.33	32.77	40.48	39.81	30.65	22.88

Table H.101: These are the resistivities after the 15th iteration using the potential-corrected adjoint method Jacobian.

118.75	499.08	469.85	456.24	468.16	496.80	489.39	469.84	450.37	435.65	447.56	444.03	434.57	431.64	416.20	268.01
93.95	719.15	803.86	834.87	813.22	765.38	797.64	818.89	828.16	51.81	42.36	45.98	50.90	54.57	64.03	94.14
154.22	187.54	120.34	112.68	116.95	115.96	101.94	98.30	174.24	38.89	44.79	45.16	38.58	28.47	17.36	31.91
887.95	299.59	158.28	139.39	148.15	154.19	173.10	226.25	197.83	12.12	5.78	3.70	4.74	9.36	12.22	20.09
590.69	370.62	632.82	1104.3	1492.1	1562.0	1485.3	1194.2	362.29	16.55	3.76	1.43	2.17	7.75	15.37	18.62
120.12	230.42	1512.3	1784.4	1784.4	1784.4	1784.4	1784.4	249.57	14.28	19.98	15.05	15.84	24.43	24.06	17.40
79.51	213.37	1784.4	1784.4	1784.4	1784.4	1784.4	1784.4	92.54	5.48	36.83	81.17	80.59	61.54	31.68	16.14

Table H.102: These are the resistivities after the 16th iteration using the potential-corrected adjoint method Jacobian.

111.42	490.68	466.23	454.60	463.61	483.28	473.79	462.88	449.08	438.53	448.83	444.24	434.99	433.52	419.72	277.10
93.03	733.25	811.65	841.44	825.69	787.41	818.48	834.81	825.55	50.54	42.37	46.31	51.05	53.41	62.14	98.72
150.52	179.66	110.94	103.54	103.62	102.29	91.02	84.86	173.90	36.54	43.54	44.43	38.32	29.74	18.30	36.15
902.12	304.22	162.62	147.34	157.66	165.55	180.89	221.81	224.34	18.85	6.01	4.24	4.98	8.81	12.76	23.47
583.60	360.01	630.85	1305.6	1784.4	1784.4	1755.39	999.20	238.00	14.28	3.79	1.62	2.37	7.44	15.91	20.78
116.94	215.77	1468.1	1784.4	1784.4	1784.4	1784.4	1784.4	165.26	10.95	22.86	18.39	18.43	24.95	24.73	18.17
73.62	195.60	1784.4	1784.4	1784.4	1784.4	1784.4	1784.4	90.20	5.03	44.24	91.48	87.55	62.07	30.96	15.48

Table H.103: These are the resistivities after the 17th iteration using the potential-corrected adjoint method Jacobian.

104.82	481.42	461.85	452.50	458.70	470.04	460.91	457.74	446.62	440.80	449.58	444.51	435.63	435.15	423.61	292.66
91.69	766.47	830.52	854.43	845.30	828.08	852.52	857.76	851.43	48.06	42.17	46.16	50.48	52.06	59.92	109.25
151.42	155.15	96.56	91.52	90.90	87.72	79.02	70.45	145.28	43.30	44.39	45.97	40.07	31.74	18.82	44.50
927.51	295.90	175.09	160.93	164.07	163.60	191.30	240.84	171.39	8.18	4.10	2.87	3.98	7.75	13.44	30.35
558.67	397.69	811.52	1784.4	1784.4	1784.4	1784.4	1664.6	543.46	31.33	4.81	1.33	2.17	7.40	18.23	25.94
109.36	239.95	1784.4	1784.4	1784.4	1784.4	1784.4	1784.4	315.95	26.82	60.05	30.23	23.90	29.57	27.91	18.54
66.62	201.60	1784.4	1784.4	1784.4	1784.4	1784.4	1784.4	75.96	4.93	92.65	181.77	135.42	79.76	32.15	12.63

Table H.104: These are the resistivities after the 18th iteration using the potential-corrected adjoint method Jacobian.

103.51	475.52	459.57	451.63	456.32	462.68	451.91	454.96	446.69	442.37	450.28	444.08	435.98	436.78	425.15	290.61
88.32	779.98	836.77	857.84	850.94	844.77	871.06	862.56	841.55	48.46	41.67	46.53	50.39	51.08	59.80	107.06
149.37	144.04	90.25	86.59	83.95	79.31	72.45	64.47	147.42	38.74	44.74	45.74	40.41	32.14	18.24	44.40
939.31	302.50	177.79	163.60	170.83	170.18	194.74	262.91	327.46	16.46	3.62	2.82	3.92	8.41	15.20	34.82
575.54	427.50	829.81	1784.4	1784.4	1784.4	1784.4	887.75	180.46	15.96	6.88	1.66	2.23	8.15	21.22	31.28
111.06	240.10	1784.4	1784.4	1784.4	1784.4	1784.4	1552.6	87.80	12.16	32.11	20.53	18.72	26.33	27.76	21.32
61.51	176.63	1784.4	1784.4	1784.4	1784.4	1784.4	1471.6	48.30	6.88	53.69	93.52	82.22	54.61	24.67	12.71

Table H.105: These are the resistivities after the 19th iteration using the potential-corrected adjoint method Jacobian.

91.36	472.51	459.05	451.07	455.28	462.25	451.86	453.19	442.79	443.15	450.42	444.50	437.20	437.60	428.70	318.04
91.91	783.48	837.38	860.14	851.60	836.10	860.76	868.93	869.88	47.46	41.84	45.90	48.88	50.58	56.99	128.35
158.32	142.95	87.14	83.46	81.99	78.74	72.23	61.81	126.36	40.55	45.85	47.97	42.33	34.52	19.33	61.09
996.69	307.24	183.32	168.53	173.15	170.95	198.03	242.41	167.15	9.30	2.02	1.91	3.12	6.21	14.65	45.53
523.09	402.05	830.62	1784.4	1784.4	1784.4	1784.4	1495.9	556.13	44.82	9.17	2.39	2.56	6.87	23.68	39.71
101.17	227.31	1784.4	1784.4	1784.4	1784.4	1784.4	1784.4	222.05	30.89	59.10	34.58	25.81	30.78	34.53	22.31
60.30	174.75	1784.4	1784.4	1784.4	1784.4	1784.4	913.59	39.96	6.58	72.07	143.87	118.41	73.10	29.80	10.40

Table H.106: These are the resistivities after the 20th iteration using the potential-corrected adjoint method Jacobian.

82.68	468.08	456.60	450.19	453.66	456.80	446.66	450.51	442.20	443.83	450.64	445.20	438.82	438.59	429.92	302.34
95.00	804.78	850.27	866.04	860.30	864.38	888.07	883.66	875.87	47.59	41.53	45.11	47.85	49.66	57.35	130.15
166.79	127.01	80.03	78.96	76.66	69.57	63.18	55.00	96.17	38.02	47.39	49.30	45.47	37.24	17.46	71.94
1039.1	312.53	197.95	175.18	182.20	183.56	234.81	338.15	458.53	11.86	1.62	.93	1.77	3.77	16.17	76.81
555.29	467.71	982.62	1784.4	1784.4	1784.4	1784.4	1676.2	392.65	37.14	32.69	5.60	3.74	9.36	55.52	95.32
109.09	248.85	1784.4	1784.4	1784.4	1784.4	1784.4	1784.4	120.85	27.40	132.90	65.99	39.65	56.77	88.78	37.75
56.55	159.61	1784.4	1784.4	1784.4	1784.4	1784.4	1477.9	32.70	10.02	109.12	169.85	134.33	105.54	43.57	7.63

Table H.107: These are the resistivities after the 21st iteration using the potential-corrected adjoint method Jacobian.

90.08	464.52	455.94	449.63	452.78	457.12	447.78	447.50	440.49	445.68	451.13	446.22	440.36	440.10	429.35	238.40
81.91	819.53	850.74	868.38	862.15	853.27	875.51	891.84	887.01	45.37	41.34	44.45	46.84	47.88	59.67	108.24
162.12	113.70	77.67	76.24	75.28	70.32	62.71	52.47	90.48	40.23	47.95	51.00	46.47	40.10	16.14	75.57
1016.8	309.18	198.99	177.98	176.27	172.14	232.08	333.07	206.18	8.61	1.61	.93	1.78	3.06	11.20	98.90
594.70	533.37	1081.2	1784.4	1784.4	1784.4	1784.4	1784.4	524.75	60.78	28.37	11.61	5.64	13.59	83.59	208.30
121.12	282.53	1784.4	1784.4	1784.4	1784.4	1784.4	1784.4	167.62	48.46	122.65	99.72	56.02	80.34	155.10	78.58
56.97	151.72	1784.4	1784.4	1784.4	1784.4	1784.4	988.16	36.91	13.11	106.00	211.52	172.45	137.30	57.78	6.40

Table H.108: These are the resistivities after the 22nd iteration using the potential-corrected adjoint method Jacobian.

122.81	462.05	455.94	450.01	452.58	456.07	447.59	447.97	440.51	446.30	451.66	447.13	441.73	440.26	426.04	206.34
58.86	824.81	849.54	866.04	863.90	859.79	879.15	883.32	886.10	46.06	40.94	43.93	46.07	48.22	64.02	103.77
145.66	107.13	78.64	75.97	73.27	67.67	60.58	52.85	81.64	39.19	49.03	51.38	46.87	39.86	14.47	83.46
878.83	294.30	182.01	173.65	181.25	183.55	248.27	339.44	361.24	8.63	1.56	1.02	1.80	3.89	5.33	86.36
639.24	598.98	1036.4	1784.4	1784.4	1784.4	1784.4	1551.0	471.50	73.19	37.53	11.94	8.48	31.68	107.75	207.90
138.14	319.99	1784.4	1784.4	1784.4	1784.4	1784.4	1784.4	156.13	67.14	166.17	132.81	120.19	248.53	285.90	74.66
60.67	143.88	1784.4	1784.4	1784.4	1784.4	1784.4	1219.79	42.07	16.04	116.52	283.36	375.91	396.94	106.11	5.95

Table H.109: These are the resistivities after the 23rd iteration using the potential-corrected adjoint method Jacobian.

131.76	459.98	453.71	449.25	451.62	454.08	448.34	447.55	440.41	446.59	450.93	446.77	441.49	440.22	422.12	119.49
55.76	831.34	861.84	872.78	868.23	865.77	878.72	887.85	894.73	45.71	41.96	44.30	47.06	48.64	67.43	57.12
134.85	102.57	73.12	72.01	70.82	67.69	59.68	51.36	69.78	38.71	48.65	50.38	45.70	37.59	13.56	73.92
709.97	284.23	202.32	182.29	186.33	167.75	251.15	446.67	387.54	6.63	1.55	.89	2.01	4.83	3.12	138.68
504.73	656.81	1640.0	1784.4	1784.4	1784.4	1784.4	1784.4	962.38	177.50	87.55	16.07	17.98	105.95	262.16	646.80
112.72	354.31	1784.4	1784.4	1784.4	1784.4	1784.4	1784.4	218.18	157.94	625.55	402.39	437.57	981.03	746.90	165.78
51.95	140.89	1784.4	1784.4	1784.4	1784.4	1784.4	933.33	46.37	22.75	469.87	1252.9	1675.1	1339.8	161.56	5.08

Table H.110: These are the resistivities after the 24th iteration using the potential-corrected adjoint method Jacobian.

137.81	458.85	452.30	448.65	451.06	452.20	447.81	447.89	440.60	446.74	449.74	446.14	440.83	439.84	420.00	99.50
53.13	831.14	865.54	875.58	870.42	871.44	881.08	884.82	891.47	45.84	42.94	44.49	47.75	49.52	68.03	58.72
131.29	102.78	70.36	68.99	68.73	66.55	58.41	51.00	68.82	37.95	47.62	50.03	44.31	35.23	14.47	120.17
622.03	279.00	202.45	193.95	191.58	166.96	267.37	446.75	389.31	6.31	1.96	.87	2.32	4.59	2.90	174.16
406.26	627.55	1642.5	1784.4	1784.4	1784.4	1784.4	1738.9	639.65	198.56	81.23	22.36	39.01	107.57	174.05	506.89
115.84	353.24	1784.4	1784.4	1784.4	1784.4	1784.4	1720.3	201.78	188.14	358.52	317.73	464.07	683.33	441.03	127.94
50.95	122.55	1784.4	1784.4	1784.4	1784.4	1784.4	979.42	54.11	27.32	235.11	662.03	1015.6	702.20	100.17	4.93

Table H.111: These are the resistivities after the 25th iteration using the potential-corrected adjoint method Jacobian.

141.83	458.46	451.52	448.41	450.72	451.08	448.12	448.76	440.36	445.98	448.85	445.78	440.35	439.38	418.64	127.37
52.19	832.36	867.54	876.46	871.71	872.86	878.18	880.15	891.53	47.03	43.21	44.66	48.08	50.04	67.99	75.33
124.61	102.39	68.20	67.10	67.36	66.36	58.88	51.84	68.28	36.69	46.96	50.13	43.16	34.65	15.72	98.78
445.39	268.85	210.51	201.30	191.91	163.84	248.17	402.34	369.87	6.01	2.21	.74	2.48	4.32	2.50	113.47
340.21	693.00	1729.4	1784.4	1784.4	1784.4	1784.4	1582.0	739.69	180.49	102.08	28.26	60.76	154.64	234.75	437.32
134.61	400.99	1784.4	1784.4	1784.4	1784.4	1784.4	1577.5	257.43	253.11	796.85	818.25	1348.7	1784.4	871.50	130.50
54.53	102.64	1784.4	1784.4	1784.4	1784.4	1784.4	862.77	60.10	49.74	684.49	1784.4	1784.4	1784.4	205.09	4.56

Table H.112: These are the resistivities after the 26th iteration using the potential-corrected adjoint method Jacobian.

143.31	457.46	450.56	447.91	449.71	448.83	447.50	449.16	440.52	445.39	447.67	445.26	440.17	438.85	418.61	158.80
52.05	840.20	871.11	880.36	878.60	883.47	883.86	879.99	891.85	47.52	44.17	44.85	47.98	50.58	66.33	79.14
118.36	96.85	66.00	63.71	63.35	62.02	55.64	50.95	66.33	35.44	45.94	50.08	43.05	34.45	18.17	112.98
341.63	278.75	216.83	228.19	219.36	194.27	347.23	638.80	467.42	5.83	2.28	.62	2.91	3.46	2.41	165.99
251.50	827.04	1784.4	1784.4	1784.4	1784.4	1784.4	1784.4	762.80	266.62	259.03	38.95	59.62	72.52	116.22	452.66
178.62	515.71	1784.4	1784.4	1784.4	1784.4	1784.4	1303.5	190.41	356.68	1527.1	1076.1	1067.9	813.91	410.28	116.04
71.10	83.80	1648.6	1784.4	1784.4	1784.4	1784.4	616.24	72.37	68.79	1107.7	1784.4	1784.4	1529.2	167.77	4.38

Table H.113: These are the resistivities after the 27th iteration using the potential-corrected adjoint method Jacobian.

143.10	456.89	450.09	447.84	449.23	448.37	448.63	450.12	440.46	444.93	446.60	444.74	440.41	438.17	419.89	198.19
52.65	843.62	872.35	879.94	878.33	879.44	874.75	872.48	891.18	47.88	44.79	45.10	47.53	51.24	63.46	104.35
111.88	93.01	64.67	62.81	62.59	62.52	57.08	53.34	68.08	34.33	45.44	50.23	42.94	34.64	21.85	128.57
283.39	269.11	218.50	216.36	207.57	175.88	285.43	416.03	302.29	5.79	2.45	.54	3.02	3.22	2.22	122.78
354.04	1059.3	1784.4	1784.4	1784.4	1784.4	1784.4	1510.9	694.96	219.34	111.41	38.46	80.13	62.22	106.98	307.83
222.52	574.39	1784.4	1784.4	1784.4	1784.4	1784.4	1026.3	289.71	505.18	1012.2	1036.1	1299.7	813.87	409.67	90.00
79.16	70.06	1346.3	1784.4	1784.4	1784.4	1784.4	401.72	86.76	151.37	1145.9	1784.4	1784.4	1693.9	197.78	4.26

Table H.114: These are the resistivities after the 28th iteration using the potential-corrected adjoint method Jacobian.

142.78	455.50	449.61	447.81	449.08	447.63	449.35	451.30	440.91	444.12	445.58	444.47	440.95	438.05	422.36	238.07
53.10	848.54	874.95	881.29	880.22	883.70	875.01	868.53	890.21	48.96	45.39	45.03	47.06	50.91	60.32	121.59
111.30	91.31	61.98	60.68	60.36	59.69	56.57	54.76	65.87	32.83	45.11	50.54	43.35	36.18	26.16	139.52
207.58	268.09	259.31	254.46	233.74	218.23	335.72	575.95	483.69	5.81	2.40	.47	3.40	2.37	2.19	124.99
268.02	1056.6	1784.4	1784.4	1784.4	1784.4	1784.4	1784.4	882.24	236.80	208.52	40.72	65.43	38.94	85.75	275.70
298.16	594.55	1784.4	1784.4	1784.4	1784.4	1784.4	1004.7	291.20	578.29	1387.9	972.88	902.68	487.39	288.53	76.58
113.22	60.03	1150.2	1784.4	1784.4	1784.4	1784.4	423.59	96.13	238.26	1437.0	1784.4	1784.4	999.96	136.89	4.22

Table H.115: These are the resistivities after the 29th iteration using the potential-corrected adjoint method Jacobian.

143.08	453.44	449.16	447.53	448.19	447.06	449.26	450.75	440.86	443.21	444.76	444.41	441.96	438.38	425.65	246.24
54.48	862.86	877.08	883.11	883.37	883.81	876.01	872.66	891.21	49.58	45.79	44.92	46.24	50.27	56.58	122.03
108.51	81.06	60.13	59.29	59.19	58.81	55.83	54.89	67.51	31.52	45.12	50.74	44.32	38.89	31.59	171.20
131.70	308.89	265.97	251.81	226.11	223.89	368.38	573.20	274.66	5.83	2.35	.45	3.94	1.44	2.14	149.74
249.32	1694.0	1784.4	1784.4	1784.4	1784.4	1784.4	1784.4	829.87	215.21	171.90	44.51	112.35	15.88	63.42	247.11
414.36	874.30	1784.4	1784.4	1784.4	1784.4	1784.4	946.79	388.68	856.27	1784.4	1784.4	1784.4	515.82	306.00	66.87
160.13	53.14	815.75	1784.4	1784.4	1784.4	1784.4	331.73	160.17	550.50	1784.4	1784.4	1784.4	1784.4	239.64	4.09

Table H.116: These are the resistivities after the 30th iteration using the potential-corrected adjoint method Jacobian.

141.69	452.07	448.70	447.25	448.27	447.91	450.26	451.63	441.67	442.13	444.12	444.32	442.92	439.38	430.92	336.34
50.48	864.61	880.82	885.31	882.22	879.28	871.99	868.25	891.31	50.76	46.07	44.87	45.79	49.00	51.22	157.58
116.39	76.24	56.52	56.99	58.80	58.96	56.77	56.06	63.09	30.25	45.23	50.62	44.94	41.87	39.95	164.70
231.69	379.06	361.67	292.56	236.36	214.69	330.01	565.40	465.97	5.89	2.22	.45	5.10	.79	2.14	86.31
352.37	1547.9	1784.4	1784.4	1784.4	1784.4	1784.4	1784.4	1309.37	306.19	170.70	38.47	70.54	15.92	61.71	129.91
295.30	540.98	1784.4	1784.4	1784.4	1784.4	1784.4	958.83	536.85	1004.1	1535.4	1112.1	1063.5	399.01	249.56	38.91
110.32	41.84	647.53	1784.4	1784.4	1784.4	1600.9	306.51	109.73	476.11	1784.4	1784.4	1784.4	1253.2	181.04	4.31

Table H.117: These are the resistivities after the 31st iteration using the potential-corrected adjoint method Jacobian.

139.39	451.37	448.75	447.42	448.02	446.64	449.06	450.85	442.08	441.21	443.57	444.40	444.35	440.72	435.24	488.11
50.69	869.41	878.76	883.05	884.93	888.43	880.46	873.41	887.38	51.45	46.18	44.78	44.97	47.68	47.84	206.06
112.95	72.05	56.42	57.38	57.70	55.70	53.50	55.00	65.73	29.19	45.73	50.30	45.78	44.96	45.09	104.91
334.10	471.17	302.77	250.40	236.62	279.42	491.19	715.32	320.24	6.04	2.25	.45	4.76	.59	2.00	33.03
284.33	1385.7	1784.4	1784.4	1784.4	1784.4	1784.4	1784.4	664.41	208.71	98.65	25.98	119.45	12.91	82.31	73.77
181.33	470.09	1784.4	1784.4	1784.4	1784.4	1784.4	823.92	556.23	976.75	1645.1	1784.4	1784.4	1304.1	571.80	26.00
48.02	39.49	578.68	1784.4	1784.4	1784.4	1444.8	244.93	230.24	818.49	1784.4	1784.4	1784.4	1784.4	684.16	4.51

H.7 Results of potential-corrected hybrid method

Table H.118: These are the resistivities after the 1st iteration using the hybrid method Jacobian.

1784.4	1784.4	1784.4	1784.4	1784.40	1784.4	1784.4	1784.4	1292.2	509.67	364.97	339.59	388.55	395.62	324.25	234.82
1784.4	1784.4	1784.4	1784.4	1784.4	1784.4	1784.4	1784.4	733.36	146.43	93.77	95.13	96.76	100.99	112.17	121.54
1605.4	1784.4	1784.4	1784.4	1784.4	1784.4	1784.4	726.73	168.26	44.34	30.42	30.10	25.02	25.86	36.73	52.02
700.65	923.50	1456.7	1784.4	1669.73	979.62	411.40	133.58	39.63	19.22	19.07	21.38	18.10	17.90	24.33	34.04
302.13	344.51	467.52	554.13	460.32	244.02	91.74	30.92	13.44	11.75	18.38	27.01	26.84	25.93	30.18	36.36
159.07	162.82	194.33	208.56	160.28	80.41	30.05	11.54	7.03	9.45	21.37	41.13	48.83	47.34	48.04	49.27
123.51	119.89	130.65	129.13	94.49	47.50	18.88	8.29	6.12	9.63	24.07	51.15	67.76	67.68	64.40	60.36

Table H.119: These are the resistivities after the 2nd iteration using the hybrid method Jacobian.

881.94	810.50	820.92	775.46	806.90	817.00	852.66	867.82	726.61	337.95	283.41	290.67	289.54	277.72	236.96	174.33
1011.0	929.54	1055.3	1055.2	996.43	938.86	979.11	928.40	536.55	131.07	92.98	99.28	101.10	105.43	109.61	99.96
1015.99	788.49	855.62	951.26	915.59	844.67	755.37	515.36	194.72	44.62	25.81	27.21	29.28	31.92	37.28	41.18
733.66	522.86	484.96	557.07	577.90	522.15	392.02	211.28	73.83	21.90	12.41	11.97	12.80	14.15	16.61	19.17
355.95	276.08	255.30	287.66	309.17	276.87	190.35	95.71	37.00	14.52	8.84	7.98	8.25	8.98	10.18	11.52
183.59	152.79	148.47	167.10	180.92	161.11	108.20	55.46	24.45	11.80	7.84	6.92	6.95	7.36	8.03	8.78
137.30	119.80	118.84	130.32	137.09	119.94	80.94	43.51	21.29	11.57	8.06	7.00	6.86	7.11	7.55	8.03

Table H.120: These are the resistivities after the 3rd iteration using the hybrid method Jacobian.

582.66	590.15	606.67	548.68	571.30	571.16	582.07	595.28	607.24	331.78	307.37	321.19	315.66	314.88	275.64	189.50
628.14	551.78	664.00	686.95	645.04	603.94	633.82	652.86	508.97	108.96	82.50	92.59	91.60	96.88	103.61	94.62
739.02	476.36	480.70	563.58	574.30	560.07	553.39	451.36	206.65	38.05	21.59	24.52	25.72	26.22	29.23	33.00
759.89	416.08	323.70	366.68	414.89	427.12	381.47	246.93	92.82	22.41	11.52	11.21	11.49	11.41	12.24	14.10
415.29	264.32	207.71	233.24	281.68	300.22	251.65	147.45	57.21	18.45	9.53	7.99	7.64	7.38	7.56	8.34
209.74	156.55	139.50	163.80	205.44	222.45	182.43	106.05	45.32	17.96	9.70	7.47	6.69	6.25	6.16	6.51
150.74	124.21	120.00	141.87	174.84	185.99	151.03	90.02	42.19	19.06	10.72	7.89	6.76	6.19	5.99	6.13

Table H.121: These are the resistivities after the 4th iteration using the hybrid method Jacobian.

332.71	546.62	516.77	504.46	552.43	593.60	561.55	524.56	506.77	423.43	386.78	408.17	409.46	416.06	387.77	229.61
364.43	547.33	656.32	636.74	573.44	497.59	523.30	588.07	680.30	75.24	69.33	71.24	68.46	72.37	83.67	84.85
540.36	340.27	351.84	369.89	360.87	346.76	415.22	460.71	285.40	30.81	20.69	23.81	22.89	22.99	22.47	25.88
848.38	298.32	214.72	254.03	303.14	334.59	369.10	303.03	120.15	20.17	12.79	14.82	15.84	14.59	11.90	11.78
371.77	182.10	163.32	245.52	361.13	421.94	379.67	220.60	70.52	16.48	9.67	10.84	12.80	11.80	8.70	7.39
132.46	101.46	141.88	286.38	491.69	566.33	415.95	184.06	51.58	14.19	8.52	9.65	11.77	10.69	7.31	5.55
87.98	85.44	146.23	322.51	563.76	619.94	407.87	162.49	45.65	14.24	8.85	9.75	11.48	10.26	6.99	5.12

Table H.122: These are the resistivities after the 5th iteration using the hybrid method Jacobian.

332.71	546.62	516.77	504.46	552.43	593.60	561.55	524.56	506.77	423.43	386.78	408.17	409.46	416.06	387.77	229.61
364.43	547.33	656.32	636.74	573.44	497.59	523.30	588.07	680.30	75.24	69.33	71.24	68.46	72.37	83.67	84.85
540.36	340.27	351.84	369.89	360.87	346.76	415.22	460.71	285.40	30.81	20.69	23.81	22.89	22.99	22.47	25.88
848.38	298.32	214.72	254.03	303.14	334.59	369.10	303.03	120.15	20.17	12.79	14.82	15.84	14.59	11.90	11.78
371.77	182.10	163.32	245.52	361.13	421.94	379.67	220.60	70.52	16.48	9.67	10.84	12.80	11.80	8.70	7.39
132.46	101.46	141.88	286.38	491.69	566.33	415.95	184.06	51.58	14.19	8.52	9.65	11.77	10.69	7.31	5.55
87.98	85.44	146.23	322.51	563.76	619.94	407.87	162.49	45.65	14.24	8.85	9.75	11.48	10.26	6.99	5.12

Table H.123: These are the resistivities after the 6th iteration using the hybrid method Jacobian.

272.69	576.49	529.70	505.12	555.04	601.70	565.77	494.24	474.49	409.08	406.85	421.28	418.10	408.62	371.55	222.40
255.89	509.46	629.54	649.33	580.48	500.83	520.52	630.44	731.14	71.53	59.89	58.78	59.85	65.04	80.60	83.54
415.13	320.07	294.65	297.15	305.94	312.65	369.80	443.17	270.99	27.99	24.11	25.64	23.04	23.08	22.90	26.45
867.74	326.15	207.97	206.27	242.15	287.73	330.68	296.34	114.35	17.23	13.50	15.77	15.26	14.16	12.02	12.33
404.45	217.72	198.22	251.41	334.49	402.11	387.85	243.12	71.93	13.61	8.04	8.78	9.81	9.78	8.31	7.80
140.98	125.26	200.78	363.21	548.25	626.11	492.03	228.48	56.33	11.53	6.00	6.24	7.32	7.60	6.62	5.96
95.65	106.72	214.33	447.22	699.89	752.01	518.52	209.59	50.71	11.68	5.97	5.85	6.61	6.82	6.10	5.45

Table H.124: These are the resistivities after the 7th iteration using the hybrid method Jacobian.

165.97	512.93	487.63	473.59	486.19	514.86	524.57	481.41	447.84	441.22	432.60	442.03	434.11	427.93	406.99	215.95
187.55	637.26	723.44	754.84	738.36	671.30	669.68	702.89	799.75	55.25	50.14	51.03	55.16	58.25	70.55	69.23
334.39	288.39	227.54	211.22	219.70	232.38	222.17	274.30	262.82	37.80	31.59	29.19	23.60	23.74	21.10	21.15
885.94	283.71	155.76	125.19	124.08	138.09	160.39	229.61	131.92	12.39	13.56	17.49	15.42	14.91	12.01	10.61
396.77	232.86	266.58	279.79	266.32	279.23	331.36	377.80	125.00	8.47	3.87	4.81	7.13	10.37	9.38	7.33
94.29	137.72	468.48	882.88	932.87	899.71	908.61	671.21	129.25	7.45	2.80	4.07	6.74	9.61	8.46	5.81
58.76	116.09	590.16	1561.5	1784.4	1697.2	1410.9	737.32	116.87	8.60	3.93	6.50	9.36	10.49	8.49	5.44

Table H.125: These are the resistivities after the 8th iteration using the hybrid method Jacobian.

148.60	514.22	483.04	466.52	483.10	525.08	509.63	464.57	443.94	439.75	431.75	447.78	441.70	430.87	409.95	215.31
158.90	637.26	747.44	781.46	743.77	655.84	701.82	773.07	820.07	55.54	48.00	46.90	50.66	55.16	66.72	67.85
289.53	272.11	184.30	179.77	194.03	200.76	183.00	189.60	204.79	33.21	36.29	33.43	27.29	25.80	21.63	21.81
901.24	314.07	154.44	121.97	132.85	146.36	151.10	193.55	164.61	17.85	13.08	15.75	15.13	15.82	13.29	11.73
386.69	256.20	309.39	346.57	394.58	431.27	446.07	435.56	173.27	11.00	3.51	3.36	4.66	8.74	9.86	8.19
102.73	158.93	539.07	1125.1	1573.9	1696.9	1447.8	814.68	149.77	7.78	2.65	2.93	4.20	7.49	8.37	6.32
72.67	146.07	680.52	1784.4	1784.4	1784.4	1784.4	877.12	117.75	7.62	3.91	5.32	6.59	8.35	8.08	5.68

Table H.126: These are the resistivities after the 9th iteration using the hybrid method Jacobian.

92.77	476.21	460.07	456.18	460.67	457.47	442.80	444.42	435.98	445.01	447.57	447.02	445.86	439.91	431.62	204.05
219.06	742.55	817.56	828.14	815.65	822.21	874.29	903.95	876.61	46.49	42.04	44.77	46.27	49.67	56.58	59.68
357.97	210.92	141.02	140.25	150.55	156.95	123.66	88.05	139.93	55.35	49.37	46.22	38.73	32.90	25.02	23.67
891.97	234.85	108.35	103.26	104.05	89.11	105.68	132.78	115.65	4.39	5.22	8.87	10.09	14.78	16.57	15.70
393.73	289.98	412.99	573.44	607.16	538.42	661.82	963.78	629.56	18.93	1.70	.63	.59	2.43	8.77	10.62
61.09	197.94	1250.9	1784.4	1784.4	1784.4	1784.4	1784.4	799.76	31.75	5.27	3.73	2.48	3.82	7.80	6.88
48.97	222.97	1784.4	1784.4	1784.4	1784.4	1784.4	1408.84	175.79	3.82	5.38	34.87	32.24	13.01	9.05	5.13

Table H.127: These are the resistivities after the 10th iteration using the hybrid method Jacobian.

96.07	468.99	455.38	452.08	453.57	443.39	429.62	447.92	438.44	440.27	446.70	445.07	443.46	442.41	430.25	212.85
179.52	776.71	844.10	851.90	848.36	889.48	915.99	893.89	863.15	48.55	42.62	44.79	46.03	46.73	54.87	66.27
324.28	172.25	105.92	110.71	114.38	106.93	90.63	63.78	138.90	46.16	45.71	48.10	45.40	40.49	28.98	28.87
894.75	251.97	139.25	123.12	107.90	93.14	116.31	207.00	306.36	8.40	9.19	4.99	4.97	9.75	15.28	15.99
410.52	320.95	539.16	1001.7	1416.4	1371.9	1001.5	524.22	116.28	5.93	4.08	.88	.47	1.36	7.53	9.23
74.30	201.78	1404.9	1784.4	1784.4	1784.4	1784.4	1007.58	61.94	6.11	30.02	9.94	4.00	5.80	12.01	6.17
48.32	185.72	1784.4	1784.4	1784.4	1784.4	1784.4	1213.34	42.98	2.81	65.48	58.61	31.70	29.23	19.72	4.70

Table H.128: These are the resistivities after the 11th iteration using the hybrid method Jacobian.

82.05	459.14	447.32	446.90	445.78	433.52	428.03	453.30	433.60	442.08	449.30	447.18	445.48	439.07	445.34	232.82
193.24	804.95	877.29	879.53	881.55	927.73	929.66	893.90	910.32	45.58	43.99	44.96	44.31	47.65	46.92	117.05
449.93	163.20	77.09	83.13	86.19	79.04	70.00	49.84	71.73	54.96	37.00	41.50	49.76	44.31	31.02	191.40
844.39	194.89	231.33	168.34	130.11	114.52	178.67	489.77	416.00	3.45	28.33	28.84	1.89	8.09	9.06	240.65
614.08	203.64	433.02	1128.3	1784.4	1784.4	947.26	846.66	1644.9	4.20	.45	.45	.45	4.51	4.15	117.57
113.45	147.00	1385.5	1784.4	1784.4	1784.4	1784.4	649.84	272.61	67.08	1191.0	98.94	20.17	49.79	16.32	33.13
35.59	227.01	1784.4	1784.4	1784.4	1784.4	1784.4	609.09	24.28	2.71	1784.4	1784.4	1447.9	265.06	11.46	2.64

Table H.129: These are the resistivities after the 12th iteration using the hybrid method Jacobian.

98.17	452.43	452.37	450.75	447.95	442.22	440.18	447.88	437.63	448.69	441.84	448.58	442.59	447.14	412.32	187.19
167.18	873.11	859.68	865.11	873.14	896.74	899.78	888.52	893.54	42.38	49.07	42.95	46.10	44.30	74.04	137.13
236.81	85.54	79.83	83.07	83.81	73.46	63.54	50.09	71.78	52.97	24.79	49.27	49.35	42.33	15.71	76.66
533.79	350.09	165.80	146.38	116.11	139.87	186.88	411.54	767.85	3.31	54.77	10.56	3.58	6.45	16.44	96.08
255.17	469.58	471.59	921.10	1650.0	1784.4	1555.3	642.60	90.18	4.45	.65	.45	.45	3.57	8.72	114.18
66.19	324.55	1191.3	1784.4	1784.4	1784.4	1784.4	1325.62	59.50	111.36	3.31	1.04	1.97	33.32	440.41	162.05
29.75	270.80	1784.4	1784.4	1784.4	1784.4	1784.4	1693.6	30.39	2.92	1.57	1.78	4.96	21.70	24.59	2.58

Table H.130: These are the resistivities after the 13th iteration using the hybrid method Jacobian.

163.49	449.95	450.79	448.28	448.12	449.43	440.68	443.19	436.45	447.01	427.23	450.05	443.30	445.94	410.56	1.06
92.21	871.73	867.77	877.29	877.05	873.95	897.06	911.23	906.43	43.78	59.72	41.77	47.64	45.46	62.62	14.04
167.03	79.72	74.50	73.05	76.15	78.80	65.80	40.13	62.52	48.25	12.26	39.69	32.54	43.87	83.76	1784.4
115.30	176.45	194.40	208.42	146.26	110.98	151.46	1784.4	755.76	2.19	90.47	37.84	1641.2	2.77	7.61	47.13
1784.4	1784.4	905.69	926.31	1784.4	1784.4	274.84	801.61	1227.8	16.07	2.48	7.87	.45	.45	.45	.45
40.89	287.87	1182.3	1784.4	1784.4	1784.4	841.90	1784.4	5.00	52.02	.88	.45	2.44	42.24	2.40	2.16
25.23	302.53	1784.4	1784.4	1784.4	1784.4	1784.4	1784.4	43.19	.45	49.07	205.92	163.84	197.69	54.22	2.14

Table H.131: These are the resistivities after the 14th iteration using the hybrid method Jacobian.

124.28	460.37	470.24	457.33	454.54	458.08	436.00	452.73	429.41	452.55	397.10	441.21	362.78	447.95	427.97	1.57
92.94	808.38	805.32	837.29	849.86	849.45	880.35	873.66	895.54	40.12	78.21	51.29	128.12	44.71	52.12	2.67
122.28	132.36	99.09	89.28	92.74	81.56	72.11	42.27	86.35	54.40	7.58	19.51	4.67	38.51	61.99	8.21
159.01	149.56	113.71	106.89	100.68	111.32	128.94	74.24	29.10	2.66	62.72	57.03	7.73	11.37	17.51	5.37
77.32	186.88	347.20	567.85	781.53	973.80	992.46	323.14	52.36	24.43	29.88	9.17	.67	.45	1.06	1.23
36.06	167.11	814.23	1784.4	1784.4	1784.4	1784.4	513.05	8.29	2.77	.49	.69	.85	.58	2.72	4.67
81.29	289.83	1429.9	1784.4	1784.4	1784.4	1784.4	1113.02	21.95	.45	.45	.55	.74	.75	1.23	1.17

Table H.132: These are the resistivities after the 15th iteration using the hybrid method Jacobian.

115.46	457.79	466.17	456.58	451.31	448.45	431.20	423.03	409.54	446.58	408.91	433.00	380.62	439.21	432.39	4.41
95.42	821.40	815.16	843.12	863.06	892.50	955.38	1002.0	991.86	42.67	71.10	50.35	96.28	47.93	50.30	.95
118.06	131.51	102.41	89.77	86.97	64.50	40.03	21.75	48.70	54.98	7.81	20.52	4.68	34.88	56.41	1.29
155.33	241.61	152.21	152.88	132.19	172.86	619.45	837.39	180.33	2.76	40.68	63.91	13.56	37.98	7.86	.47
56.16	382.63	406.30	758.27	1227.1	1784.4	1784.4	1784.4	1784.4	35.18	1.15	.76	.78	2.64	.79	.45
50.22	517.11	1458.9	1784.4	1784.4	1784.4	1784.4	1784.4	57.16	3.74	.45	.69	.49	.45	.52	.45
117.50	757.70	1784.4	1784.4	1784.4	1784.4	1784.4	1182.0	5.15	.45	4.99	9.06	.45	.45	1.75	1.31

Table H.133: These are the resistivities after the 16th iteration using the hybrid method Jacobian.

265.28	574.35	580.00	589.54	623.75	653.13	661.65	643.51	608.90	366.89	334.91	373.58	324.28	364.57	328.72	173.61
172.37	511.19	576.71	563.57	548.48	481.45	426.39	423.62	516.13	137.16	80.87	92.32	73.75	101.07	114.19	69.21
108.08	249.77	326.14	308.39	271.38	204.50	140.11	107.50	101.75	36.96	22.57	22.49	14.97	18.53	21.38	16.72
165.09	183.61	178.02	149.87	116.94	80.06	50.61	34.14	24.82	12.83	10.59	9.03	5.64	4.66	4.33	3.94
66.61	81.08	85.95	73.91	54.48	34.86	20.60	12.53	8.27	5.62	4.75	3.52	2.11	1.41	1.13	1.09
50.87	53.29	52.83	44.30	31.29	18.94	10.38	5.63	3.32	2.35	2.04	1.46	.86	.55	.45	.45
48.41	47.00	43.37	35.14	24.26	14.35	7.57	3.79	1.96	1.29	1.16	.86	.52	.45	.45	.45

Table H.134: These are the resistivities after the 17th iteration using the hybrid method Jacobian.

210.43	469.65	505.15	480.85	517.65	735.08	770.21	647.12	460.75	485.62	401.30	426.10	405.59	424.46	395.92	140.05
207.45	738.36	663.48	762.39	684.87	375.28	309.34	358.45	871.03	61.47	83.17	68.50	75.04	70.64	82.60	39.75
110.52	263.23	317.69	152.86	138.48	198.10	775.18	1784.4	74.93	36.34	6.27	12.20	9.29	19.26	24.09	12.44
142.95	94.39	167.93	257.12	1037.5	1784.4	1784.4	1784.4	198.88	70.28	139.36	152.97	67.28	22.92	15.08	7.65
106.74	100.79	317.59	946.82	1784.4	1784.4	1784.4	1784.4	232.33	73.78	256.73	142.35	22.78	6.84	6.89	3.63
47.58	78.96	433.15	1784.4	1784.4	1784.4	1784.4	1150.0	22.48	16.53	116.85	19.09	.76	.55	2.17	1.18
45.68	80.04	380.12	1181.2	1784.4	1784.4	702.00	32.60	1.48	2.53	20.48	1.26	.45	.45	.74	.45

Appendix I

Contents of CDROM

CDROM

- C — *(This contains the C code used in testing the methods used to solve the Forward Problem)*
  - Comp_inv *(The code for Complete Inversion)*
  - Point_iter *(The code for Point Iteration)*
  - Line_iter *(The code for Line Iteration)*
  - Panel_iter *(The code for Panel Iteration)*
  - Con_grad *(The code for Conjugate Gradient)*
  - tests *(This contains the test input files)*
- Fortran — *(This contains the Fortran files totally or partly written by the present author which are designed to link in with the programs written by P. Jackson.)*
- Maple — *(This contains the Maple files used in *.mws format)*
  - text *(This contains the text version of the Maple files so that they may be used in any version of Maple.)*
- Results — *(This contains the results and some of the Jacobians from solving the test Inverse Problem)*
  - Adjoint_m *(Uncorrected Adjoint Method)*
  - Mea_adj_m *(Measurement Corrected Adjoint Method)*
  - Pot_adj_m *(Potential Corrected Adjoint Method)*
  - Hybrid_m *(Hybrid Method)*
  - Pert_m *(Perturbation Method)*
- Thesis
  - Plot_jac *(The picture files for the images of the Jacobians in Chapter 7)*

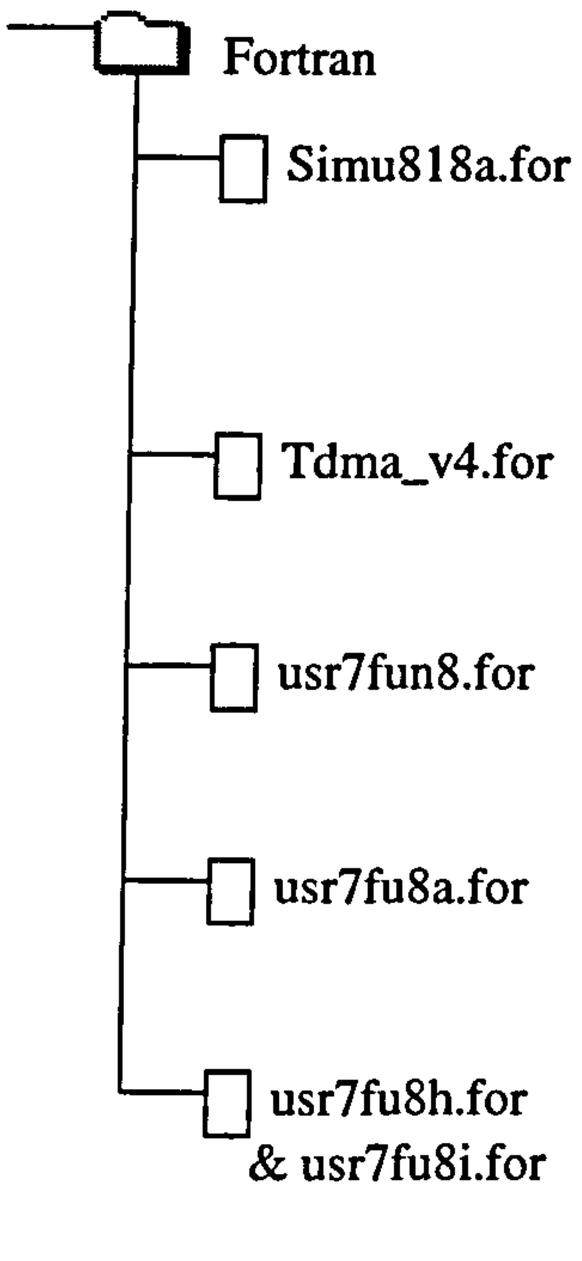

The all the files in the C directory were written by the present author. However, the direct solver engine is based on a 2D direct solver written in Pascal by G. Reece.

It is hoped that most file titles will be self-explanatory. Each directory has a readme.txt file which will distinguish all the different files. However, there are various file type which may not be self-explanatory. These are:-

- *.jac are binary files which contain the Jacobian (usually produced by the Perturbation Method.
- *.ada are binary files which contain the Jacobian produced by an adjoint method.
- *.asc are text files of Jacobians (note: these are 2Mb files)
- *.??? where ??? is a 3 digit number indicating the measurement number and the files contain the values in the Jacobian for that specific measurement (in text format).

Bibliography

Al-Chalabi, M. [1992], 'When Least-squares Squares Least', *Geophysical Prospecting* **40**, 359–378.

Babu, V. & Korpela, S. A. [1993], 'On the Direct Solution of Poisson's Equation on a Non-uniform Grid', *Journal of Computational Physics* **104**, 93–98.

Barber, C. C., Brown, B. H. & Freeston, I. L. [1983], 'Imaging Spatial Distributions of Resistivity using Applied Potential Tomography', *Electronics Letters* **19**(22), 933–935.

Barber, D. C. & Brown, B. H. [1984], 'Applied Potential Tomography', *Journal of Physics E-Scientific Instruments* **17**(9), 723–733.

Barrett, R.; Berry, M., Chan, T. F., Demmel, J., Donato, J. M., Dongarra, J., Eijkhout, V., Pozo, R., Romine, C. & Van der Vorst [1994], *Templates for Solutions of Linear Systems: Building Blocks for Iterative Methods*, SIAM, internet: http://www.netorg/templates/Templates.html.

Berryman & Koln [1990], 'Variational constraints for Electrical Impedance', *Phys. Review letters* **65**, 325–328.

Berryman, J. [1990], 'Impedance - Computed Tomography Algorithm and System', *Inverse Problems* **6**, 21–42.

Bharadwaj, K. K., Kadalbajoo, M. K. & Sankar, R. [1984], 'Symmetric Marching Technique for the Poisson Equation. 1. Dirichlet Boundary - Conditions', *Applied Mathematics and Computation* **15**(2), 137–149.

Binley, A., Ramirez, A. & Daily, W. [c. 1993], Regulariesd Image Reconstruction of Noisy Electrical Resistance Tomography Data, Lancaster University and Lawrence Livermore National Laboratory (published after 1992).

Buneman, O. [1973], 'Inversion of the Helmholtz (or Laplace - Poisson) Operator for slab Geometry', *Journal of Computational Physics* **12**, 124.

Buzbee, B. L., Dorr, F. W., George, J. A. & Golub, G. H. [1971], 'The Direct Solution of the Discrete Poisson Equation on Irregulare Regions', *SIAM Journal of Numerical Analysis* 8(4), 722–736.

Buzbee, B. L., Golub, G. H. & Nielson, C. W. [1970], 'On Direct Methods for Solving Poisson's Equations', *SIAM Journal of Numerical Analysis* **7**(4), 627–656.

Carslaw, H. S. & Jaeger, J. C. [1959], *Conduction of Heat in Solids*, second edn, Clarendon Press.

Cheng, K., Simske, S., Isaacson, D., Newell, J. & Gisser, D. [1990], 'Errors Due to Measuring Voltage on Current Carrying Electrodes in Electric Current Computed Tomography', *IEEE Trans. Biomed. Eng.* **37**, 60–65.

Chunduru, R. K., Sen, M. K. & Stoffa, P. L. [1996], '2-D Resitivity Inversion using Spline Parameterization and Simulated Annealing', *Geophysics* **61**(1), 151–161.

Chunduru, R. K., Sen, M. K., Stoffa, P. L. & Nagendra, R. [1995], 'Non-linear inversion of resistivity profiling data for some regular geometrical bodies', **43**, 979–1003.

Constable, S. C., Parker, R. L. & Constable, C. G. [1987], 'Occam's Inversion: A Practical Algorithm for Generating Smooth Models from Electromagnetic Sounding Data ', *Geophysics* **52**(3), 289–300.

Dabas, M., Tabbagh, A. & Tabbagh, J. [1994], '3-D Inversion in Subsurface Electrical Surveying 1.Theory', *Geophysical Journal International* **119**(3), 975–990.

Daily, W., Lin, W. & Buscheck, T. [1987], 'Hydrological Properties of Topopah Spring Truff: Lab. measurements ', *Journal of Geophysical Research* **92**(B8), 7854–7864.

Dey, A. & Morrison, H. F. [1979], 'Resistivity Modelling for Arbitrarily Shaped Three - Dimensional Structures', *Geophysics* 44(4), 753–780.

Ellis, R. G. & Oldenburg, D. W. [1994], 'The Pole Pole 3-D DC-Resistivity Inverse Problem - A Conjugate Gradient Approach', *Geophysical Journal International* **119**(1), 187–194.

Freund, R. W., Golub, G. H. & Nachtigal, N. M. [1991], 'Iterative Solutions of Linear Systems', *Acta Numerica.*

Friedman & Vogelius, M. [1989], 'Determining Cracks by Boundary Measurement', *Indiana Uni. Maths* **38**, 527–556.

Gallopsoulos, E. & Saad, Y. [1988], 'A Parallel Block Cyclic Reduction Algorithm for the Fast Solution of Elliptic-Equations', *Lecture Notes in Computer Science* **297**, 563–575.

Golub, G. H. & Van Loan, C. F. [1988], *Matrix Computations*, second edn, The Johns Hopkins University Press.

Isaacson, D. [1986], 'Distinguishability of Conductivities by electric current computed Tomography', *IEEE Transactions in Medical Imaging* **M1-5**, 91–95.

Jackson, P. D., Busby, J. P., Meldrum, P. & Reece, G. [1988], Identification of Hydraulically Connected Fractures by Elctrical Resistivity Methods, Technical Report WK/88/19, British Geological Survey.

Jackson, P. D., Earl, S. J. & Reece, G. [1997], 3D Resistivity Tomography - Towards Estimating Mass Properties, Technical Report WN/97/21C, British Geological Survey.

Jackson, P. D., Gunn, D. A., Meldrum, P. I. & Flint, R. C. [1994], 3D Data Processing and Tomographic presentation of Resistivity Data , Technical Report WN/94/20, British Geological Survey.

Kadalbajoo, M. K. & Bharadwaj, K. K. [1984], 'Fast Ellipitc Solvers - Overview Applied Mathematics and Computation', *Applied Mathematics and Computation* 14(4), 331–355.

Kearey, P. & Brooks, M. [1991], *An Introduction to Geophysical Exploration*, Oxford.

Keller, G. V. & Frischknecht, F. C. [1966], *Electrical Methods in Geophysical Prospecting*, Pergamon Press.

Kim, Y., Webster, J. G. & Tompkins, W. J. [1983], 'Electrical-Impedance Imaging of the Thorax', *Journal of Microwave Power and Electromagnetic Energy* **18**(3), 245–257.

Kohn & Vogelius, M. [1984], 'Determining Conductivity by Boundary Measurements', *Communic. on Pure and Applied Maths* **37**, 643–667.

Kohn & Vogelius, M. [1985], 'Determining Conductivity by Boundary Measurements II. Interior Results', *Communic. on Pure and Applied Maths* **38**, 643–667.

Kohn, R. V. & McKenney, A. [1990], 'Numerical Implementation of a Variational Method for Electrical Impedance Tomography', *Inverse Problems.*

Koln & Vogelius, M. [1984], 'Identification of an unknown Conductivity by means of Measurements of the Boundary', *Inverse Problem SIAM - AMS proc.* **14**, 113–123.

Kunetz, G. [1966], *Principles of Direct Current Resistivity Prospecting*, Geopublications Associates.

Li, Y. & Oldenburg, D. W. [1994], 'Inversion of 3-D DC Resistivity Data using an Approximate Inverse Mapping', *Geophysical Journey International* **116**(3), 527–537.

Loke, M. H. & Barker, R. D. [1995], 'Least-squares Deconvolution of Apparent Resistivity Pseudosections ', *Geophysics* **60**(6), 1682–1690.

Loke, M. H. & Barker, R. D. [1996*a*], 'Practical Techniques for 3-D Resistivity Surveys and Data Inversion', *Geophysical Prospecting* **44**, 499–523.

Loke, M. H. & Barker, R. D. [1996*b*], 'Rapid Least-squares Inversion of Apparent Resistivity Pseudosections by a quasi Newton Method', *Geophysical Prospecting* **44**(6), 131–152.

Lovell, M. A. & Jackson, P. D. [1991], Electrical Flow in Rocks, the application of high resolution electrical resistivity core measurements, *in* 'Thirty-second Annual SPWLA Symposiu'.

Marquardt, D. W. [1963], 'An Algorithm for Least-squares Estimation of Non-linear Parameters', *Journal Soc. Indust. Appl. Math.* **11**, 431.

McGillivray, P. R. & Oldenburg, D. W. [1990], 'Methods for Calculating Fréchet Derivatives and Sensitivities for the Non-Linear Inverse Problem: A Comparative Study', *Geophysical Prospecting* **38**, 499–524.

Molyneux, J. E. & Witten, A. [1994], 'Impedance Tomograghy - Imaging Algorithms for Geophysical Applications', *Inverse Problems* **10**(3), 655–667.

Nachman, A. [1988], 'Reconstruction from Boundary Measurements', *Annuals of Maths* **128**, 531–576.

Narayan, S., Dusseault, M. B. & Nobes, D. C. [1994], 'Inversion Techniques Applied to Resistivity Inverse Problem', *Inverse Problems* **10**, 669–686.

Parasnis, D. S. [1973], *Mining Geophysics*, 2nd edn, Elsevier Scientific Publishing Company.

Parasnis, D. S. [1986], *Principles of Applied Geophysics*, 4th edn, Chapman and Hall.

Park, S. [1998], 'Fluid migration in Vadose Zone from 3D Inversion of Resistivity Monitoring Data', *Geophysics* **63**(1), 41–51.

Park, S. K. & Van, G. P. [1991], 'Inversion of Pole-Pole Data for 3-D Resistivity Structure Beneath Array of Electrodes', *Geophysics* **56**(7), 951–960.

Powell, H. M., Barber, D. C. & Freeston, I. L. [1987], 'Impedance Imaging using Linear Electrode Arrays ', *Clin. Phys. Physiol. Meas.*

Press, W. H., Teukolsky, S. A., Vetterling, W. T. & B.P.Flannery [1992], *Numerical Recipes in C, The Art of Scientific Computing*, Cambridge University Press.

Raines, M. G., Jackson, P. D., Evans, C. J., Meldrum, P. & Rainsbury, M. [1989], An Evalualtion of the Resistivity of the Anisotropy of the Clays at the Down Ampney Fault Research Site, Technical Report WE/89/48, British Geological Survey.

Reece, G. [1986], *Microcomputer Modelling by Finite Differences*, Macmillan Education Ltd.

Santosa, F. [1994], 'Impedence Imaging', *SIAM News.*

Santosa, F. [1995], Imaging Corrosion in Plates, *in* 'Three-Dimensional Electromagnetics', Schlumberger-Doll Research, pp. 339–347.

Santosa, F. & Vogelius, M. [1984], 'A Backprojaction Algorithm for Electrical Impedance Imaging', *SIAM Journal of Applied Maths* **37**(50), 216–234.

Sasaki, Y. [1992], 'Resolution of Resistivity Tomography Inferred from Numerical Simulation', *Geophysical Prospecting* **40**, 453–463.

Sasaki, Y. [1994], '3-D Resistivity Inversion using the Finite-element Method', *Geophysics* **59**(11), 1839–1848.

Spitzer, K. & Wurmstich, B. [1995], Speed and Accuracy in 3D Resistivity Modeling, *in* 'Three-Dimensional Electromagnetics', Schlumberger-Doll Research, pp. 167–180.

Sylvester & Uhlmann [1987], 'A Global Uniqueness Theorem for an Inverse Boundary Value Problem', *Annuals of Maths* **125**, 153–169.

Sylvester & Uhlmann, G. [1986], 'A Uniqueness Theorem for an Inverse Boundary Value Problem in Electrical Prospection', *Communic. of Pure and Applied Maths* **39**, 91–112.

Tarantola, A. & Valette, B. [1982], 'Generalized Non-linear Inverse Problems Solved using the Least-squares Criterion', *Reviews of Geophysics* **20**(2), 219–232.

Telford, W. M., Geldart, L. P., Sheriff, R. E. & Keys, D. A. [1976], *Applied Geophysics*, Cambridge University Press.

Tripp, A. C., Hohmann, G. W. & Swift Jr., C. M. [1984], 'Two-dimensional Resistivity Inversion', *Geophysics* **49**(10), 1708–1717.

Tsourlos, P. I., Dittmer, J. K. & Szymanski, J. E. [1995], 'Nonlinear Technies for the Inversion of Earth Resistivity Data', *Proceedings of IEEE International Geoscience Remote Sensing Symposium.*

Wexler, A., Fry, B. & Neuman, M. [1985], 'Impedance - Computed Tomography Algorithm and System', *Applied Optics* **24**, 3985–3992.

Williams, C. [1996], Assessment of Electrical Resistivity Properties through development of 3D Numerical methods, PhD thesis, University of Leicester.

Yorkey, T. J. & Webster, J. G. [1987], 'A Comparison of Impedence Tomographic Reconstruction Algorithms', *Clinical Physics and Physiological Measurement* **8**(suppliment A), 55–62.

Yorkey, T. J., Webster, J. & Tompkins, W. [1987], 'Comparing Reconstruction Algorithms for Electrical Impedance Tomography', *IEEE Trans. Biomed. Eng.* **34**, 843–852.

Zhang, J., Mackie, R. L. & Madden, T. R. [1995], '3-D Resistivity Forward Modelling and Inversion using Conjugate Gradients', *Geophysics* **60**(5), 1313–1325.